Proceedings of the Fourth International Workshop

on

Laser ranging instrumentation

held at the
University of Texas in Austin, Texas, U.S.A.
October 12 – 16, 1981

Volume II

compiled and edited
by
Peter Wilson
President, Special Study Group 2.33, I.A.G.
Earth-satellite laser ranging

published by the
Geodetic Institute, University of Bonn, 1982

TABLE OF CONTENTS

THE LASER AND THE CALIBRATION OF THE CERGA LUNAR RANGING SYSTEM

by J.F. MANGIN, CERGA, France

The actual laser pulse width at half amplitude is 3 nanoseconds. In increasing the dye concentration, we can obtain 2.2 ns reliably.

The pulse energy is about 2.5 joules. The photon energy is :

$$h\nu = 6.6.10^{-34} . 3.10^{8} /0.7.10^{-6} = 2.8.10^{-19} J.$$

Then, each firing corresponds to 9.10^{18} photons. It is necessary to attenuate of 190 dB since the calibration requests "single photoelectron" event.

The target proximity forbids Flip-Flop use. Instead we have a beam splitter :

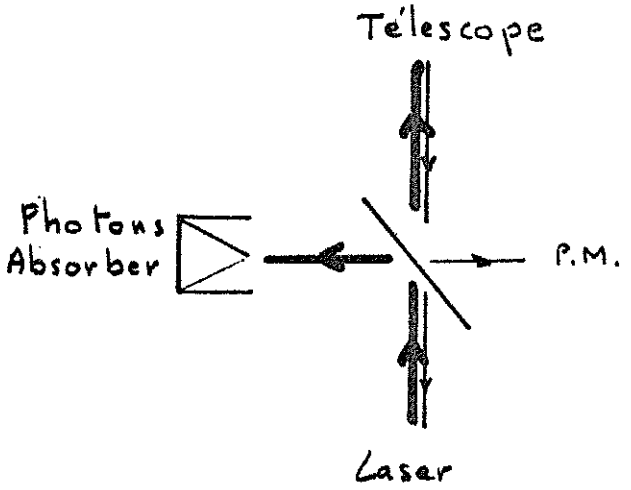

But this beam splitter permits many parasitic reflections on the P.M. (photon-absorber ; mirror II and various scattering) which could be very harmful.

To cure that and protect the laser, we decrease the laser output energy by switching-off the final amplifier. A part of the laser spot is retrieved from reflection on the final amplifier front face.

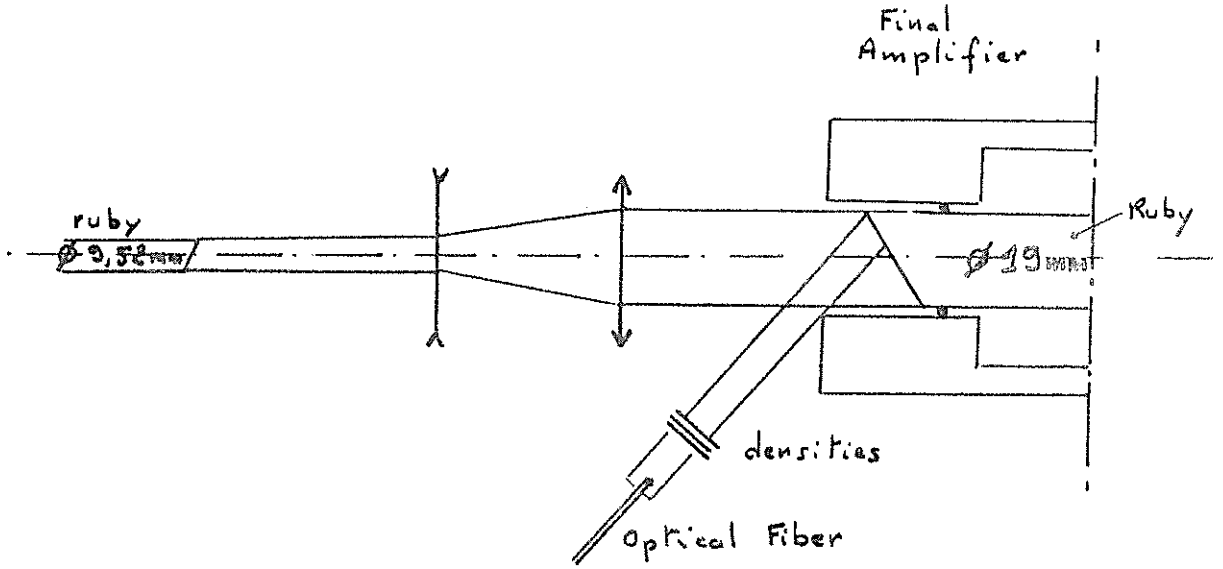

This pulse is directed via an optical fiber to the start pulse centroid detector. We have checked that energy collected by the optical fiber was independent of the final amplifier switching. Thus, the attenuation is 25 dB (5 dB : amplifier gain ; 20 dB : ruby absorption). Then, we can add 60 dB densities after the final amplifier. The target is a corner cube retro-reflector. Its aperture is a thousandth of the telescope's. So, we got 30 dB loss. Variable densities in front of the P.M. allow an attenuation from 0 dB to 80 dB. Thus it is possible to adjust the output level in order to receive statistically single photoelectron events.

The photomultiplier characteristics RCA 31034 A give 12 mV peak pulse for one photoelectron.

Reception diagram

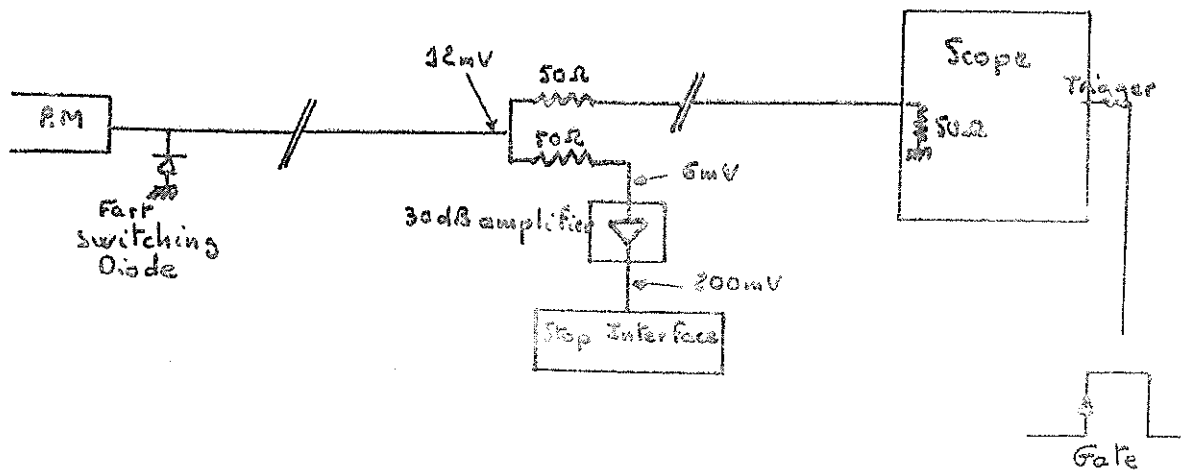

The separator allows a display on a fast storage oscilloscope of the returning event.

Start interface (fig. 1)

The start interface most provide the event-timer with a calibrated pulse synchronized with the center of the laser pulse. A start pulse centroid detector* is used. This allows to minimize the energy and width jitters of the pulse (inhomogeneity of the dicarbocyanine-methanol dye). We verified that, for a same laser pulse, two centroid detectors date this pulse with ± 120 ps r.m.s. delay. This integrator circuit is also used to display the energy of each firing by means of 7 L.E.D.

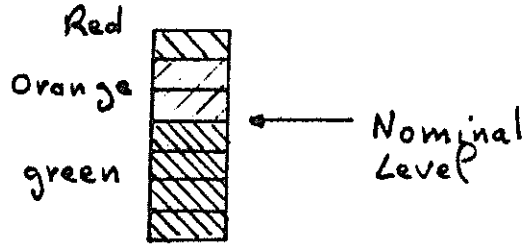

Stop interface (fig. II)

The stop interface realize several functions.

1/ Half amplitude detection, real time

Assuming that the P.M. output pulse corresponds to only one or several simultaneous photoelectrons, the half amplitude pulse width is about 4 ns. We did then an half amplitude detection dividing the amplitude by two and delaying the pulse by half its width. A comparator gives a calibrated pulse at the pulse crossing "A". Jitter from statistical gain gain variations of the P.M. are thus eliminated.

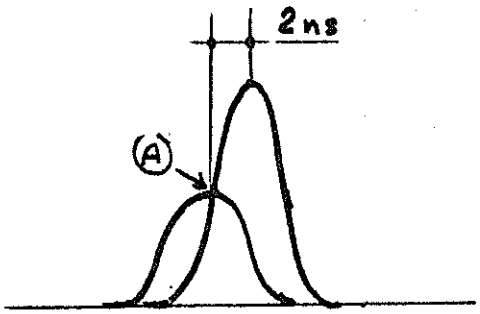

2/ Threshold setting, real time (J.M. TORRE, CERGA, France)

Post P.M. amplifier output pulse is compared with a variable level ranging from 150 mV (Moon ranging : one photoelectron about 200 mV) to 4 V (satellite ranging). A window allows to switch-on the signal only when it is above the threshold.

★ cf.: Third International workshop on laser ranging instrumentation "A start-Pulse Centroid detector", J-F Mangin and J. Gaignebet.

3/ Available output

An output from the processed pulses goes to a counter, allowing to know the noise under the experimental conditions.

4/ Gate

A signal from the "gate control" board allows transmission of the pulses to the event-timer if they are close to the predicted range. Gate width is adjusted manually from 20 ns to 50 µs by 20 ns steps.

It is possible to replace the threshold selector by a measuring system of the returning energy but the calibration target ranging did not show explicitly any correlation between the measurements and the returning pulse level if the detection works with few photoelectrons.

Calibration

- On June 17th, 1981, a calibration was realized on a target set up at Gréolière peak, 7 631.021 m distant from the mount axes crossing. The following histogram (fig. III) shows that measurements are distributed over 5 ns.

- On september 16th, 1981, two series of calibration were made, single and double round trip on the same target and one on the internal retroreflector (fig. IV, V, VI)

Calibration computing (Y. Boudon, CERGA, France).

On June 17th, 1981 : Cal. = 199.0 ns

On September 16th, 1981 :

- Single Round Trip : Cal. = 198,7 ns
- Double Round Trip : Cal. = 198,5 ns
- Silverberg method : Cal. = 198,7 ns
- Internal target : Cal. = 199,1 ns

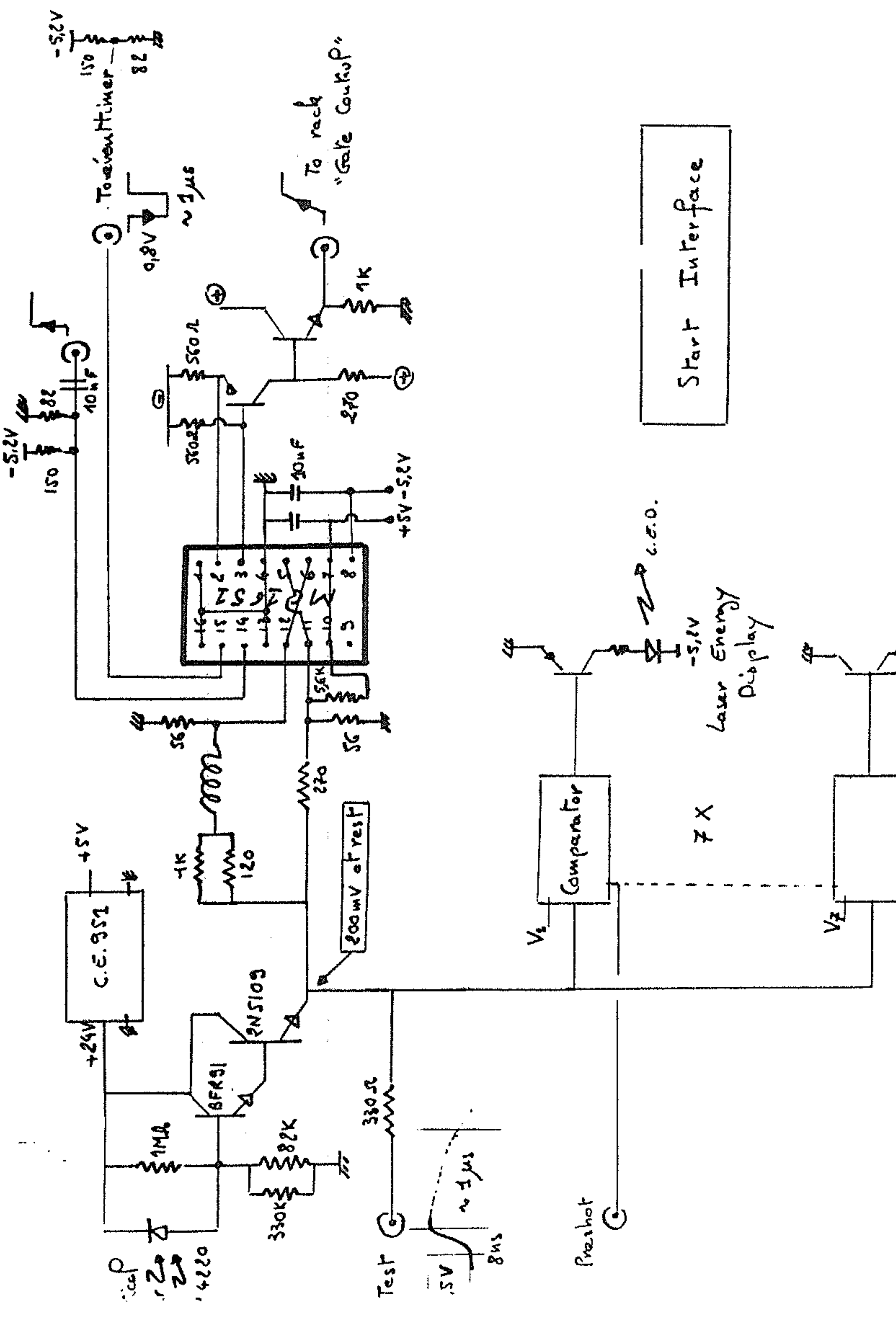
Start Interface
Comparator
Laser Energy Display
7 X
Test
Preshot
2N5109
BFR91
200mV at rest
L.E.D.
-5,2V
+5V
+24V
~1µs
0,8V
330Ω
1MΩ
82K
330K
270
1K
120

Fig I

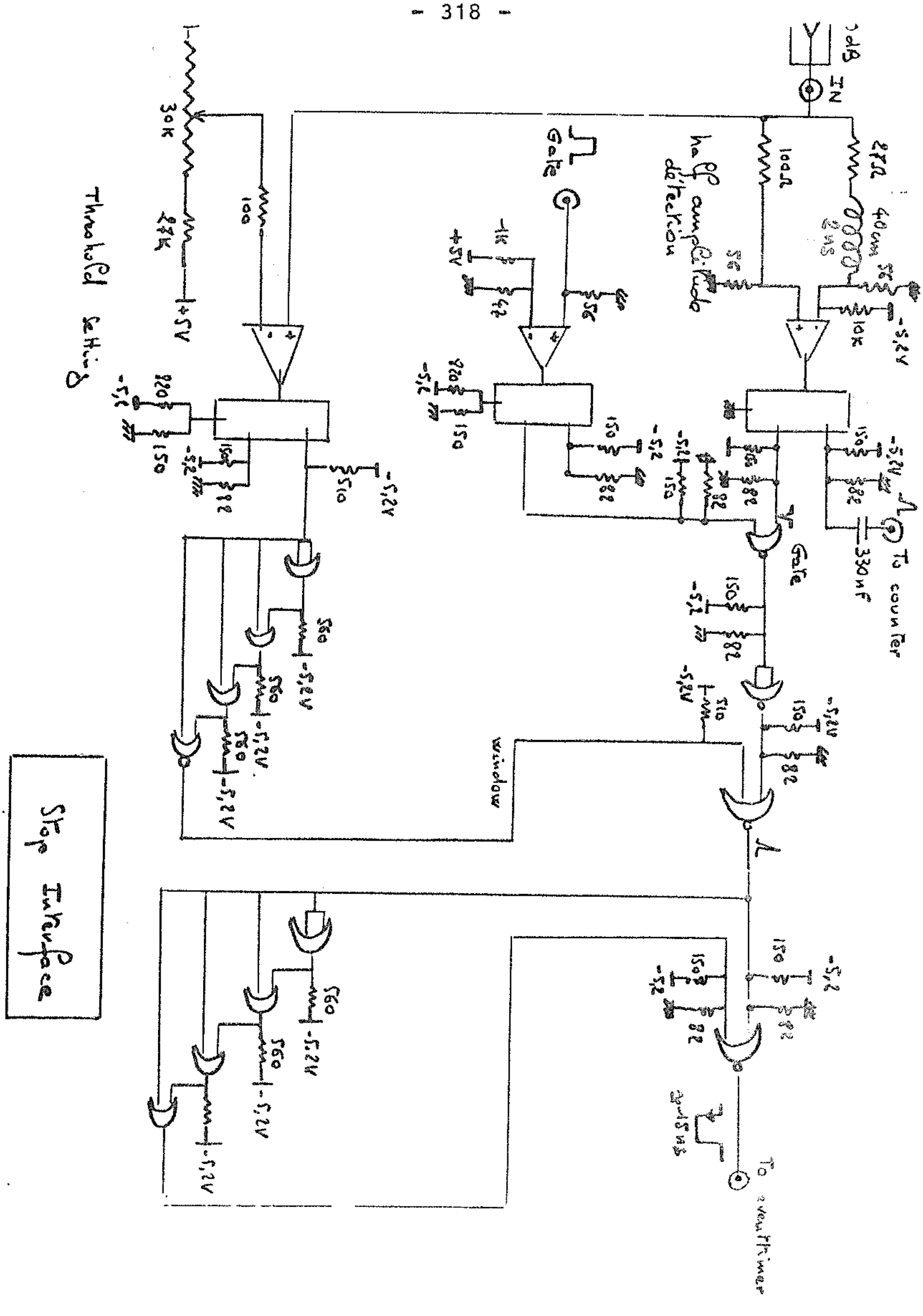
Stop Interface
Threshold setting
half amplitude detection
IN
Gate
To counter
window
To eventtimer

Fig II

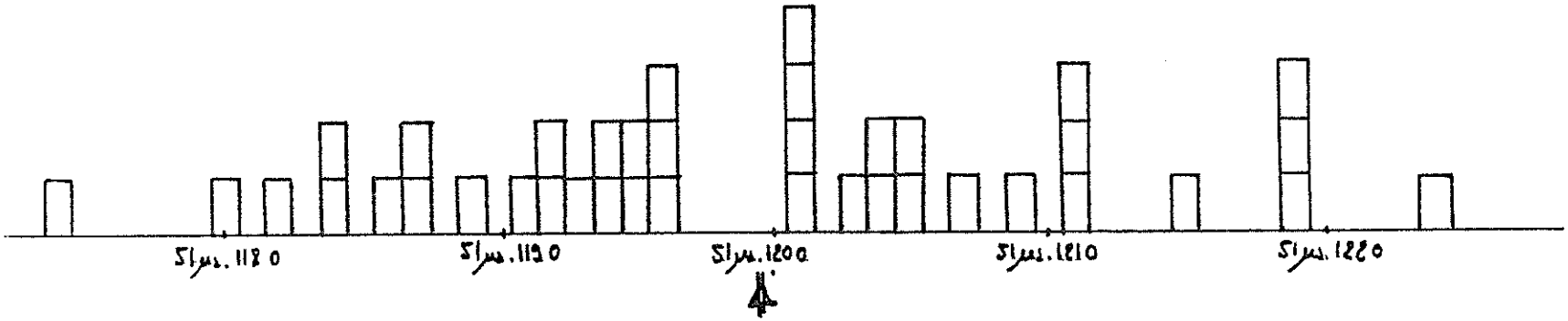

Calibration : Gréolière Target ; June 17th, 1981

T = 10,1°C D = 7631,021 m
P = 649,0 mm Hg d = 1.828 m

Asumed mean value 51µs. 119.9 | CoP = 199.0 ns

Fig. III

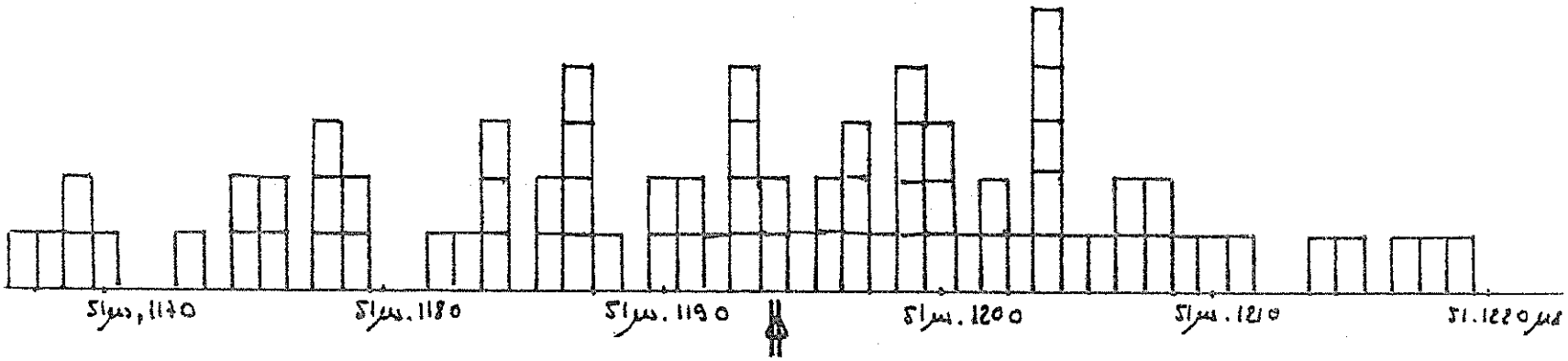

Calibration : Grésilleise Target ; September 14th, 1981

T = 16°5 C
P = 656 mm Hg

D = 7631,021 m
d = 1,806 m

Asumed mean value 51μs.1194 ⇒ **Cal = 198.7 ns**

Fig IX

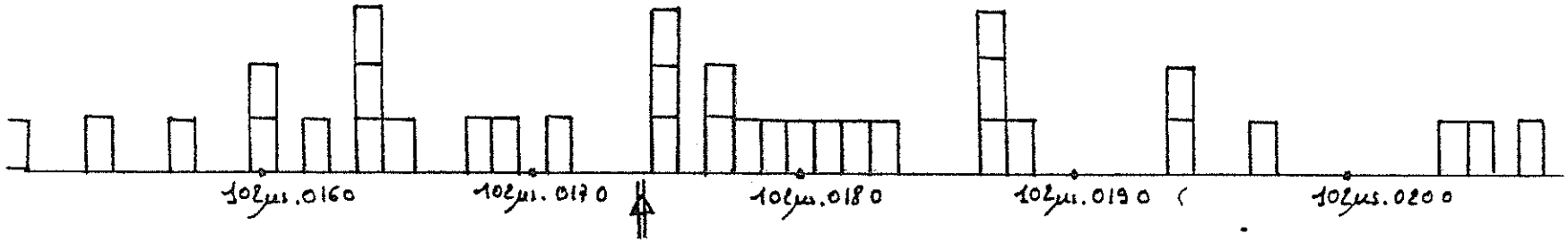

Calibration : Gréolière Target ; September 14th, 1981

T = 16,5 °C
P = 656 mm Hg

D = 7631,021 + (7631,021 - 3,387)
d = 1,806 + 1,806

Asumed mean value 102μs.017 4 ⇒ $\boxed{C_0P = 198.5}$

Fig IV

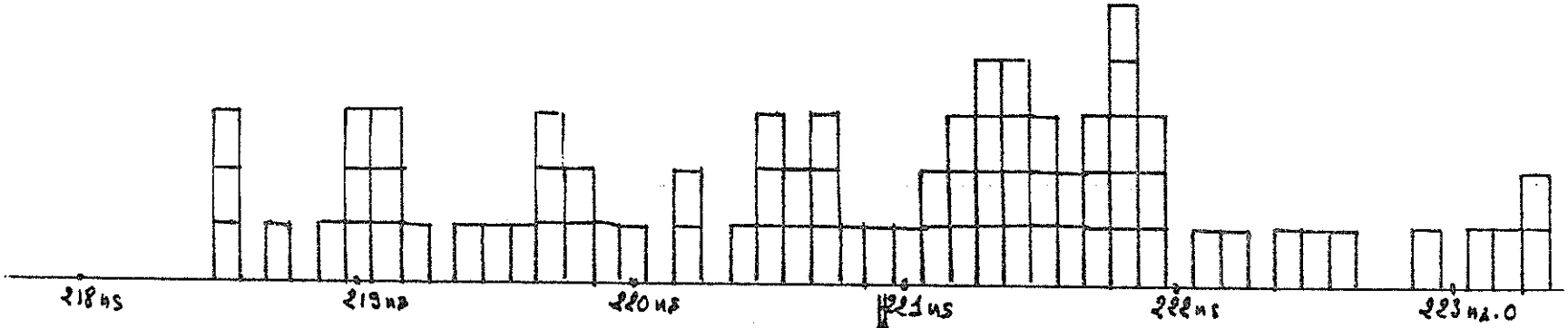

Calibration : Retroreflector September 16th, 1981

D= 3,263 m

Asumed mean value 220.9 ms ⇒ **CaP= 199.1 ms**

Fig VI

SAO CALIBRATION TECHNIQUES

M. PEARLMAN, N. LANHAM,
J. THORP AND J. WOHN

SMITHSONIAN ASTROPHYSICAL OBSERVATORY
CAMBRIDGE, MASSACHUSETTS 02138

Detailed and rigorous calibration procedures are the key to verifying system performance. In particular, as ranging accuracy requirements become more stringent the sources of data corruption become more illusive and more difficult to observe in ranging data. In fact, with the current state of geophysical models, it is unlikely that aliasing effects at the decimeter level would be recognized in long arc solutions. Calibration techniques may vary slightly depending upon system configuration. The techniques used by SAO are presented here as an example of the care that must be taken to ensure data quality and reliability. We also point out that these techniques were not invented by SAO but have evolved through experience by many participants in this field.

The SAO calibration procedures can be broken down into three categories: electronic calibration, specialized ground target calibration, and calibrations associated with satellite ranging procedures.

ELECTRONIC CALIBRATION

A full electronic calibration of the pulse processing system conducted several times per month and whenever a modification is made to the signal processing electronics provides the dependence of system delay on output pulse characteristics. It also provides a measure of electronic system jitter (post PMT). The calibration is performed by entering electronic pulses of widths 5, 6 and 7 nsec into both the output (start) channel and return (stop) channel circuitry. The input to the start channel is then varied +/-3 db from the normal operating level of the laser to encompass the effects of any variations in output signal strength that may be encountered during ranging. Regression analysis on this data gives the calibration parameter and a measure of the electronic system jitter (see Figure 1). Typical values for jitter range from .15-.20 nsec (2-3 cm). The calibration parameter and the jitter are monitored at both the stations and Headquarters to assess system performance.

Once per shift (usually at the beginning) the response of the 0.1 nsec resolution time interval counter is checked with a 100 msec period signal derived from the 1 MHz output of the station clock. Expected performance is +/-.1 nsec; 1 sigma scatter is typically 50-80 psec. Performance outside +/-.2 nsec indicates that the counter is not working properly.

SPECIALIZED TARGET CALIBRATIONS

Extended target calibrations on ground bill board targets are conducted at least once per month over the full operating range of the laser (1 - 1000 photoelectrons). This test is performed to monitor system calibrations as a function of signal strength to ensure that variations in system delay through the PMT and the pulse processing electronics are consistant with accuracy requirements. This measure also includes any long term drift effects in the system.

In practice, received optical signal strength is varied with neutral density filters in the photoreceiver to span the dynamic operating range. The calibration extends all the way down to the single photoelectron level where signal strength (pulse area) is determined from pulse counting statistics. This single photoelectron area is then used to calibrate signal strength over the full dynamic range. In the calculation, the data are divided up into subsets by

signal strength for convenience. Subsets have a minimum of 100 photoelectrons at the very lowest signal strengths and as many as several thousand at higher signal strengths.

An example of a calibration result is shown in Figure 2. In the present configuration, the calibration response is typically "flat" to better than +/-.4 nsec (6 cm). Error bars denote the standard deviation of the individual measurements.

The standard deviations are examined to assess the noise performance of the system (see Figure 3). In the intermediate regions we expect the sigma to follow a $1/\sqrt{n}$ dependence. At high signal strengths, sigma tends asymptomatically toward a fixed level characteristic of system jitter (electronic and PMT) which is typically .2 - .3 nsec. At very low signal strengths (~1 photoelectron) aside from effects of photon-quantization, the data also include corruption from degradation in pulse shape due to PMT response, and inadequate pulse sampling with the digitizer.

Ground target calibrations using a single retroreflector have been used to map the wavefront distortion of the laser. This distortion which arises from internal mode structure in the laser was particularly illusive because it could not be seen with the standard billboard target. Measurements of wavefront give us one of the fundamental limitations on the accuracy of a particular ranging system because in some cases error signatures may not be separable from geophysical effects.

In the calibrations taken by SAO, we probed the beam with a 3 by 3 or 4 by 4 matrix with a minimum of a 1000 photoelectrons (20 shots) at each point. See Pearlman, et al 1981. The results of a number of calibrations show a maximum variation of 9 cm across the beam with a r.m.s. variation of about 3 cm. The pattern of the wavefront distortion changes over a time period of several hours, but the magnitude values above are quite typical.

CALIBRATIONS ASSOCIATED WITH SATELLITE RANGING

To account for any possible changes or drift in system delay, calibrations are performed on the ground target before and after each pass. These precalibrations and postcalibrations, which consist of 20 points each at the 25 photoelectron level (for a total of 500 photoelectrons), are submitted with the pass data. System calibration is determined on a pass-by-pass basis as the mean value of the two calibration runs. The difference between precalibration and postcalibration values and the rms are used to estimate the short term system stability and the system noise. These numbers are monitored and compared with historical data. An example of calibration differences is shown in Figure 4. RMS calibration noise is typically .3 - .4 nsec as would be anticipated for a 6 nsec pulse.

In the process of ranging on satellites, we also record (digitize) several examples of the outgoing laser pulse. This is used for reference for centroid detection, and is also available for assessment of laser performance.

In all cases where the waveform is recorded (electronic calibration, target calibration, output pulse, satellite ranging, etc.), the digitizer baseline (or zeroset) is recorded for use in normalizing pulse shapes.

CONCLUSION

Calibration is an essential part of ranging. It should not be surprising that the laser in many cases must be fired as many times for calibration purposes as for ranging. On the otherhand, we must recognize that systematic errors can be extremely difficult to observe and that great care must be taken to design the hardware and the calibration procedures to isolate and measure these effects.

REFERENCES

Pearlman, M. R., N. W. Lanham, J. Wohn and J. Thorp, 1981. The Current Status and Upgrading of the SAO Laser Ranging Systems, to be presented at the Fourth International Workshop on Laser Ranging Instrumentation, Austin, Texas.

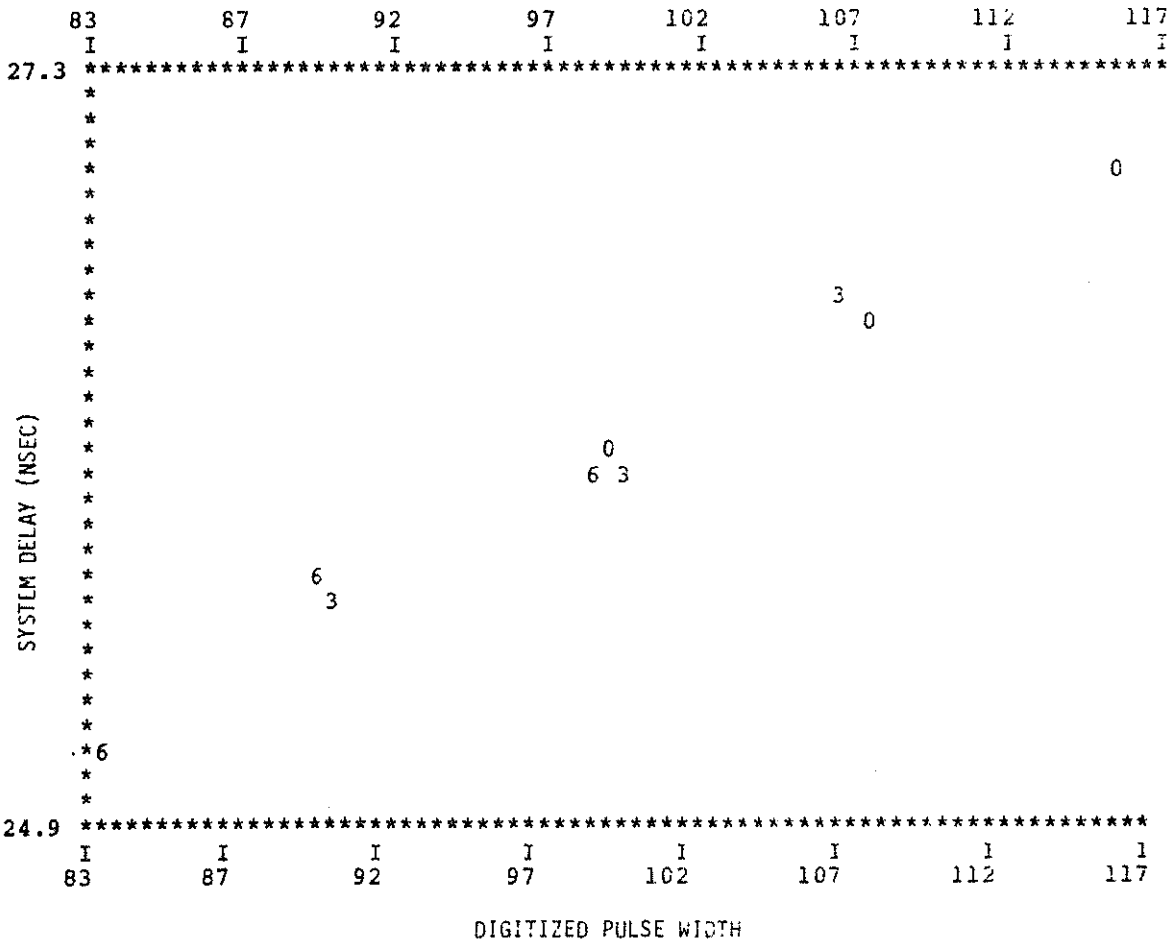

Figure 1.

Electronic system calibration showing change in start system delay with pulse width. Points on the graph represent averages of data sets taken at 5, 6 and 7 nsec with 0, 3 and 6db attenuation (denoted as 0, 3 and 6) in the signal line. The middle 3db point represents the nominal performance of the SAO laser with 6 nsec pulse width.

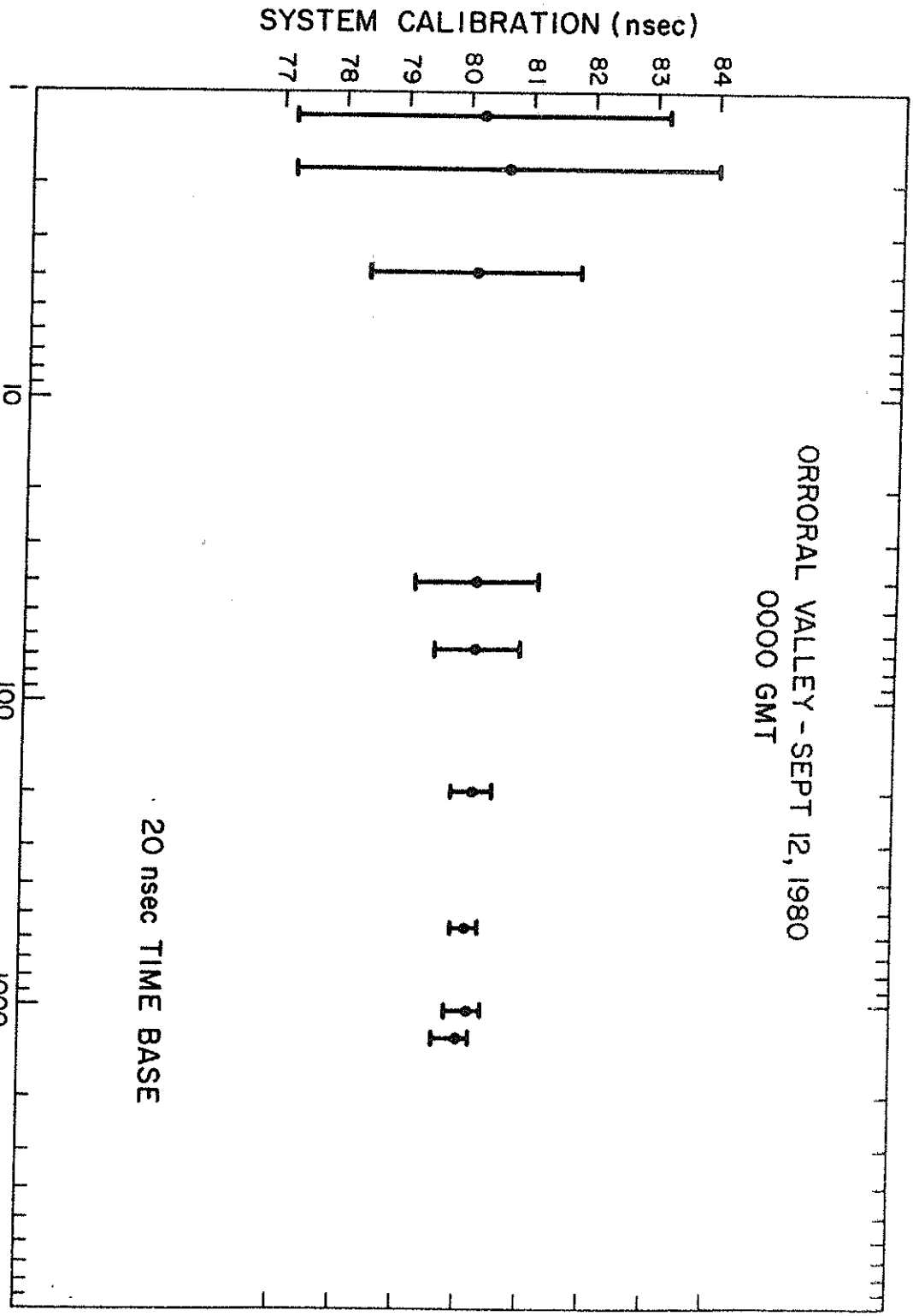

Figure 2.

Extended target calibration with single point uncertainties shown with brackets.

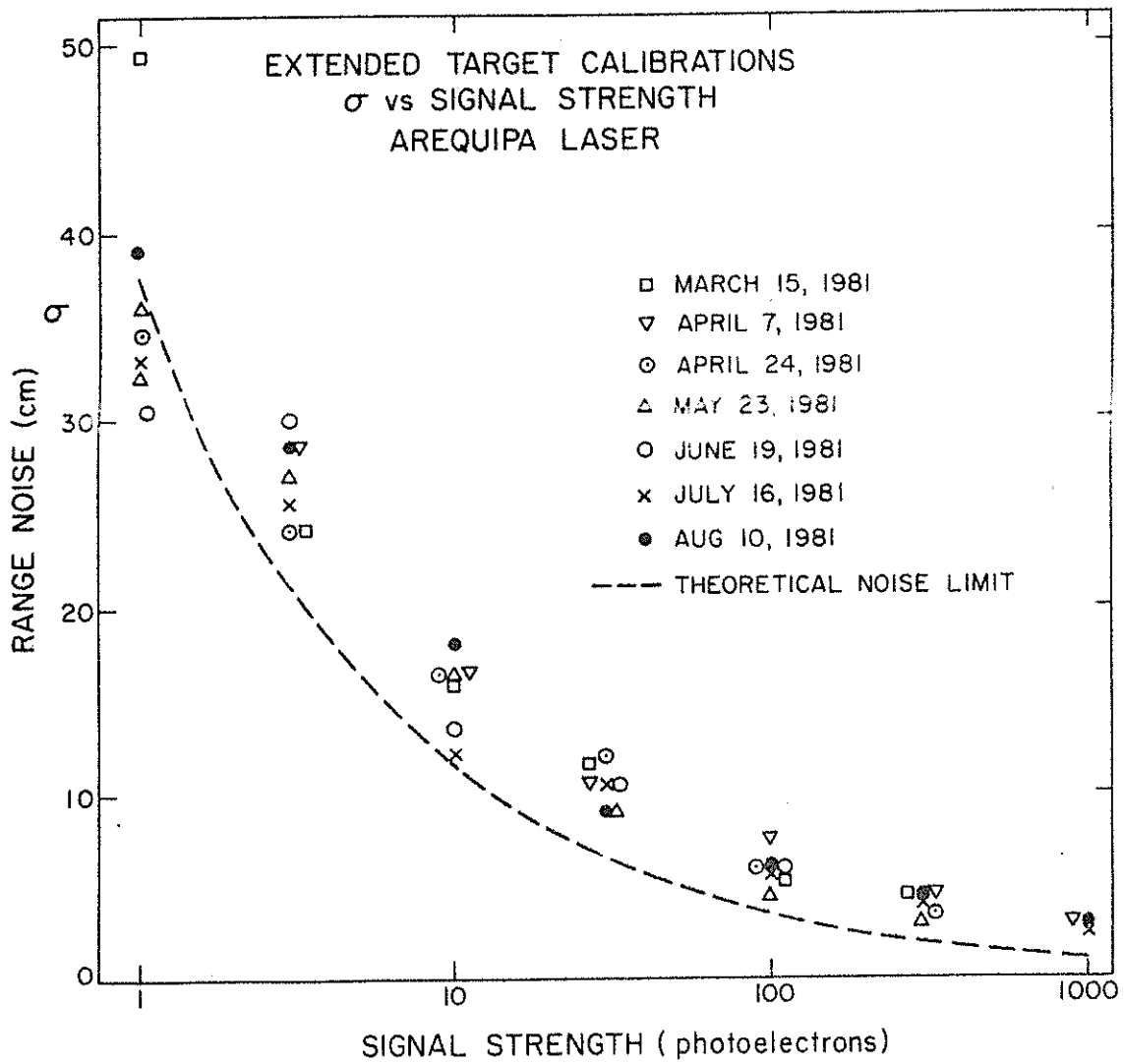

Figure 3.

Extended target calibrations, σ versus signal strength with theoretical limit shown.

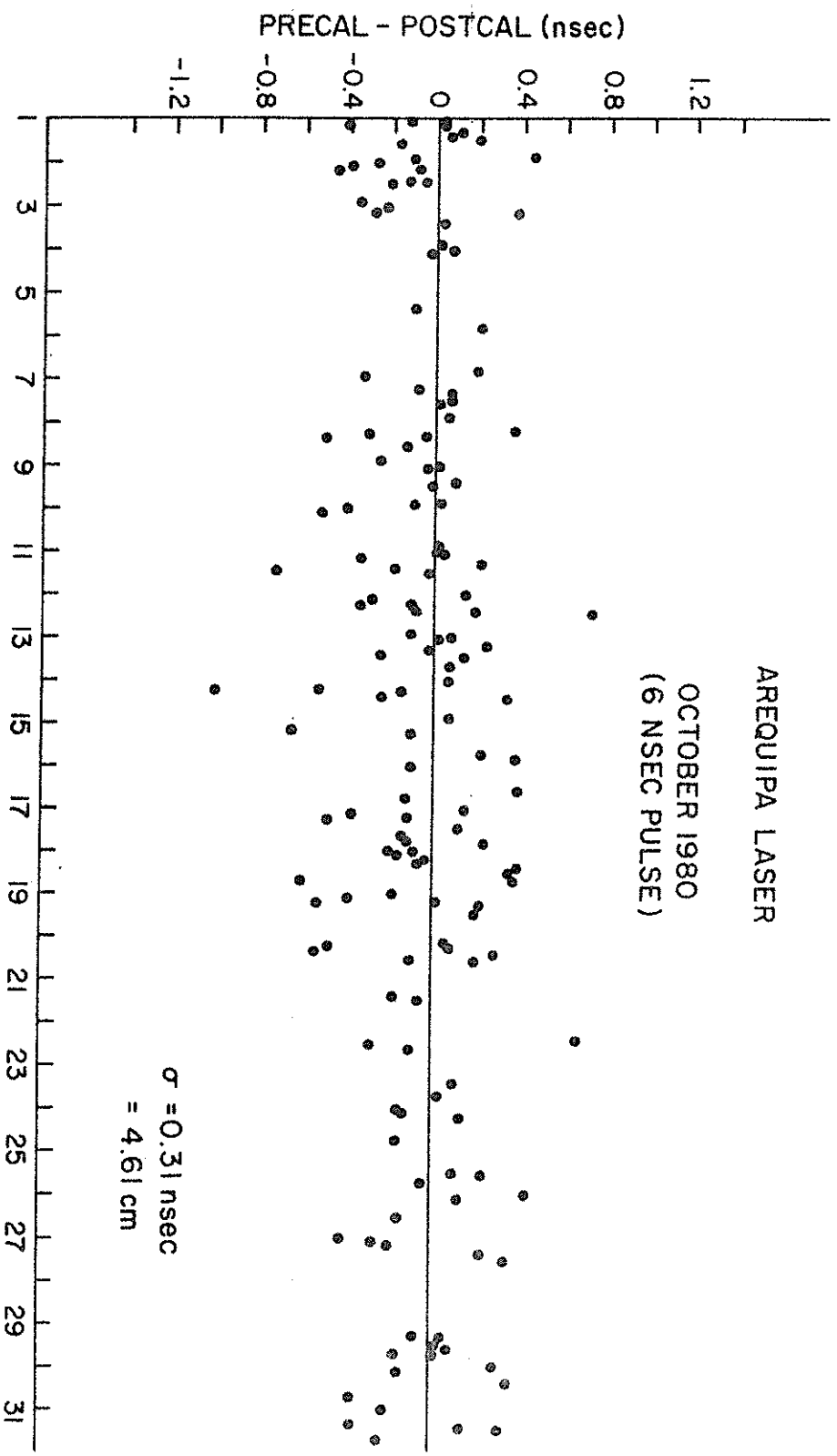

Figure 4.
Precalibration minus Postcalibration; 4 differences based on 20 shots each.

THE FEEDBACK CALIBRATION OF THE TLRS RANGING SYSTEM

BY

ERIC C. SILVERBERG
UNIVERSITY OF TEXAS McDONALD OBSERVATORY
AUSTIN, TEXAS 78712

The transportable laser ranging station (TLRS) which was constructed under a NASA Contract by The University of Texas, uses a multipulse mode-locked laser. The system relies on the use of real time feedback calibration to correct the time-of-flight data for the system delays. As such the system is truly self-calibrating, in the sense that it monitors the relevant system delays without operator interaction during each satellite pass.

The main features of this calibration scheme can be understood with the aid of Figures 1 and 2, the optical and electronic diagrams respectively. After the laser fires, a small amount of the output beam is diverted by an antireflection coated glass plate and immediately attenuated another factor of 10^6. It is then further attenuated to the single photoelectron level by a rotating attenuater which is located directly in front of the system spacial filter. Meanwhile, the signal from the system start diode travels through the discriminator circuitry and simultaneously starts the three system verniers which are contained in a commercial EG&G TD811 time digitizer unit. The start diode signal also latches the current epoch in a five megahertz, 28 bit circulating count register. The counter is phased by cable delays (D_3) to the TD811 to eliminate any 200 nsec ambiguities in the interpretation of the two readings. If a photoelectron pulse was created by the feedback light, it then travels through the discriminator units, through delay box D_1 to vernier 0. Vernier 1 of the TD811 stops

on the next 5 megahertz pulse which is delayed about 100 nanoseconds and also fed into vernier 2. (The program automatically selects the use of either vernier 1 or vernier 2 depending on which is closest to its mid-range.) All the verniers are, for convenience, adjusted to have the same slopes, but this is not absolutely necessary. The initial reading of vernier 0 is saved as the principal calibration constant.

When a return from the satellite travels through the system some tens of milliseconds later, the rotating mirror and rotating attenuater have moved to new positions so that the photons are routed through the spacial filter along the same path as the feedback. If a photoelectron is created, the latch again records the number of counts in the 5 megahertz counter, since the receiver "and" gate is open. The return photon also reactivates the start of the same TD811 used for the start sequence. In addition the return signal travels through the delay box to stop vernier 0. The true calibration constant i.e., the difference between the stop and start sides of the system is therefore $V_{01} - V_{02}$. By adjusting the length of the start cable, it is possible to hold $V_{01} - V_{02}$ close to 0 so that any error in the measurement of the vernier 0 calibration constant is not propagated into the range accuracies.

The time of flight is measured by the difference in the counter, as recorded by the two operations of the latch, plus the difference in verniers 1 and 2 which have been selected as mentioned earlier. Per usual, we correct the time of flight to that which would be measured if an infintessimally small telescope was observing from the first non-moving point on the receive path. This requires that we subtract twice the distance from the rotating mirror to the intersection of the axes (2a+2b+2d+2e+2f) and twice the additional size which the telescope implants from that point forward (2g). Note that the measurement of the path length from the beam splitter to the photomultiplier or from the beam splitter to the start diode is not important, since it affects both the calibration feedback path and the range path in exactly the same manner. The stability of the calibration vernier can, furthermore, be monitored independently by watching the numbers which are derived for V_{02}, since this merely represents a fixed cable delay.

So far all of these comments could be applied to any system which provides a feedback pulse which is at the same intensity as the satellite return. In the case of a single photoelectron system, however, the distribution in V_{01} will statistically build up the pulse shape of the laser system over a matter of hundreds of shots. We can use this information to not only determine the exact jitter which the total ranging system is undergoing at the time, but to further improve the accuracy of the results. Our calibration constant is removed by cross-correlating the array of $V_{01} - V_{02}$ readings with the array of returns from the satellite as plotted in residual space (o-c). This

allows the system to work with any laser pulse shape which can be monitored during a reasonable interval of time by the statistical sampling process. In the TLRS, for instance, a multiple pulse, dye mode-locked laser produces a return from the satellite such as shown in Figure 3a. When the data from this strong 3-minute burst was cross-correlated with the calibration data for that particular 3-minute span (3b), the cross-correlation function locates the calibration displacement with unerring accuracy. The point at which the calibration data and the returns from the satellite show the best match immediately realize the formation of a normal point which takes advantage of the full information available in the data. It also identifies with which laser pulse the returns should be identified and thus results in a calibration for each of the various return groups. When each return group was calibrated and folded together the resulting residuals form Figure 4. These data show an RMS deviation of approximately 8 centimeters.

The advantage of a real-time feedback calibration system is that it is capable of monitoring subtle pulse shape changes, discriminator settings and other factors during the actual ranging process thus preventing errors which might otherwise be possible. This is especially important in long duration LAGEOS runs where changing light levels, voltages and discriminator settings can make pre/post pass calibrations suspect. While it is bit more difficult to realize the real time calibration scheme than to calibrate off a target board, our experience in this area has been universally good and we recommend its use whenever possible.

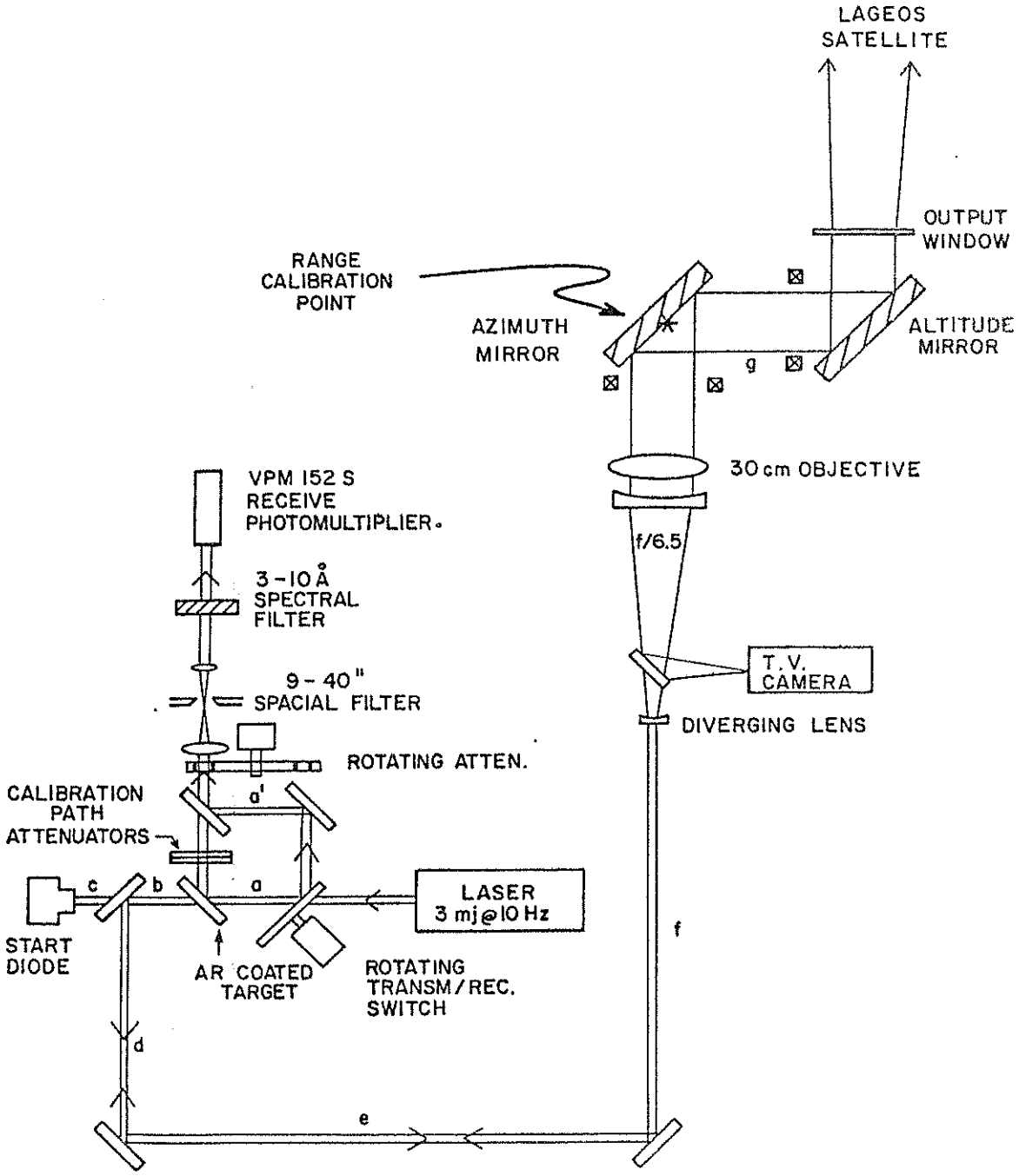

Figure 1: A schematic drawing of the major optical components in the TLRS.

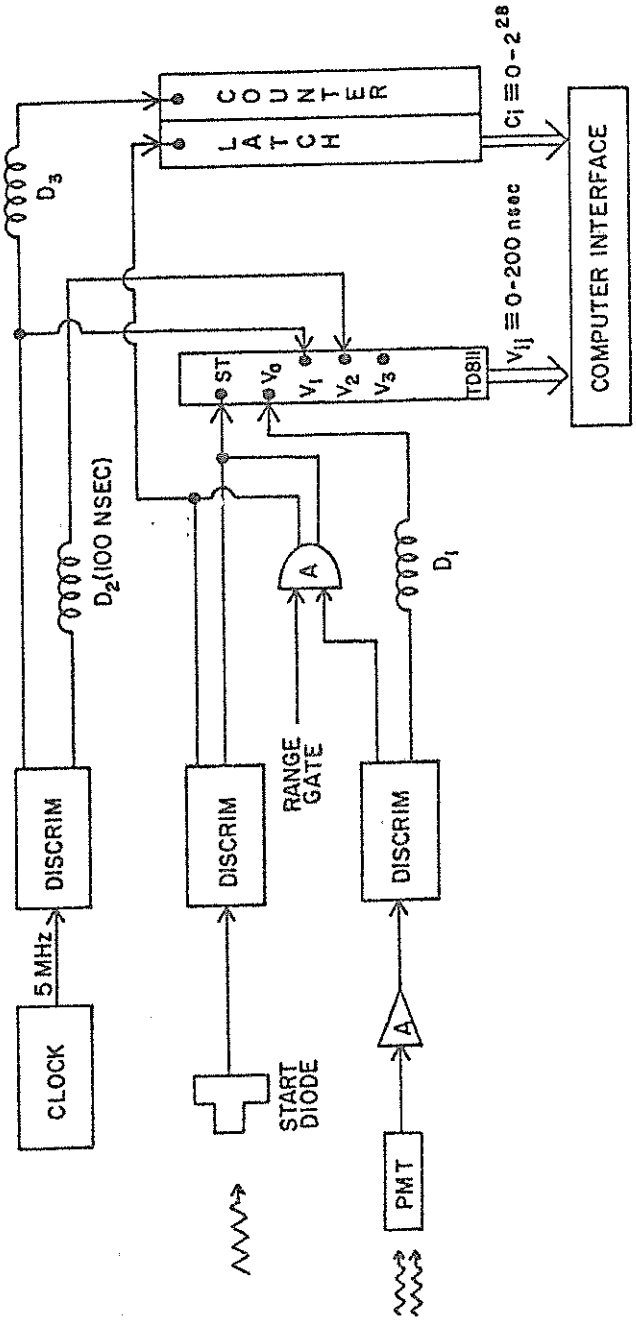

Figure 2: Shown is a schematic drawing of the critical components in the TLRS time-of-flight (TOF) system which are evolved in the real-time calibration scheme.

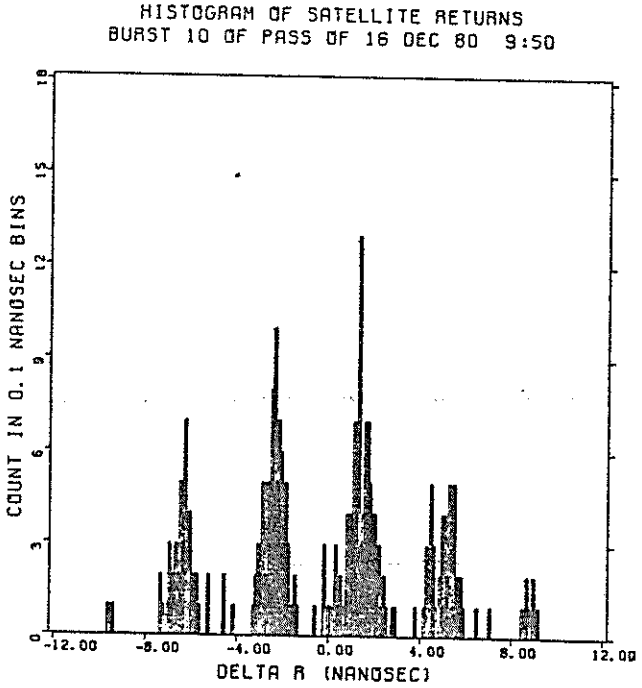

Figure 3(A): Shown is a histogram of the range residuals from a three minute burst on the LAGEOS satellite plotted relative to the average for the entire burst. Note the multipulse character of the laser and the fact that, in this case, the earlier pulses are slightly oversampled.

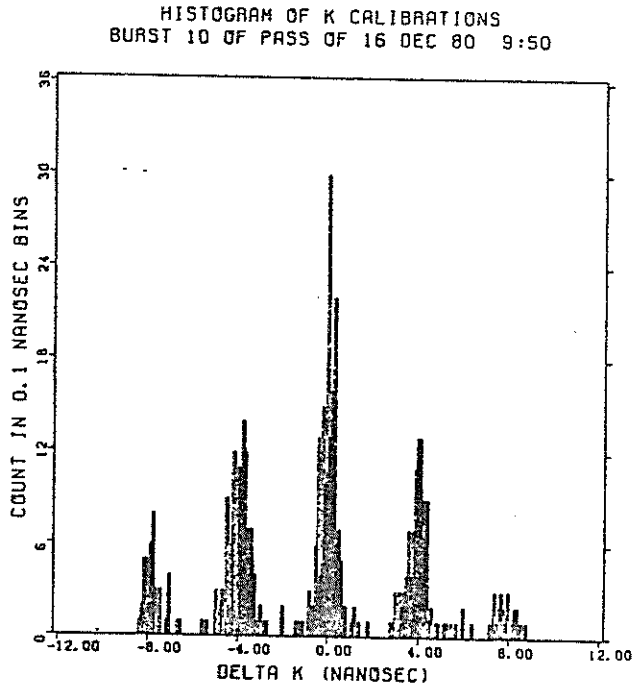

Figure 3(B): The feedback calibration data from the same time interval as in Figure 3(A) indicates not only the calibration bias, but also the true limitations of the system at that time.

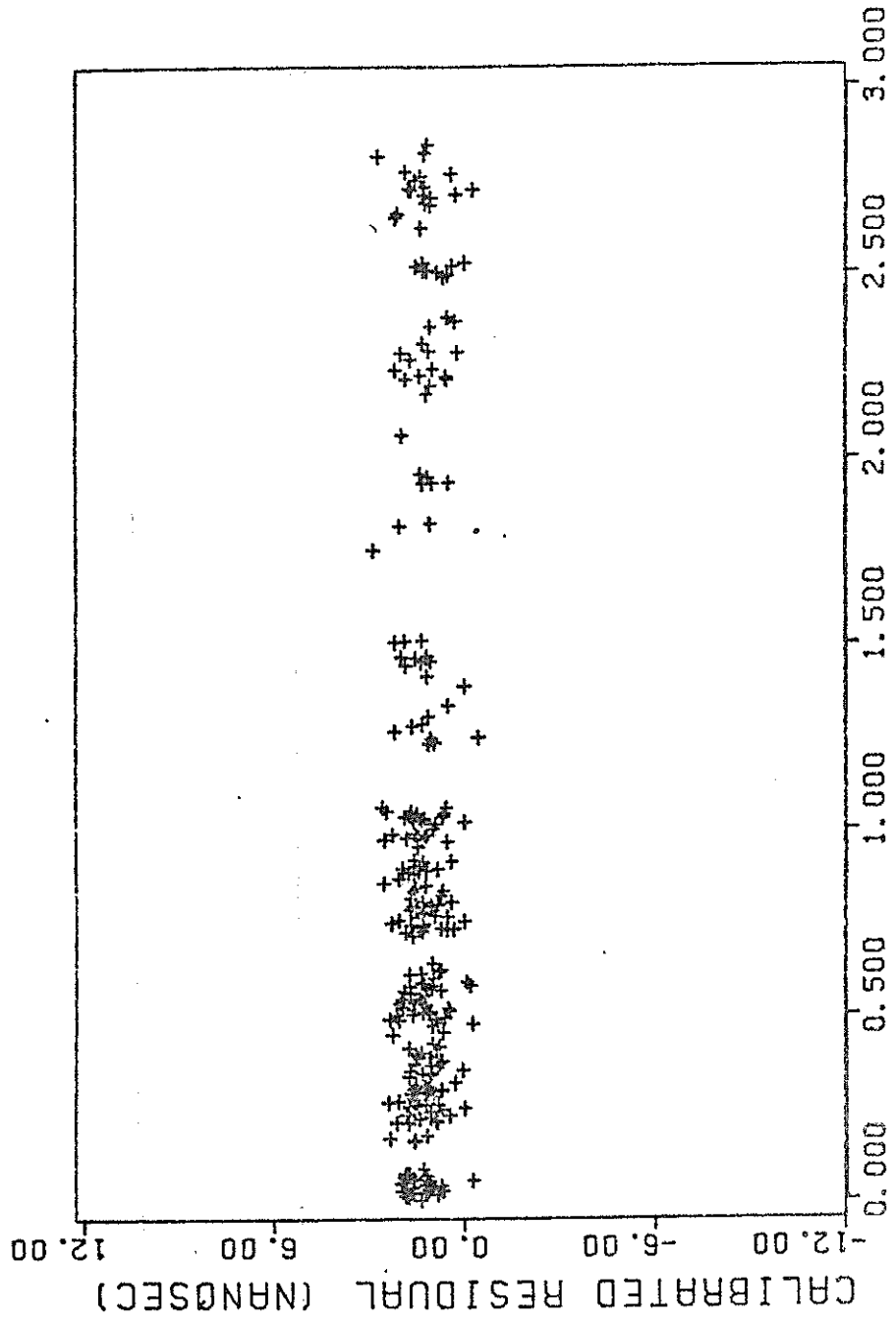

Figure 4: This drawing shows the calibrated residuals from the Figure 3 data. Good bursts show an RMS scatter of 7-8cm with as many as 550 returns.

GPS TIME TRANSFER RECEIVERS FOR THE NASA TRANSPORTABLE LASER RANGING NETWORK

O. Jay Oaks and James A. Buisson
Naval Research Laboratory
Washington, D.C. 20375

Schuyler C. Wardrip
NASA/Goddard Space Flight Center
Greenbelt, MD 20771

ABSTRACT

Present time synchronization techniques used within the Laser Network will be discussed. LORAN-C and portable clock data taken over the past year at various installations will be presented.

Future applications of the Global Positioning System (GPS) to achieve worldwide submicrosecond timing within the Laser Network will also be discussed.

The theme of the presentation will center on the performance of the NRL developed GPS receiver which was recently field tested at Kennedy Space Center, Florida. Portable clock measurements were made during the tests for comparison, with all measurements referenced to the Naval Observatory. Nine GPS timing receivers will be built for use in the Laser Network and other NASA facilities.

BACKGROUND

Present time synchronization techniques within the NASA laser network utilize LORAN-C and portable clocks. To use the highly accurate laser ranging data, it is necessary to time tag data from the laser stations very accurately. In applications where the data from two or more stations will be merged to determine baselines for geodetic work and polar motion determinations, it is necessary that the clocks at the several stations be synchronized to within ± 1 microsecond with respect to a master clock, such as that of the U.S. Naval Observatory (USNO). Best synchonization results using the LORAN-C system were obtained from the West Coast chain at the Goldstone, California laser tracking station (MOBLAS 3) and have an RMS of a half microsecond (Figures 1 and 2). Worst results have been a four microsecond RMS obtained in Australia (MOBLAS 5) using a wave hop from the Northwest Pacific chain (Figures 3 and 4). Portable clock measurements allow worldwide synchronizations of less than a microsecond but require frequent, therefore costly, travel to the remote stations.

Time transfers by satellite have been performed by NASA Goddard Spaceflight Center (GSFC) and the Naval Research Laboratory (NRL) initially using the NRL Navigation Technology Satellites (NTS).[1,2] Accuracies of several hundred nanoseconds were obtained.[3] As an outgrowth of the NTS effort, a Time Transfer Receiver (TTR) which operates with the NAVSTAR Global Positioning System (GPS) satellites is presently being developed jointly by GSFC and NRL. GSFC will

use the GPS TTR in the Laser Ranging Network. The network consists of eight mobile vans, a permanent installation at GSFC, and eventually four highly transportable laser systems. The laser systems will be deployed to various locations around the world (Figures 5 and 6) and will be used in support of the NASA GSFC Crustal Dynamics Program.

NAVSTAR GPS is a tri-service Department of Defense (DOD) program.[4] The first GPS satellite flown was NTS-II[5,6] which was designed and built by NRL personnel. GPS will provide the capability of very precise instanteous navigation and transfer of time from any point on-or-around the earth. At present six NAVSTAR satellites are on-orbit, providing instanteous navigation over selected areas for limited parts of each day. This constellation is part of the GPS Phase I configuration. Additional space vehicles (SV) are to be launched during the next year with the NAVSTAR 7 launch scheduled for December 1981.

The major objective of a satellite time transfer receiver is to determine precise time differences between a given satellite and a local ground clock referenced to the TTR (Figure 7). Precise time can then be obtained between the SV and a single remote ground station clock or between the SV and any number of remote stations. The remote sites could then be synchronized among themselves.

THE NAVSTAR GLOBAL POSITIONING SYSTEM (GPS)

GPS is comprised of three segments. The space segment consists of a constellation of satellites for global coverage.[7] Phase

III GPS will have a total of 24 satellites, eight in each of three orbital planes (Figure 8). The GPS orbits are near-circular at an altitude of approximately 10,000 nautical miles, inclined at 55 degrees to the equator. The period is adjusted such that a repeating ground trace is obtained for a given ground tracking station. Each satellite transmits its own identification and orbital information continuously. The GPS signal is spread spectrum in nature, formed by adding the data to a direct sequence code which is then biphase modulated onto a carrier.

The control segment consists of a master control station (MCS) and monitor stations (MS) placed at various locations around the world.(8) The current Phase I MCS is located at Vandenberg Air Force Base with the supporting monitor tracking stations at Alaska, Guam, Hawaii, and Vandenberg (Figure 9).

The monitor stations collect data from each satellite and transmit to the MCS. The data is processed to determine the orbital characteristics of each satellite and the trajectory information is then uploaded to each satellite, once every 24 hours as the spacecraft passes over the MCS.

The user segment consists of a variety of platforms containing GPS receivers which track the satellite signals and process the data to determine position.(9,10) Coverage of the Phase III constellation is such that at least four satellites will always be in view from any point on the earth's surface.

TIME TRANSFER METHOD

To perform a satellite time transfer with GPS, pseudo-range measurements are made that consist of the propagation delay in the signal plus the difference between the satellite clock and the ground station receiver reference clock. Data from the satellite is processed to obtain satellite position and satellite clock information (offset from GPS time). The propagation delay is subtracted from the pseudo-range by knowing the exact locations of the satellite and the station. This result is then corrected by the GPS time offset to determine the final result of ground station time relative to GPS time. The Phase I GPS time is maintained at the Vandenberg MCS using a cesium oscillator. The Phase III GPS time is planned to be referenced from the MCS to the U. S. Naval Observatory (USNO) Master Clock. The final results obtained from a single-frequency receiver, such as the one described in this paper, will contain a small error due to the ionospheric delay which may be modeled and corrected.

GPS TIME TRANSFER RECEIVER (TTR)

The GPS TTR is a microcomputer based system which was designed to replace existing receivers that formerly used the NTS satellites for time transfer. The design used hardware and software from these receivers whenever possible. The following is a summary of the design requirements:

A. GPS Signal Detection Characteristics

1) Operates at the single L1 frequency of 1575 MHz

2) Has sufficient bandwidth to track satellites throughout their doppler range from horizon to horizon

3) Uses only the course/acquisition (C/A) code of 1.023 MHz

4) Tracks the C/A code to within 3% of a chip (30 nanoseconds)

5) Tracks any GPS satellite by changing to the appropriate code

6) Detects and decodes the navigation data as required to determine a time transfer

B. Operational Characteristics

1) Requires a stationary platform during operation

2) Determines the time difference between the 1 pps input station reference and GPS system time

3) Measures the time difference once every six seconds

4) Has an RMS of less than 50 nanoseconds on the time difference measurements

5) Controls the operation of the receiver by inputs from a keyboard

6) Outputs data to the CRT display and records on a flexible disc

C. Input Requirements

1) Antenna position in WGS-72 coordinates

2) 1 pps from the station time standard

3) 5MHz from the station time standard

With these design requirements, the receiver block diagram in Figure 10 was implemented. The following is a description of the major components shown in the diagram.

RF SUBSYSTEM

The RF subsystem provides carrier and code tracking capabilities for the GPS signal. It demodulates the data message into the non-return to zero (NRZ) format and provides the voltage controlled crystal oscillator (VCXO) frequency for coherent code generation. An external control voltage input to the VCXO is used for acquisition tuning.

C/A CODE GENERATOR

The C/A code generator accepts the code sequence of any GPS satellite from the microprocessor. It then derives the 1.023 MHz C/A code from the VCXO frequency and outputs it to the RF subsystem for code tracking. A satellite time epoch is derived from the C/A code period and output for the time interval psuedo-range measurement.

TIME INTERVAL MEASUREMENT

A time interval counter is controlled by the microprocessor to measure the time difference between the satellite epoch and the station reference. This measurement occurs once every six seconds as commanded by the microprocessor. The time difference, which is psuedo-range, is output to the microprocessor for determining the time transfer. The time interval counter is also used to determine the VCXO frequency for tuning control.

I/O TERMINAL

The receiver contains a CRT display with a keyboard and a dual flexible disc drive recorder. Operator control of the receiver is through keyboard inputs. The time transfer results are displayed on the CRT and recorded on the flexible disc.

MICROPROCESSOR

The microprocessor controls hardware functions in the receiver, decodes the navigation message, and calculates the time transfer. Receiver tuning is provided during acquisition by taking frequency measurements of the VCXO, comparing these measurments to predicted values and outputing corrections to the control voltage through a digital-to-analog converter.

The appropriate satellite C/A code is loaded into the code generator after being calculated using a linear feedback shift register algorithm implemented in the microprocessor. The code phase is also controlled by the microprocessor until a correlation or "code lock" is established in the RF subsystem. After signal acquisition, the microprocessor decodes the navigation data and commands pseudo-range measurements to be performed using the time interval counter to calculate the final time transfer result. This result is output to the CRT display and recorded on a flexible disc once every six seconds.

TIME TRANSFER FIELD TEST

The prototype GPS TTR was installed and tested at NASA's Merrit Island tracking site (MILA) at Kennedy Spaceflight Center, Fla.

Figure 11 shows the horizon of the MILA facility and the portion of the orbit of NAVSTAR 5 in view at the MILA site. Figure 12 shows the orbits of all five NAVSTAR satellites along with approximate rise and set times for the period during which the tests were performed. Most of the data was taken during a segment of time when all the satellites passed through a high elevation angle (60° to 90°) with approximately the same azimuth. Figure 13 shows the segments of each orbit where the data collection was concentrated. Figures 14 through 18 present the clock difference between the MILA station ground clock and the GPS spacecraft clocks as determined from individual satellite passes observed during the test. On each graph a calculated time transfer is presented for an epoch close to the mid-time of the observed period. The RMS of a least squared data fit is also presented. The RMS of any one pass varies from 11 to 13 nanoseconds for a given satellite.

Figure 19 is an extended track (two hour) of a NAVSTAR 6 pass. NAVSTAR 1 has a quartz crystal oscillator, NAVSTAR 3 and 4 have rubidium oscillators, while NAVSTAR 5 and 6 have cesium oscillators.

Figure 20 shows the time transfer results taken through each satellite and referenced to USNO master clock over a seven day period. Figure 21 shows the same results as an equal weighted average of all satellites. Results from individual satellites appear to vary as much as several hundred nanoseconds. The most well-behaved data on a day-to-day basis is that obtained from NAVSTAR 5. Figure 22 shows a comparison

of the five satellite average results with measurements made through LORAN-C and with portable clock measurements referenced to the U.S. Naval Observatory Master Clock.

Even though, during Phase I of the GPS, no attempt is being made by the MCS to precisely synchronize the five NAVSTAR space vehicles (SV), the results of the GPS data taken on all SVs during this experiment compares to the portable clock data to within 200 nanoseconds. It is planned during Phase III to maintain SV synchronization to within 100 nanoseconds.

Improvements were made to the receiver as a result of this field test, and data has subsequently been taken at NRL. Figure 23 is a typical plot of data taken from NAVSTAR 4 over a period of 22 days. A fit to this data produces a 25 nanoseconds RMS over the observed time period.

SIRIO/LASSO TIME TRANSFER EXPERIMENT

Future activities include joint participation by GSFC, USNO, and NRL in the European Space Agency (ESA) SIRIO/LASSO time transfer experiment during 1982. The missions of SIRIO-2 are twofold; meteorological data dissemination and synchronization of intercontinental atomic clocks.

The aim of the LASSO experiment is to provide a repeatable near-real-time method for long-distance (intercontinental) clock synchronization with nanosecond accuracy at a reasonable cost. The pioneering aspects of this first experiment will provide the opportunity to compare

the international network of atomic clocks with the internationally adopted atomic time scale (TAI) and with each other. It will also have an impact on such practical applications as the tracking of deep space missions, the calibration of other time transfer techniques such as Very Long Baseline Interferometry (VLBI), Tracking Data Relay Satellite System (TDRSS), the Global Positioning System (GPS), and future generations of space navigation and telecommunciation systems.

SIRIO-2 will be launched during March of 1982 from Koarou, French Guiana in South America into a synchronous orbit at 25 degrees west longitude, just off the West Coast of Central Africa near Liberia (Figure 24). The satellite has a 2-year lifetime design and will remain in this position for about 9 months to permit time measurments between the United States (Goddard Space Flight Center referenced to the Naval Observatory) and major observatories and time keeping facilities in Europe--principally with the Bureau International de l'Heure (BIH) in Paris, France. SIRIO-2 will then be moved over Central Africa at 20 degrees east longitude and will remain there for meteorological data dissemination until the completion of its 2-year mission.

SPACECRAFT CHARACTERISTICS

The LASSO experiment is based on the use of laser ground stations firing monochromatic light pulses at predicted times directed toward the geosynchronous SIRIO spacecraft.

SIRIO-2 is a spin-stabilized geostationary satellite spun around an axis vertical to its orbital plane (Figure 25). The spacecraft

consists of a drum-shaped central body covered with solar cells. On top is mounted a mechanically despun S-Band (1689.6 MHz) antenna for support of the meteorological, timing missions, and housekeeping data. Omnidirectional antennas (VHF 136.14 MHz) serve for command, ranging and backup telemetry.

The LASSO payload is composed of retroreflectors, photodetectors (for sensing ruby and neodyme laser pulses), and a stable clock for time tagging arrival times of laser pulses.

LASSO EXPERIMENT GOALS

The goals of the LASSO experiment are as follows:

1. Verify that lasers can be used to perform a two-way time transfer from a geostationary satellite to within nanoseconds or sub-nanoseconds.
2. Determine the limations and problems of such a laser time transfer technique.
3. Verify the accuracy of other techniques, such as the Global Positioning System (GPS) time transfer technique, using receivers being developed for use in the Mobile Laser Network.

FUTURE PLANS

Increased receiver performance and capabilities development is continuing based on results and operational feedback from field tests and on-going experiments. Extensive evaluation of the receiver

is planned through several additional field tests. A joint experiment is scheduled with the Jet Propulsion Laboratory (JPL), to evaluate ionospheric delay error. Co-location tests are planned to compare nanosecond accuracy VLBI data with GPS TTR data. The co-location tests will involve VLBI stations at NRL Maryland Point, Haystack/ Westford Observatory, NASA Deep Space Network (DSN), Goldstone, CA., and NASA DSN, Madrid, Spain. Analysis will also be performed from the data obtained during the SERIO/LASSO experiment.

The first operational field test of the GPS TTR is scheduled in the second quarter of fiscal year (FY) 1982 with the deployment of the NASA GSFC Transportable Laser Ranging System (TLRS) prototype to Easter Island. Four additional receivers are scheduled to be deployed with mobile laser systems later in FY 1982.

REFERENCES

1. L. Raymond, O. J. Oaks, J. Osborne, G. Whitworth, J. Buisson, P. Landis, C. Wardrip, and J. Perry, "Navigation Technology Satellite (NTS) Low Cost Timing Receiver," Goddard Space Flight Center Report X-814-77-205, Aug. 1977.

2. J. A. Buisson, T. B. McCaskill and O. J. Oaks, "Initial Design for Navigation Technology Satellite Time Transfer Receiver (NTS/TTR)," NRL Report 8312, 16 May 1979.

3. J. Buisson, T. McCaskill, J. Oaks, D. Lynch, C. Wardrip, and G. Whitworth, "Submicrosecond Comparisons of Time Standards via the Navigation Technology Satellites (NTS)," Proc. PTTI, Nov. 1978, pp 601-627.

4. B. W. Parkinson, "NAVSTAR Global Positioning System (GPS)," National Telecommunications Conference, Conference Record, Vol. iii, 1976, pp 41.1-1 to 41.1-5.

5. J. A. Buisson, R. L. Easton, and T. B. McCaskill, "Initial Results of the NAVSTAR GPS NTS-2 Satellite," NRL Report 8232, May 25, 1978.

6. R. L. Easton, J. A. Buisson, T. B. McCaskill, O. J. Oaks, S. Stebbins, and M. Jeffries, "The Contribution of Navigation Technology Satellites to the Global Positioning System," NRL Report 8360, Dec. 28, 1979.

7. J. A. Buisson and T. B. McCaskill, "TIMATION Navigation Satellite System Constellation Study," NRL Report 7389, June 27, 1972.

8. S. S. Russel and J. H. Schaibly, "Control Segment and User Performance," J. Inst. Navigation 25(2), Summer 1978, pp. 166-172.

9. J. J. Spilker, "GPS Signal Structure and Performance Characteristics," J. Inst. Navigation, 25(2), Summer 1978, pp. 121-146.

10. A. Dierendock, S. Russell, E. Kipitzke, and M. Birnbaum, "The GPS Navigation Message", J. Inst. Navigation, 25(2), Summer 1978, pp. 147-165.

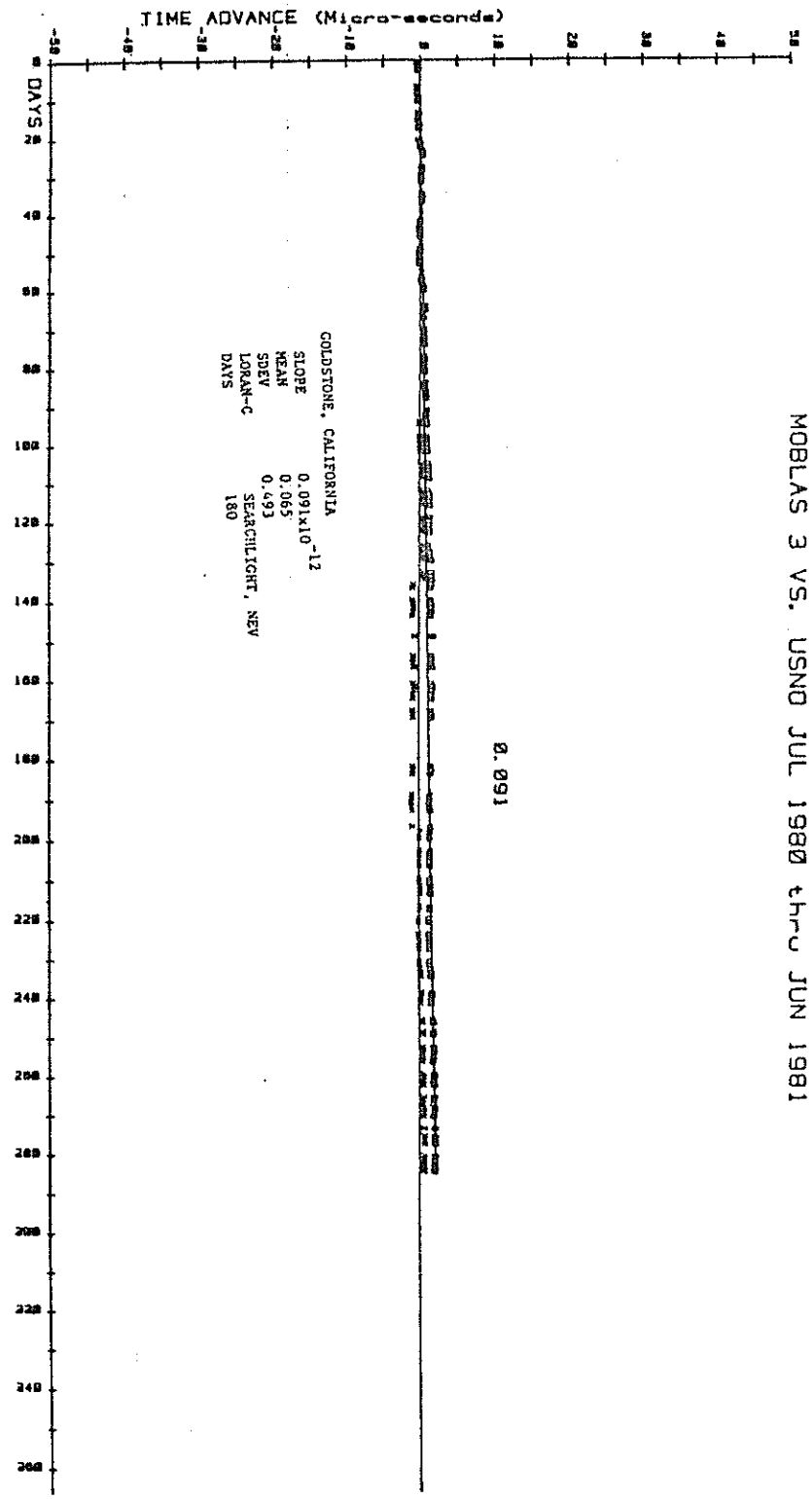
TIME ADVANCE (Micro-seconds)
DAYS
GOLDSTONE, CALIFORNIA
SLOPE 0.091x10-12
MEAN 0.065
SDEV 0.491
LORAN-C SEARCHLIGHT, NEV
DAYS 180
0.091
MOBLAS 3 VS. USNO JUL 1980 thru JUN 1981

Figure 1

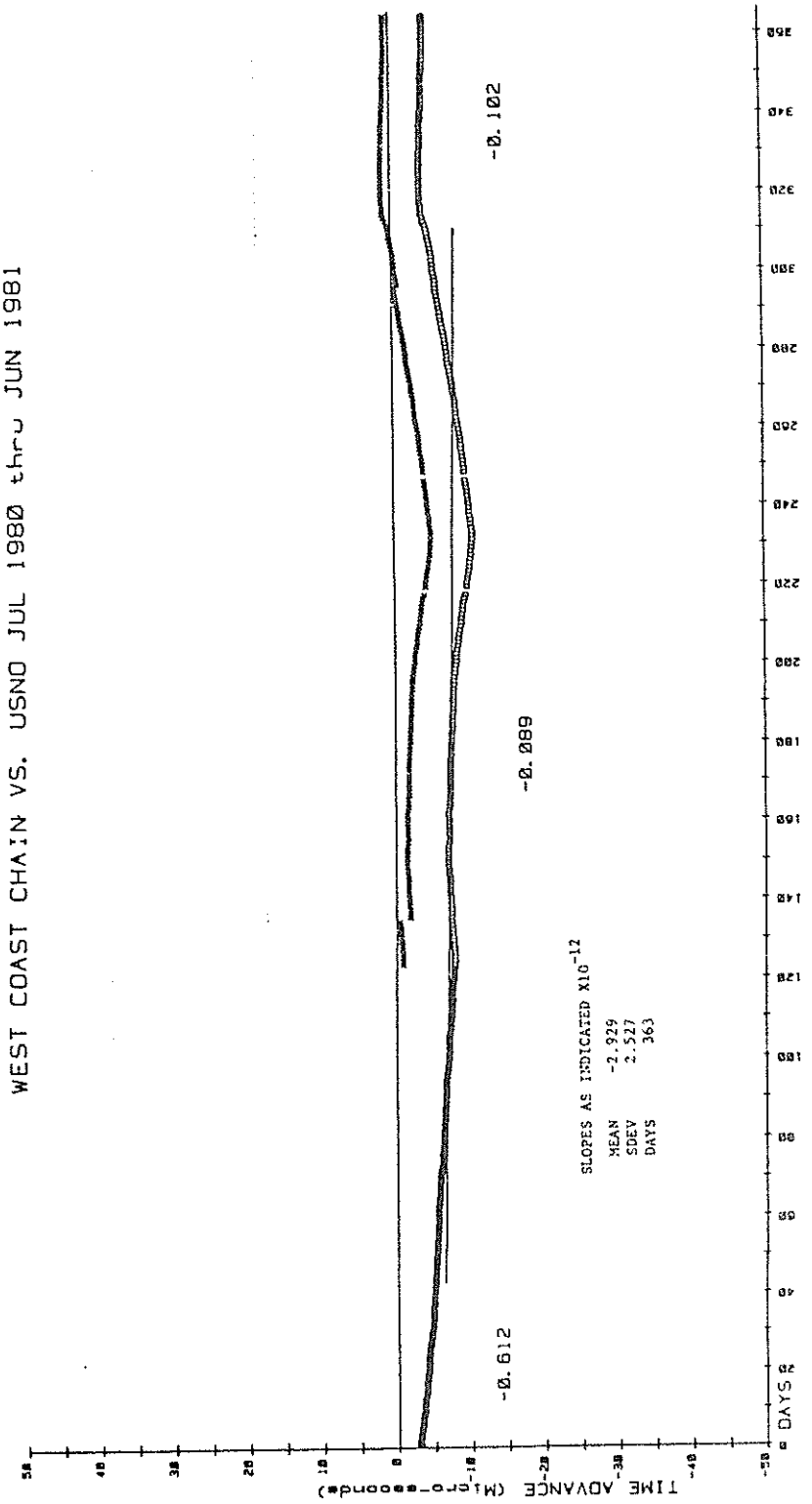
WEST COAST CHAIN VS. USNO JUL 1980 thru JUN 1981
TIME ADVANCE (Micro-seconds)
DAYS
-0.102
-0.089
-0.612
SLOPES AS INDICATED X10-12
MEAN -2.929
SDEV 2.527
DAYS 363

Figure 2

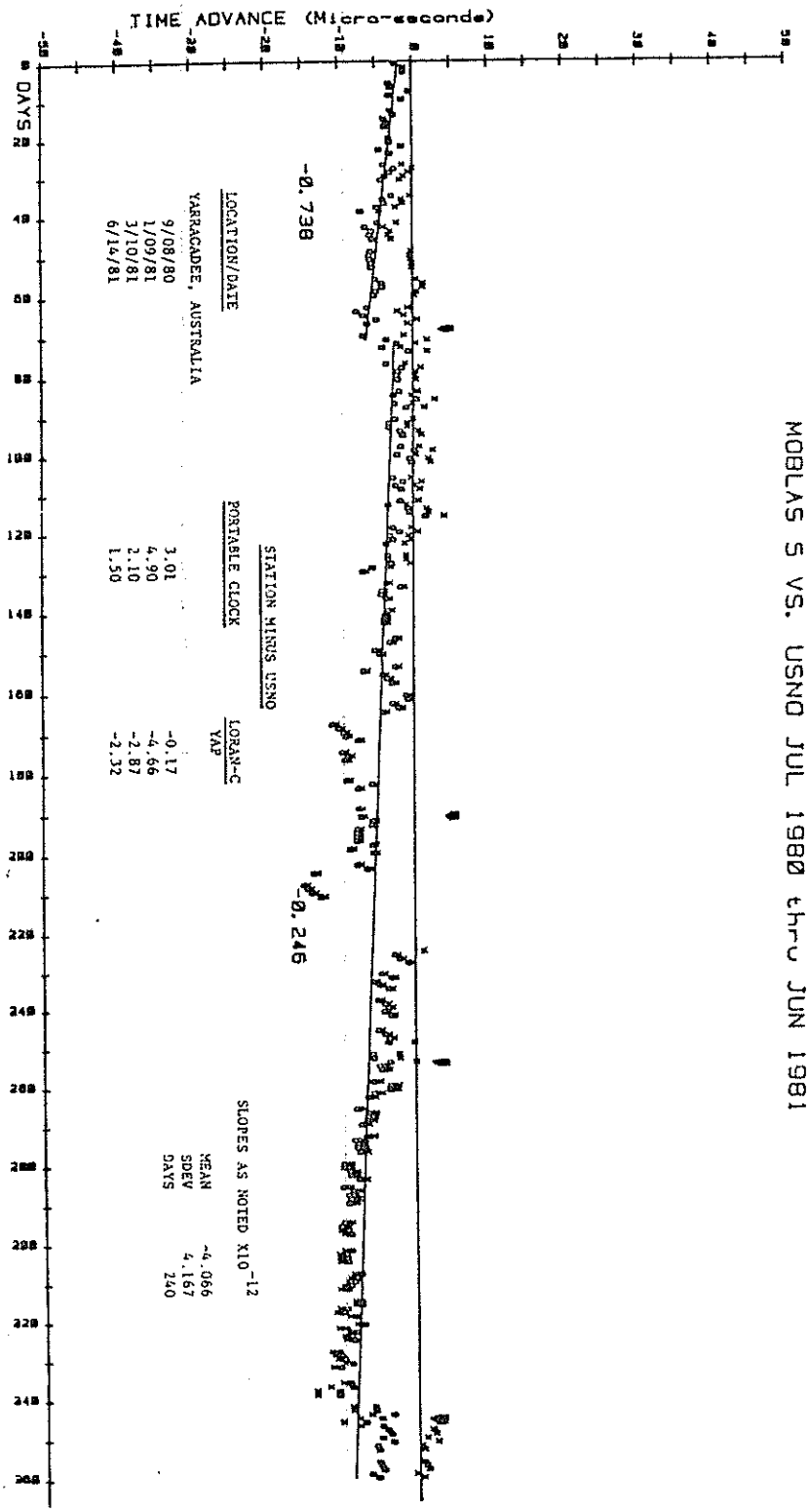
TIME ADVANCE (Micro-seconds)
DAYS
MOBLAS 5 VS. USNO JUL 1980 thru JUN 1981
-0.738
-0.246
STATION MINUS USNO
LOCATION/DATE
PORTABLE CLOCK
LORAN-C
YAP
YARRAGADEE, AUSTRALIA
9/08/80
1/09/81
3/10/81
6/14/81
3.01
4.90
2.10
1.50
-0.17
-4.66
-2.87
-2.32
SLOPES AS NOTED X10-12
MEAN -4.066
SDEV 4.167
DAYS 240

Figure 3

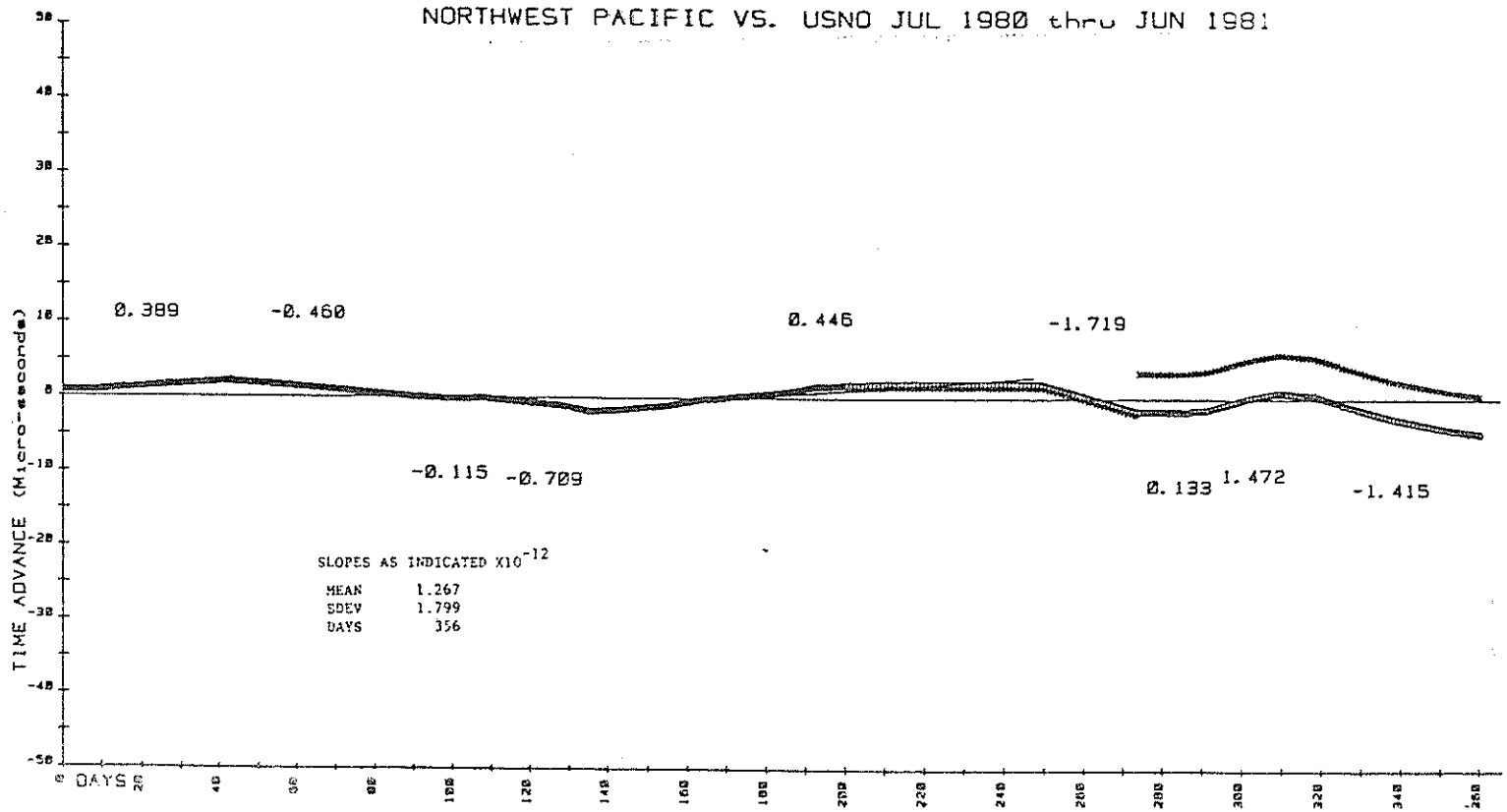
NORTHWEST PACIFIC VS. USNO JUL 1980 thru JUN 1981
TIME ADVANCE (Micro-seconds)
DAYS
0.389
-0.460
0.446
-1.719
-0.115
-0.709
0.133
1.472
-1.415
SLOPES AS INDICATED X10^-12
MEAN 1.267
SDEV 1.799
DAYS 356

Figure 4

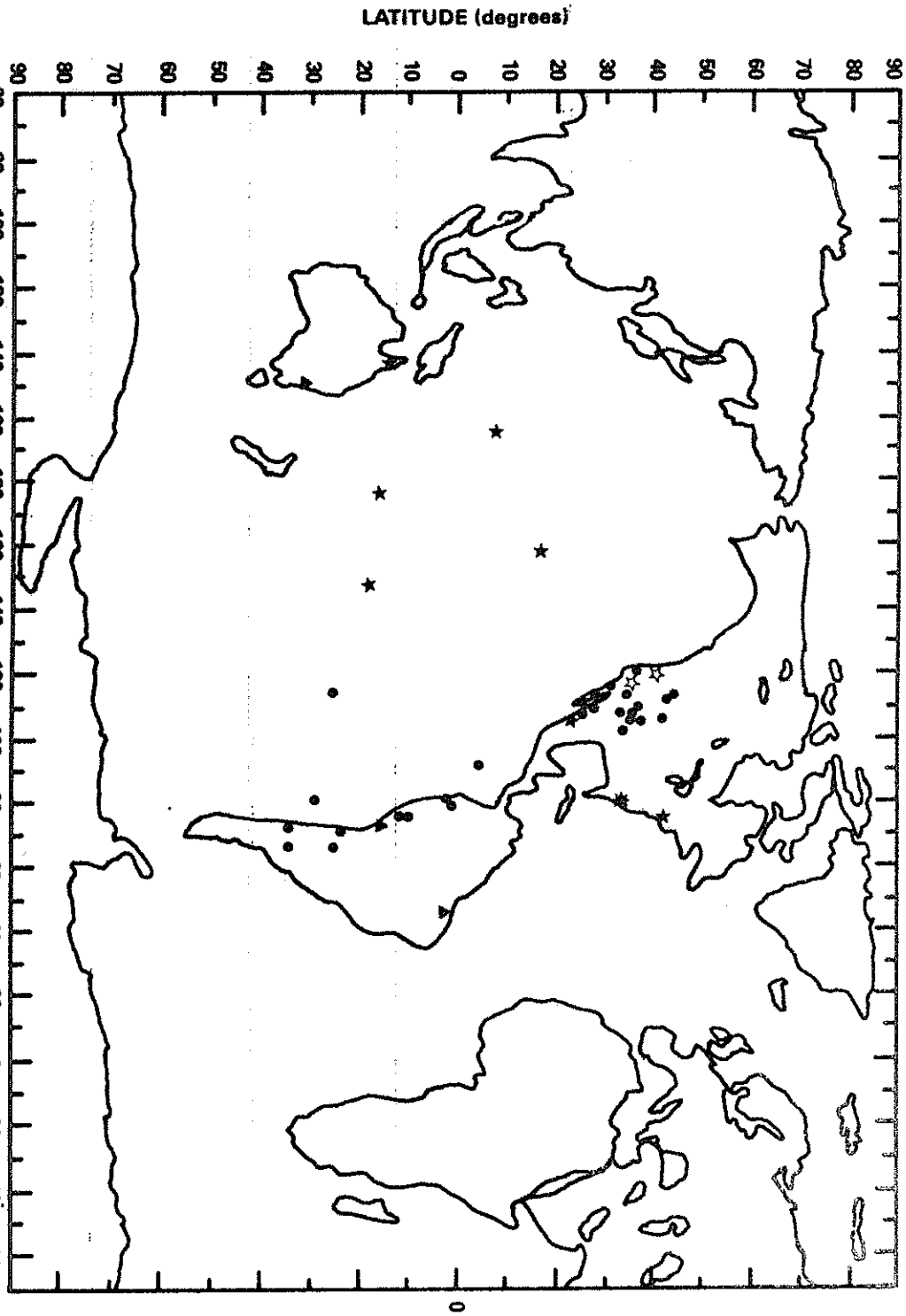
NASA-GSFC LASER TRACKING SITES 1980 - 1986
LATITUDE (degrees)
WEST LONGITUDE (degrees)
* STALAS
★ MOBLAS
● TLRS
☆ MOBLAS/TLRS
▲ SAO

Figure 5

TENTATIVE LASER DEPLOYMENT SCHEDULE

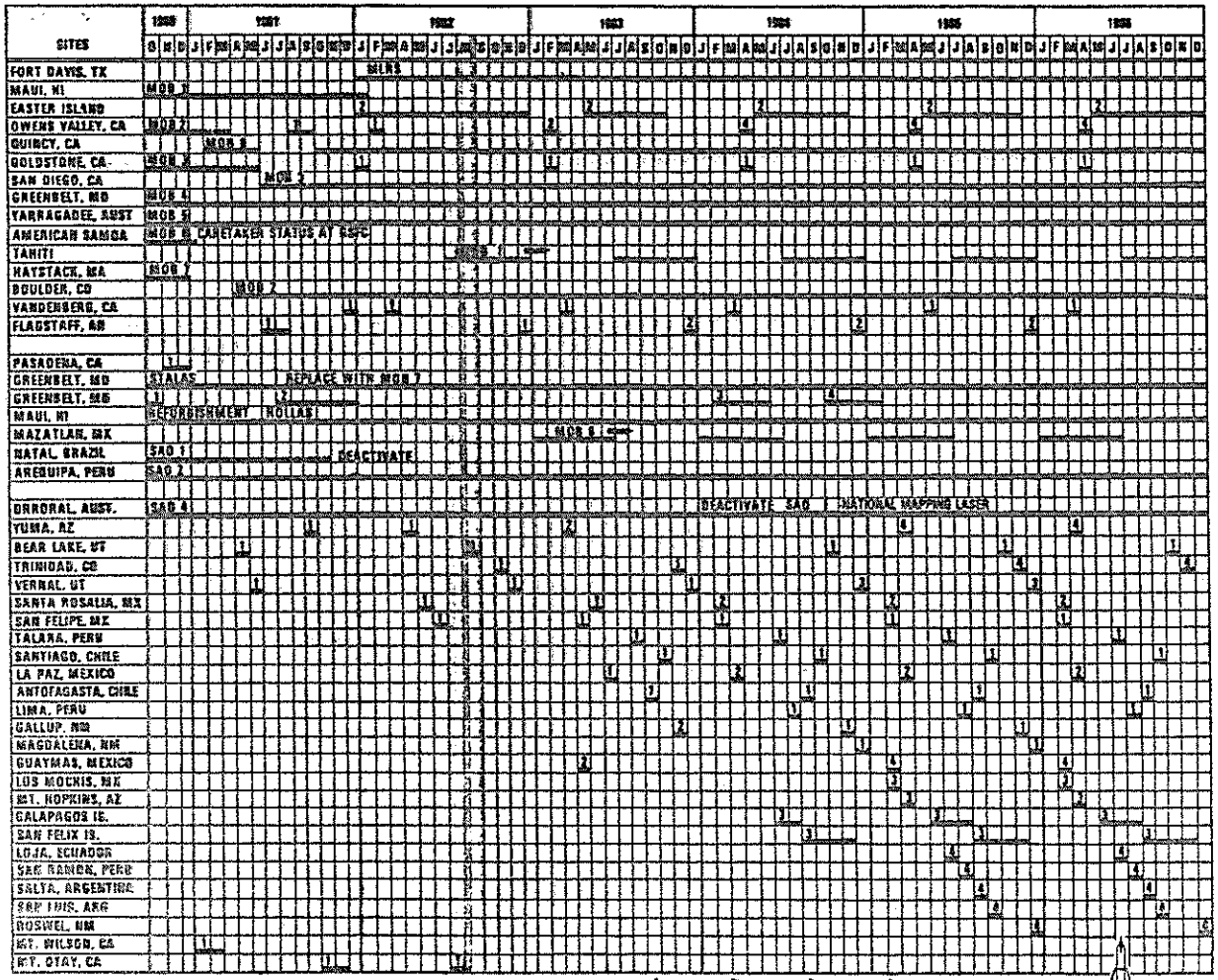

LASER NETWORK MANAGER

LASER PROJECT MANAGER

CRUSTAL DYNAMICS PROJECT MANAGER

Figure 6

NAVSTAR GPS
STATION SYNCHRONIZATION
BY
TIME TRANSFER

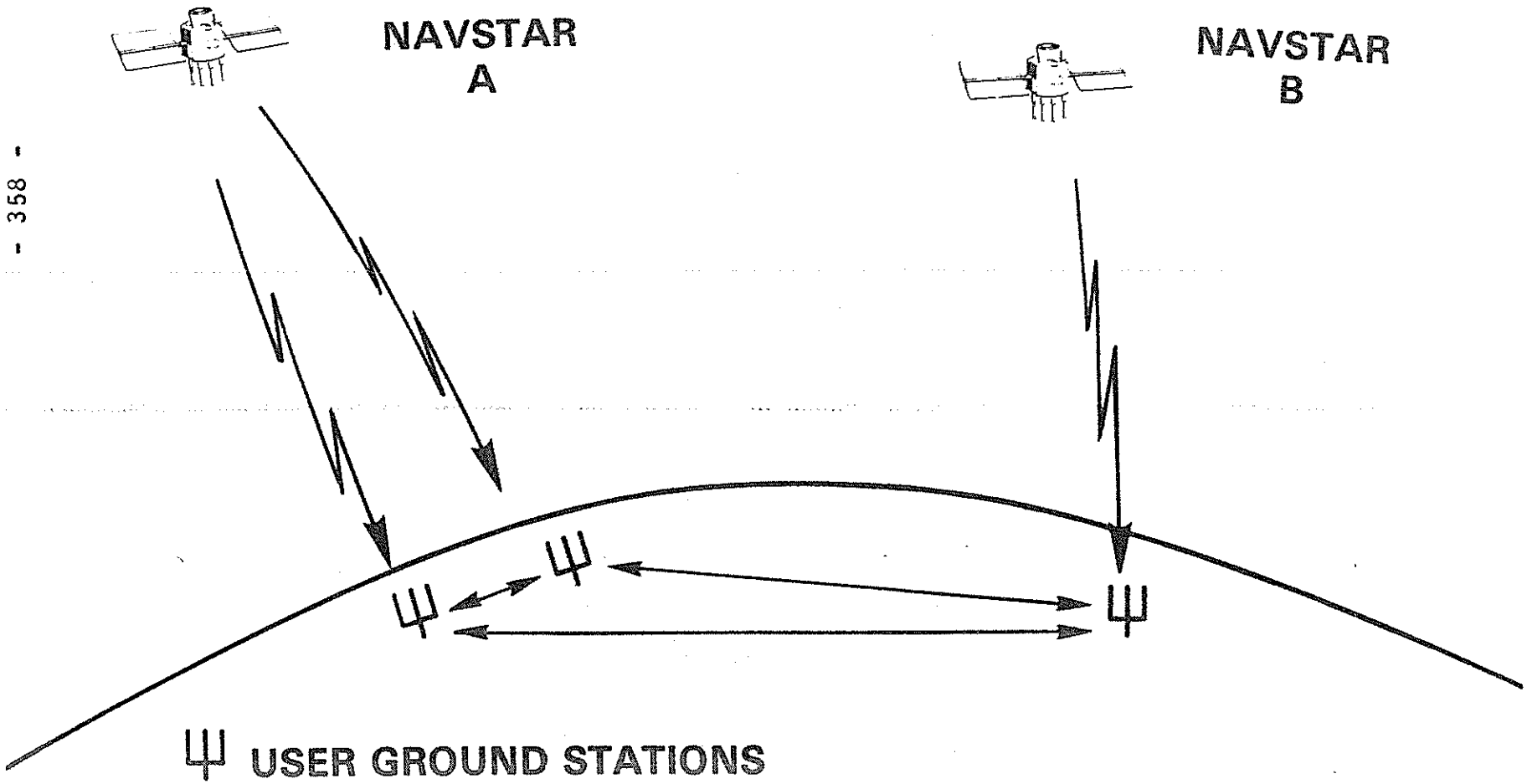

NAVSTAR

Global Positioning System

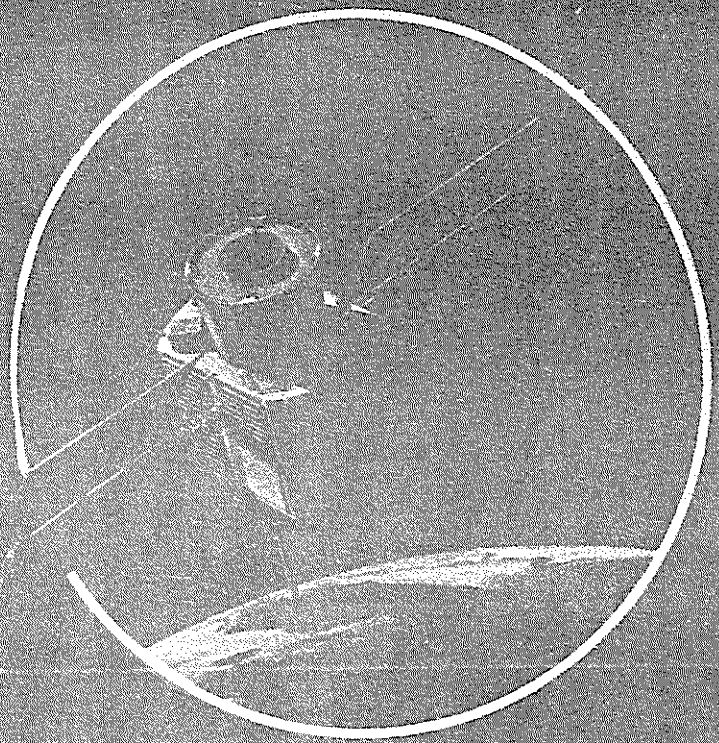

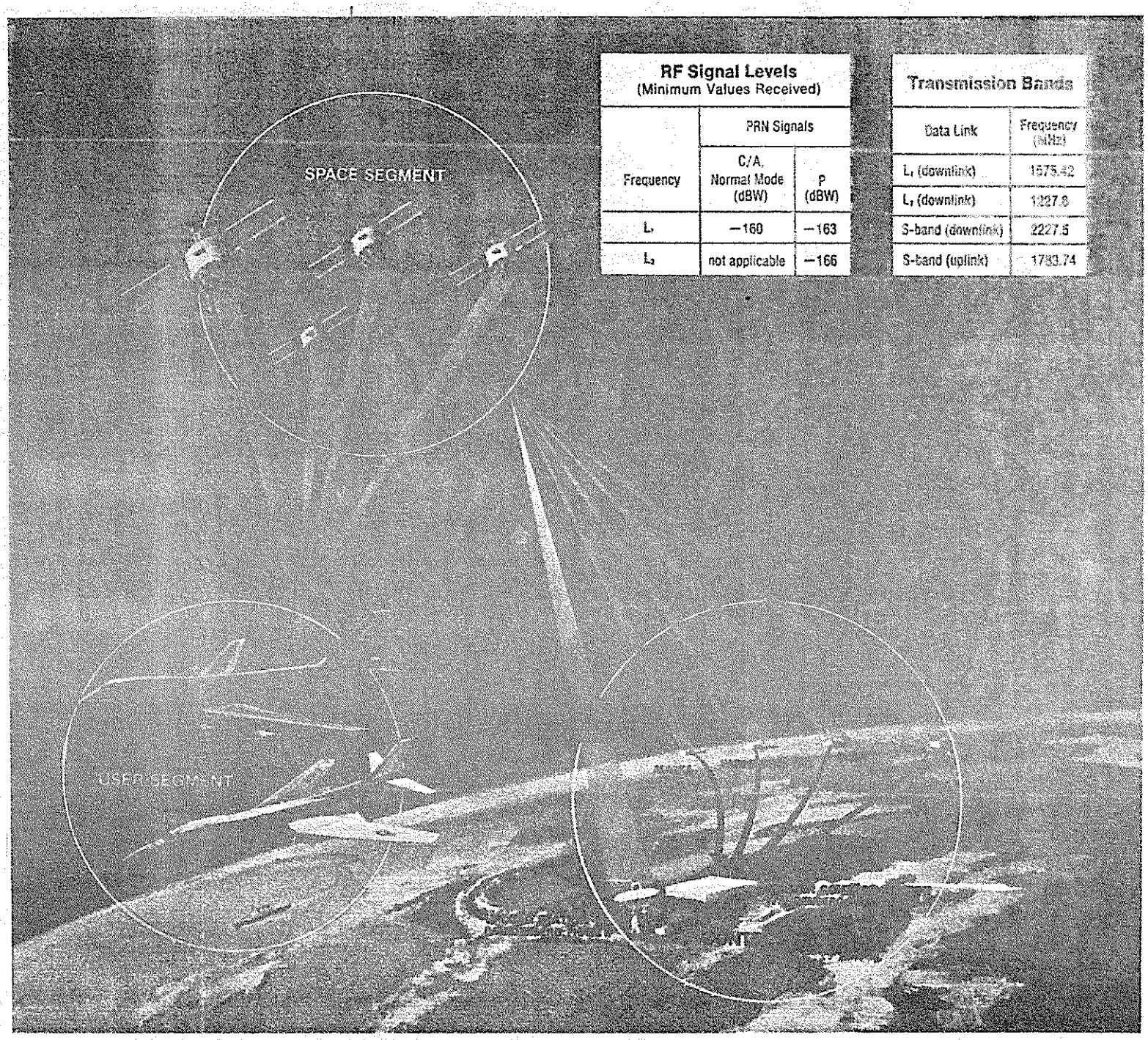

RF Signal Levels
(Minimum Values Received)

Frequency	PRN Signals	
	C/A, Normal Mode (dBW)	P (dBW)
L_1	−160	−163
L_2	not applicable	−166

Transmission Bands

Data Link	Frequency (MHz)
L_1 (downlink)	1575.42
L_2 (downlink)	1227.6
S-band (downlink)	2227.5
S-band (uplink)	1783.74

Figure 9

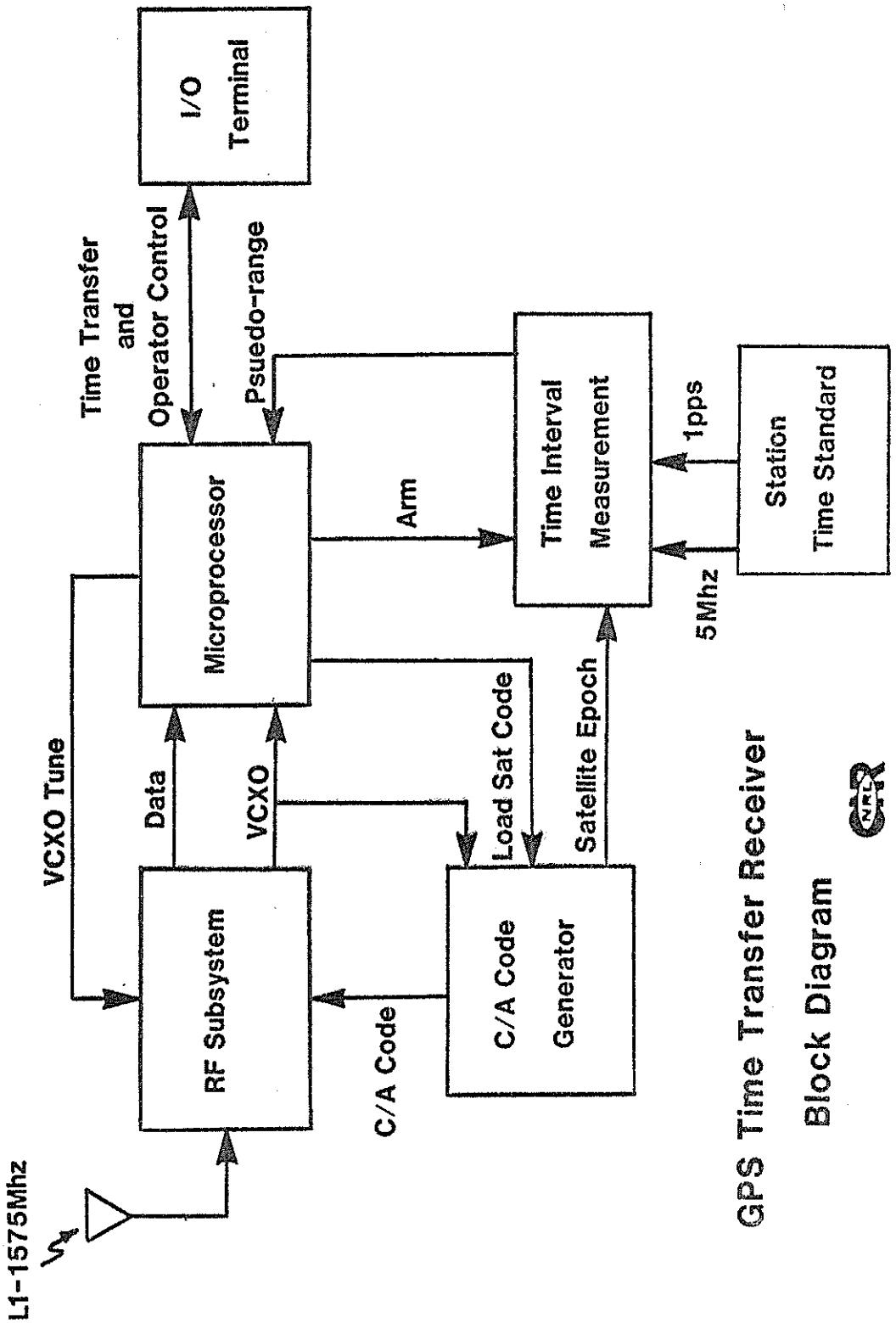
I/O Terminal
Time Transfer and Operator Control
Psuedo-range
Microprocessor
Arm
Time Interval Measurement
1pps
Station Time Standard
5Mhz
VCXO Tune
Data
VCXO
Load Sat Code
Satellite Epoch
RF Subsystem
C/A Code Generator
C/A Code
L1-1575Mhz
GPS Time Transfer Receiver
Block Diagram
NRL

Figure 10

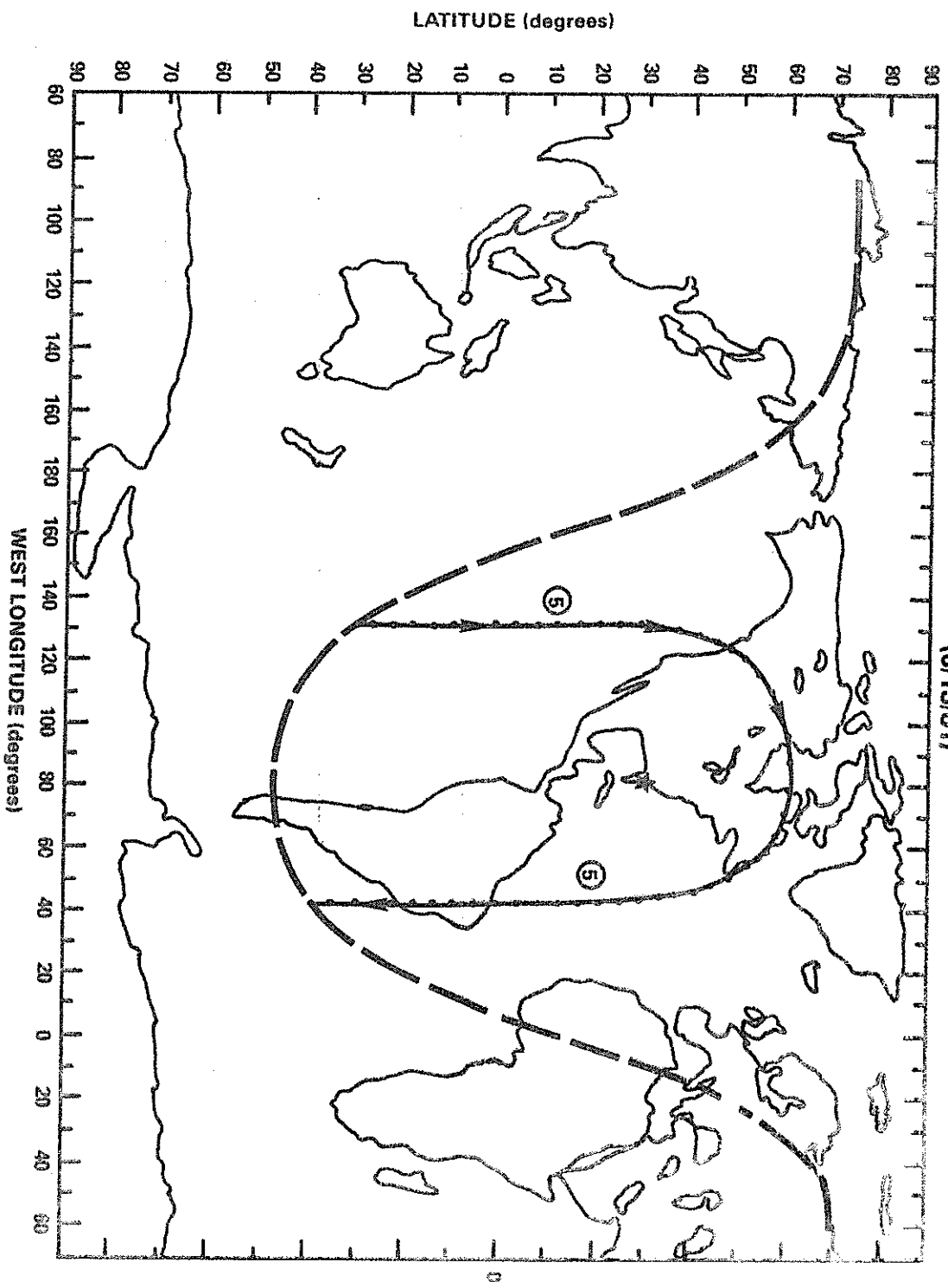
GPS NAVSTAR
MILA
GROUND TRACK
(6/15/81)
LATITUDE (degrees)
WEST LONGITUDE (degrees)
5
5

Figure 11

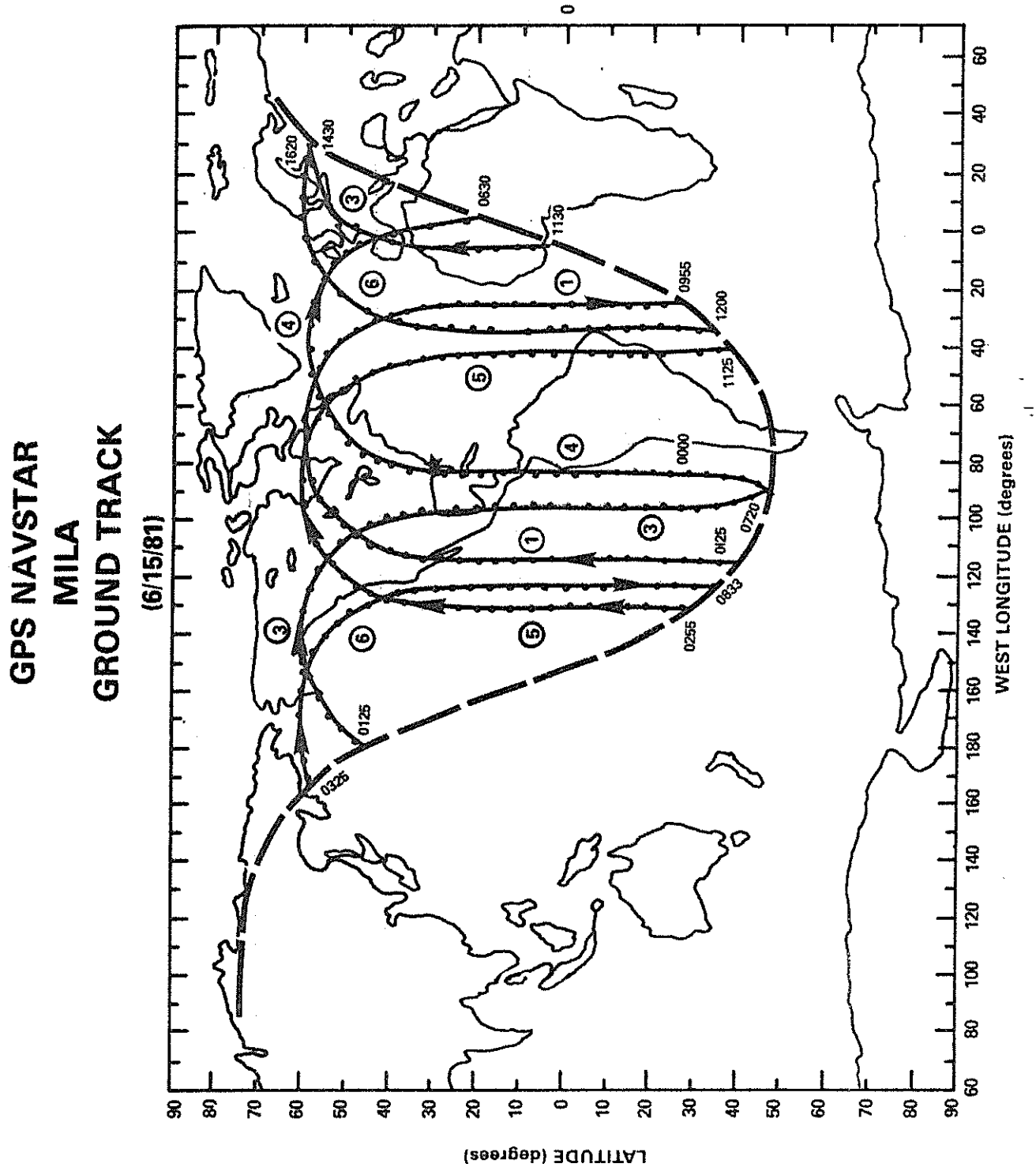
GPS NAVSTAR
MILA
GROUND TRACK
(6/15/81)
LATITUDE (degrees)
WEST LONGITUDE (degrees)
0
1620
1430
0630
1130
0955
1200
1125
0000
0720
0125
0833
0255
0125
0325

Figure 12

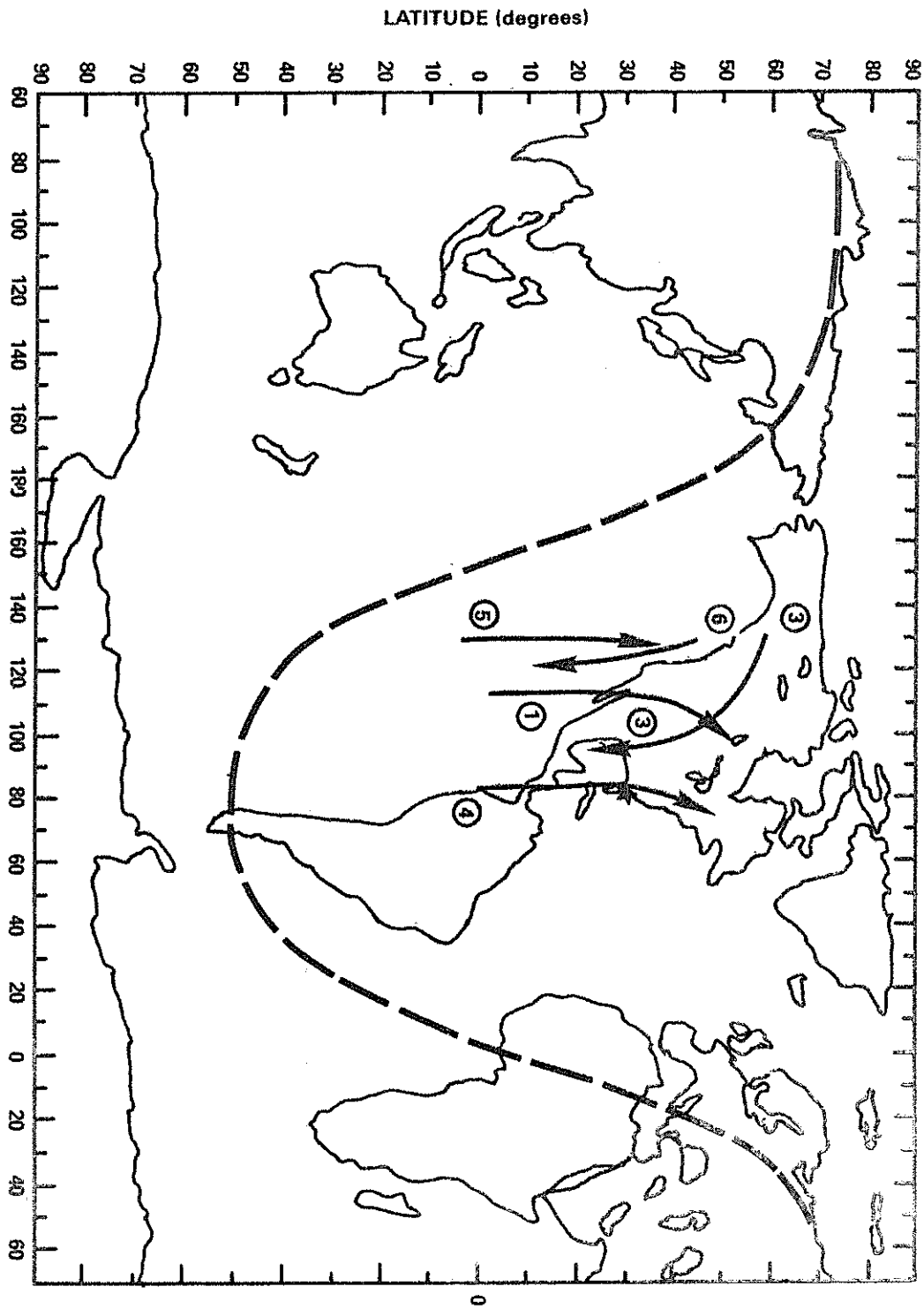
GPS NAVSTAR
MILA
GROUND TRACK
(6/15/81)
LATITUDE (degrees)
WEST LONGITUDE (degrees)
90 80 70 60 50 40 30 20 10 0 10 20 30 40 50 60 70 80 90
60 80 100 120 140 160 180 160 140 120 100 80 60 40 20 0 20 40 60
0
1
2
3
4
5
6

Figure 13

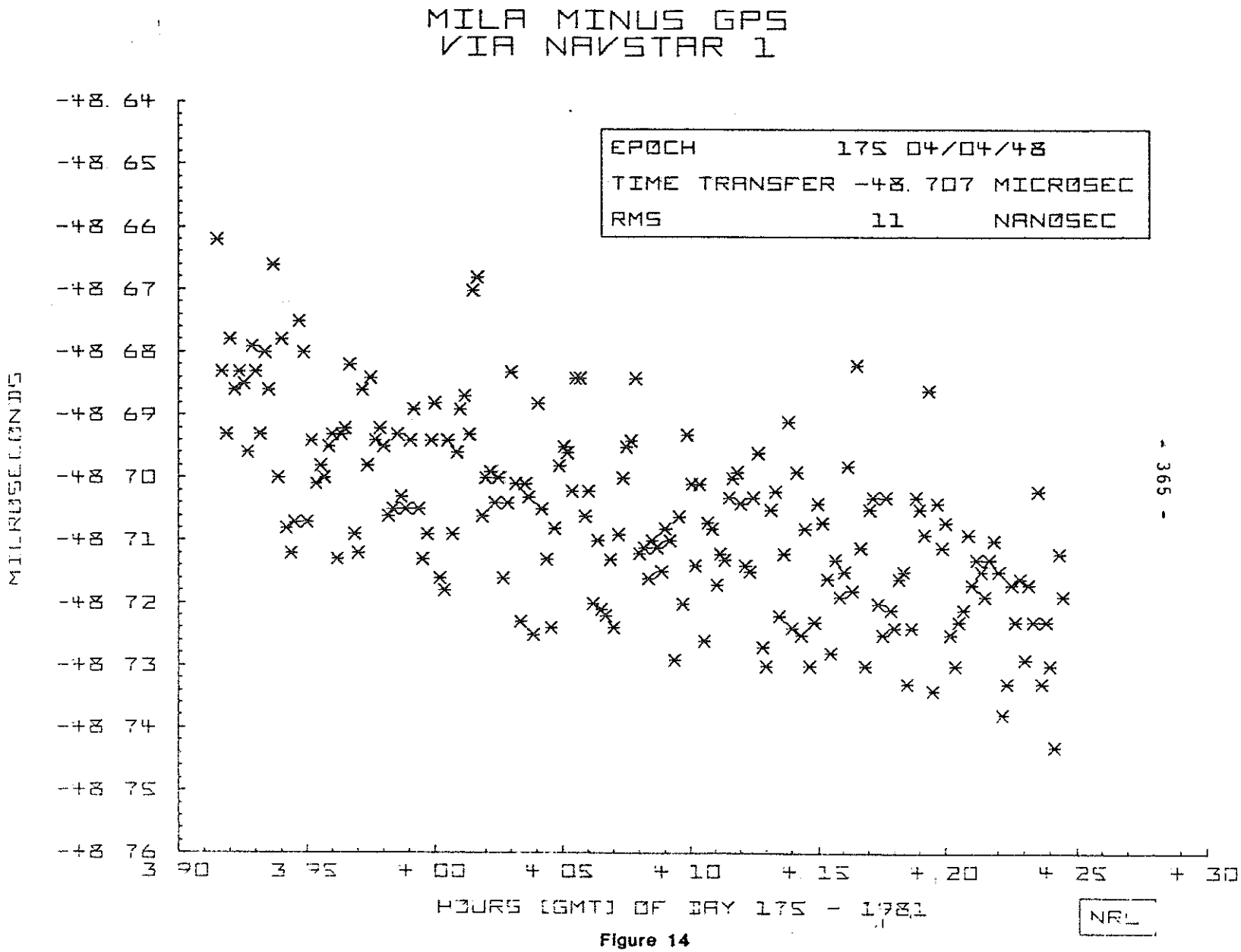

Figure 14

- 365 -

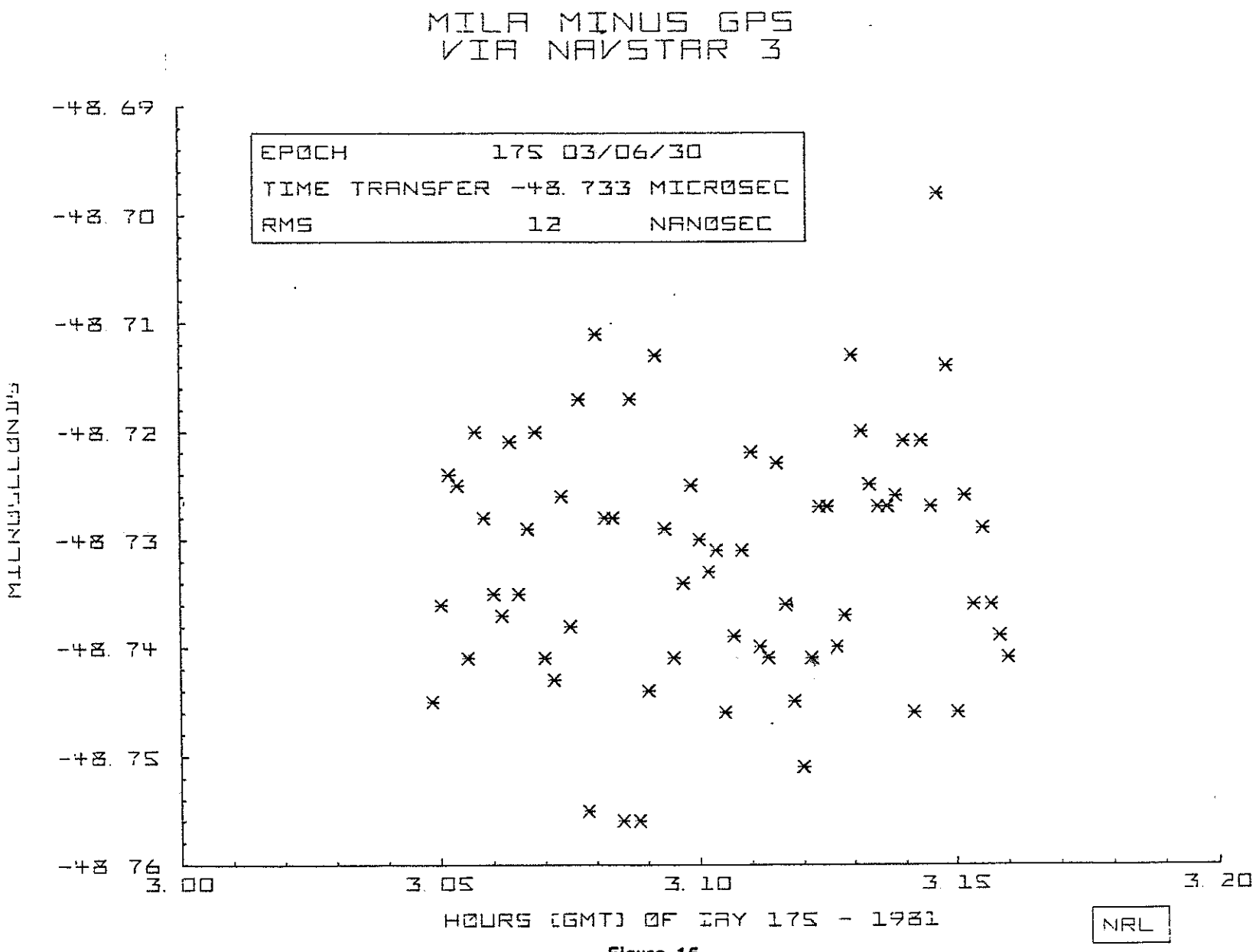
MILA MINUS GPS
VIA NAVSTAR 3
EPOCH 175 03/06/30
TIME TRANSFER -48.733 MICROSEC
RMS 12 NANOSEC
-48.69
-48.70
-48.71
-48.72
-48.73
-48.74
-48.75
-48.76
MICROSECONDS
3.00
3.05
3.10
3.15
3.20
HOURS (GMT) OF DAY 175 - 1981
NRL

Figure 15

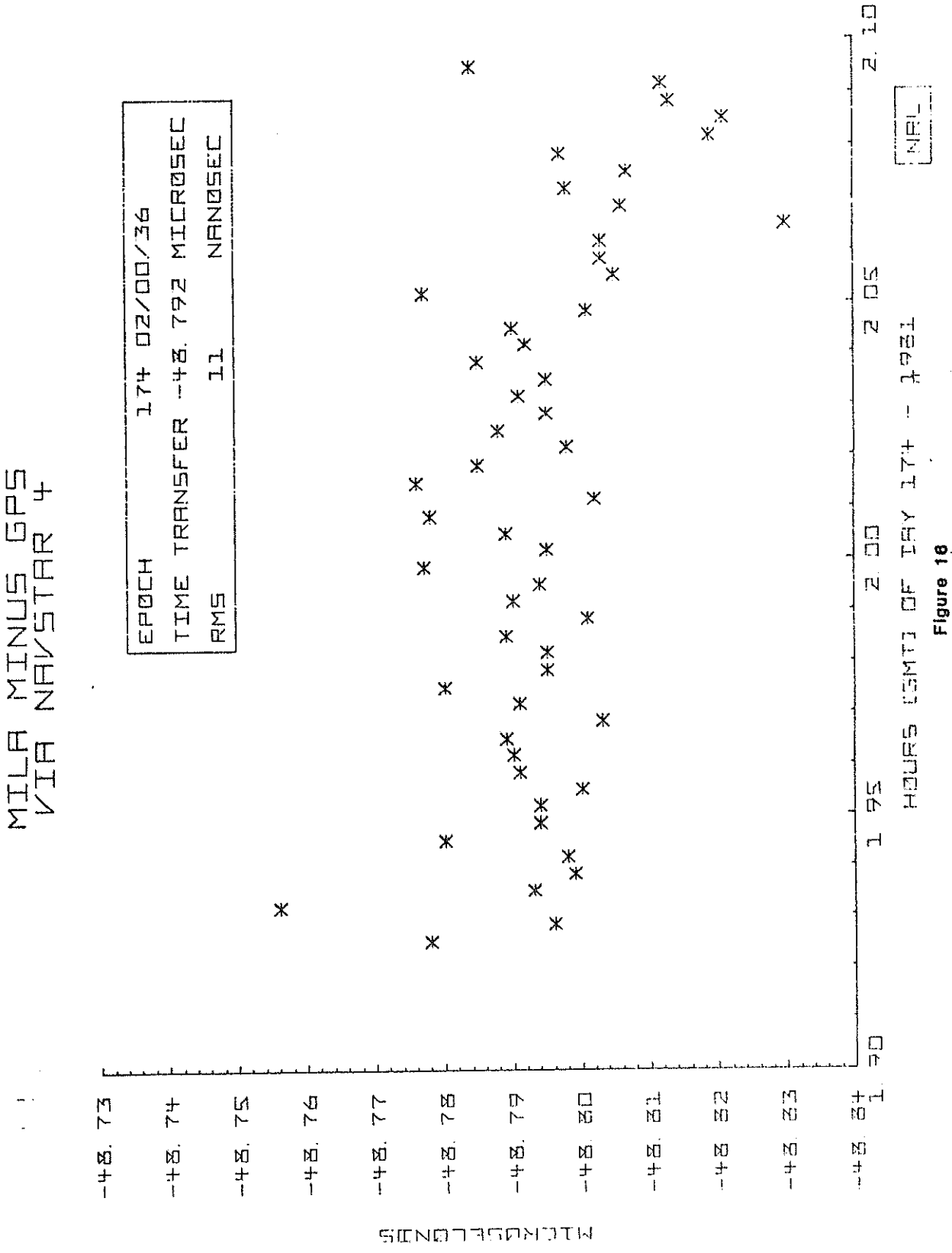
MILA MINUS GPS
VIA NAVSTAR 4
EPOCH 174 02/00/36
TIME TRANSFER -48.792 MICROSEC
RMS 11 NANOSEC
MICROSECONDS
-48.73
-48.74
-48.75
-48.76
-48.77
-48.78
-48.79
-48.80
-48.81
-48.82
-48.83
-48.84
0
1.95
2.00
2.05
2.10
HOURS GMT OF DAY 174 - 1981
NRL

Figure 16

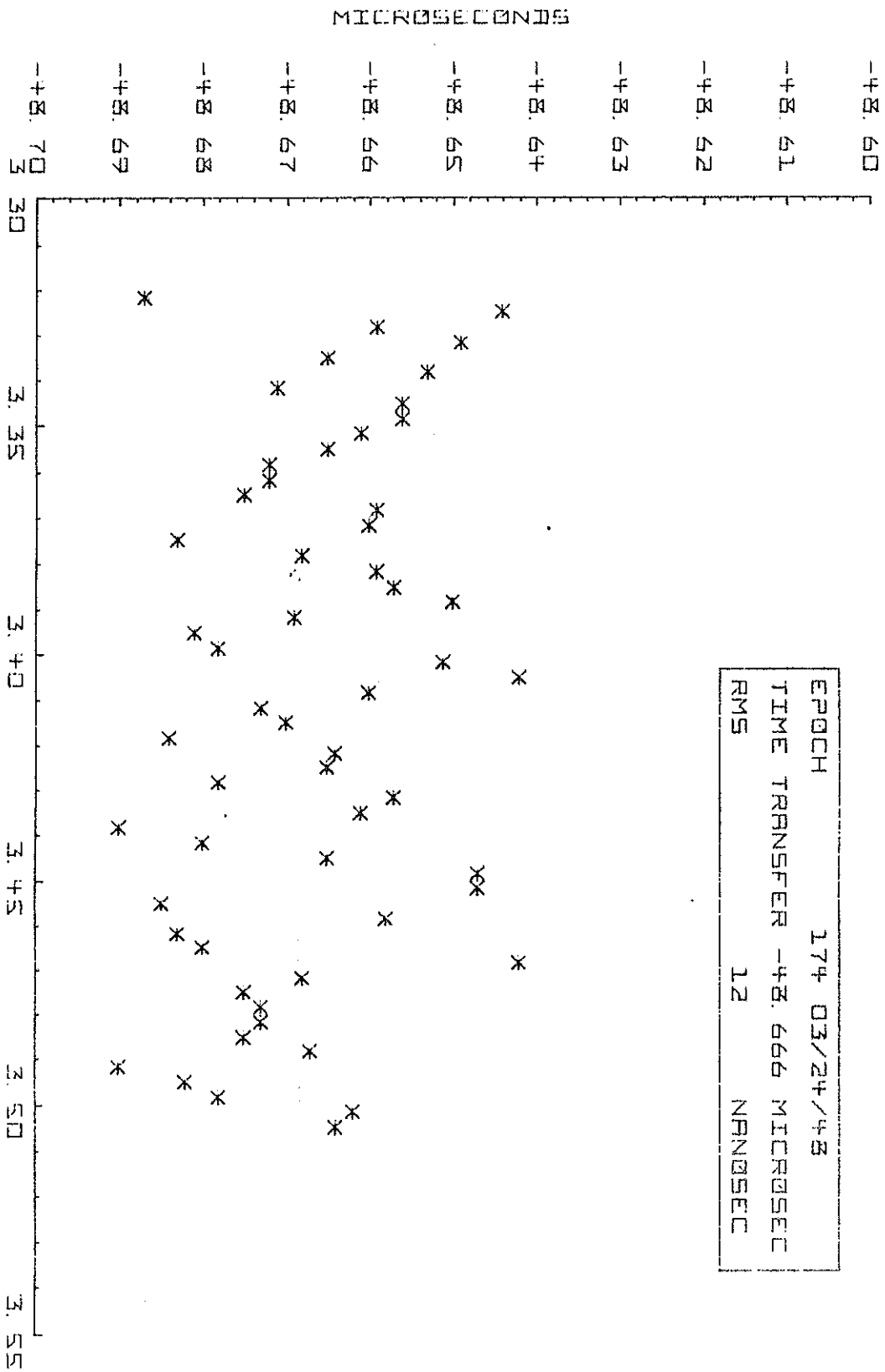
MILA MINUS GPS
VIA NAVSTAR 5
EPOCH 174 03/24/43
TIME TRANSFER -43.666 MICROSEC
RMS 12 NANOSEC
MICROSECONDS
-43.60
-43.61
-43.62
-43.63
-43.64
-43.65
-43.66
-43.67
-43.68
-43.69
-43.70
3.30
3.35
3.40
3.45
3.50
3.55
HOURS GMT OF DAY 174 - 1981
NRL

Figure 17

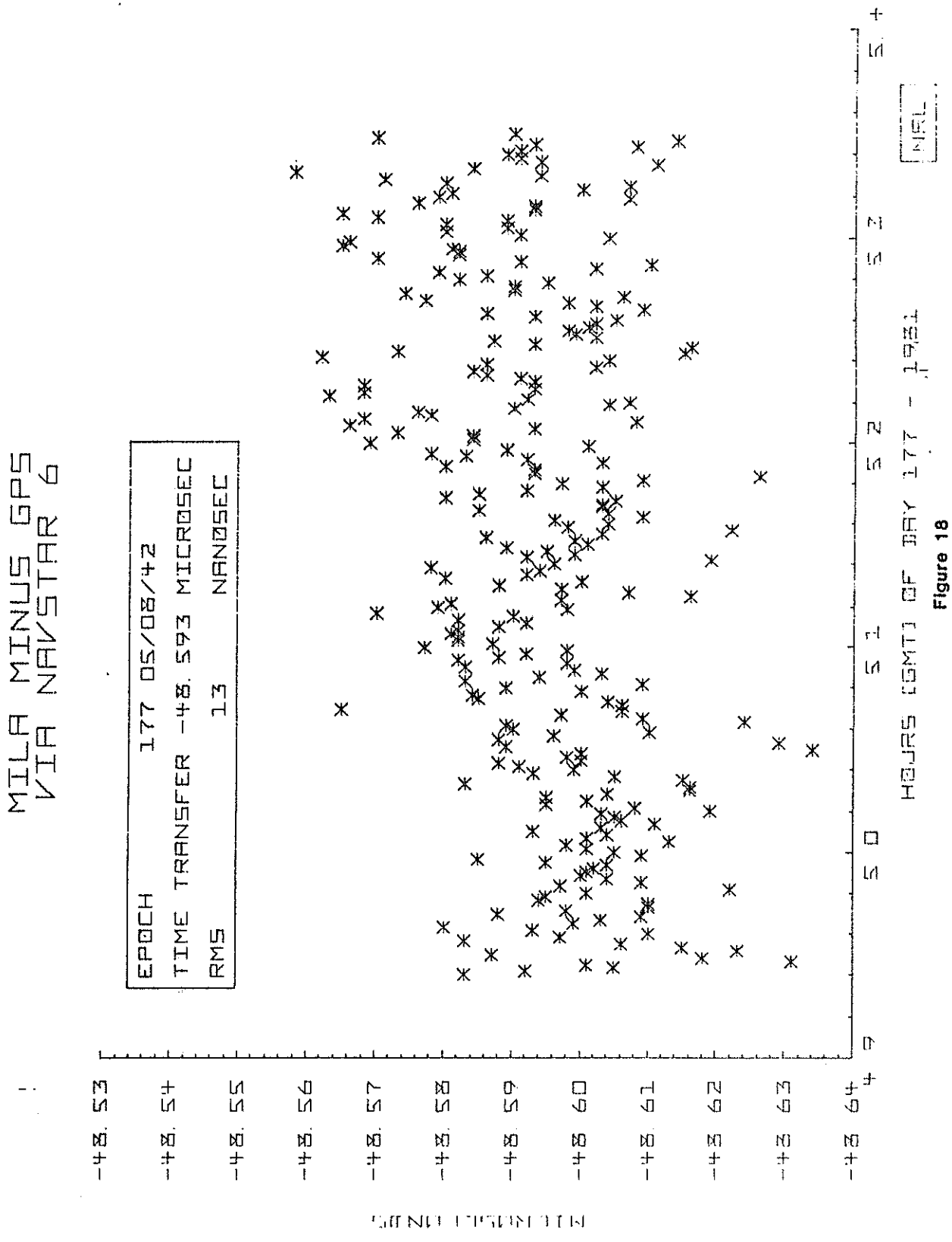
MILA MINUS GPS
VIA NAVSTAR 6
EPOCH 177 05/08/42
TIME TRANSFER -48.593 MICROSEC
RMS 13 NANOSEC
HOURS GMT OF DAY 177 - 1981
NBS

Figure 18

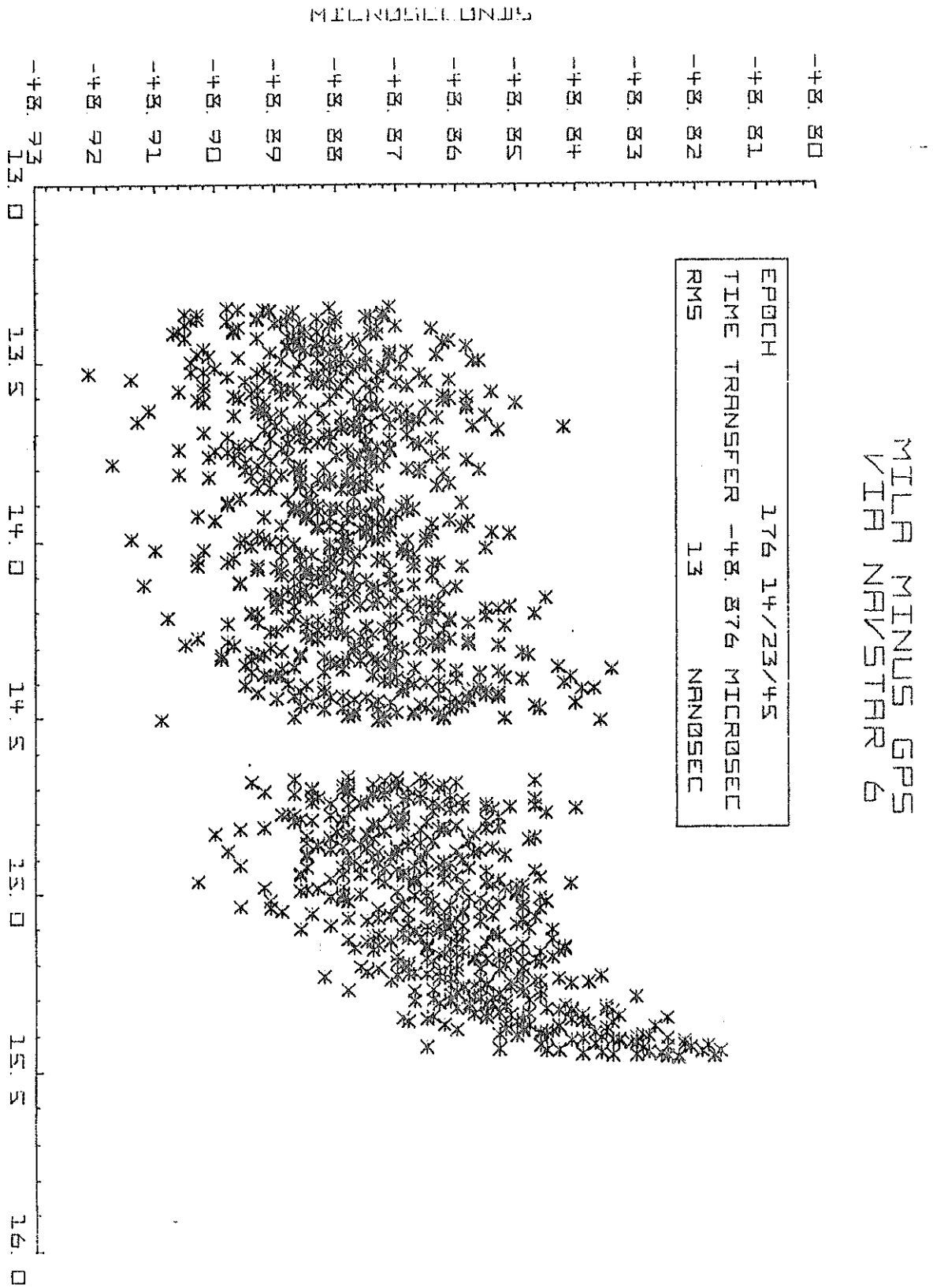
MILA MINUS GPS
VIA NAVSTAR 6
EPOCH 176 14/23/45
TIME TRANSFER -48.876 MICROSEC
RMS 13 NANOSEC
MICROSECONDS
-48.80
-48.81
-48.82
-48.83
-48.84
-48.85
-48.86
-48.87
-48.88
-48.89
-48.90
-48.91
-48.92
13.0
13.5
14.0
14.5
15.0
15.5
16.0
HOURS (GMT) OF DAY 176 - 1985
NRL

Figure 19

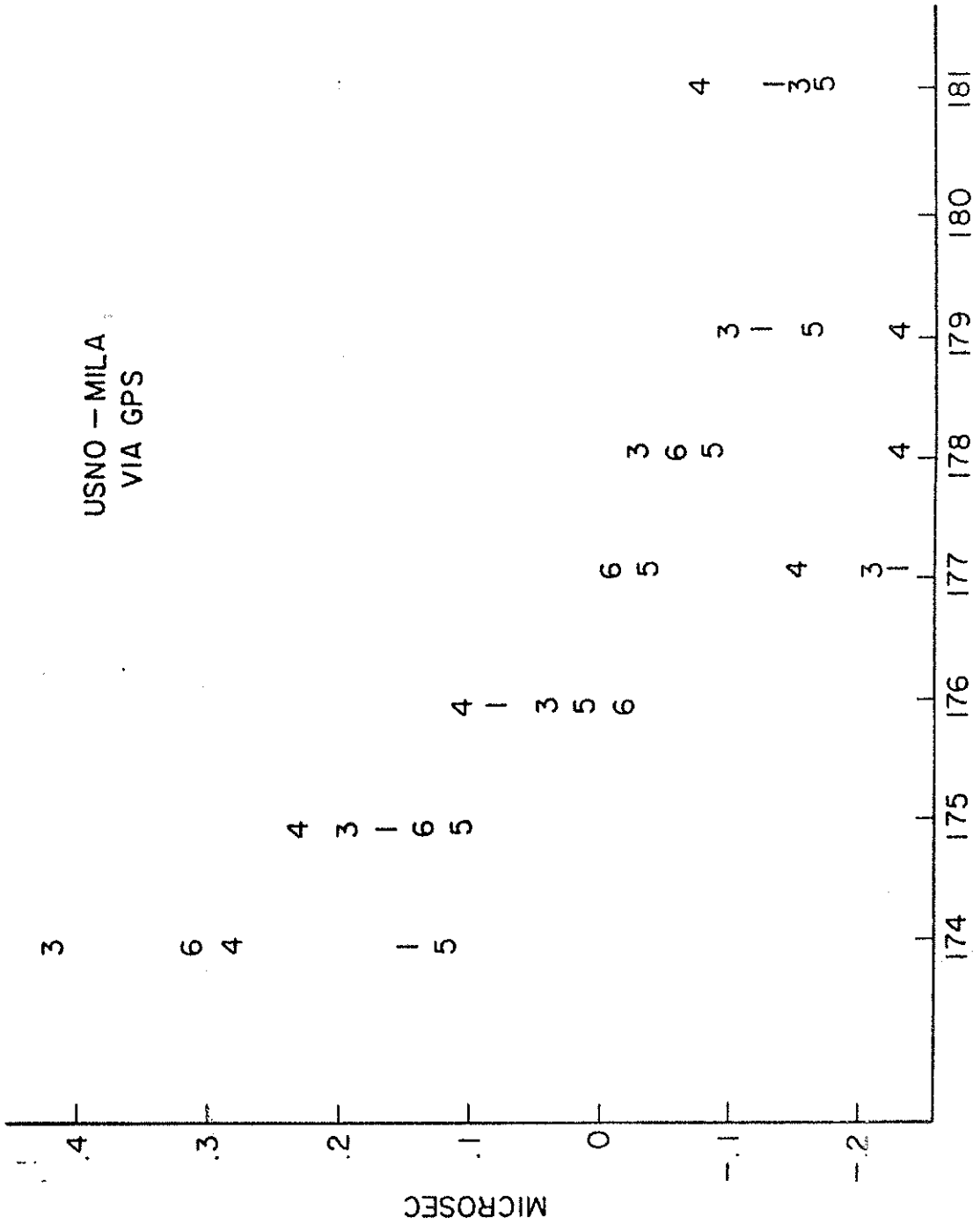
USNO – MILA
VIA GPS
MICROSEC
.4
.3
.2
.1
0
-.1
-.2
174
175
176
177
178
179
180
181
DAY (1981)

Figure 20

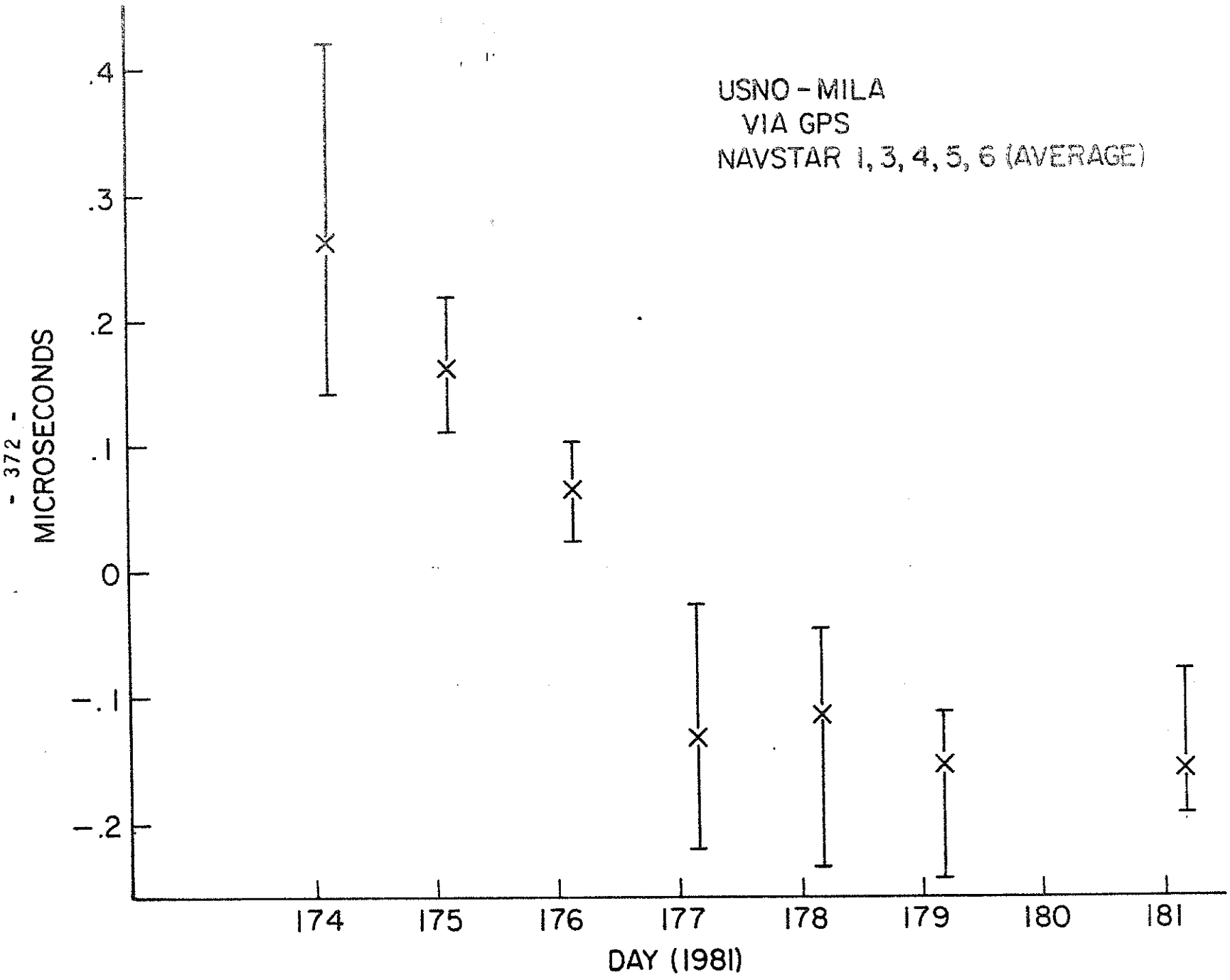
USNO - MILA
VIA GPS
NAVSTAR 1, 3, 4, 5, 6 (AVERAGE)
- 372 -
MICROSECONDS
.4
.3
.2
.1
0
-.1
-.2
174
175
176
177
178
179
180
181
DAY (1981)

Figure 21

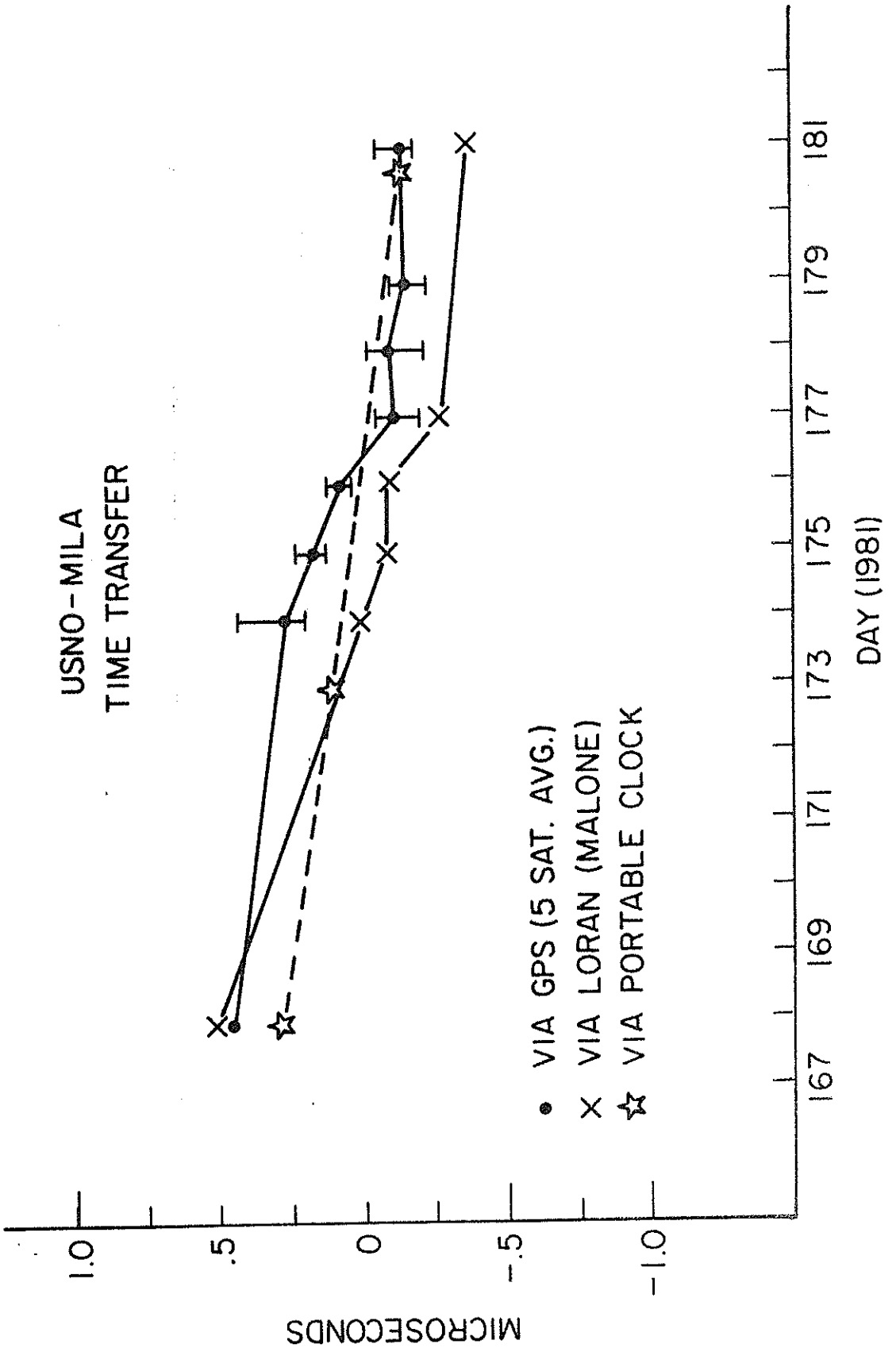
USNO-MILA
TIME TRANSFER
VIA GPS (5 SAT. AVG.)
VIA LORAN (MALONE)
VIA PORTABLE CLOCK
MICROSECONDS
1.0
.5
0
-.5
-1.0
167
169
171
173
175
177
179
181
DAY (1981)

Figure 22

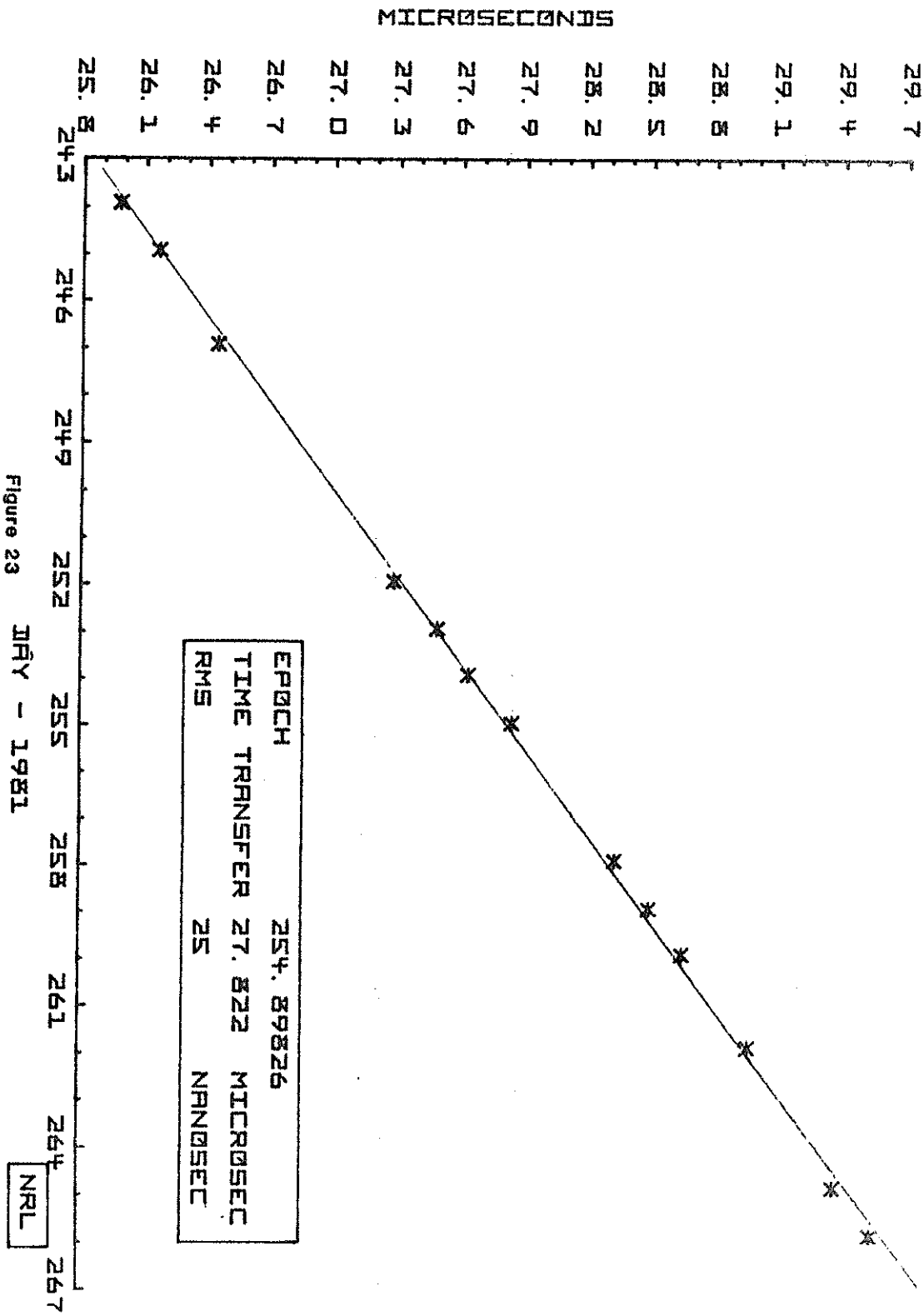

Figure 23 MAY - 1981

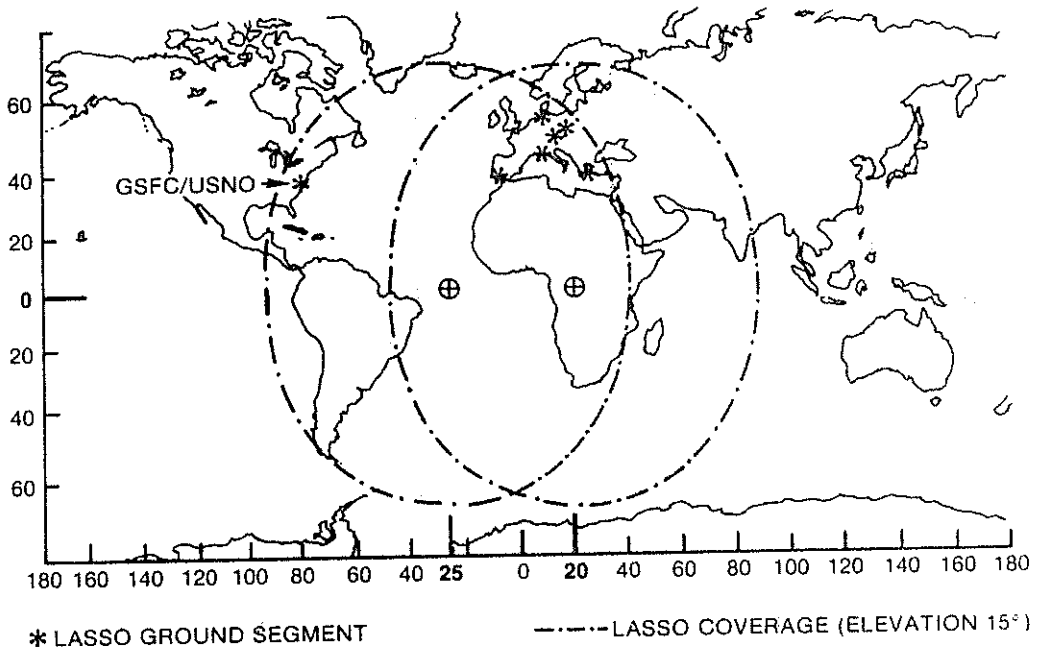

Figure 24. Provisional LASSO Coverage Zones

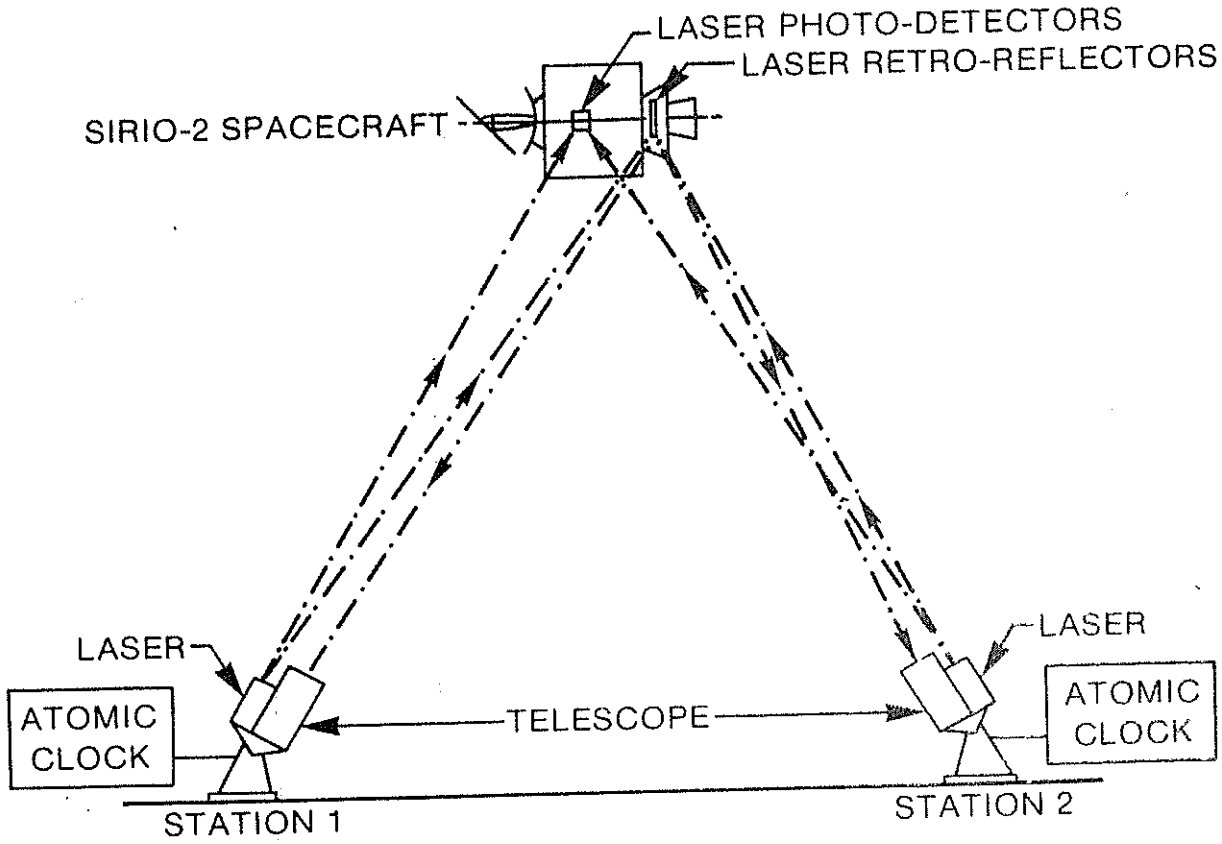

Figure 25. Schematic Diagram of LASSO Experiment

TRANSIT/NOVA SYSTEM WORLDWIDE TIME DISSEMINATION POTENTIAL CAPABILITY

LAUREN J. RUEGER
THE JOHNS HOPKINS UNIVERSITY APPLIED PHYSICS LABORATORY
JHU/APL
JOHNS HOPKINS ROAD
LAUREL, MD 20707

ABSTRACT

The Navy Navigation Satellite System (NNSS) has been in continuous operation providing UTC time marks at even two minutes since 1963. These time marks are presently traceable to the United States Naval Observatory (U.S.N.O.) master clock to uncertainties of 10 to 50 microseconds; a new spacecraft, (NOVA) was recently launched that has the potential capability of time mark traceability to less than 50 nanoseconds error to users anywhere in the world.

SYSTEM DESCRIPTION: Polar orbiting satellites at 600 nautical miles altitude transmit 150 and 400 MHz carriers modulated with a data message that mathematically describes the orbit position as a function of time. The data message is a prediction of the satellite position based on data from fixed ground stations making precise measurements of the frequency shift in the 150/400 MHz carriers as the spacecraft passes each ground station. There is sufficient information in the frequency shift on the received carriers to calculate the geometric position of the satellite relative to any receiving station. Therefore, knowing where the satellite is and knowing your position relative to the satellite provides a navigation fix. Part of this navigation solution provides the propagation path length at each two minute mark between the satellite and the ground-based receiver from which a time mark correction can be determined for setting local ground clocks.

OSCAR

The modulation in use since 1963 is recovered in a receiver phase-locked to the carrier as $\pm 60^{\circ}$ phase modulation in a binary code

bit (Fig. 1) period of 19.6 milliseconds (approximately 50 bits per second). The phase modulation is generated in T^2L logic with rise times of 20 nanoseconds. Antennas receiving signals from the overhead hemisphere provide signals at about — 120 dBm $^{+0}_{-20}$; the signal level fluctuations are due to multipath, and Faraday rotation, of the propagated signal and is due to variations in the signal polarization and attitude of the spacecraft. The time marks are kept in step with UTC by planned deletions of cycles in the clock divider circuits (Fig. 2); the steps being 9.6 μsec in size and occurring approximately 56 times each 2 minutes. Successive two minute periods will vary + or - one count from the average number of deletions. Therefore, to realize time from such a clock, it is desirable to average as many two minutes marks as possible. Seven or 8 time marks can be recovered each time the spacecraft passes the receiving station. Typically 2 successive revolutions are visible each 12 hours. Therefore, in 3 days as many as 84 time marks can be averaged.

$\frac{9.6}{\sqrt{42}}$ = 1.48 μs is the timing uncertainty W/O oscillator drift

2×10^{-11}/Day → 1.7 μs/DAY is a typical drift rate of orbiting oscillators and is predictable to

$\pm 2 \times 10^{-13}$ → 17 ns/DAY

2×10^{-12}/Day → 0.17 μs/DAY would be considered to be a low rate for an oscillator in orbit.

NOVA

The new generation of spacecraft for NNSS, has a much improved reference oscillator and a programmable synthesizer to normalize the frequency against drift so that a fixed divider chain drives the clock without any deletions of cycles. The same modulation for message data is used, however, another higher frequency modulation has been designed into the system 1.6 MHz bit rate for a pseudo random code (PRN) that repeats every 19.6 ms in synchronism with the message data. The NOVA timing chain is shown in (Fig. 3).

Experiments performed in 1977 using receivers modified to recover the PRN code on the 2 minute marks have demonstrated a 3 day average at each of two stations permitted time transfer at the 40 ns level. The experiment was set up at U.S.N.O. in Washington, D.C. and the National Bureau of Standards (NBS) in Boulder, Colorado. The reference measurements were two clock trips bracketing the experiment, one of which had probable errors of less than 3 ns, the other clock trip had errors as large as 25 ns.

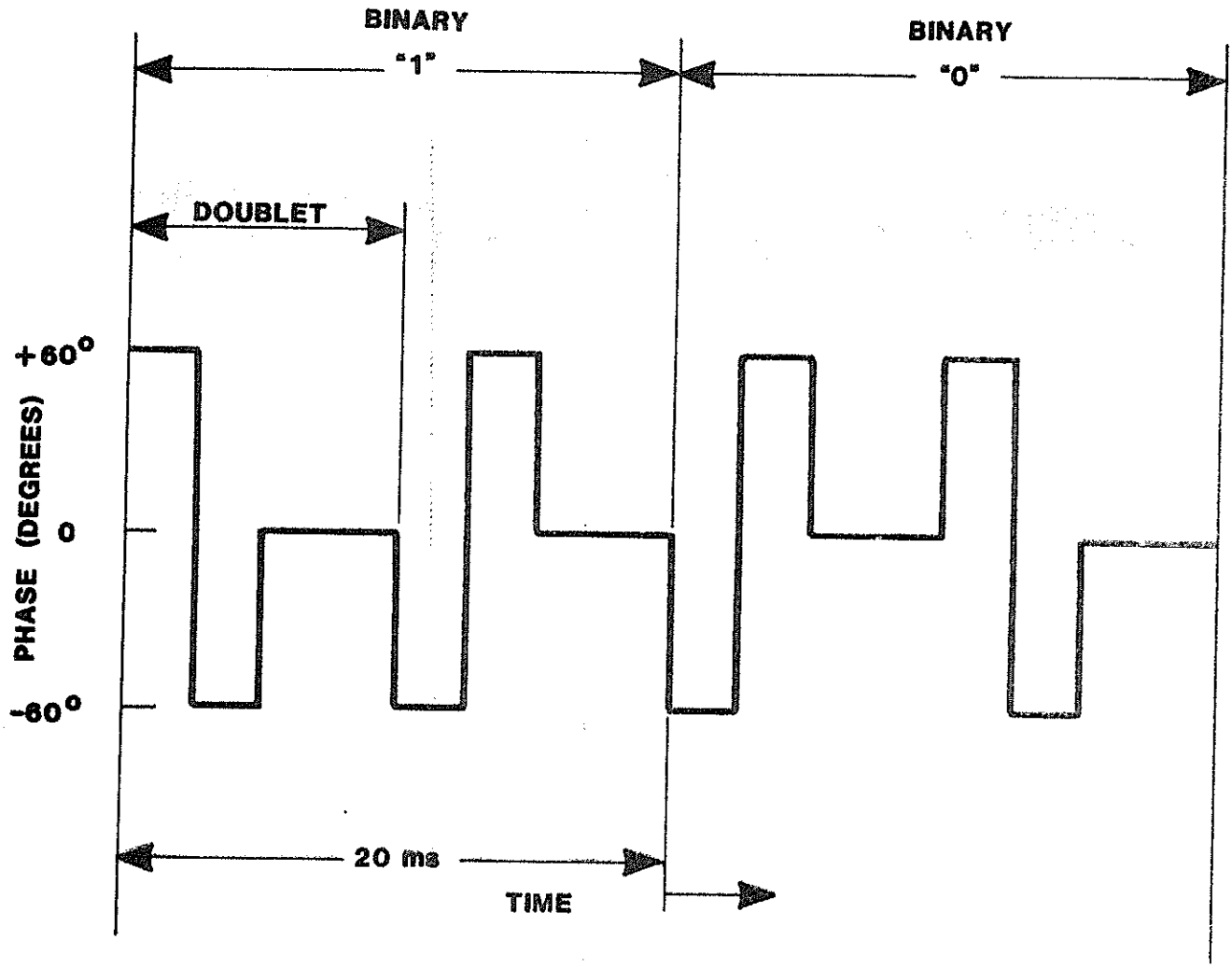

Fig. 1. MODULATION CHARACTERISTICS IN BINARY CODED FORM

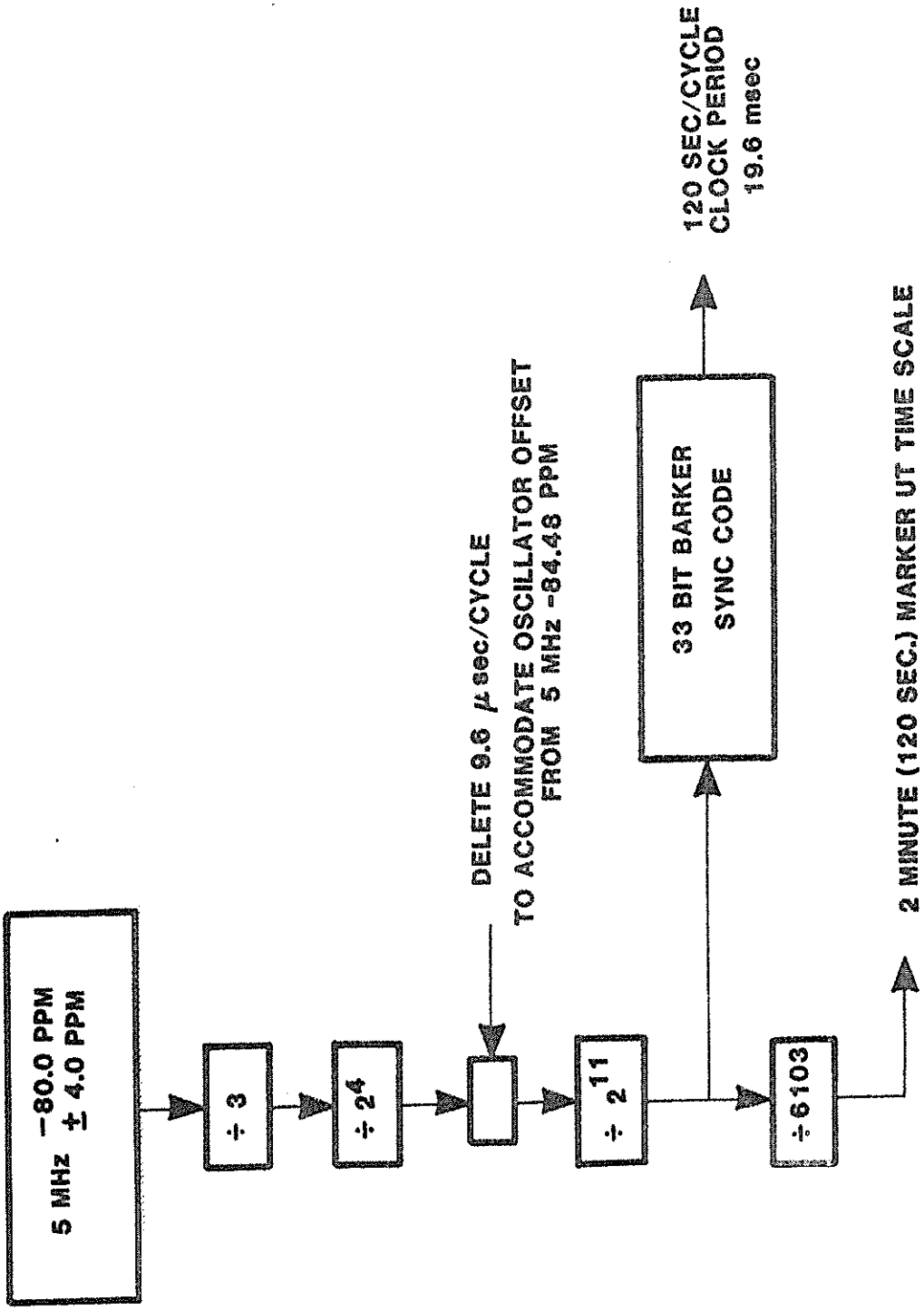

Fig. 2. OSCAR SPACECRAFT TIMING CHAIN

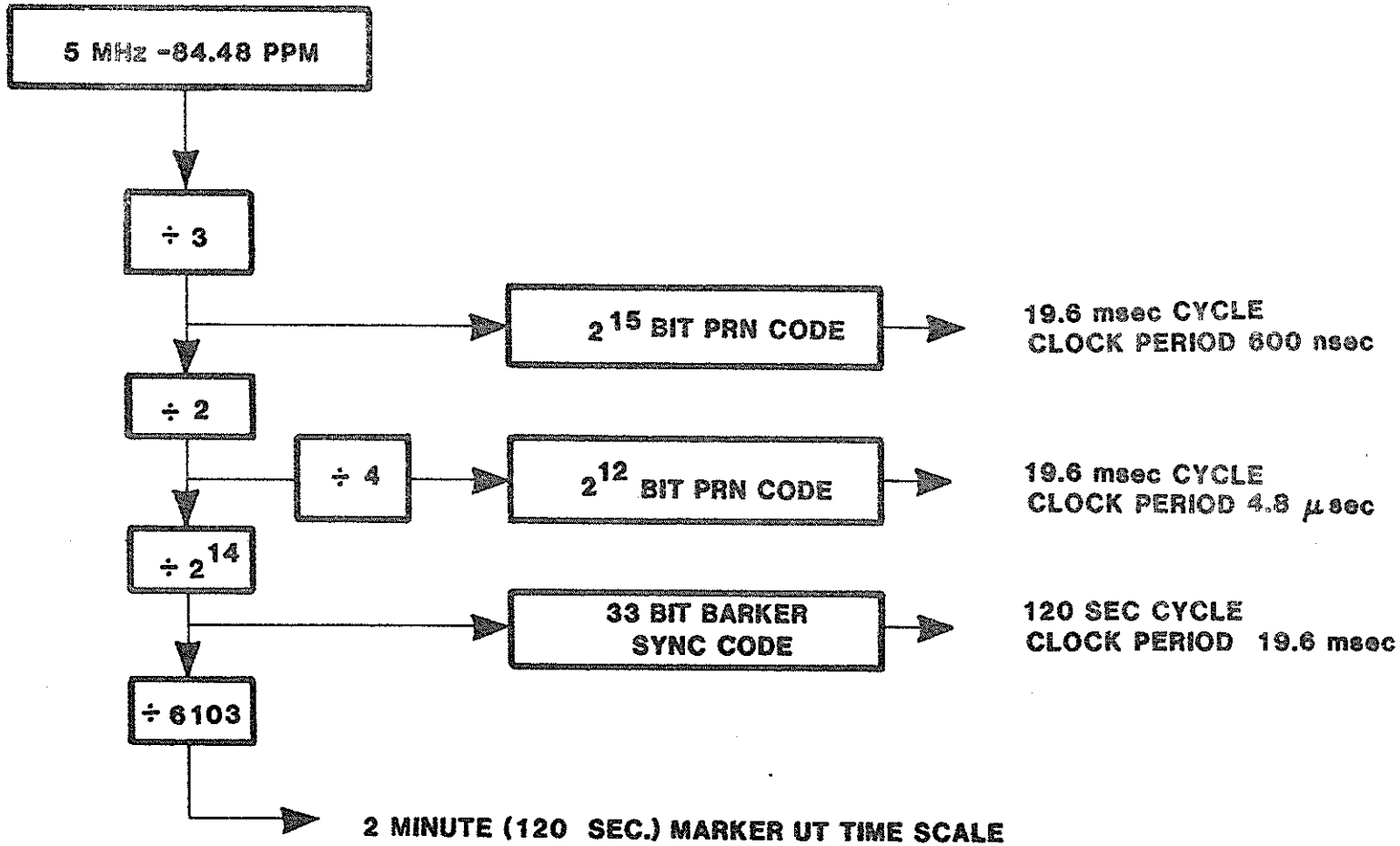

Fig. 3. NOVA SPACECRAFT TIMING CHAIN

Ground test data before launch on the satellite oscillators (Fig. 4) showed that in 3 days the clock could be steered to errors less than 50 ns and after 1 week the clock could be steered to within 2 ns of the reference clock using single measurements spaced 12 hours apart. The algorithm to steer the clock has Kalman filtering and clock modeling to accommodate the typical Allan variance of the specific oscillator being steered.

RECEIVERS

Since Pseudo Random Noise (PRN) modulation is not required to operate the NOVA satellite in the navigation mode, no plans to turn on PRN modulation exist. There is a commercial source for the standard OSCAR signal modulation time recovery priced between $10,000 and $20,000 depending on the optional features desired. Frequency & Time Systems, Inc. calls the receiver Model T-200. Units of these designs are operating at the U.S.N.O. and at several other sites in the U.S. The original Model T-200 receivers have Right Circular Polarized 400 MHz antenna and the antenna must be changed to either linear or Left Circular Polarized to recover NOVA signals.

NOVA PRN

The NOVA PRN modulation is expected to be turned on for a short period of operational tests in the near future as a diagnostic tool to make precision measurements on the oscillator performance in orbit. It is desired to determine the in-orbit predictability of drift rates as a reference mark for this oscillator and to examine the resolution to which the drift rates can be canceled and indexed to UTC time. The single measurement time resolution with PRN can be as small as 1 nanosecond with the laboratory instrumentation available at JHU/APL. Clock steerage is a software function; the operators of the spacecraft system need only know the clock corrections to be made and do not have to have direct access to the precision measurement receivers. Eventually, only one master clock facility like the U.S.N.O. would need to have the precision clock reception instruments to control the NNSS NOVA satellite.

If the remote site to be timed can see the exact same 2 minute time marks as the reference time station and measurements are made when the ionospheric activity is low (i.e. at night), the system can function at the 1 to 10ns level of time transfer.

If a valid requirement develops for the NNSS PRN timing system, it is understood that the U.S.N.O. would accept the monitoring role to obtain clock steerage data for the operational system. The use of the clock error data to steer the clock in NOVA satellites is within the current operating charter of Naval Astronautics Group (NAVASTROGRU) who control the NNSS.

TIP-III OSCILLATOR AND IPS LABORATORY TESTS

TIME STEERING:

- 50 nsec AFTER THREE DAYS
- 1-2 nsec AFTER SEVEN DAYS

Fig. 4. TIP-III TIME STEERING RESULTS

THE LASER STATIONS FOR THE SIRIO-2 LASSO EXPERIMENT

Dr. B.E.H. SERENE
LASSO Payload & Mission Manager

EUROPEAN SPACE AGENCY
Centre Spatial de Toulouse
18, avenue Edouard Belin
31055 TOULOUSE CEDEX
France

Summary

1. Introduction

The SIRIO-2 satellite will be launched in the spring of 1982. One of the satellite payloads is called LASSO (LAser Synchronisation from Stationary Orbit). It will enable time synchronisation between distant atomic clocks on the ground to the nanosecond level (1 nsec = 10^{-9} sec). LASSO will employ the services of existing laser stations in Europe, Asia and the Americas. As described in detail below, the stations will fire laser pulses towards the satellite at predetermined times according to their local time standard. The arrival times of these laser pulses at the satellite, and of their reflected "echos" at the originating stations, provide a measure of the asynchronism between the participating local time standards, or "clocks".

2. The LASSO Experiment

Principle:

The LASSO experiment is based on the use of laser stations emitting monochromatic light impulses at pre-determined times and directed towards a geosynchronous spacecraft (Fig.1). An array of retro-reflectors on board the spacecraft sends back a fraction of the received signal to the originating laser station. An on board electronic device detects and time-tags the arrival of the laser pulses. Each station measures the two-way travel times of the laser pulses and computes the one-way travel time between station and spacecraft, taking into account the station's geographical coordinates, the spacecraft position, and the Earth's rotation.

./.

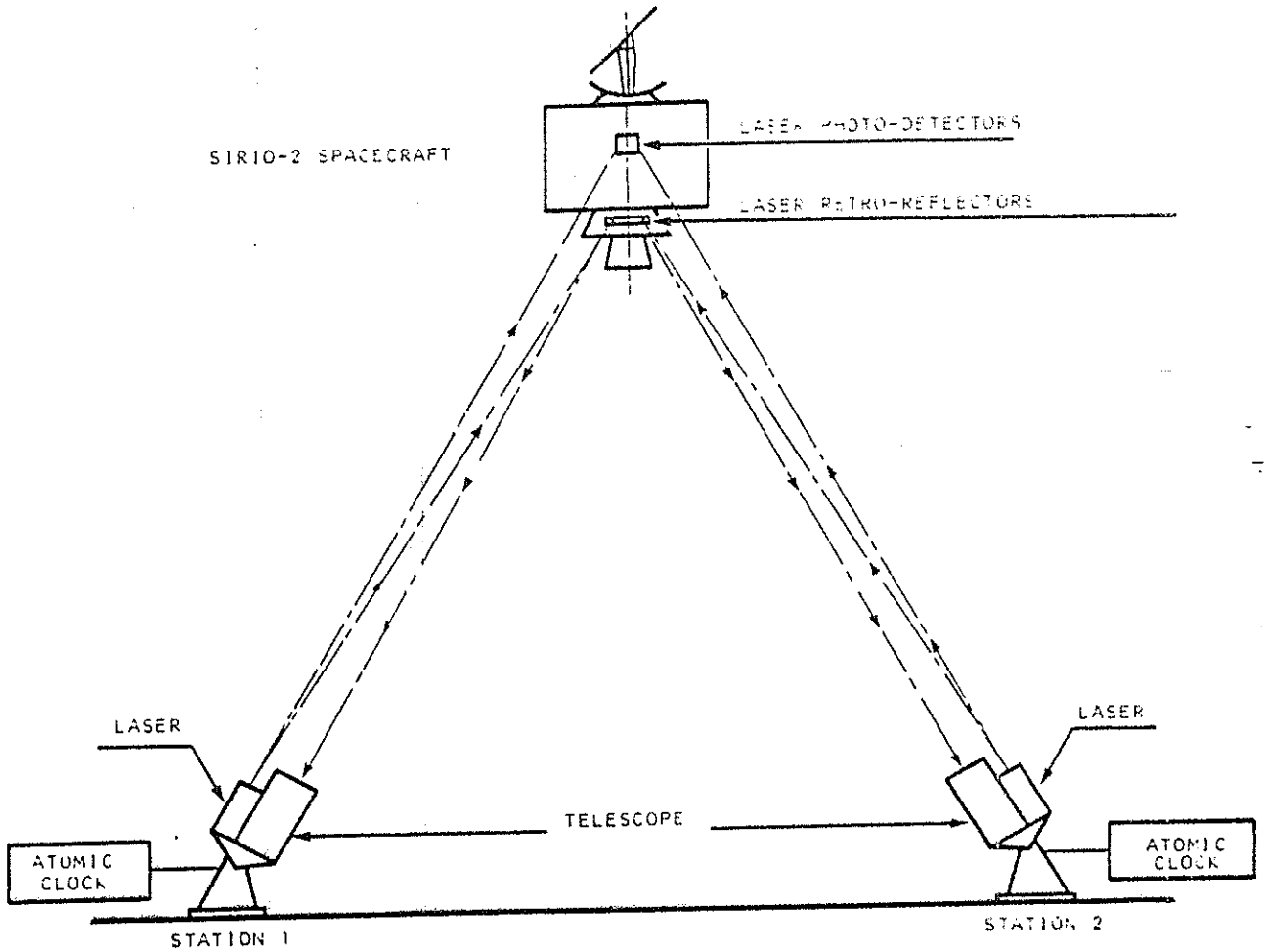

Figure 1

The differences between the clocks that provide the time reference for each of the laser stations can be deduced from the data emanating from the spacecraft and the ground stations (Fig.2).

For two stations, we have :

$$D_{21} = (H_D^2 - H_D^1) + (T_2 - T_1) - (H_S^2 - H_S^1), \qquad (1)$$

where :

D_{21} = time difference between the clocks at stations 2 and 1

H_D^1, H_D^2 = departure times of laser pulses from stations 1 and 2

./.

T_1, T_2 = travel times between stations and spacecraft, with $T = [(H_R - H_D)/2] + \varepsilon$

H_S^1, H_S^2 = arrival times on board the spacecraft of the laser pulses from stations 1 and 2

H_R^1, H_R^2 = return times of laser pulses from stations 1 and 2

ε = corrective factor depending on the station and satellite positions.

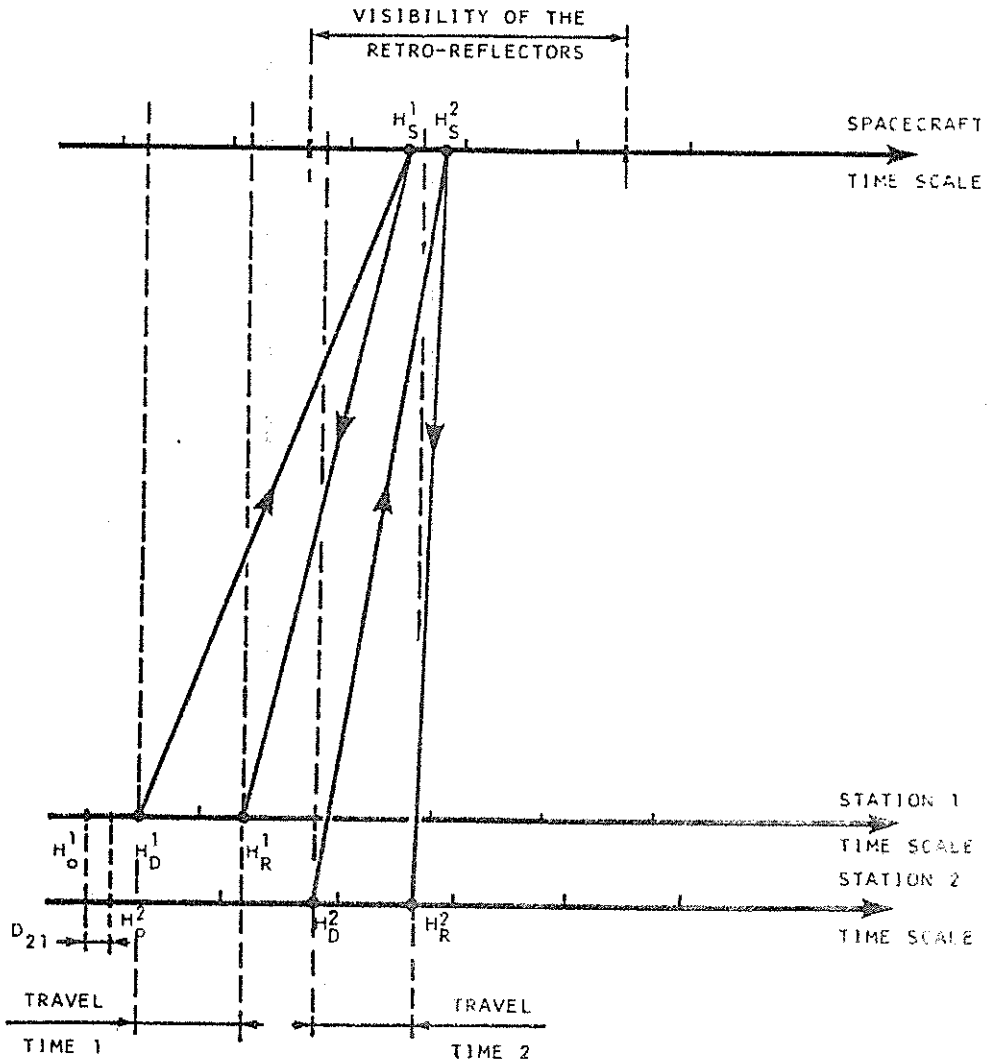

Figure 2

./.

Thus :

$$D_{21} = \left(\frac{H_D^2 - H_D^1}{2}\right) + \left(\frac{H_R^2 - H_R^1}{2}\right) + (\varepsilon_2 - \varepsilon_1) - (H_S^2 - H_S^1) \qquad (2)$$

Performance:

Error Analysis

Using the above information, the global error is:

$$\Delta D = \Delta H_D + \Delta H_R + 2\Delta\varepsilon + 2\Delta H_S \qquad (*)$$

where ΔH_D = error in departure time
ΔH_R = error in return time
$\Delta\varepsilon$ = in correction factor
ΔH_S = error in arrival time on board the spacecraft.

Link Budget

Bearing in mind the two planned orbital positions for the SIRIO-2 spacecraft (25°W and 20°E), the parameters of the on board equipment, and the assumed characteristics for a number of laser stations, different algorithms have been used to compute :

- P_r the power density received by the spacecraft :

$$P_r = K \frac{J}{T} \cdot \frac{T_A}{\frac{4}{\pi}\theta^2 D^2}$$

where :

J = emitted energy (joules)
T = pulse width (ns)
θ = beam divergence (arc.s)
D = station - spacecraft separation (km)
$T_A = (0.7)^{1/\cos z}$: atmospheric transmission coefficient (z= zenithal distance)
K = 0.7 coefficient of energy distribution.

./.

(*) B. Serène & P. Albertinoli, 1980

For LASSO,

$$P_r \ (mW/cm^2) = 3.79 \times 10^{12} \cdot \frac{J}{\tau} \frac{1}{\epsilon^-} \frac{1}{D^2} T_A$$

- $\bar{N}_d$, the mean number of photons received by the photo-detector:

$$N_d = \frac{N_d}{T} = P_r \ A_{op} \ s \ \frac{\lambda}{hc} \ \text{(photons/ns)}$$

where: A_{op} = 4.25 gain of optical detection
s = 0.2 mm^2 photodiode sensitive surface
λ_R = 694.3 nm (ruby)
λ_N = 532.0 nm (neodyme)
h = 6.6256×10^{-34} joules.s
c = 2.9979×10^{8} m/s

Consequently :

$$\bar{N}_d = kP_r \begin{cases} k_R = 29710 \\ k_N = 22760 \end{cases}$$

- N_e, the number of photo-electrons collected at the laser station, from the Fournet formula :

$$N_e = E \cdot TR_1 \cdot R \cdot TR_2 \cdot D$$

where :

$E = KJ \frac{\lambda}{hc}$ — photons emitted by the laser station

$TR_1 = \frac{T_A}{\frac{\pi}{4} \left(\frac{\pi}{180} \cdot \frac{\theta}{3600} 10^5 D\right)^2}$ — travel effect station-spacecraft

$R = R_{cc} \Sigma f(G_i)$ — retro-reflector effect

R_{cc} = 0.84 (coefficient of reflection)

$\Sigma f(G_i)$ = 23.8 for ruby (mean value)
= 22 for neodyme

$TR_2 = 0.328 \ T_A / D^2$ — travel effect station-spacecraft

$D = AT_r\rho$ — station detection effect ./.

where A (cm^2) is the receiving surface of the telescope, T_r the transmission coefficient of the telescope optics, and ρ the quantum efficiency of the photo-multiplier.

3. The Ground Segment Requirements

The LASSO mission is planned to last a total of two years. The experiment 'working sessions' will occupy an average of one hour per day. There will be no constraints at the satellite level on the time of day at which one or more 'sessions' can be performed, but the constraints will rather be of a procedural nature.

After a 2-month period of satellite commissioning, each daily working session will consist in synchronisation of the pulse transmissions from each participating station with respect to the rotation of the spacecraft and associated time measurements.

Because of the design of the satellite's on-board equipment, the laser pulses from the various ground stations must be timed to arrived at the spacecraft with the temporal distribution shown in Figure 3.

Each sequence of measurements lasts approximately 4 to 6 s (bound to the minimum pulse rate of the laser stations), and in each sequence a time slot of 5×10^{-3} s is reserved for the arrival of the pulse from a particular station (this figure is bound by the accuracy of the time of departure of the pulse from the station and by the accuracy of the computation of the travel time of light from the station to the spacecraft).

Consequently each subsession lasts about 3 min and is separated from the next subsession by a time interval of 10 min, to allow laser stations to reset the firing time based on the spin rate drift of the spacecraft.

Successive sequences differ from one another since not all of the laser stations send pulses in each sequence. The use of pattern recognition techniques in the ground processing ensures that any false pulses detected by the on-board equipment is discarded.

./.

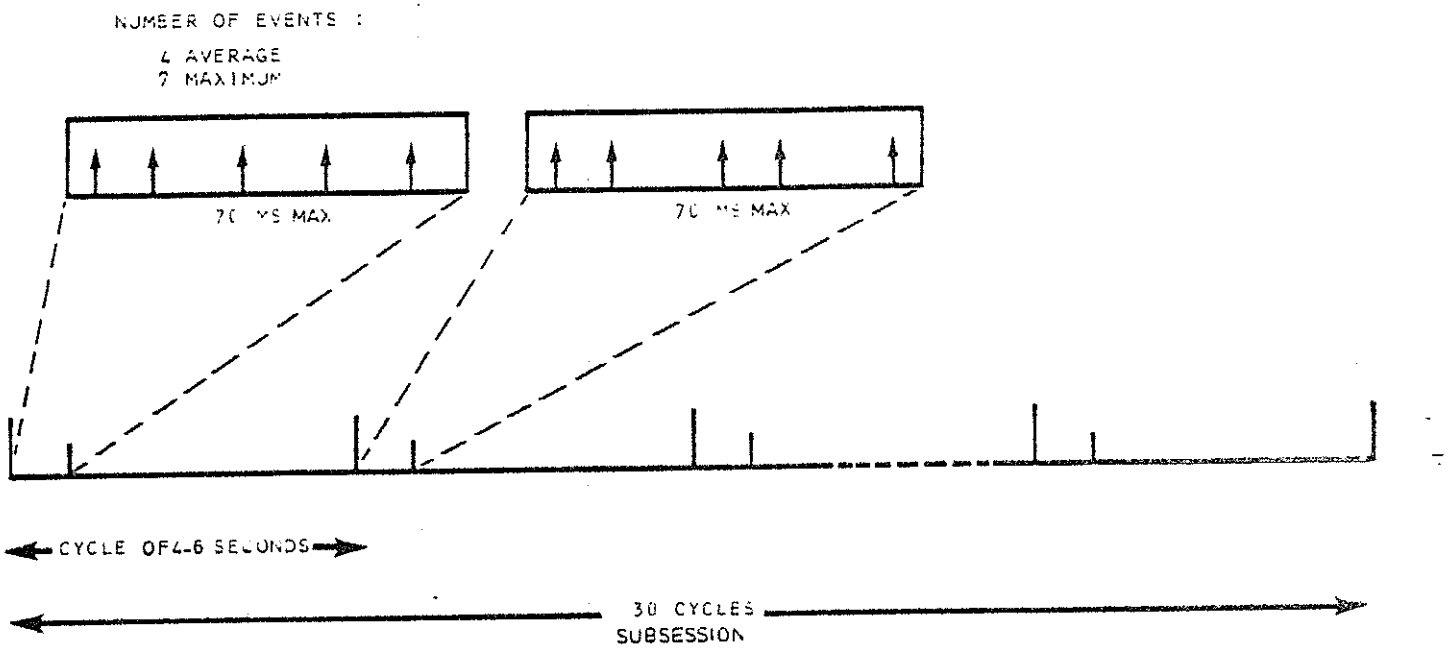

Figure 3

An alternative spin-asynchronous mode of experiment operation is currently being investigated. Several data processing modes are also under study in consultation with the various principal investigators.

Station location and performance

Because of the need to correct the transit time of light from the laser station to the spacecraft, the laser station should be located in a common Earth reference frame with a minimum specific accuracy :

- latitude : ± 10" (or ± 300 m)
- longitude : ± 10" (or ± 300 m)
- altitude : ± 10 m

Two sets of conditions are imposed on laser-station characteristics : one by the satellite-detector and retro-reflector characteristics, the other by the laser station detector system.

./.

In order to ensure laser detection on-board the spacecraft, the laser station must deliver sufficient energy in a sufficiently narrow beam for a finite time. If J is the total energy (in joules) of the light in the beam during one pulse from the laser station, T the equivalent pulse duration in nanoseconds, and θ the laser station beam divergence in arc seconds, bearing in mind the link budget and the two sensitivities (nominal and high) of the on-board detectors, the laser station should satisfy the performance relationship :

$$\theta \leqslant \alpha \left(\frac{J}{T}\right)^{1/2}$$

where α is a coefficient given in figure 4.

In order to detect the return pulse from the retro-reflectors on board SIRIO-2 (544 cm^2 of surface, reflection coefficient = 0.84, efficiency > 20), the laser station should also satisfy the relationship giving the number of photons received by the station :

$$N = \beta \left(\frac{J}{\theta^2}\right) T_R A$$

where β is a coefficient given in figure 5.

A = effective area of the telescope used to collect the light (cm^2)

T_R = transmission factor of the telescope

J = energy of the laser flash (joules)

θ = beam divergence (arc.s)

N = number of photons collected by the telescope equipment

A minimum of 10 photons must be detected by the laser station from the retro-reflected signal.

The number of photo-electrons detected is :

$Ne = N.\rho$ where ρ = quantum efficiency of the photon-multiplier.

./.

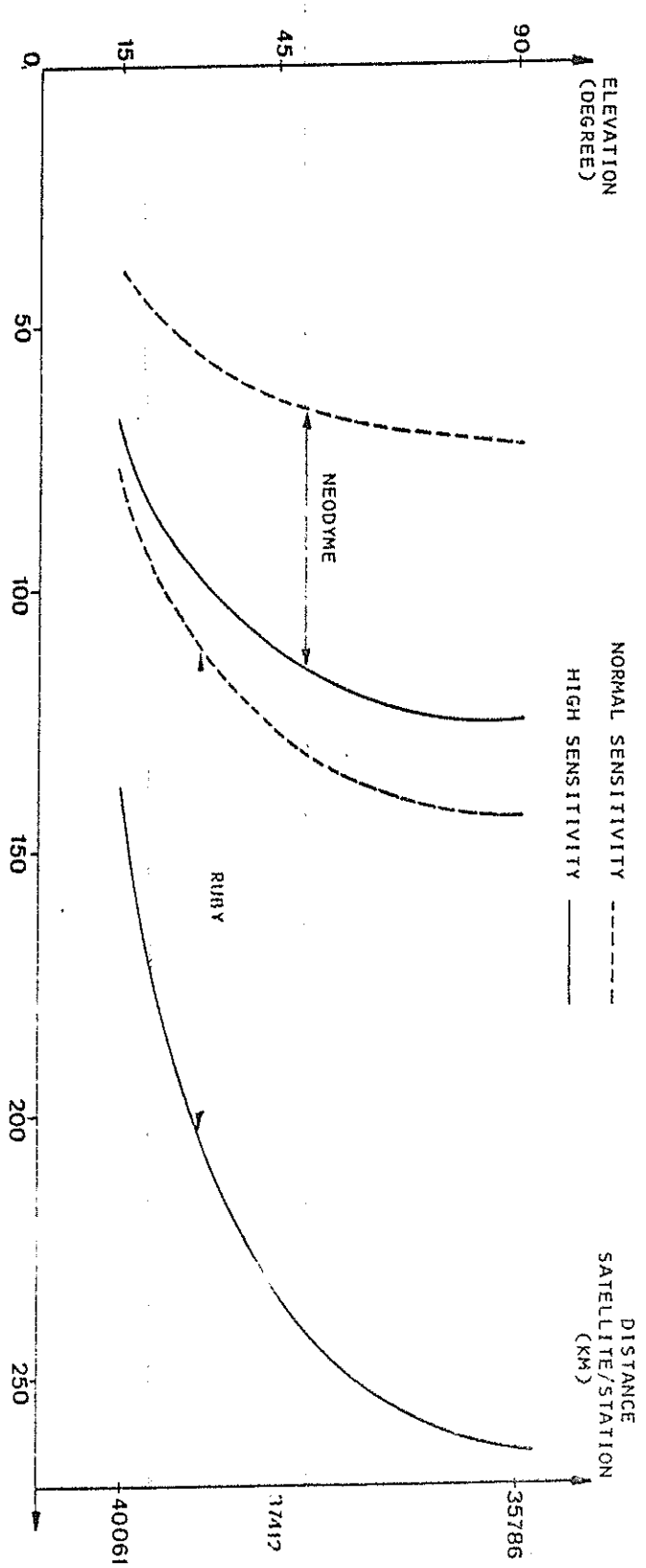
ELEVATION (DEGREE)
0
15
45
90
COEFFICIENT α
50
100
150
200
250
NEODYME
RUBY
NORMAL SENSITIVITY
HIGH SENSITIVITY
DISTANCE SATELLITE/STATION (KM)
35786
40061

Figure 4

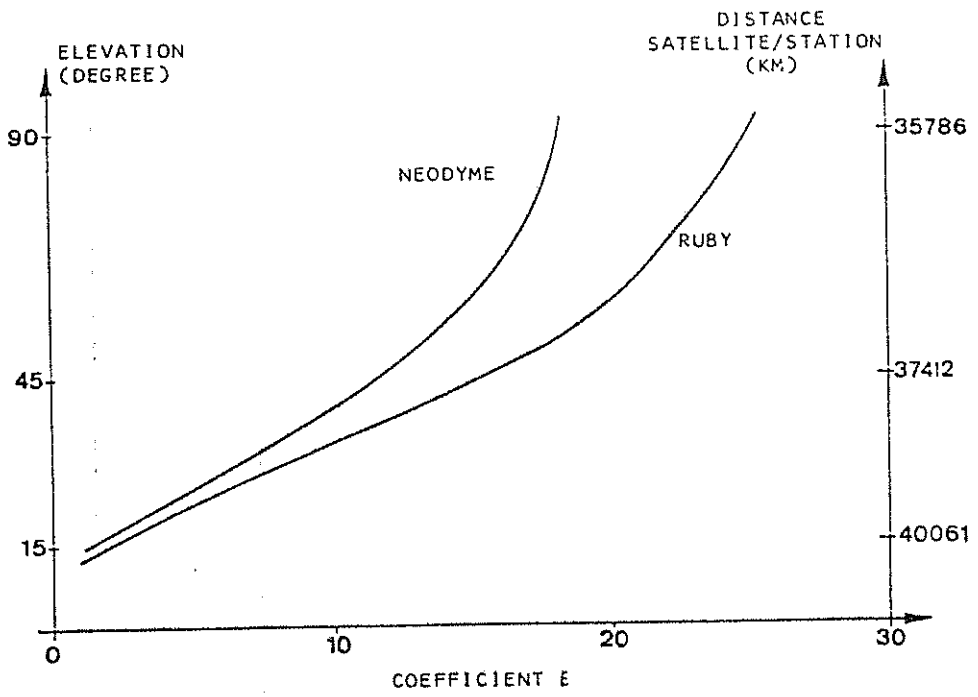

Figure 5

Sufficient beam divergence is necessary at each laser station to ensure that the pulse does in fact arrive at the satellite, taking into account small errors in satellite position (known 'à priori' within ± 1 km). The laser stations must therefore have a beam divergence of :

$\theta \geq 10'' + 2 \times$ (angular error of tracking).

The time-measurement devices at the participating laser stations must also satisfy a number of criteria. They should permit synchronisation with a standardised time source in their zone (e.g. IAT) by terrestrial means on a daily basis, with a precision of a few microseconds. ./.

The maximum error in synchronisation between two stations participating in the experiment should be less than 1 ms before LASSO measurements commence.

Each pulse transmitted by the laser station should be pre-programmed at T_0. If T_1 is the real time at which the laser pulse was transmitted, one should have :

$(T_0 - T_1) < 1$ ms.

T_1 should be measured with an accuracy of $\pm$ 0.1 ns 'à posteriori'

T_2 the time of arrival of the pulse returning from the satellite, should be measured with an accuracy of $\pm$ 1 ns, and the maximum elapsed time from transmission to return of a given pulse should be conditioned by :

270 ms $< T_2 - T_1$.

4. Status of Laser Stations

Using the technical specifications provided by the laser stations, a computer programme has been run. The results are used as the basis for laser station classification :

- two-way laser stations

  power density received by the satellite detection unit above the threshold; number of photons detected by telescope;

- one-way laser stations (type N)

  power density received by the satellite detection unit above the threshold for normal sensitivity;

- one-way laser stations (type H)

  power density received by the satellite detection unit above the threshold for high sensitivity;

- laser stations unable to participate without modifications.

./.

The classification is made purely as a mathematical exercise to estimate the probability of successful participation. It does not, in any way, prejudge the interest of accommodating a particular user in the LASSO mission as a whole.

4.1 Two-way laser stations

France	Grasse 'Satellite' Grasse 'Lune'
Spain	San Fernando
F.R.G.	Wettzell
Netherlands	Kootwijk (marginal)
Austria	Lustbuhel
U.S.A.	NASA/GSFC 1 NASA/GSFC 2

4.2 One-way laser stations, type N

Netherlands	Kootwijk (possibly two-way)

4.3 One-way laser stations, type H

G.D.R.	Potsdam	$50 < \theta < 90$ arc.s
Italy	Cagliari	(marginal)
Brasil	SAO Natal	(marginal)

4.4 Laser stations apparently unable to participate without modifications

India	Kavalur

./.

5. Laser Station Calibration

A problem of calibration arises at the laser stations due to the fact that they have been designed for laser ranging rather than for clock synchronisation. The need for calibration is caused by a small but inevitable discrepancy between the measured and actual emission times of laser pulses. The magnitude of the discrepancy varies from station to station and can be translated directly into a laser travel time uncertainty which, in turn, degrades the potential time synchronisation accuracy between the clocks.

5.1 Necessity

The basic equation (1) masks in fact a rather sophisticated technological application. The calibration consists theoretically in three types of measures :

i/ Measure of the travel time 2Γ

Such a calibration is classical in laser ranging. It could be done either by firing on a target at a very well known distance or by double round trip using an additional retro-reflector (E. Silverberg method). One thus obtains the time delay difference between emitting and receiving channels. The delays are due to the time elapsed between the moment when the laser pulse passes through the reference point and the internal triggering of the event timer.

ii/ Satellite time-tagging

LASSO relies only upon the short term stability of the on board oscillator; stability drift calibration is therefore not necessary.

iii/ Definition of the emission time

The moment when the emitted laser pulse is passing through the reference point must be time tagged with an accuracy better than 1 nsec if the LASSO objectives are to be met. This implies that the delay τ between this moment and the memorised time H in the event-timer must be

./.

calibrated with an uncertainty of less than 1 nsec. It is this third type of calibration which will be solved by the mobile calibration device.

5.2 Concept

We will consider here only the aspect relevant to the definition of the emission time.

We have : $H_D = H - \tau$

$$D_{21} = (H^2 - H^1) - (\tau^2 - \tau^1) + (T_2 - T_1) - (H_S^2 - H_S^1) \qquad (4)$$

This new relation shows that keeping the accuracy of the time synchronisation does not involve the knowledge of the absolute values of τ, but only their differences. A method of solving the problem is to use a second laser ranging equipment, in parallel with the laser station to be calibrated, bearing in mind that potential drift will be monitored by an internal return path.

5.3 Equipment

The European Space Agency is in the process of procuring a calibration device in order to establish a relative measure of this discrepancy between stations, thus allowing the necessary time corrections to be made in the calculation of atomic clock asynchronisms. The intention is to obtain a facility which is sufficiently small, light, rugged, and stable that it can be transported in a jeep-type vehicle and by air to participating laser stations all over the world without suffering any degradation on performance.

6. CONCLUSION

It appears that the most critical parameters for a successful participation of the laser stations are :

- a small divergence of the laser beam,
- a good pointing accuracy,
- at least a medium size telescope (60 cm)
- a photo-multiplier with high quantum efficiency.

./.

Laser stations with marginal link performance will often be able to raise the probability of success by improving only one or two of these parameters, the choice of modifications being subject e.g. to the planning and cost considerations at the laser station.

- o0o -

References:

Serène B. & Albertinoli P., 1980, The LASSO Experiment on the SIRIO-2 Spacecraft, ESA Journal 4, 1, pp 59-72

Serène B., 1980, The Progress of the LASSO Experiment, Proc 12th Annual Precise Time & Time Interval (PTTI) Conference, NASA-GSFC, Greenbelt, Maryland, 2/3/4 Dec. 1980.

Serène B., February 1981, The LASSO Experiment and its operational organisation, International Symposium on Time and Frequency, New Delhi.

COMPARISON OF MEASURED AND THEORETICAL PERFORMANCE OF A MAXIMUM LIKELIHOOD LASER RANGING RECEIVER

CONTACT: J.B. ABSHIRE
CODE 723
NASA/GODDARD SPACE FLIGHT CENTER
GREENBELT, MARYLAND 20771 USA

Abstract and Summary

A maximum-likelihood laser ranging receiver recently has been built and tested. Its configuration includes a high quantum efficiency (30% at 532 nm) detector, a single start-stop channel, and a matched filter followed by a peak detector to implement the maximum-likelihood signal processing algorithm in real time. The receiver was designed to operate with signals from 5 to 5000 photoelectrons per 7 nsec laser pulse, with a 50:1 dynamic range on a shot-to-shot basis. It can operate with background rates of up to 375 pulses/μsec, which are the rates expected when the receiver and its 20 cm telescope are pointed at sunlit clouds. Measured receiver detection probabilities were in excellent agreement with theory for signals in the 3 to 62 photoelectron level. Measured false alarm rates also agreed with theory for low receiver thresholds, but exceeded theory for high threshold values due to photomultiplier feedback events. Range jitter values were 0.8 db from theoretical at the 10 cm level, and increased to 2.7 db from theoretical at the 2 cm ranging level.

System Description

A block diagram of the laser receiver is shown in Figure 1. The fire signal from the minicomputer triggers the laser and the generation of a start gate signal. The optical pulse from the laser is divided by a beam splitter and approximately 0.1% is reflected into a variable optical attentuator used to control the the start pulse amplitude. The pulse from the attenuator is directed to the single photomultiplier, and the amplitude of its electrical signal output is controlled by a variable attenuator. The attenuator output signal is amplified, matched-filtered, reamplified, and split into four paths. One output triggers the peak detector, which is enabled by the start gate signal. The gate generator triggers only the start charge-digitizer, after

it is triggered by the discriminator output. The input to the charge digitizer is delayed by a coaxial cable, to compensate for the peak detector and the gate generator propagation delays. The event timer also registers the peak detector output, and records it as the start occurence time.

The remainder of the laser output energy is transmitted through the beam splitter, and is directed through a pointing system to the target corner cube. The return signal is collected by the telescope, and is spatially and spectrally filtered. The return signal then is recollimated, and focused onto the photomultiplier. This signal passes through the same electrical path as the start signal, and triggers the same peak detector as the start pulse. The peak detector is only enabled for the return pulse during the range gate generated by the event timer. This gating signal also enables the stop charge-digitzer, which measures the received pulse energy. The event timer is triggered by the peak detector output and registers the occurence time of the return pulse.

Both the start and return pulse energy readings from the charge digitizers are used in a feedback loop to control the signal levels in the single channel receiver. The electrical attenuator is controlled by the return pulse amplitude through an averaging algorithm in the minicomputer. This technique allows the average return signal level to be kept within the center of the dynamic range of the common signal channel. The start optical attenuator is then controlled to compensate the optical level of the start pulse, also to keep it centered in the receiver's dynamic range. This is feasible since the 2000:1 dynamic range of the photomultiplier is much larger than the 50:1 range of the electronic channel.

A summary of the specifications of the receiver is given in Figure 2. Both the telescope and the filter are standard commercial products. The photomultiplier is a Varian 152 model, with a high quantum efficiency "S"-type photocathode. The value of photomultiplier gain was selected to be sufficiently high that thermal noise from the preamplifiers would not dominate the system's ranging performance, but low enough to prevent saturation of the last few photomultiplier dynodes

SGRS LASER RANGING RECEIVER

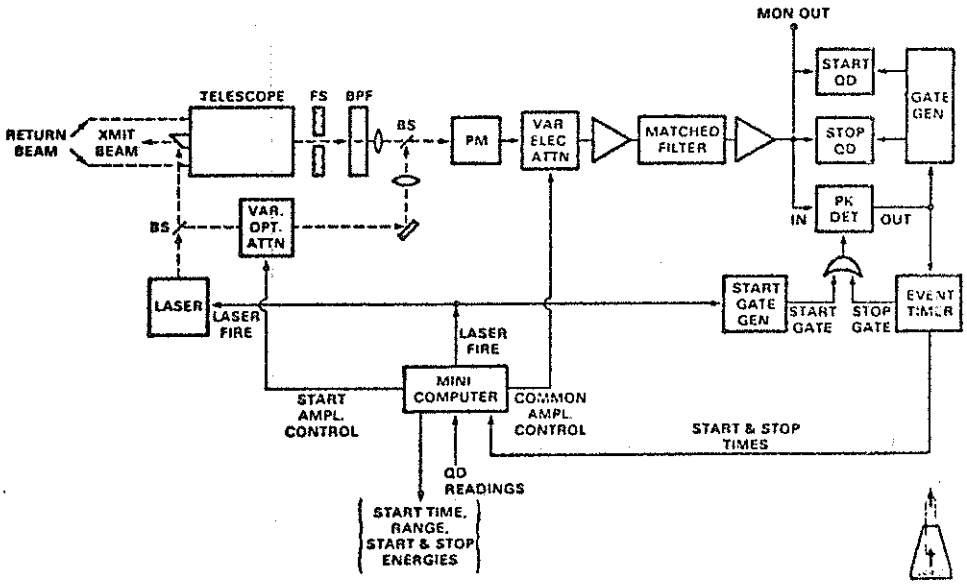

Fig. 1 - Block diagram of SGRS receiver

RECEIVER SPECIFICATIONS

TELESCOPE	: 20 cm DIA, f10 CASSEGRAIN, FOV = 1.4 mrad
BANDPASS FILTER	: 10 Å FWHM
DETECTOR	: 10^5 GAIN, 30% QE @ 532 nm, 2000:1 DYNAMIC RANGE
AMPLIFIERS	: 25 & 35 dB GAIN, 400 MHz BW
MATCHED FILTER	: TAPPED DELAY LINE CORRELATOR, 8 TAPS AT 2nsec/TAP
TIMING DISCRIMINATOR	: GATABLE PEAK DETECTOR,
TIME WALK	: { UNCORRECTED = ± 500 psec; CORRECTED = ± 75 psec
LEVEL DETECTOR	: CAMAC COMPATIBLE CHARGE DIGITIZER, 10 BIT RESOLUTION
EVENT TIMER	: RMS ACCURACY = 17 psec, DEAD TIME = 5.3 μsec, TIME LIMIT = 131 DAYS
MINICOMPUTER	: DEC PDP 11/40
PACKAGING	: SINGLE CAMAC CRATE & NIM BIN

Fig. 2 - Summary of receiver specifications

during reception of large amplitude signals. The amplifiers in the system compensate for the signal loss in the matched-filter and the various power splitters in the channel, and give the low photoelectron signals sufficient gain to trigger the peak-timing discriminator. The matched filter was constructed in a tapped delay line configuration, to allow adjustment of its impulse response. This is accomplished by adjusting variable attenuators in each of the 8 taps.

The peak timing discriminator was a custom unit built by Lawrence-Berkeley Laboratories. It triggers on the peak of the matched filter output, and includes a gating capability. The time-walk for the unit was measured to be ±500 psec. However, by measuring and storing the time walk curve before ranging, the charge-digitizer readings can be used to correct for the time-walk on a shot-by-shot basis. By using this technique, the residual time walk was reduced to ±75 psec. The charge digitizers in this system are commercially available 10-bit units, and are read through the CAMAC dataway. The event-timer was also custom built by Lawrence-Berkeley Labs, and has a timing resolution of 17 psec. Since it also has a single input channel, the minimum dead-time between start-stop events is 5.3 μsec. It can unambigiously record the occurence times of start-stop event pairs for a period of 131 days. A PDP 11/40 minicomputer was used as the controller of for the development of this receiver, although almost any mini- or micro-computer which can control a CAMAC crate would have been adequate. The ranging receiver is packaged in a single CAMAC crate and NIM bin.

Receiver Testing

The LED pulse shape used to test the performance of the receiver is shown in Figure 3. This 7.6 nsec full-width at half-maximum (FWHM) pulse was generated by driving the LED from a fast-risetime pulse generator through a pulse shaping network. The impulse response of the matched-filter is shown in Figure 4. It had a 7.3 nsec FWHM for these tests, and the shape was adjusted to give a close match to that of the laser transmitter of the SGRS system.

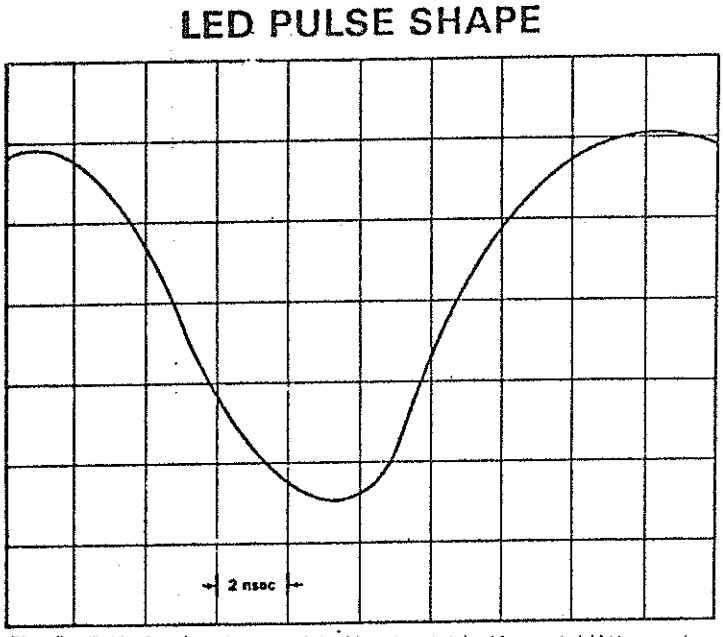

Fig. 3 - Optical pulse shape used in timing and detection probability tests

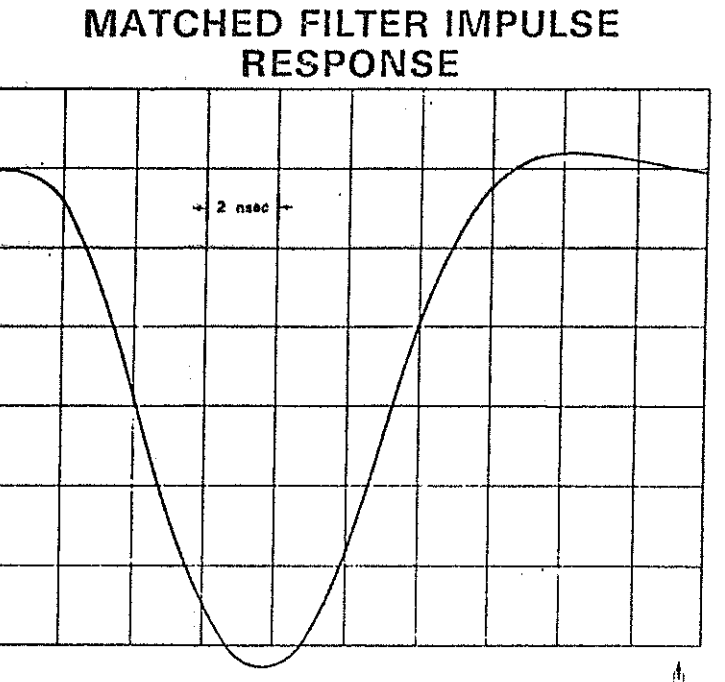

Fig. 4 - Impulse response of receiver matched filter

The receiver photoelectron calibration was performed by measuring the single photoelectron voltage from the photomultiplier, and then measuring the receiver channel amplitude response to the same level signal. A plot of the results is shown in Figure 5, where Monitor Point 2 is labeled as MON in Figure 1. This calibration data was used to determine the received photoelectron level on all subsequent tests.

The test configuration for measuring the receiver performance is shown in Figure 6. The pulse generator output was used to drive the LED, which emits a shaped optical pulse. This pulse was used to simulate the laser pulse incident to the photomultiplier. The output trigger from the generator was used to start the time interval unit when measuring the system timing performance. The LED output was attenuated by a variable ND stack, and focused onto the photomultiplier photocathode. A small flashlight bulb controlled by a variable DC supply was used to provide optical background for timing and false alarm measurements. The photomultiplier output was connected to either a meter to measure the average photomultiplier anode current, or to the SGRS receiver. The threshold of the receiver was adjusted by varying the electrical attenuator preceding the peak detectors. The average photoelectron level in the detected pulses was measured by a waveform digitizer connected to the MON port of the receiver. The discriminator output was connected to the time interval unit for timing tests, and to the frequency counter for detection probability and false alarm tests.

For the timing measurements, the optical pulse energy was varied by using the ND filters, and the RMS timing jitter was measured using the time interval unit. The detection probability tests were performed by varying both the optical pulse strength and the receiver threshold, and by measuring the percentage of the optical pulses which exceeded the receiver threshold with the frequency counter. False alarm measurements used only the DC background illumination, and the rate of receiver triggering was measured as a function of average illumination level and threshold setting.

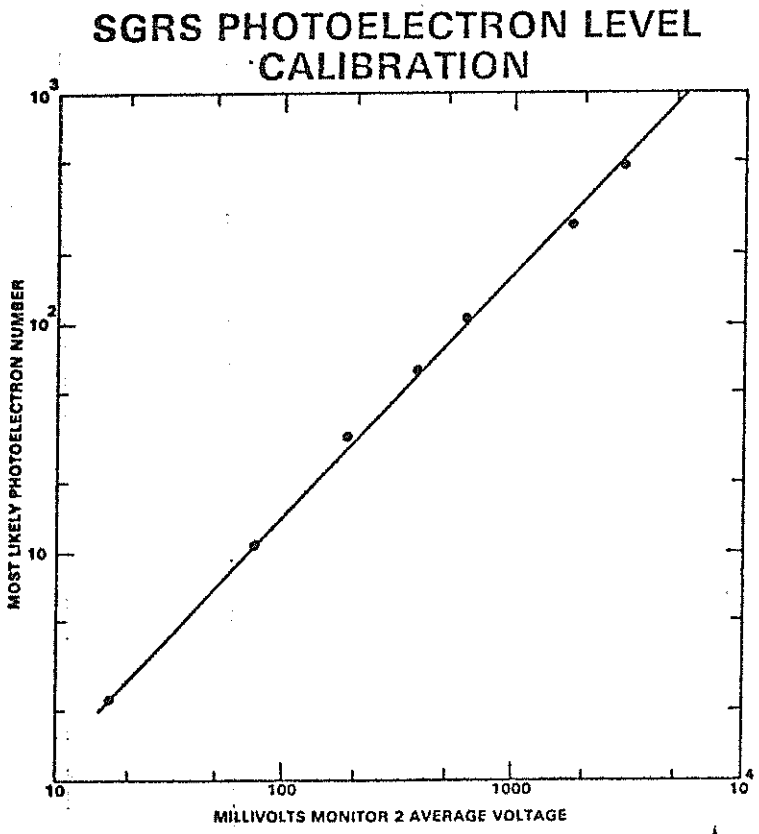

Fig. 5 - Photoelectron calibration of receiver

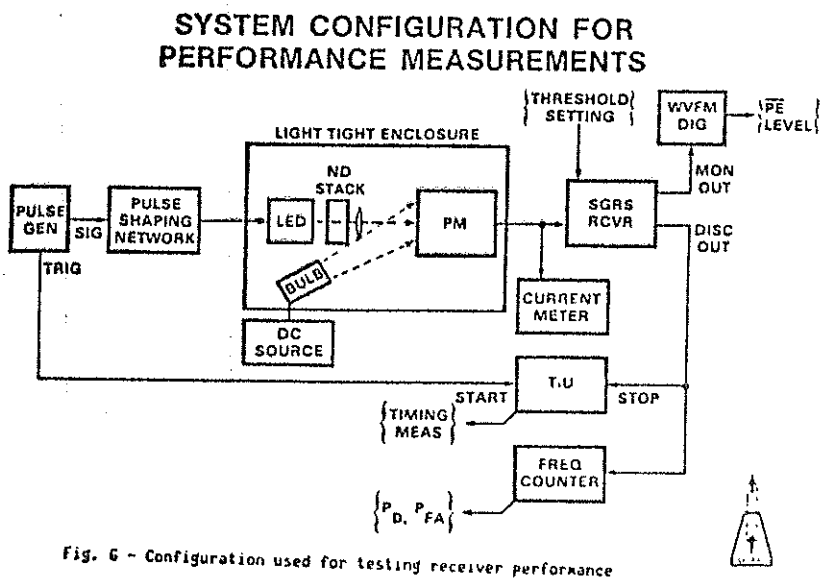

Fig. 6 - Configuration used for testing receiver performance

Theoretical and Measured Results

The theoretical calculations shown in Figure 7 are based on the assumption that the receiver is a sliding window photon counter. Further assumptions were made that the receiver observation window was much longer than its integration time, and during its integration time the receiver simply counts the input photoelectrons. For this analysis the integration time was taken to be equal to the FWHM of the receiver impulse response. For the false alarm calculations, the noise count rate was assumed to be constant over the observation time. Finally, the occurence of false alarms and optical pulse detections were assumed to be independent events, so that their probabilities could be calculated independently. This assumption is not strictly true for actual single channel receivers, since a false alarm will trigger the channel, and preclude detection of a laser pulse following it in the observation window. However, it is a very good approximation for such systems operating under low false alarm probabilities.

Measured detection probabilities and point theoretical calculations are shown in Figure 8. The plot shows excellent agreement between the theory and the measured detection rates, for average optical pulse levels from 10 to 62 photoelectrons. Agreement was not as good for the 3 photoelectron level. The spread in the single photoelectron voltage from the photomultiplier is thought to be responsible for this discrepency.

The measured and calculated false alarm probabilties are shown in Figure 9. There is good agreement between the theory and measurements for low threshold values and low photomultiplier anode currents, but substantial differences at higher thresholds and currents. These are due to receiver dead-time effects at low threshold levels and high background rates. For high threshold settings, the measured false alarm rates considerably exceed those predicted by theory. This is caused by the ion-feedback mechanism in the photomultiplier, which causes a small fixed percentage of photoelectrons to generate large amplitude bursts of photoelectrons. This mechanism is more evident in photmultipliers with more open dynode structures, such as static-crossed field types.

SIMPLIFIED THEORY

DETECTION AND FALSE ALARM PROBABILITIES:

- **ASSUME:**
  - RECEIVER IS SLIDING WINDOW INTEGRATOR, WIDTH τ
  - OBSERVATION WINDOW OF TSEC, $T \gg \tau$
  - RECEIVER COUNTS PE OVER LAST τ SEC
  - NOISE COUNT RATE n_b IS CONSTANT OVER T
  - DETECTION & FALSE ALARMS ARE INDEPENDENT
- $P_D = P_r\{N_{s_\tau} \geq \text{THRESH (L)}\} = 1 - e^{-Q} \sum_{k=0}^{L-1} \frac{Q^k}{k!}$
- $P_{FA} = P_r\{N_{n_\tau} \geq L, \text{ SOMETIME DURING } T\} = 1 - \exp\left\{\frac{-n_b T (n_b \tau)^{L-1}/(L-1)!}{\sum_{k=0}^{L-1} (n_b \tau)^k/k!}\right\}$
- REF: LEE & SCHROEDER, IEEE TRANS. INF. THY, IT-22, 114 (1976).

Fig. 7 - Theoretical basis for detection and false alarm calculations

PROBABILITY OF DETECTION VERSUS THRESHOLD LEVEL

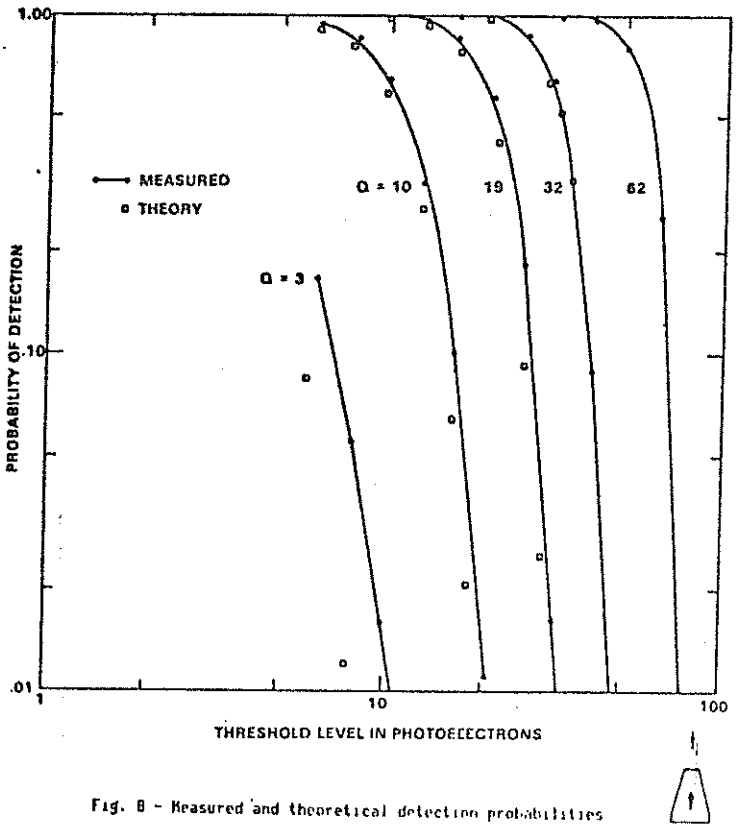

Fig. 8 - Measured and theoretical detection probabilities

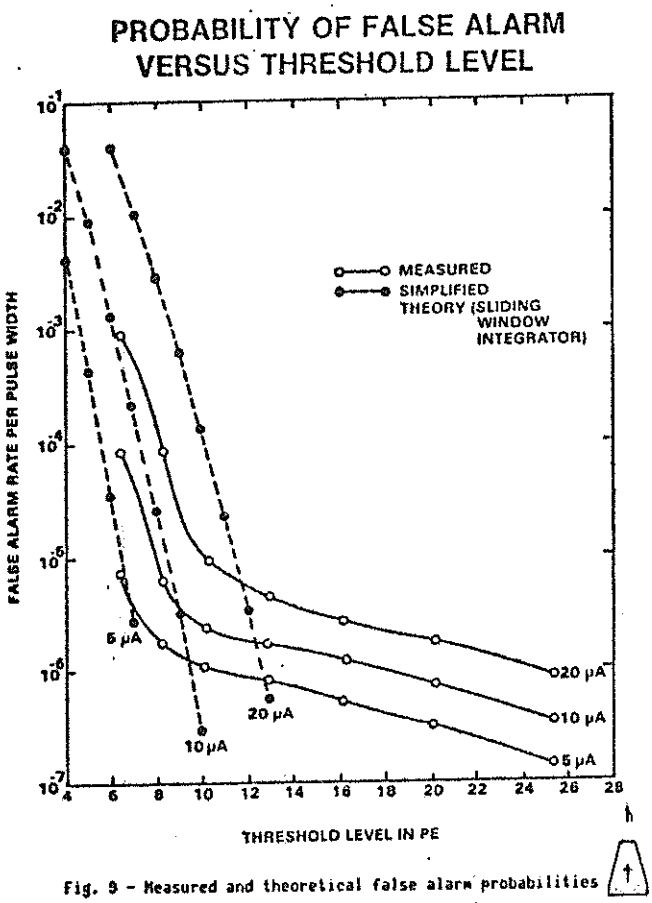

Fig. 9 - Measured and theoretical false alarm probabilities

SIMPLIFIED THEORY

TIMING PERFORMANCE:

- ASSUME:
  - ML RECEIVER WITH RAISED COSINE
  - OPTICAL PULSE
  - $\lambda n = 0$

- $\sigma_R = \frac{\tau}{2\pi\sqrt{Q}}$, τ = TRANSMITTED PULSE FULL WIDTH AT BASE,

  $Q = \int_{T/2}^{T/2} \lambda_s(t)dt$ = EXPECTED SIGNAL COUNT

- REF: BAR-DAVID, IEEE TRANS. INF. THY, IT-15, 31 (1969)

Fig. 10 - Theoretical basis for receiver timing performance

The theoretical timing performance for a maximum-likelihood receiver operating with a raised-cosine optical pulse is shown in Figure 10. For background rates which are less than 10% of the expected signal count within the optical pulse width, the simple formula in the figure is adequate. This was always the case for the SGRS receiver, since the false alarm probability would have been excessive for higher background rates.

A comparison of theoretical and measured timing performance is shown in Figure 11. The receiver performance was only 0.8 db from theory at the 10 cm ranging level, and 2.7 dB from theory at the 2 cm level. The growth in the difference between the curves is due to the fixed jitters of the amplifiers and the time interval unit in the measurement system. These effects are small compared to the timing jitter caused by the photon-limited signal at low photoelectron levels, but are a relatively larger source at higher photoelectron levels.

A summary of the receiver description and calibration results is shown in Figure 12. The single channel design of the receiver was used to minimize drifts between start and stop channels, while amplitude measurements of both the start and return pulses were used to correct for discriminator time walk. These measurements also were used in a feedback arrangement with variable optical and electrical attenuators to control the gain of the receiver. The timing and detection probabilities were in good agreement with simple theoretical models. The false alarm probabilities were considerably higher than those predicted by theory, due to photomultiplier feedback events. The rate of these events depends upon both the illumination level and the design of the photomultiplier, and must be taken into account when designing multiphotoelectron ranging receivers for daylight operation.

SGRS TIMING PERFORMANCE WITH 7.3 NS LED PULSE

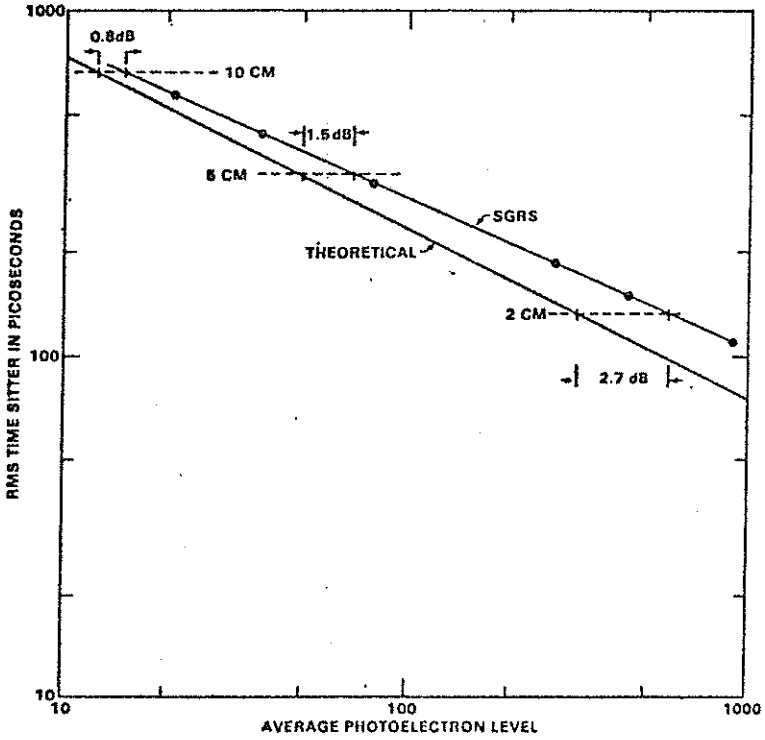

Fig. 11 - Measured and theoretical timing performance

SUMMARY

- SINGLE CHANNEL ML LASER RANGING RECEIVER HAS BEEN DESIGNED BUILT & TESTED
- SINGLE CHANNEL MINIMIZES DRIFTS
- START & STOP AMPL. MEAS. MINIMIZE DISC TIME WALK
- SYSTEM TESTED WITH 7.6 NSEC LED PULSE & CW BACK-GROUND
- TIMING PERFORMANCE { 0.8dB FROM THEORY AT 10 cm / 2.7dB FROM THEORY AT 2 cm
- USED SLIDING WINDOW INTEGRATOR AS THEORETICAL BASIS FOR P_D & P_{FA}
- MEASURED P_D AGREED WITH THEORY FOR SIGNALS IN 10-32 PE RANGE
- MEASURED P_{FA} AGREED WITH THEORY FOR LOW RATES & THRESHOLDS
- FOR HIGH RATES & THRESHOLDS P_{FA} DEPARTS FROM THEORY DUE TO DISC DEAD-TIMES AND PM FEEDBACK EVENTS

Fig. 12 - Summary of receiver description and performance

ATMOSPHERIC TURBULENCE EFFECTS ON LASER RANGING EXPERIMENTS

by P. ASSUS
CERGA, Grasse, France

Abstract. In the recent years, the speckling phenomena have arrested the special attention of many investigators (1,2,3,4) from their fundamental properties and applications in scientific and industrial fields. We study here the effect of this phenomenon on laser ranging (Moon and satellites).

I. INTRODUCTION

The theoretical models and experimental studies on atmospheric turbulence allow us to know light intensity distribution of a star image given by a telescope.

First, let us assume that we have a diffraction limited telescope (D.L.T.).The image of a star through atmospheric turbulence given by a D.L.T. is shown in fig. 1 (very narrow bandwidth):

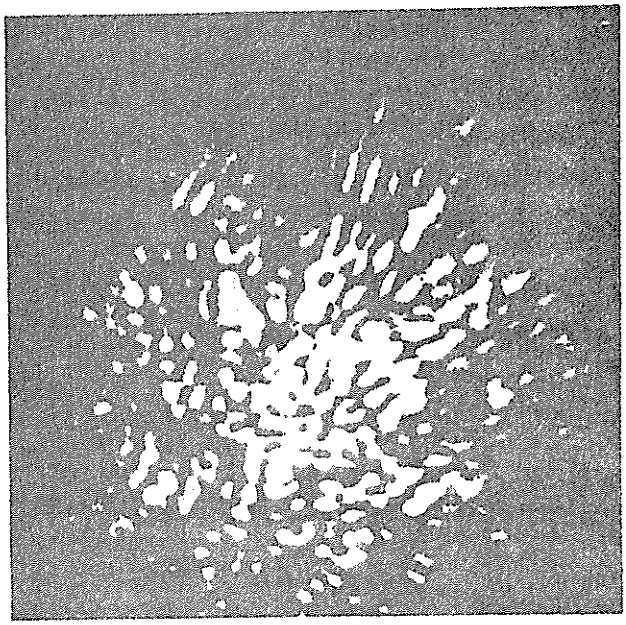

Fig. 1. Speckled image of a stellar point source at the Palomar 200" telescope (by courtesy to Labeyrie)

The diameter of the speckle pattern is given by atmospheric turbulence but the mean diameter of speckles is only given by telescope resolution.

Any variation on the turbulence changes only the number of speckles and the diameter of the speckle pattern.

Example : Lunar laser ranging at CERGA (telescope looking at an unresolved star filtered with a narrow bandwidth) :

$$\text{Speckle diameter} \qquad \alpha = \frac{1.22\lambda}{D} = 0.1 \text{ arc sec.}$$

taking $\lambda = 6943$ Å and telescope diameter $D = 1{,}5$ meter.

II. LASER EMISSION TOWARDS SPACE THROUGH ATMOSPHERE

We have the same phenomenon when the light is a point source in the focal plane of a D.L.T. and the observer is outside Earth atmosphere (light inverse return principle).

The very short duration of laser shooting allows us to consider atmospheric turbulences as frozen during the impulse. Between two following impulses, the position of speckles is completely decorrelated (more than 2 seconds).

III. NATURAL DIVERGENCE OF LASER, OPTICAL POLISHING IMPERFECTIONS, ABERRATIONS.

The natural divergence of lasers is mainly due to inhomogeneities in the amplifying medium. The spatial coherence of laser implies that the laser beam is the result of a diffraction limited beam through an inhomogeneous medium.

This effect is the same for polishing imperfections of "coudé" mirrors or aberrations of the telescope.

The spot diameter grows up with this effect while speckle diameters stay the same. So, the number of speckles grows up with the spot diameter.

We must note that without turbulence, this effect lets conservative positions of speckles in the speckle-pattern during the tracking. For an Alt.Az. mount for instance without "coudé" or telescope mirror imperfections, the position of speckles only turns with the field rotation.

IV. APPLICATION

A/ Lunar laser ranging of CERGA

Ruby pulsed laser natural divergence is about $\beta = 2.5.10^{-4}$ radian for an output diameter, $d = 19$ mm.

At the output of the 1.5 m telescope, the natural divergence will be :

$$\beta' = \beta \frac{19.10^{-3}}{1.5} = 3.2 \cdot 10^{-6} \text{ rad} \qquad \sim 0{,}6 \text{ arc sec.}$$

Atmosphere turbulence is very often situated between 1 and 3 arc sec. which is morely higher.

Taking an average atmospheric turbulence of 2 arc sec., we have about 600 speckles of 1/10 arc sec. diameter each (near 200 m on the Moon) in a spot of 2.6 arc sec. diameter (5 km). Between speckles, there are dark zones where light intensity can decrease down to total extinction. So there is a great difference of light efficiency between bright zones and darker zones.

So, statistic repartition of return power is very influenced by speckled aspect of laser spot. The signal possessing must take it into account(5).

B/ Satellite laser ranging of CERGA

Emission : D = 20 cm
speckle diameter : α = 0.8 arc sec. (about 4 m at 1000 km)

For a pointing problem of the mount, the beam is defocalised and the spot diameter is about 20 arc sec. (100 m at 1000 km). The speckle diameter does not stay the same in a defocalised beam but we can assume that there are a few hundred speckles in the spot. Thus, we have also a great power difference between the returns on account of this phenomenon.

Discussion : is it possible to change these effects of atmospheric turbulence ?

By modifying the emission diameter, the speckle dimension changes. For example, taking an emission diameter of 5 cm * , speckle dimension is about 3.5 arc sec. Turbulence agitation is lower.

Without natural divergence of the laser beam, this hypothesis would nearly neutralize the speckle effect by having only one speckle. But the minimal speckle number is given by laser natural divergence. With the same pulsed ruby laser, we have here :

$$\beta' = \beta \frac{19.10^{-3}}{5.10^{-2}} = 9.5 \cdot 10^{-5} \qquad \sim 19 \text{ arc sec.}$$

---

* Fried defines a correlation length of wavefront perturbation r_0. Usually, 5 cm < r_0 < 10 cm according to turbulence.

The speckle pattern diameter is corresponding to the size of r_0 and speckle diameter to the size of telescope (6)

So we could have therefore about 30 speckles in a spot with diameter of 19 arc sec.

The speckle position in the spot would be conservative. It would be better to have lasers with less natural divergence. In that case, it would be necessary to have :

- good optical surfaces in emission afocal optics,
- good "coudé" mirror adjustments,
- a good relative pointing quality of the mount.

REFERENCES

(1) RODDIER C & F, 1975, J. Opt. Soc. Am. 65, p. 664.

(2) LABEYRIE, A., 1978, "Stellar Interferometry Methods", Ann. Rev. Astron. Astrophys., 16, p. 77.

(3) DAINTY, J.C., "Laser speckle and related phenomena".

(4) ERF, R.K., 1978, "Speckle metrology", Academic Press, New York.

(5) COLLATO, M., 1981, "Possibilités d'utilisation des photodiodes à avalanche pour la détection du laser-Lune du CERGA. Influence de l'existence des speckles sur le nombre de photons de retour", rapport de stage de DEA, Nice University.

(6) FRIED, D.L., 1965, J. Opt. Soc. Am., 55, p. 1427.

A Receiver Package for the U.K. Satellite Laser Ranging System

P.S. Cain, D.R. Hall, R.L. Hyde, D.G. Whitehead

Applied Physics Department
Hull University, Hull, England.

The U.K. Satellite Ranging Facility is to be sited at the Royal Greenwich observatory at Herstmonceux. It will utilise a Contraves Goertz tracking telescope, in common with the Observatory Lustbühel, Graz.

The receiver package is to be mounted in the Cassegrain focus region, and has been designed and is being constructed at the University of Hull.

The object of this receiver is to:

(a) Image the system entrance pupil onto the detector photocathode.

(b) Accommodate a narrow band filter to reduce background signals.

(c) Provide an area for density filtering and a protection shutter.

This has all to be contained in a volume situated within the telescope yoke.

To satisfy all these requirements it is necessary to produce an overall demagnification of x 15 in two stages.

(a) A beam reducing telescope reduces the collimated telescope output by a factor 3 to enable the narrow band filter étendue to be accommodated The density filter and a backscatter shutter is also sited in this part of the beam.

(b) A lens, situated within the detector housing demagnifies by 5 to finally image the telescope mirror onto the photo cathode (0.5m to 2mm). The detector is a Varian photo-multiplier (152S) and the sub system is designed to detect single photo-electron events using the four stop Event Timer designed and built by the University of Maryland.

Fig. 1 shows the receiver package and Fig. 2 the overall scheme.

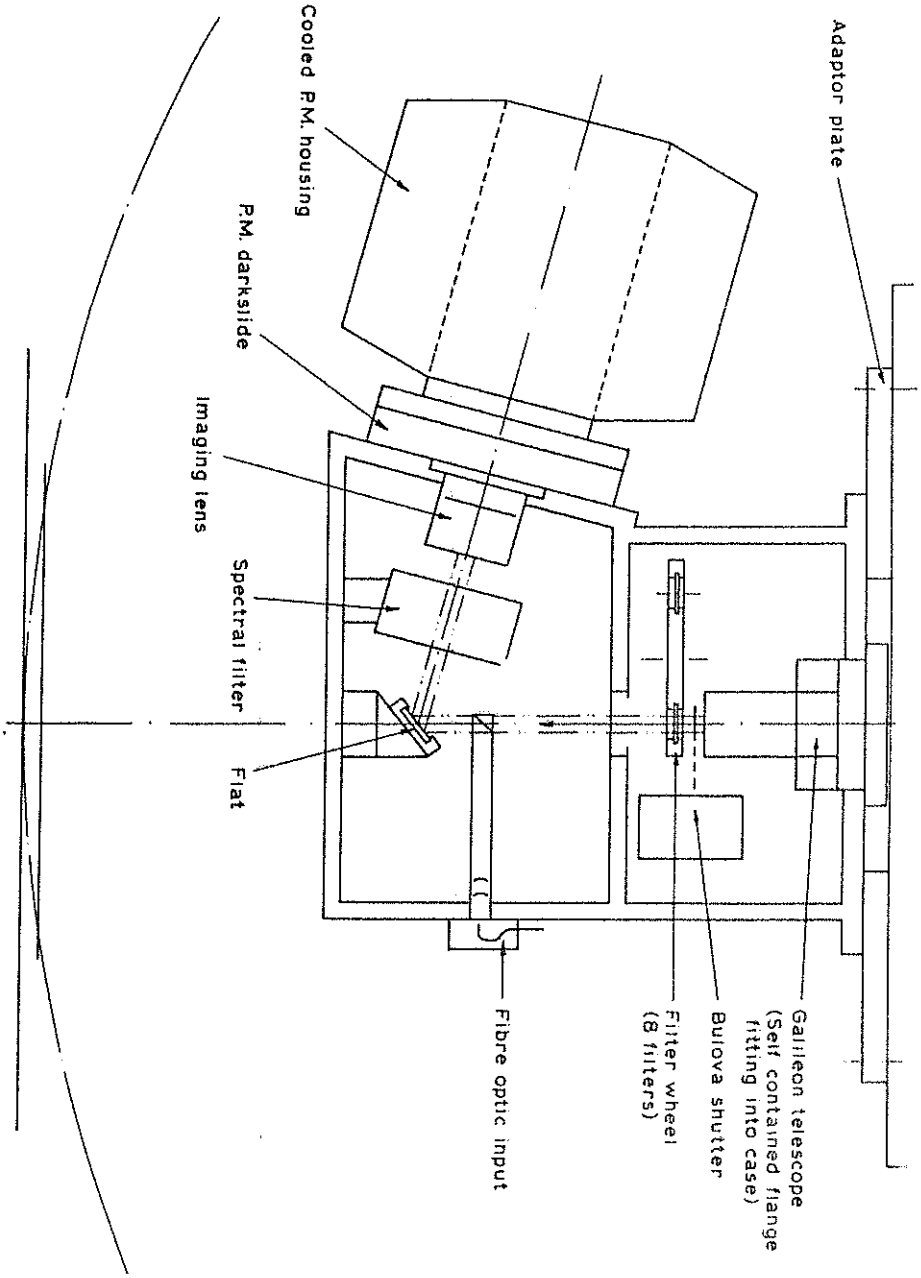

Fig. 1 Receiver: Optical Package.

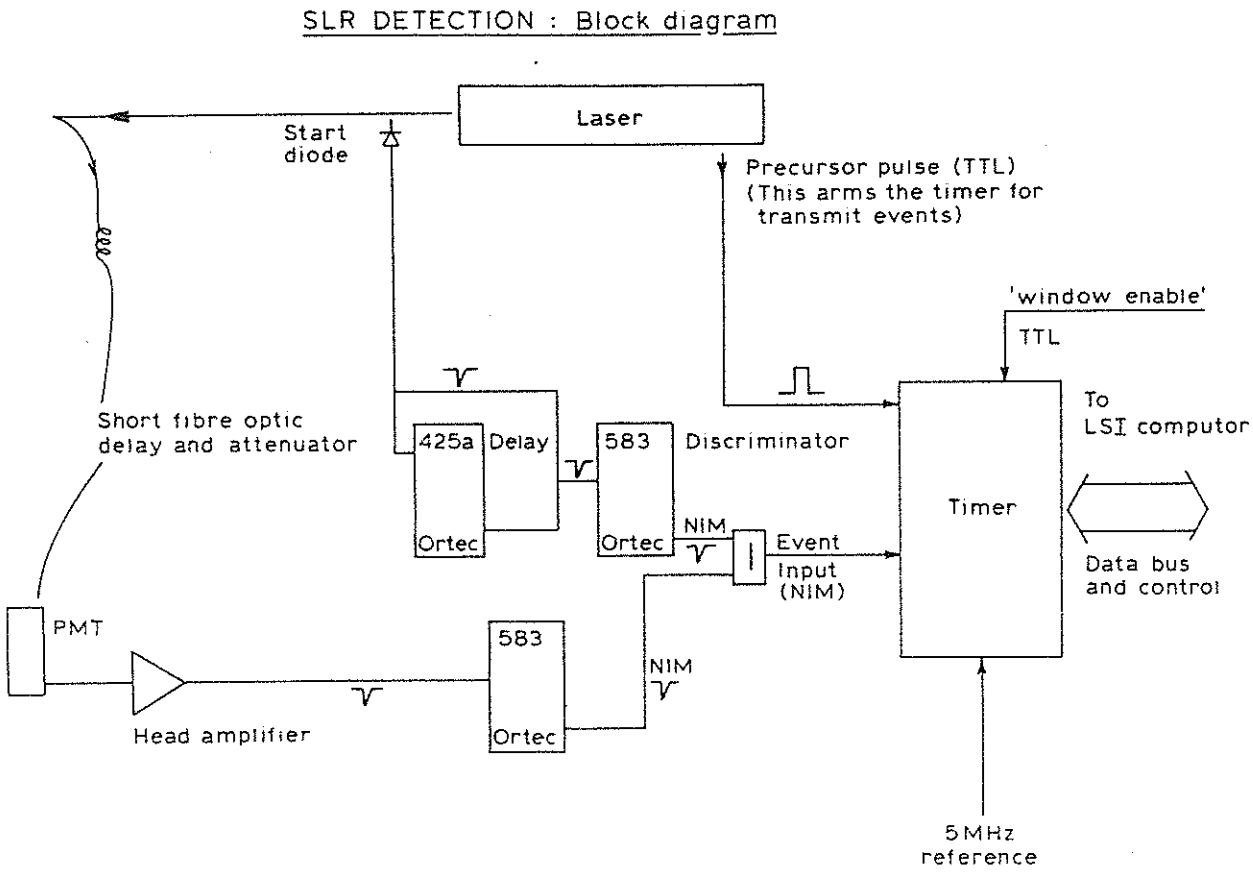

Fig. 2 Receiver: Overall Scheme.

DIGITAL VS ANALOG RECEIVED SIGNAL PROCESSING RESULTS IN 4 NS PULSE LASER RADAR

W.KIEŁEK, A.JASTRZĘBSKI

Technical University of Warsaw, Poland

and

K.HAMAL

Technical University of Prague, Czechoslovakia

INTERKOSMOS group

I ABSTRACT

The results of experimental comparison between some analog and digital estimates of delay at Interkosmos Laser Radar at Helwan for 4 ns laser pulse are described. Results indicate that the digital, software implementations are much better than analog ones for the mean value of result change with signal level. For digital case, there are also results of the influence of number of digitized points on the accuracy.

II INTRODUCTION

We tried to compare the quality of some analog and software digital implementations of the delay estimates using the 4 ns laser station calibration link in Helwan. Comparisons were done for the following estimation methods: analog fixed threshold and half area /median/, and digital software half area /HA/, center of gravity /CG/, half max /HM/, and filtering matched to the signal shape with subsequent finding of the maximum /NML/.

III METHOD OF MEASUREMENTS

The received signal strength control was done via the iris change at the photoelectric receiver. The connections of the electronic instruments used are shown at Fig.1. To make comparisons for the same trials of the signal, we used parallel connection of 2 systems. The analog system of half-area estimate implementation [1] consists of analog integrating circuit, followed by analog constant 0.5 fraction discriminator [2], and PS 500 time interval meter. Constant threshold system consists of constant threshold discriminator built according to [3], followed by minimum range gating circuit and Hewlett-Packard 5360 time interval meter. The digital system consists of the previous one, equipped additionally with Tektronix type 7912AD Programmable Digitizer and Hewlett-Packard 9830 desk-top calculator. The shape of the received signal, at the output of photomultiplier tube PMT, f/t/, /Fig.2./. was digitized and stored in HP 9830. The time interval from the start pulse to the t_R moment of time at Fig.2. was registered in time interval meter. This t_R moment of time occurs when the input signal level crosses, for the first time, the discrimination level of the constant threshold discriminator /set at approx. 120 mV/. The t_R moment of time should be always at the same place at the digitizer screen independent of the input voltage level. But due to some instability of the threshold, and also due to inadequate model of the threshold, there is some instability of this time value.

IV ESTIMATION METHODS

Reiffen and Sherman [4] have showed that the maximum likelihood estimate of delay, for Poisson statistics, can be implemented by the filtration of the incoming pulse signal with the filter matched to the logarithm of the signal shape /quantum limited case/, or matched to the signal shape /high level of additive noise case/ followed by locating the maximum in time. In our case, characteristics of the matched filter must be

composed of the response of the photomultiplier tube, and additional filter. Registering of signal shape of PMT, we need to filter this signal by addi onse only. This additional filter can be obta 1PE pulse time shape and transmitted pulse d of troubles with de-convolution in ti screte fast Fourier transforms of transmi nals, matched and additional filters, he width of matched filter time response r than the width of f_{SER}. From this pe of additional filter time response f such filter in time domain are, may ency domain such filter is fully re mputations of Fourier coefficient

The tim s stable. To compensate for tr ability, there exists the possib btain the additional filter ch ed pulse. Having 1 digitizer tics of additional filter usin the transmitted pulse from uares method.

Othe xed threshold, analog and etector, and digital imp tector. This last one 5], maximum likeli- error/ estimate

that the maximum l t for the ones tatistics, can be ng pulse signal wi nd the digitization e signal shape /qu g using only al shape /high lev e receiving sig- ting the maximum in error, we inter- matched filter must s interpola- hts and 3-d

degree polynomial to approximate the signal between each pair of digitized points.

V RESULTS

Examples of laser pulse used are given at Fig.1 together with mean shape of this pulse obtained using least squares method. Some deterioration of shape when using semiconductor photodiode is visible. Table 1 gives the correlation coefficients between some characteristic time moments in this pulse, and also the standard deviations of them from position of the same moment in mean pulse. Some statistics of signals received from ground target as obtained on 18.07.79., are given in Table 2.

We obtained in some cases non - Poisson results for the number of photoelectrons distribution in the signal reflected from the target. We obtained the variance smaller than expected, the coefficients of this decrease are given in Table 2. It is somewhat strange, when having in mind, that besides of Poisson fluctuations, there are here also transmitted energy fluctuations /± 15%/, atmospheric turbulence and eventually target fluctuations from coherent effects. Probably the last effect does not exist due to, may be, greater than 120 kcps bandwidth of our laser or due to reflecting properties of our wooden, painted, flat target.

The results of comparison of the estimation methods quality, can be seen at Figs 3 and 4 for the material obtained on 18.07.79. In tables and 6 there are the comparisons of results for matched to the signal shape filtering and half-max, when using time steps 98 ps and 686 ps.

The material obtained on 17.07.79. is similar; then, statistical error is of no great influence for the results. The results can be summarized as follows:

a/ time interval bias change with signal level is substantially greater for analog systems than for digital ones

b/ the improvement in standard deviation of results for near maximum likelihood estimate is also substantial

c/ unexpectedly, we obtained better results of both parameters for digital half area, than for digital center of gravity estimate. Also unexpectedly, the results for digital halfmax are better in standard deviation than for both above mentioned. The best are results for near ML estimate /filtration matched to the signal shape/.

We are not succesful up to this time in developing good digital ML estimate. Our filter matched to the logarithm of the signal is not in order - there are fluctuations at the signal after filtering. Due to this effect, the results for such filter are better in standard deviation than for other processing methods for smallest number of photoelectrons only /Fig.3/. We plan to improve this filter, but we have no idea about the fault yet.

The interpolation method used for the signal digitized with the big time step of 686ps was fully succesful. The results of processing for such signal are nearly the same as, for original signal digitized with the 98 ps time step. The differences obtained for such signal in relation to the results of Figs 3 and 4 are summarized in Table 3.

Due to slowness of the measurements /hours/, the long-term stability of measuring system is of value for the results. Also the statistical error can be big for used sample size. But the results obtained on 18.07. are similar to the ones obtained on 17.07., so the influence of the statistical error can be much smaller than bounds.

The analog components of digital circuit, such as constant threshold discriminator, or digitizer and time interval meter trigger circuits can be the sources of errors, especially for long passes. Using adequate model of work of threshold discriminator is of some value for the results too.

The tables of correlation coefficients /Tables 4, obta-

ined for original received signals/ reveal above 90% correlation between half-max and near maximum likelihood estimates. The difference in results between them is small for standard deviation and, unexpectedly, for bias too /Figs 3 and 4/.

VI REFERENCES

1. Hamal, K.et al. Observations of Artificial Satellites of the Earth, No 19 /Interkosmos publication/
2. Polish patent No 102469
3. Basiładze, S.G., 1972; International Institute of Nuclear Research, USSR,Dubna, Report No 13-6331
4. Reiffen, B., Sherman, H., 1963; IEEE, p.1316
5. Bar-David I., 1969. IEEE Trans. IT-15, p.31
6. Bar-David I., 1975. IEEE Trans. IT-21, p.326

Table 1. Laser signal data

Moment of interest	Stand. dev. ns	Cross-correlation coefficients					
		CG	HA	MX	HMX	FR	MR
CG	.12						
HA	.10	.70					
MX	.14	-.34	-.48				
HMX	.11	-.08	-.34	.02			
FR	.11	-.10	-.36	.12	.87		
MR	.20	.04	-.38	.15	.39	.28	
FT	.18	.44	.27	-.34	.55	.49	.24

where:
CG-center of gravity
HA-half area
MA-maximum
HMX-half max. at front
FR-half /in voltage/ of the fast rise region at front of the pulse
MR-Point in time, at which the derivative of voltage is first time half of its max. value at front of the pulse
FT-fixed treshold

Table 2. Signal from target data.

Iris No	7	8	9	9
Mean value of the amplitude /mV/	848	413	209	205
No of trials of the signal	29	26	24	27
RMS value of deviations of the amplitude /mV/	202	103	77	57
Mean value of the area /mV.ns/	8130	4128	1723	1820
RMS value of deviations of the area /mV.ns/	1645	1038	592,5	535
Variance of area decrease coefficient in relation to Poisson distribution	1	1,25	1,6	2,1

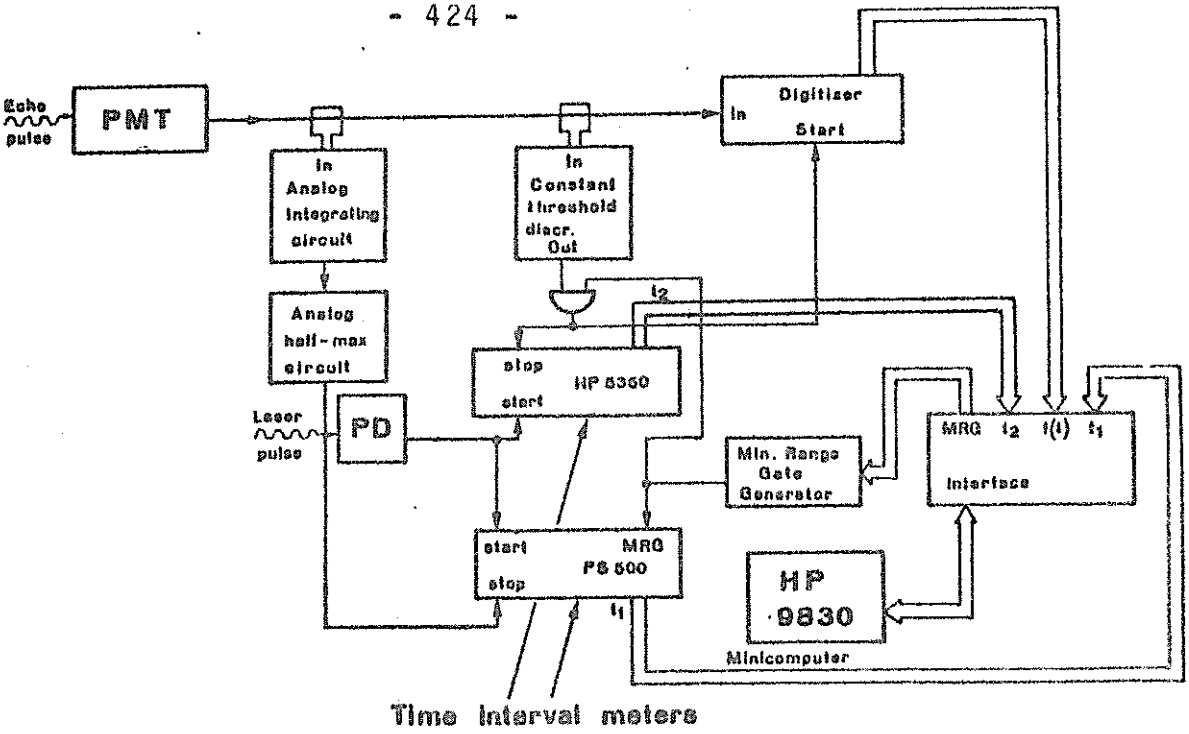

Fig.1. Scheme for the analog and digital time delay estimates comparisons.

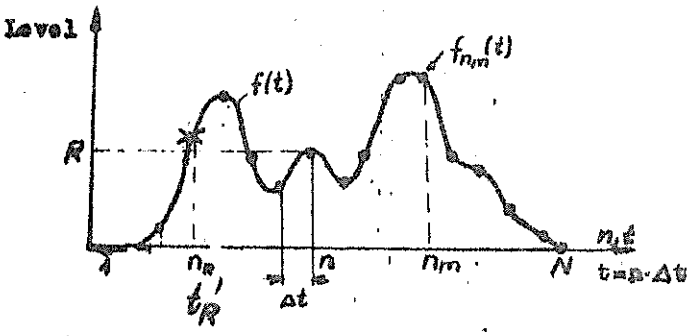

Fig.2. f(t) example at the digitiser

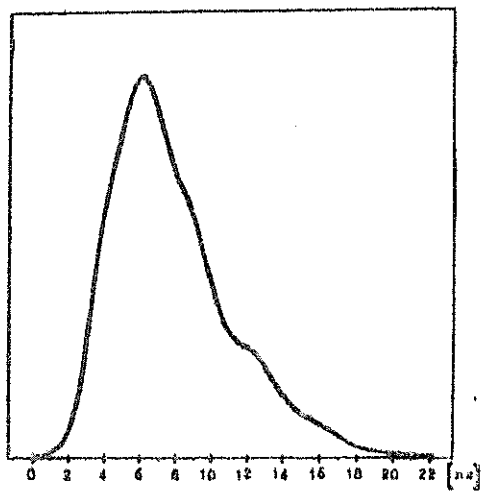

Fig.5. Averaged shape of transmitted pulse from the sample on 21.07.

Influence of digitization time step - differences in cm

for mean value - Table 5 for standard dev - Table 6

PE	CG	HA	HM	ML	NML	CG	HA	HM	ML	NML
5,37	0	0	-1,5	-4,5	-1,5	-0,15	-0,3	-0,15	+0,07	-0,3
6,25	-0,7	+0,4	-0,6	-3	0	+0,15	+0,15	-0,15	+1,9	+2,1
14,6	0	0	0	0	0	+0,3	+0,15	0	+0,3	-0,15
28	0	0	0	-1,5	-1,5	0	-0,15	0	-0,15	-0,15

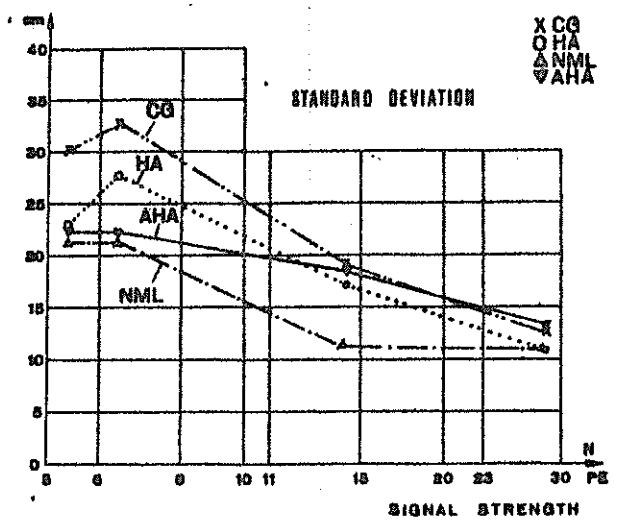

Fig. 3a

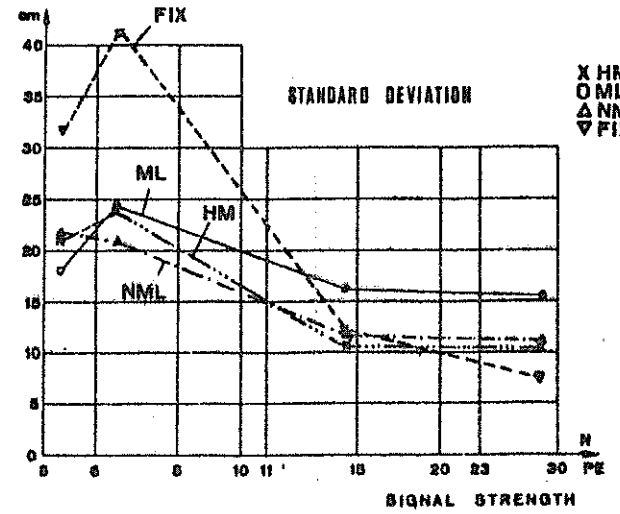

Fig. 3b

CG center of gravity

HA digital half area

HM half max

NML filter matched to the signal shape

AHA analog half area

FIX fixed threshold

Tables 4. Correlation coefficients in %

6 photoelectrons

	CG	HA	HM	NML	AHA
HA	93				
HM	68	74			
NML	63	74	96		
AHA	80	92	75	77	
FIX	77	83	95	93	76

11 photoelectrons

	CG	HA	HM	NML	AHA
HA	90				
HM	38	46			
NML	57	66	91		
AHA	66	69	34	47	
FIX	57	58	63	66	83

23 photoelectrons

	CG	HA	HM	NML	AHA
HA	87				
HM	61	62			
NML	71	75	97		
AHA	50	67	47	37	
FIX	52	54	45	50	67

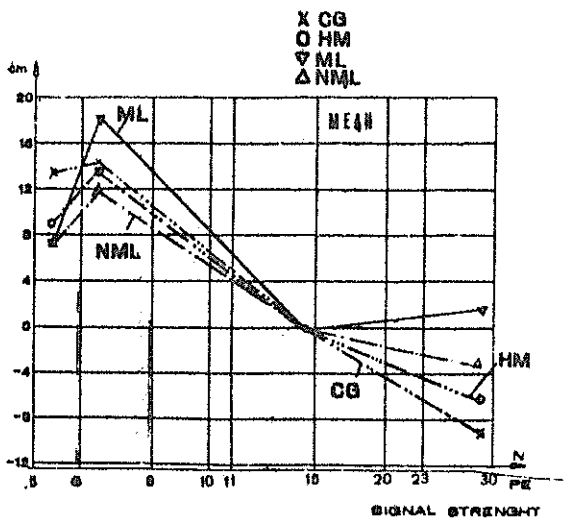

Fig. 4a

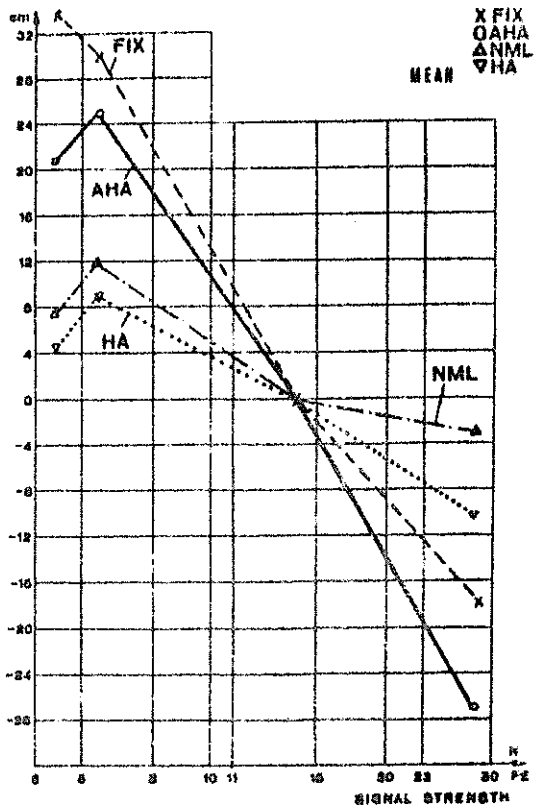

Fig. 4b

COMMENTS ABOUT RECEIVED ENERGY FLUCTUATIONS

W.KIEŁEK

Technical University of Warsaw, Poland

K.HAMAL

Technical University of Prague, Czechoslovakia

S.SCHILLAK

Borowiec observatory, Poland

INTERKOSMOS group

There exists the opinion, that laser reflections from goedetic satellites, in multielectron case, fluctuate nearly exponentially in energy due to coherence effects at retroreflector([1], [2], [3], [4]). Some experimental results are in agreement with this opinion (see Fig.1 drawn from [5]). But some our results from Borowiec 1-st generation station in Poland are only of little fluctuations (Fig.2).
Coherence effects are independent on energy, and are of the type, that when do not exist once, do not exist at all.
Our opinion is, that this effect does not exist, at least in the case of our multimode 20 ns laser. One possible explanation of this phenomenon can be as follows: Suppose, that the laser is not of single frequency, but the spectrum occupies some bandwidth, and is continuous or discrete but uniformly filled with energy. The retroreflector array normally has got some depth, or is tilted. When the difference in number of wavelengths at the target depth is near one or greater for extreme frequencies of laser frequency band, all possible phases instead of one phase from each individual corner cube are present at the receiver aperture. This is the situation as in the case of incoherent light, and amplitude fluctuations are absent.

This realizes typically for about 700 MHz bandwidth, which means spectral line width of 0.05 A^{o}. The bandwidth of laser

can be smaller than this value or as great as 10 GHz for some multimode YAG, and both possibilities exist, to have or not to have coherency effects in the case of satellite retroreflections.

After inventing of this explanation, we found the similar opinion in [7].

The difference in wavelength number for extreme frequencies of laser frequency band at the distance between the plane at the satellite, parallell to the receiver aperture, and this receiver aperture, can not give similar averaging effect. But the explanation given in [7] at page 112 is unconvincing for us. Due to lack of space, our own explanation is available at request.

For the calibration link and flat, wooden, painted target we obtained, in our opinion, Poisson and PMT gain fluctuations only, in case of 4 ns laser at Helwan, summer of 1979 - see Table 1 and Fig.3.

For the sample of 60 calibrations of 20 ns laser at Borowiec, for approx. 200 PE signals, the fluctuations are greater than Poissonian, but can be explained by PMT gain, atmospheric turbulence and transmitted power fluctuations, being typically 17 % for standard deviation in relation to mean value.

Then, in our opinion, the "rough target" concept, developed for radio and microwave region targets [6] is inapplicable for our case.

Literature

1. J.I.Bufton, R.S.Iyer, L.S.Taylor. Applied optics vol.16 No 9, p.2408-2413
2. J.L.Bufton. Applied optics, vol.16 No 10, 1977, p.2654--2660
3. D.A.Arnold. SAO Special Report No 382, p.117-149
4. D.A.Arnold. Optical and IR transfer function of the Lageos retroreflector array. SAO Report for NASA, May 1978, p.159-178
5. M.Pearlman et al. Lageos orbital acquisition and initial assessment. S.A.O. report, 1976
6. R.L.Mitchell. Radar signal simulation. Artech House, 1976 pp.17,22,23,32
7. R.H.Kingston. Detection of optical and IR radiation. Springer, 1978, pp.110-113

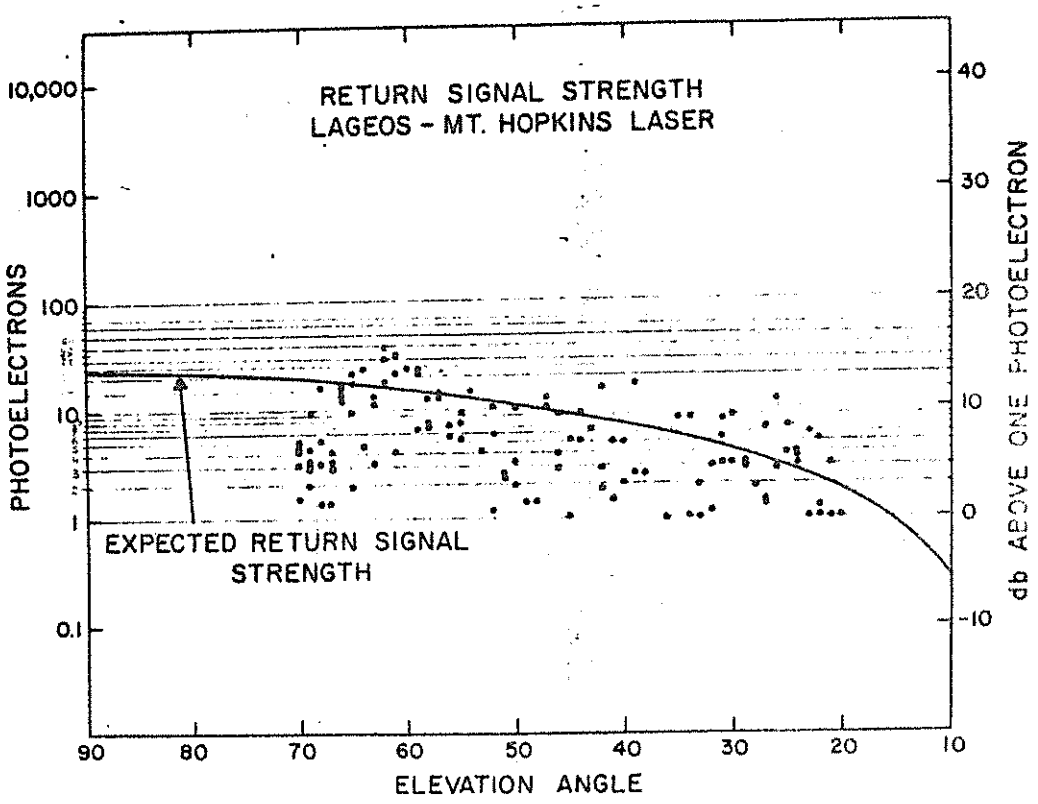

Fig. 1 Example of satellite signal strength data, Mt Hopkins USA

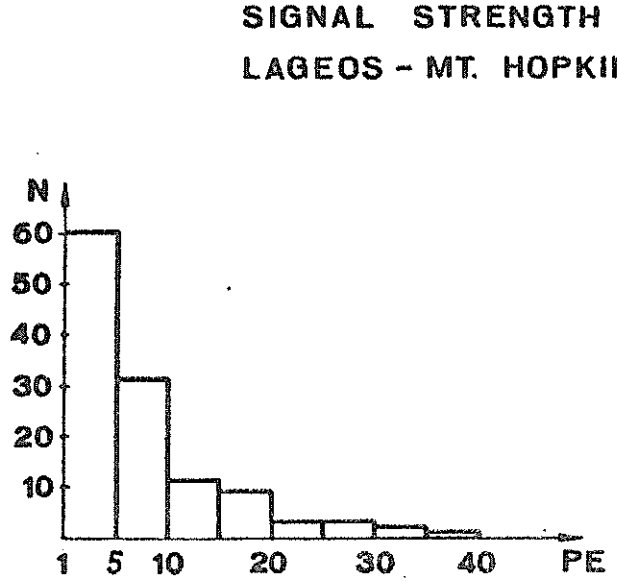

Table 1. Characteristics of target calibration signals, Helwan

Mean signal strength in PE	5,3	6,3	14,6	26,5
Standard deviation in PE	2,36	2,44	2,36	5,36
Variance decrease coefficient in relation to Poisson density	1,5	1,95	1,2	0,92

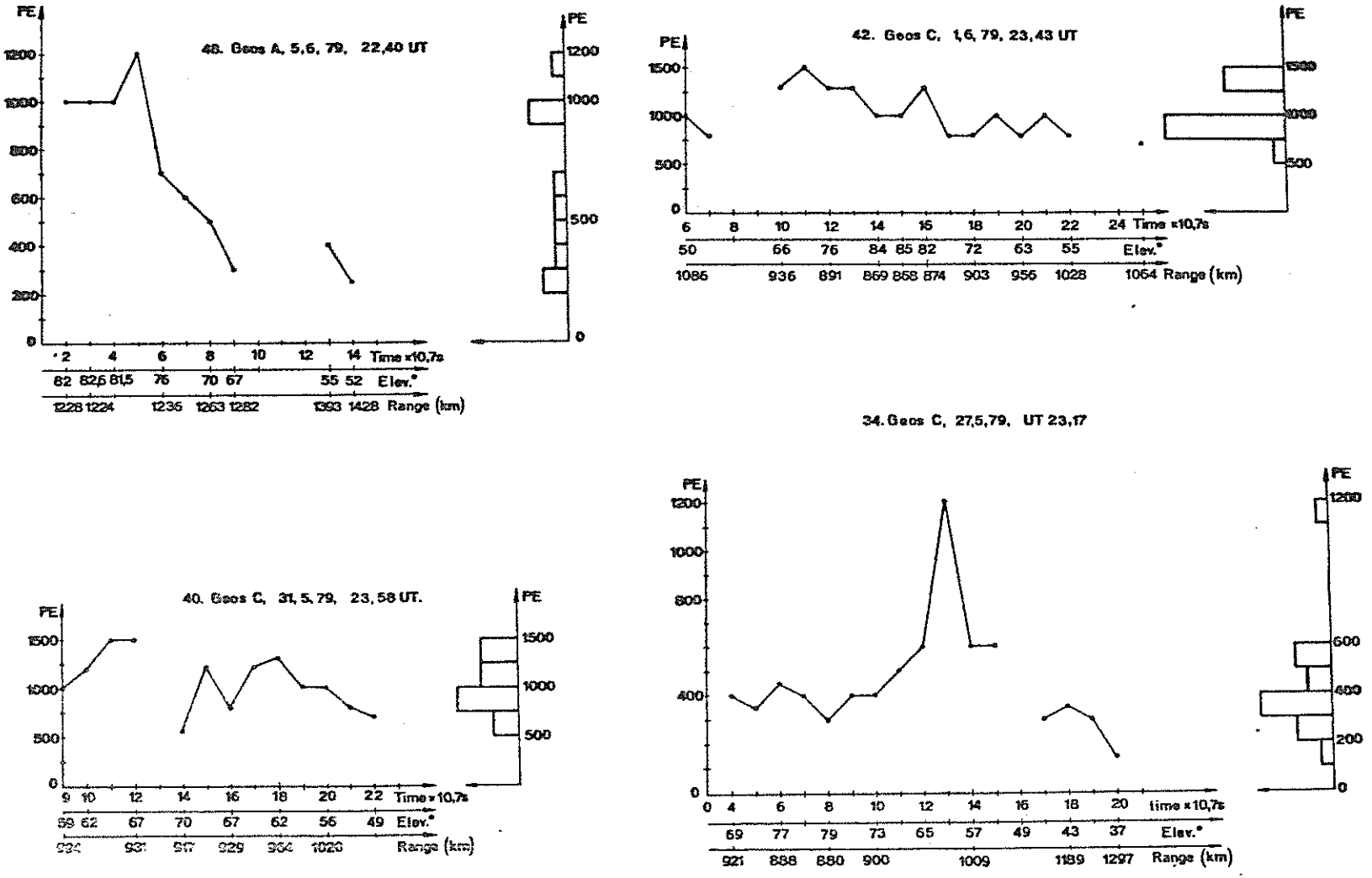

Fig.2. Examples of satellite signal strength data, Borowiec, Poland

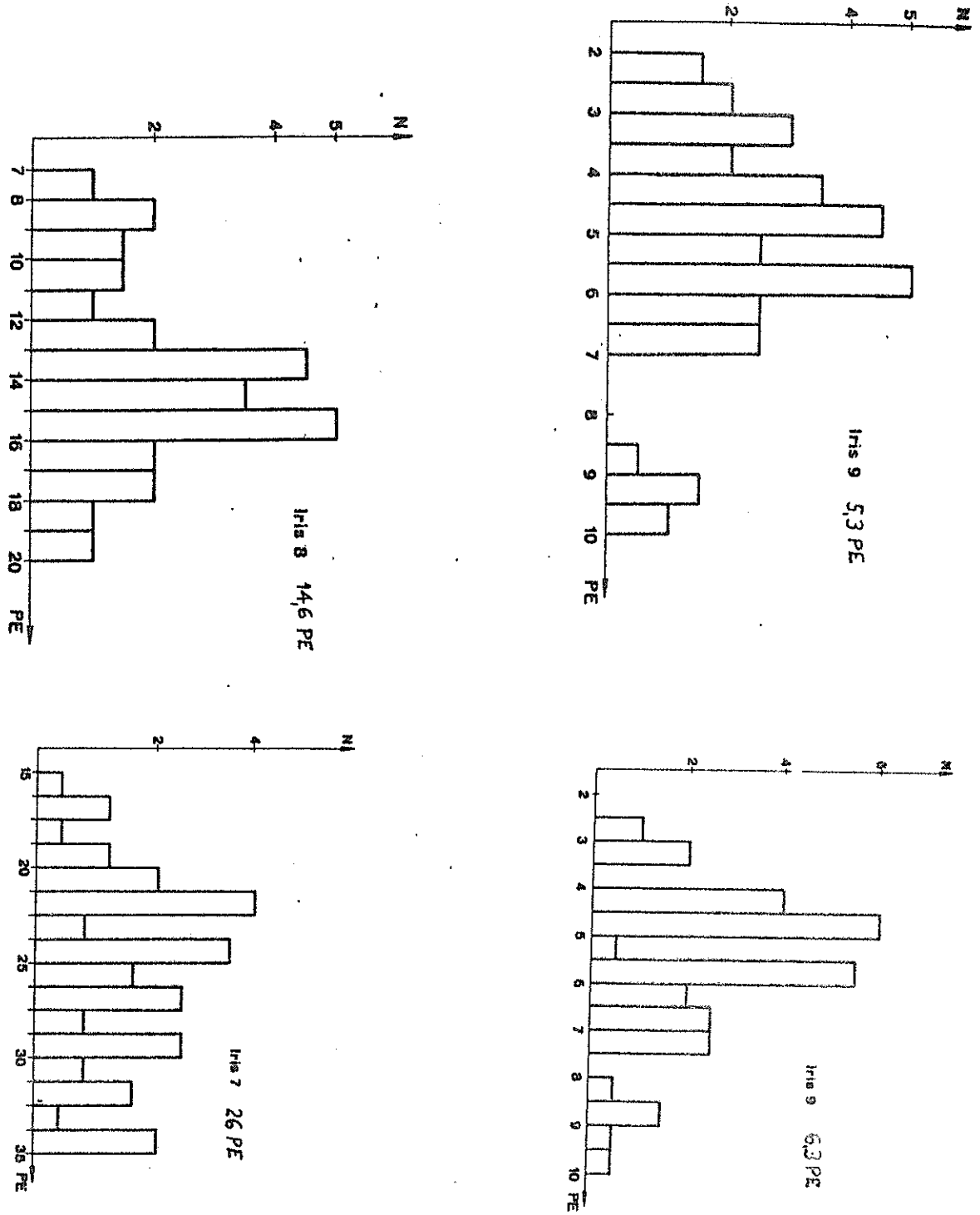

Fig.3. Calibration target signal strength densities, Helwan, Egypt.

USE OF APPROXIMATED MATCHED FILTERING AND PHOTON COUNTING IN SATELLITE LASER RANGING

Matti V. Paunonen*

Finnish Geodetic Institute
Ilmalankatu 1 A
SF- 00240 Helsinki 24, Finland

1. INTRODUCTION

The application of matched filtering in estimating the arrival time of a light pulse is well known /1-3/. The photoelectron impulses are applied to a filter with an impulse response of $\ln [1 + S(T_d-t)/n_B]$, where $S(T_d-t)$ is the delayed, time-inverted shape of the signal intensity, and n_B is the background noise rate. The peaking time is then the best estimate of the arrival time (the maximum likelihood estimation). The filter shape $S(T_d-t)$ has also been shown to give good results with Q-switched laser pulses, especially under high background noise/4/.The implementation of these filters can be somewhat tedious, and so approximate forms are also worth studying /5,6/.

The return signal from the distant LAGEOS satellite (height 6000 km) is about 1000 times weaker than the signal from the close Earth satellites and may contain only single photoelectrons. A technique called photon counting can then be used.

This report describes the detection equipment and some results of the use of approximated matched filtering both during night and daylight operation and photon counting

---

*Also with the Communications Laboratory, Helsinki University of Technology, SF- 02150 Espoo 15, Finland

in satellite laser ranging at the Metsähovi laser station.

2. EQUIPMENT

The ranging apparatus is described elsewhere /6/. In the receiver the photoelectron impulses from the photomultiplier (RCA 8852 and C 31034 are used) are filtered using an amplifier-filter with an impulse response shape best described by

$$h(t) = t \cdot \exp(-t/\tau), \quad t \geq 0 \qquad (1)$$

which is a low-order approximation (two low pass stages) of the Q-switched laser pulse shape, adequately given by $\exp(-t^2/2\sigma^2)$, with proper τ and σ to give equal half-widths. The time interval counter (Nanofast 536B, M/2 half-maximum timing unit, resolution 0.15 ns) detects the 50% point of the incoming pulse. The duration of the laser pulse and the impulse response of the detector system are about 25 ns. The start pulse is filtered in the same way, to lessen the effects due to laser mode interference. Theoretical degradation in the resolution with respect to the optimal scheme is by a factor of 1.47 /8/, if no background noise is present. Because the average timing point depends on the photoelectron content of the received pulse /9,10/, it is necessary to calibrate the system using the signal levels expected in the ranging. The trigger levels used are 1, 6 and 15 photoelectrons for LAGEOS, STARLETTE and GEOS-3, respectively. The level of amplification is adjusted by the feed voltage to the photomultiplier.

3. RESULTS

3.1. Calibration measurements

Calibration measurements are performed using a flat target at a distance of 333 m. The resolutions of an analog median detector /11/(integration with long RC-time constant and 50% detection) and the approximated matched detector under discussion were found to be very similar when the return energy was high (more than 200 photoelectrons). The r.m.s. resolutions of a single shot were in the range 0.5 to 0.8 ns using about 600 photoelectrons. When the average return was 10 times smaller, the performance of the approximated matched detector appeared to be somewhat better. The return signal at the signal levels was highly fluctuating. The timing shift was less than 1 ns.

In order to test the instrumental resolution the ranging operation was performed to a diffusely reflecting plate at a distance of 4 m from the photomultiplier. The standarddeviation of a single measurement was 0.23 ns after removing a slight timing drift and observations deviating by more than three times the standard deviation(5 out of 116 observations).

3.2. Ranging to satellites

Range observations to satellites have been performed since 1978. Two examples of range residuals after short arc orbit fitting are shown in Fig. 1. The standard deviations are 0.27 m and 0.22 m. No deletions were made. Generally the precision has been in the range of 0.3 m to 1 m in night work.

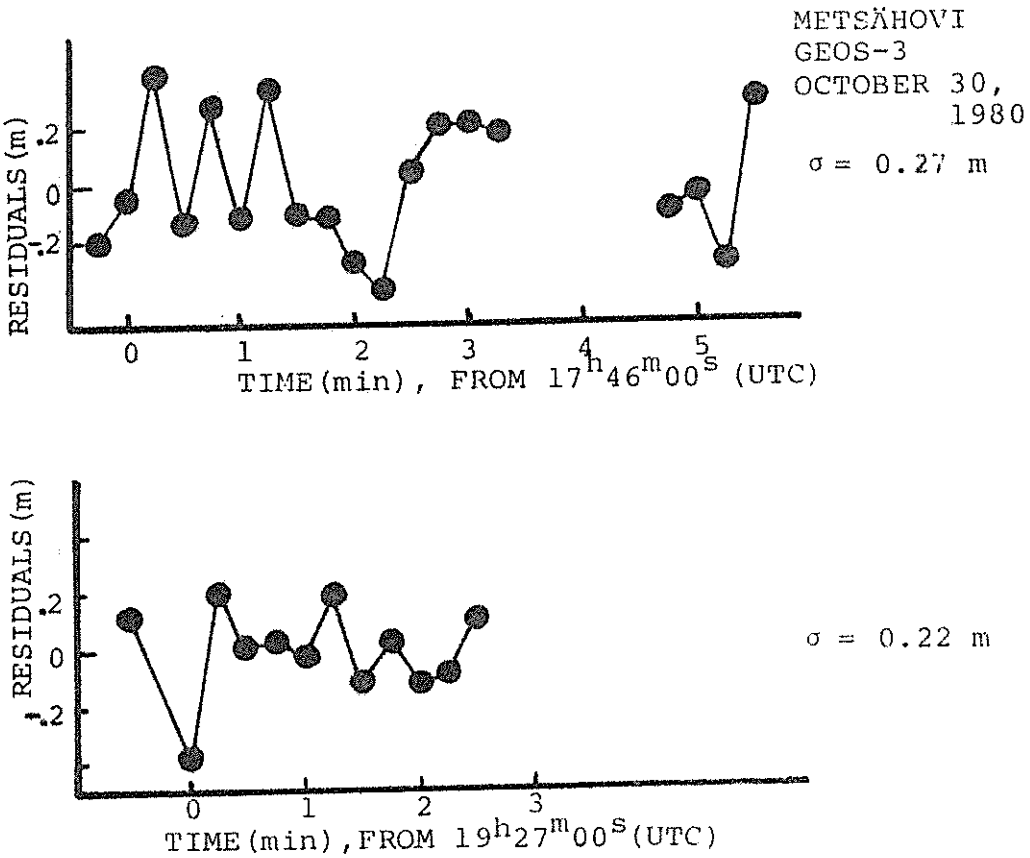

Fig.1. Two examples of range residuals after short arc fitting.

Some improvement in performance could be obtained, at least theoretically, by preintegration before the filter (i.e. moving towards median detection). The error performance of this method, both in resolution and bias, has been found to closely approach the ideal /10/ if the pulse and filter shapes are equal Gaussian. The method could also be called filtered median detection. This principle, using the filter given by Eq. 1, is at present being tested in ranging to satellites.

3.3. Daylight ranging

Daylight operation was recently found feasible with the equipment in use. The field of view of the receiver was reduced to 1.2 mrad and the voltage of the photomultiplier RCA 8852 to -1650 V, which produced an anode current of 0.3 mA. The appropriate PMT voltage was obtained by adjusting the voltage until the counter was stopped by the background noise not more than once per 10 dummy trials. The time offset of GEOS-3 and its time derivative were determinated from the preceding night's observations. On November 5, 1980, six concecutive passes of GEOS-3 were observed. The first two of these were under a bright sky, the next just after the sunset and three passes were observed in darkness. The data from short arc orbit fits are shown in Table 1. The quality of the measurements of the daylight passes differs little from that obtained in darkness. This demonstrates the advantage of the approximated matched filtering under high background noise conditions.

Table 1. Short arc orbit fits of GEOS-3, Nov. 5, 1980

Time (UTC)	Pass duration	Observations	Obs.	Fit (m)	Light conditions
$11^h20^m31^s.4$	3^m45^s	13	13	0.57	Daylight
12 59 31.4	5 45	19	17	0.52	"
14 38 16.4	6 00	14	13	0.53	Sunset 14^h17^m
16 17 01.35	5 15	15	15	0.51	Dark
17 54 31.4	7 15	18	18	0.83	"
19 34 01.55	5 15	17	17	0.91	"

3.4. Photon counting and ranging to LAGEOS

The range equation for LAGEOS predicts a signal about 1000 times weaker than that from GEOS-3. For this reason its ranging is generally considered difficult for systems designed mainly for close orbiting satellites. Because signal prediction left some hope to acquire LAGEOS, attempts at ranging have been made at the Metsähovi station from the very beginning. The gain of the photomultiplier (RCA 8852) was increased (voltage -2500 V, gain about 10^8) until single photoelectrons triggered the timing discriminator. Hence the first photoelectron within the range window, whether signal or noise, stops the counter. This method is called single photoelectron detection, or photon counting. It is well known in nuclear electronics and is also regularly used in ranging to the Moon /12 / and now also in satellite laser ranging/13,14/.

The propability of occurrence of the first photoelectron is /15/

$$R_1(t) = NS(t)\exp[-N\int_0^t S(t')dt'] , \qquad (2)$$

where N is the average photoelectron content of the pulse and S(t) its normalised shape. When the signal is very weak, say less than 0.1 photoelectrons on average, $R_1(t)$ can be approximated as /15/

$$R_1(t) \propto S(t) . \qquad (3)$$

The probability also follows the illumination curve. The variance of the occurrence time is the same as the variance of the pulse shape. For Gaussian light pulses the timing standard deviation is

$$\sigma_t = 0.425\ T,$$

where T is the pulse duration (FWHM). The effect of single electron time jitter of the RCA 8852 photomultiplier is insignificant with 25 ns long laser pulses.

Use of a higher threshold quickly invalidates the photon counting method. If the average return rate is 30% , use of the threshold of two photoelectrons would give six times fewer signal counts.

The photon counting method can effectively be used only under low noise conditions, i.e. dark sky and a cool detector, without multistop counters. The range gate used, 10 - 20 μs, has been sufficient to give a satisfactory signal-to-noise ratio. Noise counts have sometimes amounted to 10-

20 %,but this does not yet represent any significant loss in signal counts or difficulties in signal recognition.

The summary of the LAGEOS observations for the period of March-April 1980 are shown in Table 2. The average precision is 0.9 m after slight statistical screening of the observations.

Table 2. LAGEOS observations in March-April 1980

Date	Time (UT)	Pass duration	Obs.	Sterne orbit fit Deleted	σ/m	Polynomial O-C fit Deleted	σ/m	Degree
10 III	$18^h22^m15^s$	20^m30^s	16	0	1.52	o	1.46	4
13	17 50 15	26 00	39	4	0.84	4	0.87	6
13	21 28 30	18 15	27	2	0.69	2	0.63	4
14	19 58 45	28 30	60	-	-	3	0.51	6
15	18 36 15	28 15	42	3	0.80	2	0.53	6
16	17 12 00	27 15	15	2	1.28	2	1.09	4
19	20 11 45	29 45	27	1	0.97	1	0.76	6
20	18 46 45	34 15	50	-	-	4	0.93	6
22	19 46 15	21 45	18	3	0.82	2	1.17	4
23	18 12 45	33 30	48	-	-	3	0.78	6
23	22 05 00	9 15	8	0	0.60	0	0.93	2
24	20 28 30	22 30	21	1	0.96	1	0.86	4
25	19 02 00	33 15	29	4	1.20	3	1.34	6
22 IV	19 45 30	25 00	20	0	0.83	0	0.88	4

Median 0.88 m
Arithmetic mean 0.91 m
Deletion level 6.5 %
Quadratic mean 0.95 m
Weighted mean (pooling) 0.88 m

An example of range residuals in a short arc fit are shown in Fig. 2. Three observations with deviations of 4.1 m, 1.9 m and 1.8 m were deleted. It is probable that not all events are single photoelectron ones. This does not adversely affect the ranging precision because of the smoothing property of the approximated matched filtering. In a monitored pass (April 22) there were 20 signal events from 102 trials and 5 noise events. Most events were seen to contain a single photoelectron and only two larger pulses containing two photoelectrons were noticed (RCA 8852 tube with high gain first dynode is suitable for estimating the photoelectron content at this level). The fit obtained, 0.83 m, conforms well with the data obtained in March.

In ranging to LAGEOS averaging can be used over three

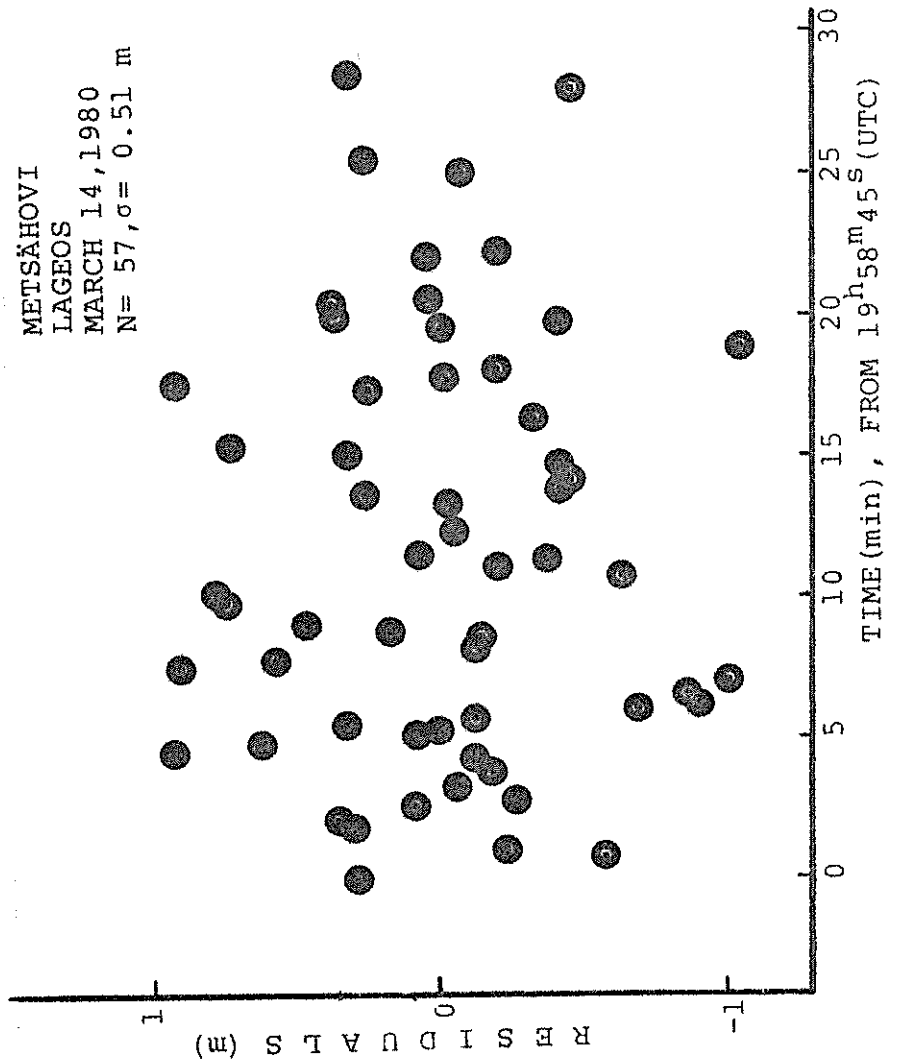

Fig. 2. Range residuals in a LAGEOS pass

minutes, the so-called normal point method /16,17/. Hence the 60 % return rate achieved allows an improvement in precision by a factor of 2.8 (time interval between shots is 15 s). Because the single shot precision has been 0.9 m, the normal point precision could be 0.3 m. This figure corresponds to a relative precision of about $4 \cdot 10^{-8}$. Some passes have shown an even better precision. In the light of these figures, ranging to LAGEOS and the close-Earth satellites gives equal range precision, which is perhaps an unexpected result. The precision achieved is also close to the theoretical value.

4. CONCLUSION

The use of approximated matched filtering in receiving Q-switched laser pulses has been found experimentally to be advantageous, especially in a low-signal regime. Performance in daylight operation was also found to be satisfactory. The same equipment can be effectively used in photon counting, simply by increasing the gain of the photomultiplier.

5. REFERENCES

/1/ B.Reiffen and H.Sherman, An optimum demodulator for Poisson processes: Photon source detectors. Proc. IEEE 51,10(1963)1316-1320.

/2/ I.Bar-David, Communication under the Poisson regime. IEEE Trans. Information Theory IT-15,1(1969)31-37.

/3/ J.B.Abshire, Comparison of measured and theoretical performance of a maximum likelihood laser ranging receiver. J. Opt. Soc. Am. 70,12(1980)1595.

/4/ E.Gatti and S.Donati, Optimum signal processing for distance measurement with lasers. Appl. Opt. 10,10 (1971)2446-2451.

/5/ V.A.Ovsyannikov and A.M.Romanov, Accuracy of timing photoelectron pulses. Sov. J. Opt. Tech. 40,10(1973) 651-652.

/6/ M.Paunonen, Estimation of the arrival time of light pulse using approximated matched filtering. Paper presented at the Third International Workshop on Laser Ranging Instrumentation, Lagonissi, Greece,May 23-27, 1978.

/7/ M.Paunonen, Metsähovi satellite laser ranging station. This conference.

/8/ O.Ojanen, unpublished (1977)

/9/ W.A.Kiełek, Influence of detecting system on the accuracy of laser pulse range meters. Proc. European Conf. on Precise Electrical Measurement (Euromeas.-77), IEE Conf. Publ. 152, 1977, 44-46.

/10/ O.Ojanen, On the analysis of the return pulse of the satellite laser. Reports of the Finnish Geodetic Institute, 79:1, Helsinki 1979, 38 pp.

/11/ A.B.Sharma and S.J.Halme, Receiver design for laser ranging to satellites. IEEE Trans. Instrum. Meas. IM-30, 1(1981)3-7.

/12/ S.K.Poultney, Single photon detection and timing in the lunar laser ranging experiment. IEEE Trans. Nucl. Sci. NS-19,3(1972)12-17.

/13/ C.O.Alley, J.D.Rayner, R.F.Chang, R.A.Reisse, J.Degnan, C.L.Steggerda, L.Small, and J.Mullendore, Experimental range measurements at the single photo-electron level to the GEOS-A and BE-C satellites. Paper presented at the Third International Workshop on Laser Ranging Instrumentation, Lagonissi, May 23-27, 1978.

/14/ E.C.Silverberg, Early laser ranging data with the TLRS. CSTG Bulletin, No 2, Nov. 1, 1980, 70-73.

/15/ S.K.Poultney, Single photon detection and timing: experiments and techniques. Advances in Electronics and Electron Physics (Ed. L.Marton),vol. 31, 1972, pp. 39-117.

/16/ R.I.Abbott, P.J.Shelus, J.D.Mulholland, and E.C.Silverberg, Laser observations of the Moon: Identification and construction of normal points for 1969-1971. Astron. J. 78,8(1973)784-793.

/17/ P.L.Bender and C.C.Goad, Probable Lageos contributions to a worldwide geodynamics control. Proc. Int. Symp. on the Use of Artificial Satellites for Geodesy and Geodynamics (Ed. G.Veis and E.Livieratos), National Technical University of Athens,Athens 1979, pp. 145-161.

DETECTION PACKAGE FOR THE GERMAN/DUTCH MOBILE SYSTEM

H. Visser
Institute of Applied Physics, Delft, The Netherlands

F.W. Zeeman
Delft University of Technology, Delft, The Netherlands

1. Introduction

In a paper entitled "Mount and Telescope for the German/Dutch mobile system", that has been presented during this Workshop, the mechanical and optical configuration of the mobile ranging system has been described. The detection package was left out of the description and this will be presented here. Especially the optical configuration of the detection package has some details that are new in laser ranging. Although the optical/mechanical hardware of the detection system is considerably more complicated than in most laser ranging systems, the operation of the detection system will be simple. In many circumstances the detection system can provide the operator with immediate information on the position of the satellite in the field of view and in the window of the range gate generator. With this information it will be possible to optimize the adjustments of the ranging system so that once the satellite has been acquired it will not easily be lost again because of bad predictions and/or background noise problems.
Because the received light is also directed through the coudé optical train the detection package is mounted in a fixed position at the base of the telescope mount. Such a configuration has the advantages of a less stringent space and weight limitation for the detection package, the controls on the package are always accessible and the number of cables in the telescope mount is considerably reduced.

2. Description of the detection package

In figure 1 the optical configuration of the detection package is presented in a somewhat simplified form. For the ease of the explanation the optical system is drawn entirely in the plane of the paper although in reality this is not true.
As already described in the paper about the telescope mount the received light coming from the telescope is split up at a "dichroic beamsplitter". A wavelength band around the laser wavelength (539 nm or 532 nm, depending on the laser rods) is reflected to the detection optics while the rest of the visual spectrum is transmitted to an eyepiece. The reflected wavelength band is focussed on the "entrance diaphragm" of the detection system. This adjustable entrance diaphragm limits the field of view (FOV) of the detection system to values ranging from 0,05 mrad (10 arcsec) to 1,75 mrad (0,1 degree) in ten discrete steps.
Just in front of the adjustable entrance diaphragm a chopper rotates at a velocity of 10 r.p.s. This chopper is synchronized to the firing of the 10 p.p.s. repetition rate of the pulse laser. The phase of the chopper blade is adjusted so that the hole in the blade is in front of the entrance diaphragm (chopper open) when the return signal from the satellite is expected. The chopper will be closed then at the moment of firing of the pulse laser also for the low satellites. The chopper protects the detectors from stray light of the pulse laser coming from the common telescope system and coudé optics. It also limits the average detector current during day time measurements.

The light transmitted through the entrance diaphragm is directed to a "concave mirror" where it is collimated to a parallel beam of 50 mm diameter. This parallel beam is dispersed by a higher order diffraction grating ("echelle grating").
The theory of diffraction gratings will not be discussed here, it is described in many optical handbooks.

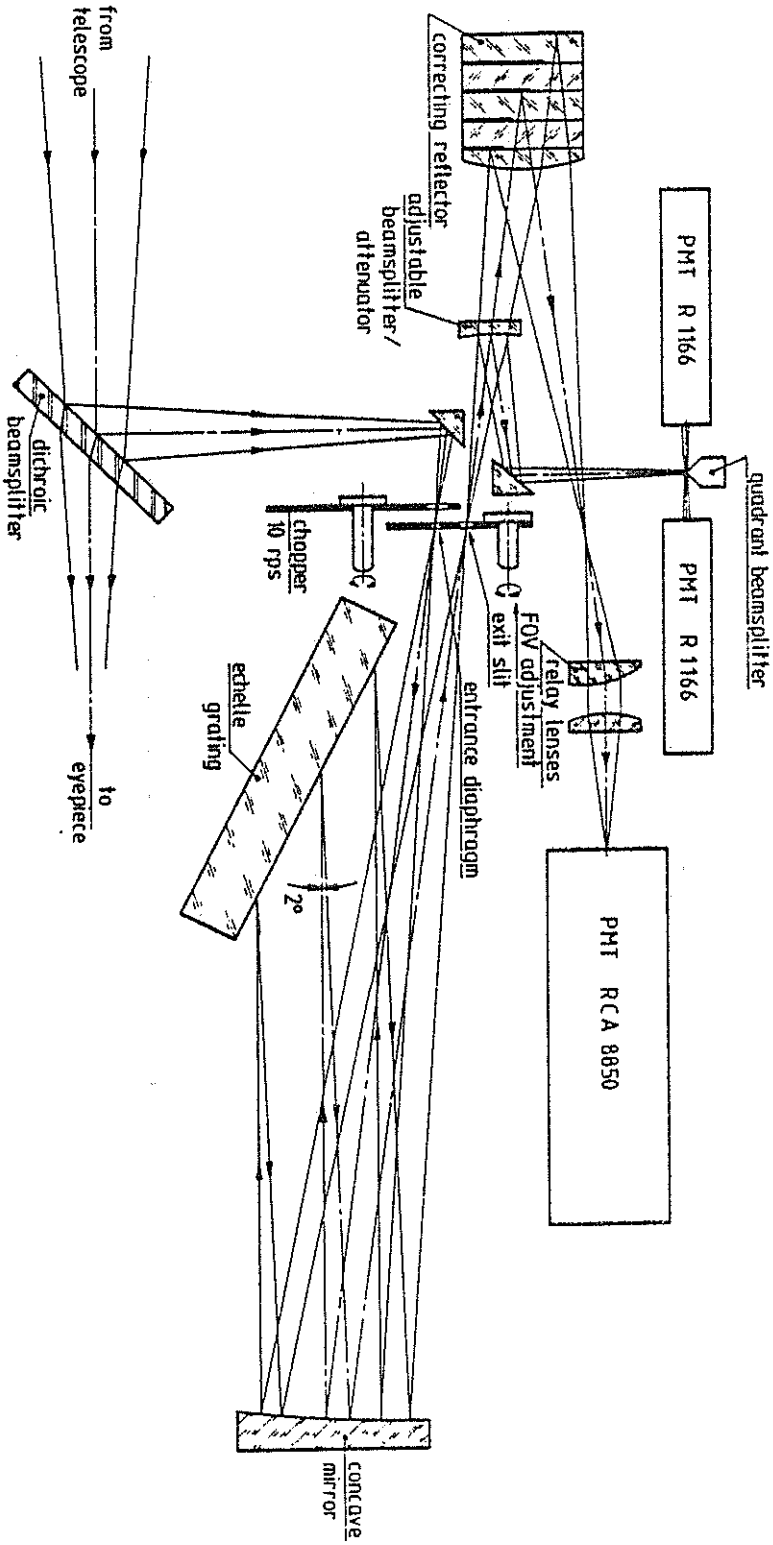

FIGURE 1 OPTICAL CONFIGURATION OF DETECTION PACKAGE

The echelle grating of figure 1 has 300 grooves per millimeter and a blaze angle of 63 degrees. The angle between the incident beam and the diffracted beam of the grating that will be transmitted through the "exit slit" is chosen at 2 degrees. For the laser wavelength the maximum efficiency of this echelle is reached in the 11th order. At the exit slit, that has the same width as the diameter of the entrance diaphragm, a narrow wavelength band around the laser wavelength will be transmitted. The dispersion of the monochromator of figure 1 is such that a one arc minute field of view (FOV) entrance diaphragm corresponds to a wavelength bandwidth of about 0,35 nm. The bandwidth of such a monochromator is proportional to the dimension of the entrance diaphragm in contrast with the fixed bandwidth of an interference filter. The presented monochromator has for instance a bandwidth of 1,2 nm for a 1 mrad FOV and 0,1 nm for a FOV of 17 arcsec; corresponding to 0,35 nm per arcmin FOV.

The use of an echelle grating instead of one or more interference filters has some advantages and some disadvantages. The main disadvantages are:

- A more complicated optical system that requires a good mechanical stability is necessary.
- It can be difficult to get a good high efficiency echelle. Although in theory an efficiency of almost 100% is possible, in practise values between 30% and 70% can be expected. A realistic grating efficiency is about 60% although it is not sure at this moment that grating manufacturers are able to deliver that efficiency at the laser wavelength from their present standard delivery programs. One grating has been delivered now and that one showed a disappointing efficiency of 40% although the manufacturer claimed 60% in his catalogue. We are still in contact with several suppliers about the possibility to get a high efficiency grating.

The main advantages are:

- No temperature control necessary. Grating blanks are made out of borosilicate glass or fused silica. The thermal expansion coefficient of borosilicate glass is about 4×10^{-6}, which results in a wavelength change of 0,1 nm over a temperature range of 50 ^{o}C. With fused silica even considerably better temperature stability is obtained.
- Easy and direct wavelength adjustment over a limited wavelength range. By rotating the grating about an axis normal to the plane of the paper of figure 1 the wavelength is scanned. An angular rotation of a few degrees results in a wavelength scan of about 10 nm without noticeable change in efficiency.
- One optical arrangement for day and night time ranging. Day time operation usually requires a smaller field of view and a narrower wavelength bandwidth due to the background signal of the bright sky. Because for the described grating monochromator the field of view and the wavelength bandwidth are proportional to each other this coupling is automatically obtained.

The exit slit transmits a narrow wavelength band around the laser wavelength to an "adjustable beamsplitter/attenuator".
For the high accuracy range measurements the transmitted light of this beamsplitter is used while the reflected light is focussed on a "quadrant beamsplitter" that will be described later. The transmitted light is reflected at the "correcting reflector". This reflector refocusses the beam and corrects for the not completely negligible range differences over the echelle surface (almost 100 mm top-top). In the correcting reflector the beam is split up by five mirrors with different optical path lengths so that the 100 mm top-top range difference over the grating surface is reduced to 20 mm top-top. Finally two "relay lenses" image the FOV on the cathode surface of a photomultiplier tube (PMT).

The preliminary PMT choice is the conventional RCA tube 8850. This tube will be used at the single photo-electron level. The amplified PMT signal will trigger a high accuracy counter (HP 5370) via a constant fraction discriminator. Although the rise time of the RCA tube is not extremely fast the stability of its single photo-electron response (transit time, pulse height, etc.) seems adequate in combination with a good constant fraction discriminator. Installation of any other PMT, amplifier, discriminator or HPIB interfaced counter will be a more or less plug-in operation.

Because the ranging system will be operated at the single photo-electron response level the received signal usually has to be attenuated to this level. This can be achieved by adjusting the transmitted energy, the divergence of the transmitted beam or by an attenuator in the detection optics. In the mobile ranging system all these three adjustments can be executed. The continuously adjustable attenuator in the detection system is the already mentioned "adjustable beamsplitter/attenuator". Two concave spherical mirrors can be turned into the beam from both sides perpendicular to the plane of the drawing of figure 1. The slit between the two mirrors transmits the central part of the beam to the "correcting reflector" while the two side parts of the beam are reflected to the "quadrant beamsplitter". By changing the slitwidth between the two mirrors the ratio of the number of transmitted and reflected photons can be adjusted from 100% transmission to almost 100% reflection. The photons that are not used for the accurate range measurement are not lost but they are reflected to the quadrant detection system. At the quadrant beamsplitter an image of the field of view, as transmitted through the "entrance diaphragm" and the "exit slit", is located. This image of the field of view is split up into four quadrants and the light in each quadrant is directed to its own small PMT of which two of the four are shown in figure 1. For these PMT's the less expensive Hamamatsu tube R 1166 has been selected.

These PMT's have sufficient gain to be operated at the single photo-electron level. If possible however they should be operated at a higher level (2 photo-electrons or more) so that the sky background noise of these detectors is considerably reduced. Information on where the satellite is located in the field of view is obtained from which of the four PMT's is triggered by the return signal of the satellite. With this information an immediate correction to the predictions will be possible. This correction can result in a better divergence of the transmitted beam which leads in turn to a higher signal level on the four quadrant PMT's, and therefore to better information on the position of the satellite in the field of view, etc. In practise each of the four PMT's will be connected via a discriminator to one channel of a four channel timer with moderate resolution and accuracy (50 ns).
This timer also gives information about where the satellite is within the window of the range gate generator so that the window, which is the same for the four quadrant PMT's and the RCA 8850 tube, can be adjusted to a very narrow band around the return signals.

AIRBORNE LASER RANGING SYSTEM FOR RAPID LARGE AREA GEODETIC SURVEYS

CONTACT: JOHN J. DEGNAN
CODE 723
NASA/GODDARD SPACE FLIGHT CENTER
GREENBELT, MARYLAND 20771 USA

1. Introduction

Geophysicists investigating phenomena such as fault motion, dilatancy, and strain buildup and relief have expressed a desire for an instrument capable of monitoring crustal deformation at hundreds of locations within an extended seismic region (e.g. 200Km X 200Km). In order to deduce the needed strain rates, the instrument must be able to measure 100 Km baseline distances with centimeter accuracies and in a time frame short compared to the scale of expected motions on the earth's surface.

During the past year, the Goddard Space Flight Center has been engaged in the design of a centimeter accuracy, multibeam, Airborne Laser Ranging System (ALRS)[1]. The basic philosophy is to invert the usual laser ranging configuration by placing the ranging and pointing hardware in a high altitude aircraft and replacing the expensive ground stations by low cost (<$1000) passive retroreflectors. The instrument would be constructed on a standard aircraft pallet so that it can be easily removed and reinstalled. This capability eliminates the need for a dedicated aircraft and allows special flights to be scheduled quickly in response to increased seismic activity.

The system is necessarily multibeam since the location of the aircraft is not known with cm precision at each point where a set of range measurements is made. Thus, a minimum of four simultaneous range measurements is required- three to resolve the new coordinates of the aircraft and one to acquire information on the relative locations of the ground targets. The ALRS system will be capable of ranging simultaneously to six retroreflectors. At a laser repetition rate of 100 pps, a potential 1.3 million individual range measurements can be made and an area as large as 60,000 square kilometers can be surveyed during one six hour flight. Computer simulations have demonstrated

that, with range biases and single-shot RMS standard deviations on the order of 1 cm, the ALRS will be capable of resolving baseline distances on the order of 100 Km to the subcentimeter level. Furthermore, the data reduction technique simultaneously resolves the aircraft position to the cm level at each point in the flight path where a laser pulse is transmitted. The system is expected to be a powerful new research tool for monitoring regional crustal deformation and tectonic plate motion because it will provide a "snapshot" of the target positions (all three axes) over an extended area with high spatial resolution (20 Km or less).

2. Ranging and Pointing Subsystems

A block diagram of the ALRS system is described in Figure 1. The current system concept is as follows. The on-board system computer generates a fire command to the short pulse laser transmitter at the rate of 10 pulses per second. The transmitter is a modelocked, PTM Q-switched Nd:YAG laser oscillator followed by a double-pass Nd:YAG laser amplifier and KD*P frequency doubler and generates a single, 150 picosecond (FWHM) pulse containing several millijoules of energy at the 5320 A green wavelength. The energy of the outgoing pulse is split six ways and directed toward six independently controlled pointing systems which are in turn directed at six different ground targets via pointing commands from the system computer.

The outgoing start pulse, as well as the incoming stop pulse, is recorded in each of the six receiver channels. In this way, most instrument-related systematic biases, which may vary slowly with time, are cancelled out automatically. In addition, biases related to the amplitude of the received signal will be compensated for by recording the integrated energy in the start and stop waveforms and applying a software-generated range correction which is based on extensive receiver testing and calibration. Provisions will also be made for on-board calibration of the instrument. The instrument-related random errors are expected to be on the order of six millimeters RMS based on projections of recent laboratory data.

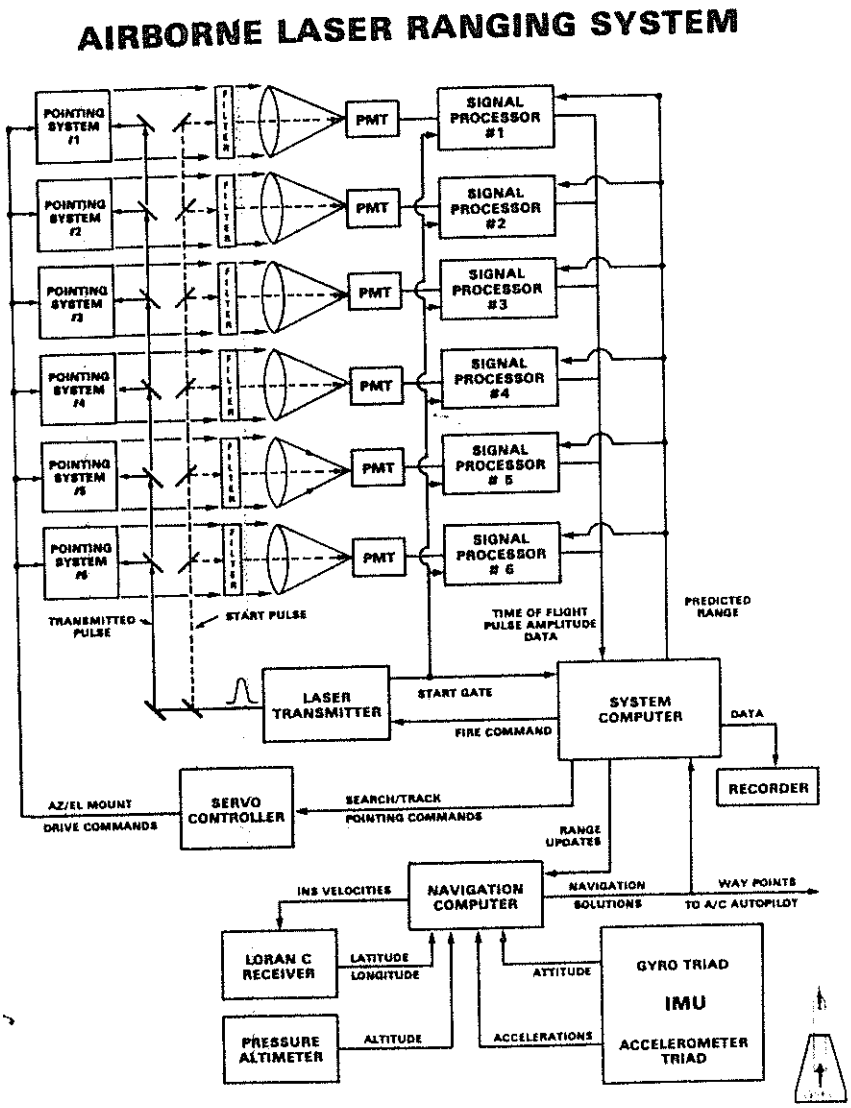

FIGURE 1: BLOCK DIAGRAM OF THE AIRBORNE LASER RANGING SYSTEM

The laser transmitter, beam splitting optics, receiver optics, and photomultiplier tubes are mounted on an optical baseplate which is isolated vibrationally from the aircraft fuselage. Six azimuth-elevation pointing mounts with 5 cm receive apertures are rigidly attached to the bottom of the optical bed. Each pointing system consists of a four mirror coelostat mounted on an azimuthally rotating stage. The laser beam enters the pointing system through a hole in the optical baseplate and the rotation stage. The final mirror rotates about an axis parallel to the optical bench to a given elevation angle. This particular configuration was chosen because it can be placed very close to the aircraft window to provide near hemispherical viewing capability.

Each pointing mount is equipped with two servo systems (azimuth and elevation). A single computer servocontroller drives all twelve stepper motors. Optical encoders attached to the motor shafts provide an independent measurement of angular position for error detection. Command angles and predicted range gates are generated by the system computer using aircraft navigation solutions provided by the navigation and attitude determination subsystem.

With laser beam divergences on the order of eight milliradians, absolute pointing accuracies at the mrad level are adequate. This performance is a factor 10 to 20 times less stringent than typically required for ground based satellite laser ranging systems.

3. Target Acquisition and Tracking

The approximate coordinates of the ground targets are stored in the system memory. The accelerations and angular rates of the optical bed are continuously monitored by a dedicated inertial measurement unit (IMU) mounted to the bed. The latter is isolation mounted to the aircraft pallet to eliminate high frequency vibrations. The navigation computer performs coordinate transformations and integrates the equations of motion to provide estimates of velocity, position and attitude relative to a set of initial conditions. In addition, independent latitude and longitude information from a LORAN C receiver is utilized to update and stabilize the corresponding INS solutions via a Kalman filter algorithm

in the NC. Similarly, barometric altimeter measurements of altitude are processed in the NC to stabilize the equations for vertical velocity and altitude. The Kalman filter also updates attitude information and provides best estimates of sensor errors such as misalignments, accelerometer biases and scale factors, gyro drift rates, etc. The INS velocity solution assists the LORAN C receiver in the acquisition of Doppler-shifted signals from the LORAN ground network. In the event of certain types of failure, the proposed navigational system can be restarted and calibrated in flight. Flight tests of a LORAN-aided INS performed for the U.S. Air Force have demonstrated a 60 meter absolute position accuracy (one sigma) and a 15 meter RMS random noise error (one sigma) and angular accuracies of a few tenths of a milliradian[2].

The navigation data is combined with the stored apriori target positions to compute the estimated range gates and the pointing mount command angles. As the targets come within range, the laser is activated and the presence or absence of range returns is noted. If no returns are detected, a search pattern is executed until range data is acquired. Selected range data is then passed to the navigation Kalman filter to update the estimate of aircraft position. The ALRS then shifts from the acquisition to the tracking mode.

In the tracking mode, triangulation on the highly accurate laser returns results in an aircraft position estimate which is virtually error free (better than a meter standard deviation) so that, except for aircraft attitude estimation errors contributed by the gyros, the computed command angles and range gates are essentially correct. The instrument remains in the tracking mode as long as sufficient range data is available to maintain an accurate estimate of aircraft position. In making the transition to a new set of six targets, the system triangulates on laser returns which are common to the new and the previous set. In this way, the aircraft position is known with better than meter accuracy during the transition.

4. Mission Scenario and Simulation Results

Simulations[3] have shown that range measurements must be taken at two widely separated altitudes in order to strengthen the geometry sufficiently to recover baselines at the centimeter level. Thus, in a typical mission, the aircraft approaches the target grid at an altitude of 40,000 feet (assuming the RB-57 A/C) as in Figure 2. After

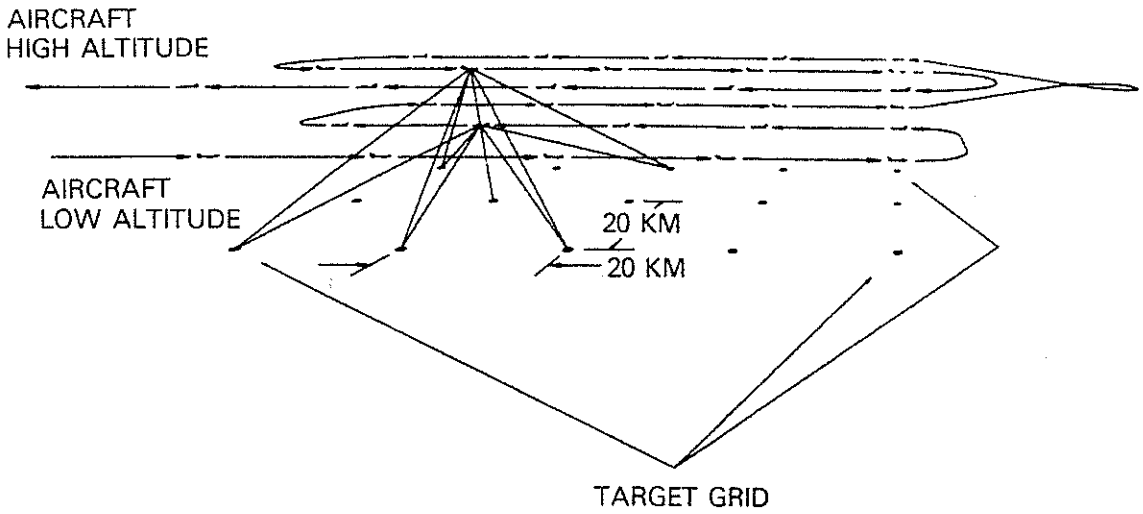

FIGURE 2: TYPICAL ALRS MISSION SCENARIO PERSPECTIVE SHOWING RANGING FROM TWO DIFFERENT ALTITUDES

acquiring the first few targets, the instrument shifts to the tracking mode for the remainder of the mission. After overflying the rows of targets at 40,000 ft, the aircraft climbs to its maximum cruise altitude (60,000 ft) for a second set of passes over the target grid.

The spacing between targets will depend on several factors including the scientific objectives of the mission, the maximum aircraft altitude, and terrain limitations. For the RB-57, the spacing is nominally 20 to 27 Km. The baseline errors grow linearly with the length at a rate of 60,000 feet. The maximum target spacing varies linearly with the maximum aircraft altitude while the baseline error growth rate varies inversely with the altitude. The simulations have also demonstrated that it is not necessary to provide meteorological instrumentation at all of the target sites in order to correct for atmospheric refraction errors. Instrumentation at one site at the center of the grid provides sufficient information to resolve the other site positions to the centimeter level even if one assumes that the site surface pressures are totally uncorrelated. This is a consequence of the simultaneous multibeam trilateration approach at two altitudes and the exponential dependence of pressure with altitude. In effect, the surface pressure at each site can be solved for along with the site coordinates.

5. Program Plans

A demonstration system is currently being constructed for use onboard the NASA NP3A Research aircraft. Initial tests will take place in the vicinity of Mary's Rock, VA in late 1983. The latter location is well surveyed and reasonably close to the aircraft's home base. The aircraft's maximum altitude of 20,000 feet will require target sites 7 km apart and increase the baseline error growth rate to about .036 cm/km.

REFERENCES

1. J.J. Degnan, "Airborne Laser Ranging System for Monitoring Regional Crustal Deformation," Proceedings of the 1981 International Geoscience and Remote Sensing Symposium, pp. 234-244, June 8-10, 1981, Washington, D.C.

2. R.D. Wierenga, Lear-Siegler, Inc., Grand Rapids, Michigan, 49508, private communication.

3. T.S. Englar, Jr., C.L. Hammond, and B.P. Gibbs, "Covariance Analysis of the Airborne Laser Ranging System," Business and Technological Systems, Inc., BTS-FR-81-143, February 1981.

SATELLITE LASER RANGING AT 10μm WAVELENGTH

D.R. Hall

Department of Applied Physics, Hull University,
Hull, England.

There has been increasing discussion in recent years concerning the possibility of developing systems operating at wavelengths around 10μm and based on carbon dioxide lasers which have the capability of ranging to satellites (1). For such systems to be of any significant interest, the resolution attained must be comparable with the centimetric performance of existing 'third generation' visible systems. Moreover, given the large investment in the technology of high resolution visible ranging systems over the last fifteen years, any potential competitive system should exhibit some decided advantage(s).

This paper considers three main aspects of this topic: First of all a summary is presented of the potential benefits which could accrue from operation in the mid infra-red 9-11μm spectral region. This is followed by a brief discussion of the techniques and hardware most likely to form the basis of such a system and finally a short assessment of the present state of the art in terms of available hardware, coupled with an indication of the technological development which would be necessary to allow a 10μm based system capable of ranging to the main satellites of interest (Lageos, Geos, Starlette) to be realised.

WHY CONSIDER 10μm SYSTEMS

There has been near continuous development of visible wavelength (based on ruby or Nd:YAG lasers) satellite laser ranging (SLR) systems during the past 15 years, and we have heard during this Workshop of the success of the most recently developed systems based on passively mode-locked, frequency doubled Neodymium YAG lasers, in achieving

night and day time ranging to Lageos with resolution at the level of a few centimetres, under ideal atmospheric conditions. Given this impressive level of performance, any potential new system, such as we are discussing here, must be shown to have clear advantages before any significant level of development is undertaken.

The evidence presently available suggests that with reasonable care and maintenance, the third generation systems presently operational can be made to achieve a level of range resolution which is adequate for modelling purposes and an acceptable level of reliability in terms of the 'down' time made necessary by equipment malfunction. The clear limitation, however, of present systems relates to their dependence on near perfect weather conditions with zero or minimal cloud and haze, and the impact this has on the frequency with which satellite ranging activities are possible. This problem obviously manifests itself to a greater or less extent, depending on geographical location, but it is apparently a significant limitation at all stations. One benefit which has been claimed for 10μm systems is that they can take advantage of the 8-14μm 'atmospheric window'. This topic has been the subject of considerable interest, particularly as it affects 'terrestrial' ranging and is one of the reasons for the recent upsurge in interest in the development of 10μm wavelength military surveillance systems, including rangefinding.

Unfortunately, despite considerable experimental and theoretical studies, the relative merits of visible and IR wavelengths as regards atmospheric extinction is not clear cut, and much depends on atmospheric conditions. Atmospheric extinction is due mainly to molecular absorption and scattering by aerosols, and whereas the latter is most effective in attenuating near and IR visible signals (i.e. Nd:YAG and frequency doubled Nd:YAG wavelengths) they have negligible effect on 10μm signals. Conversely, broad-band water vapour and CO_2 molecular absorption is effective in attenuating 10μm radiation but has very little effect on visible signals. Thus, while 10μm radiation has superior penetration through aerosols (such as water droplets in fog and light cloud), it is severely attenuated in conditions of high water vapour content (high humidity).

Consequently, although 10μm radiation can be claimed to have superior penetration in certain "artificial" atmospheres dominated by dust, smoke and hydrocarbons, the same cannot be universally claimed for 'natural' atmospheres under all conditions. Thus, it is by no means clear that 10μm systems will provide any significant improvement over the visible under a wide range of atmospheric conditions and geographic locations.

A second area of concern with regard to visible systems is the question of eye safety. It is desirable to operate SLR systems in an intrinsically eye-safe manner, so that one could dispense with the aircraft detection and laser lock-out systems currently causing headaches for some groups. Even with large transmitting apertures and using very sensitive (single photo-electron) receiving techniques, this does not appear to be feasible with visible systems because of the low value of maximum permissible exposure (MPE) in the green (2). The MPE in the infra-red allows a benefit of a factor of 10^5 in using a 10μm wavelength as compared with using the green, so that an intrinsically eye-safe IR system could in principle be built.

Existing visible wavelength SLR systems rely on direct detection, whereas any feasible 10μm based system will, for detection sensitivity reasons, be required to use a heterodyne receiver. With such a receiver it is possible to determine a single component of the satellite velocity from measurements of the Doppler shift on the return signal. Thus, a 10μm based system could, in principle, be designed to produce velocity and/or range information. From the standpoint of the data users, certainly in the context of crustal dynamics, any such 'range rate' data would need to achieve a resolution of about 10μm per second in order for the orbit model to produce useful results(3). This implies the need to measure Doppler shifts with a precision of a few hertz. Carbon dioxide lasers, operating in the continuous wave mode at 28.4 THz, have been stabilised to 1 part in 10^{12} under laboratory conditions, but this is not likely to be routinely achievable in the field. Moreover, atmospheric turbulence introduces a degree of frequency 'smear' and a resolution of 100 Hz - 1 kHz is likely to be the best achievable in practice. The conclusion, therefore is that the use of cw CO_2

lasers, heterodyne detection and Doppler tracking is unlikely to produce data on range rate with adequate resolution to be useful for geodesy.

One final reason which has been advanced for consideration of 10μm systems is the advanced level of technology available in this spectral region, based on carbon dioxide lasers and mercury cadmium telluride photon detectors. This question is examined later.

EXISTING 10μm RANGING SYSTEMS

There has been a rapid increase in interest during the past 5-7 years in the use of 10 micron systems for terrestrial rangefinding particularly in a military context. Such systems typically operate over ranges of less than a few tens of kilometers and with relatively coarse range resolution in the 1-5 meter bracket. They are however, typically used against "uncooperative" diffuse reflecting targets, i.e. no retroreflectors. Three types of system can be identified. The first to be employed, and probably still the most common, are the pulsed laser-direct detection systems (4). These employ a pulsed TEA (transverse, electric, atmospheric pressure) CO_2 laser which produces pulses of about 1 Mwatt peak, 50 nanoseconds duration at a repetition rate of 1-2 Hz. Transmit and receive optics (which may be common) are $\lesssim$ 15cm in diameter and a cryogenically cooled photon detector is employed in a direct detection mode.

A second general type of system uses a modulated cw transmitter and a heterodyne receiver. One such system (5) uses a cw waveguide CO_2 laser and an acousto-optic modulator to produce a linear frequency chirped output of less than 1 watt average power. The receiver uses part of the transmitter base signal as a local oscillator and a surface acoustic wave device as a good approximation to a matched filter. This type of system is modulator bandwidth limited to about 15 MHz/5 metre resolution and has a range $\lesssim$ 10km. The third type of system couples the peak power of the pulsed CO_2 laser with the additional sensitivity of the heterodyne receiver and is the most likely candidate for a long range (satellite) ranging system of high resolution. To date, systems have been built which produce approximately 100 mJoules in a 40 usec pulse producing range resolution of 5 metres over near horizontal range

up to 35km (6).

Although no systems have been reported which employ subnanosecond CO_2 lasers for ranging this is due in large measure to the absence of any real requirement to date for any increased range resolution in such systems. In fact subnanosecond pulses may be produced by modelocking techniques in pulsed CO_2 lasers operating at atmospheric or super-atmospheric pressure, and have been extensively studied in the content of target interaction and inertial confinement research.

The use of 10μm laser systems employing heterodyne receivers has become an important technique for velocity measurements, particularly in atmospheric studies, where the Doppler shift suffered by radiation scattered by aerosols in a natural or artificially induced air flow is used to monitor the air motion itself. Such systems, employing stabilised cw CO_2 lasers, have been used to monitor turbulent air flows associated with aircraft landing and take off, and mounted in the nose of an aircraft, to measure real air speed and as a means of detecting windshear (7). Resolution in the range 0.1-1 meters/sec is achieved.

Work is currently in progress on a proposed satellite born system which would be used to monitor the development of wind systems on a global basis. It is suggested that such a system would operate with a 10 Joule CO_2 laser producing pulses of a few microseconds duration at about 8 Hz with a velocity resolution of 1 metre per second (8). Doppler tracking of Lageos at 10.6μm has been achieved by the group at Lincoln Laboratory Firepond Facility (9) who have used a very stable master oscillator to drive a power amplifier to produce an output of several hundred watt chopped pulses of about 1 msec duration. Doppler tracking with a resolution of about 1 KHz was achieved, and the relatively complex Doppler spectrum could be interpreted in terms of the spin of the satellite, which is equipped with 4 germanium retroreflectors (intended for use at 10μm) located at the vertices of a tetrahedron.

PERFORMANCE OF POSSIBLE SYSTEM

As indicated above, any potential IR SLR system will require the use of a heterodyne receiver, where the dominant noise source is photon fluctuation in the local oscillator laser signal, as opposed to the

background noise dominated situation of direct detection receiver commonly used in the visible.

If we assume a pulsed CO_2 laser transmitting pulses of peak power P_T and duration $\tau \sim 1/B$ where B is the receiver bandwidth, from a telescope of effective transmitting and receiving aperture A_T, then the received signal power P_s after reflection from a retro at range R is given by

$$P_s = \frac{P_T A_T^2 A_R^2}{\lambda^4 R^4} \quad (1)$$

where L represents total system losses including atmospheric transmission, retroreflector losses and receiver losses, and A_R is the retroreflector area.

The receiver noise power P_N is $h\nu B/\eta$ where η is the detector quantum efficiency, h is Planck's constant and ν is the optical frequency (2.8×10^{13} Hz), so that the IF receiver signal-to-noise ratio is given by

$$(S/N) = P_s/P_N \sim \frac{E_p A_T A_R L\eta}{\lambda^4 R^4 h\nu} \quad (2)$$

where E_p is the pulse energy, assuming a perfect match between pulse duration and receiver bandwidth.

If we assume a value of 50cm for the diameter of both the transmitting and receiving telescope, a retroreflector diameter of 4 cm and system losses of 10^{-2} then the required laser characteristics are approximately as indicated in Table 1.

SATELLITE	P_T (peak)	E_p	τ_p	P(av) (10 Hz)
Lageos	12 GWatt	6 Joules	5×10^{-10} sec	60 watts
Geos	12 Mwatt	6 mJ	5×10^{-10} sec	60 Mwatts

Table 1 Required Laser Performance

To achieve the necessary pulse duration of $\lesssim$ 500 picoseconds, it would be necessary to use a multi atmosphere pulsed CO_2 laser, probably in the 2-5 atmosphere bracket, with the preferred modelocking technique

probably involving injection from a master oscillator. In this context achieving 6 mJ (for Geos) is a reasonable target but 6 Joules (for Lageos), even in a pulse train as opposed to a single pulse, represents a very difficult and expensive task, and one which would need very considerable development. Aside from achieving the necessary discharge performance one very significant problem could be the fundamental limitation of damage to optical components. A receiver for a potential IR SLR system would be required to operate with a cryogenically cooled detector element and to exhibit an IF bandwidth in excess of 1.5×10^9 Hz. This has been achieved but is difficult and expensive. The laser local oscillator could be required to frequency track over approximately ± 500 MHz to compensate for Doppler shift and would need to maintain frequency lock with the transmitter to a few MHz. The alignment of the receiver optics is critical to obtain efficient heterodyning and although there is a tolerance benefit of about factor of 20 in going to 10μm, considerable investment would be necessary like in new telescopes or in modification to existing hardware.

CONCLUSION

It is apparent from the above discussion that there is at present no overwhelming case in favour of developing 10μm wavelength SLR systems. There is a definite advantage at 10μm in terms of eye safety, a marginal benefit in terms of atmospheric transmission, no real advantage accruing from range rate data and in fact, although 10μm technology can be said to be in a relatively advanced state, there are very significant problems associated with producing a system which could range to Lageos with the requisite range resolution.

References

1. B. Greene. Third International Satellite Laser Ranging Workshop. Lagonissi 1978.

2. British Standard BS 4803.

3. D. Smith. Private Communication.

4. M.J. Taylor, P.H. Davies, D.W. Brown, W.F. Woods, I.A. Bell, C.J. Kennedy. Appl. Opt. 17, 885 (1978).

5. K.F. Hulme, B.S. Collins, G.D. Constant, J.T. Pinson. Opt. Quant. Elect. 13, 35 (1981).

6. J.M. Cruickshank, Appl. Opt. 18, 290 (1979).

7. R. Callan, J. Cannell, R. Foord, R. Jones, J.M. Vaughan, D.V. Willetts, A. Woodfield, Fifth UK Quantum Electronics Conf. Hull, September, 1981.

8. M. Huffaker, Paper presented at Coherent Laser Radar Conference, Aspen, July, 1980.

9. Leo J. Sullivan, SPIE Vol. 227 (1980).

THE LASER RANGING SYSTEM GRAZ - LUSTBÜHEL, AUSTRIA

G. KIRCHNER

Institute for Space Research
Austrian Academy of Sciences
Department: Satellite Geodesy

1. INTRODUCTION

In October 1978 the project "Construction of a Laser Ranging Facility" was approved by the Austrian Science Research Council. Until December 1979 the main components of the sytem had been specified using partly the advantage of a common planning together with the RGO, UK.

In December 1980 the two Laser emitters have been installed; in August 1981 the Mount and Telescope System has been delivered and placed in the dome at the Observatory Lustbühel in Graz. The computer and most of the instruments are already installed and operational.

2. SYSTEM CONSIDERATIONS

Originally it was planned to use a Nd:YAG short pulse laser system with estimated accuracy level of 10 cm or better; in December 1979 the decision was made to add a second laseremitter - a ruby laser with more energy output, but with longer pulses than the Nd:YAG laser to the ranging system to have more flexibility.

The philosophy throughout the system is:
- to use commercially available units for most instruments to simplify and accelerate the integration of the whole system;
- to use one standard interface for connecting all instruments, the two lasers and the mount electronics to the computer; this ist the IEEE -488 (HPIB, GPIB, IEC-Bus) interface. This enables simple and fast changing of instruments, adding new devices and reduces programming problems;
- and to make extensive use of computer power to control the whole laser ranging station. This allows great flexibility for the whole system.

3. THE LASER EMITTER SYSTEM (Figure 1)

a) The Nd:YAG-Laser

The oscillator is passively mode locked by KODAK 9740 dye; the oscillator mode is TEMoo. The pulse Selector extracts one single pulse out of the pulse train; this pulse is then amplified in

the double pass configuration amplifier (POLAREX method) and an additional amplifier. After frequency doubling - with a $KD^{x}P$ crystal - the remaining infrared light is removed and the YAG beam brought up to the Ruby beam diameter.

Pulse Width .....100 Picoseconds
Energy per Pulse .....100 Millijoules at 530 nm
Energy Stability .....$\pm$ 10 % for 90 % of the shots
Repetition Rate .....10 Hz, 5 Hz, 2.5 Hz
Beam Divergence .....0.1 milliard

b) The Ruby - Laser

The oscillator is passively Q-switched, the mode is TEMoo. This pulse is then amplified in the double pass amplifier.

Pulse Width .....3 ns, 6 ns; selectable
Energy per Pulse ..... 2.5 J; 4 J; according to pulse width
Repetition Rate .....up to 0.25 Hz
Beam Divergence .....0.1 milliard

c) General Remarks to both lasers

Both lasers are mounted on a common granite bench (320 x 100 cm) and placed in an air conditioned clean room in the main building of the observatory. Both laser beams are brought up to 40 mm diameter by means of the same beam expander telescope and directed with four mirrors within a closed, airtight path to the mount. Optical switching between YAG and Ruby laser is done by two mirrors, mounted on a high precision, computer controlled (IEEE-interface) translater on the granite bench.

Safety shutters in both oscillators prohibit unwanted laser pulses and enable - in the Nd:YAG oscillator - repetition rate selection without changing the flash lamp repetition rate.

Firing and charging of both lasers is computer controlled (IEEE - 488); repetition rates can be varied continously up to the specified maximum; epoch of firing can be predetermined with an accuracy of better than 50 Microseconds.

4. THE MOUNT AND TELESCOPE SYSTEM

Angular Coverage .....$\pm$ 290° Azimuth
$-$ 5° to 185° Elevation
Axis Wobble .....2 arc secs, both axis
Encoding System and Control:
Resolution .....0.0001°
Accuracy .....$\pm$ 1 arcsec,
Rate Commands .....0.0001 to 20 Degrees/s Azimuth
0.0001 to 5 Degrees/s Elevation

Receive Optics
Clear Aperture .....20 inches
Field of View .....23 arc secs to 3.9 arc min, selectable
Equipped with ISIT - TV Camera.

Transmit Optics
Clear Aperture.....2 inches; 4 inches beam diameter after beam expander output
Divergence .....5 to 200 arc secs variable
Mount Control .....Manual Mode; Computer Mode via IEEE-488 interface; Joystick Mode.

5. COMPUTER AND ELECTRONICS

The HP - 1000, Model 40, minicomputer with 128 kB memory and 19.6 MB cartridge disc is installed since 1980; it controls all instruments, the two lasers, the mount and the complete data flow. Standard I/O is the HP-IB (IEEE-488) interface. Via modem a connection to the UNIVAC 1100/81 computer is possible.

For time interval measurements the HP 5370A counter is used; the HP 5359A Time Synthesizer enables range gate control. Epoch time is determined with the HP 5328 Universal Counter.

For the echo detection originally it was planned to use Varian Crossed Field and Varian All-Electrostatic High Speed Photomultipliers; since these are not available in the moment, two RCA 8852 photomultipliers will be installed for the initial phase. This detection package with 3-A-filters, variable neutral-density filters and leading-edge, fixed-level discrimination is now unter construction.

A second HP 5370A counter can be used for high precision epoch time determination.

6. TIME KEEPING

The primary time standard is provided by the Lustbühel time keeping station which generates the time scale UTC(TUG) and contributes to TAI by two Cesium Beam Frequency Standards and four LORAN-C receivers. Further comparisons are performed, on a regular basis, via TV (terrestrial and satellite) and portable clock visits.

Time connection between this time standard and the laser station has been accomplished by fibre optics (1 Hz pulse and 10 MHz reference frequency).

7. SAFETY

Due to the location of the observatory Graz-Lustbühel - about 9.5 km distance to Graz Airport, within the controlled area - the authorities put heavy restrictions on the operation of the laser ranging system:

- Installation of a passive aircraft detection system with automatic stop of the laser activity (similar to the Kootwijk system); this system is already operational; the function will be tested by the authorities during the next weeks;
- Operation of the laser station only when Graz-Airport is closed (at present this is from 23^{oo} to 6^{oo}). This restricted operation time will probably be extended after the first, experimental period.
- Operation only after contacting the Air Traffic Control Center in Vienna and getting "clearance";
- In addition, a human observer is mandatory

8. CONCLUSION

If detection package construction and software integration continue without major problems, the beginning of the testphase can be expected early 1982.

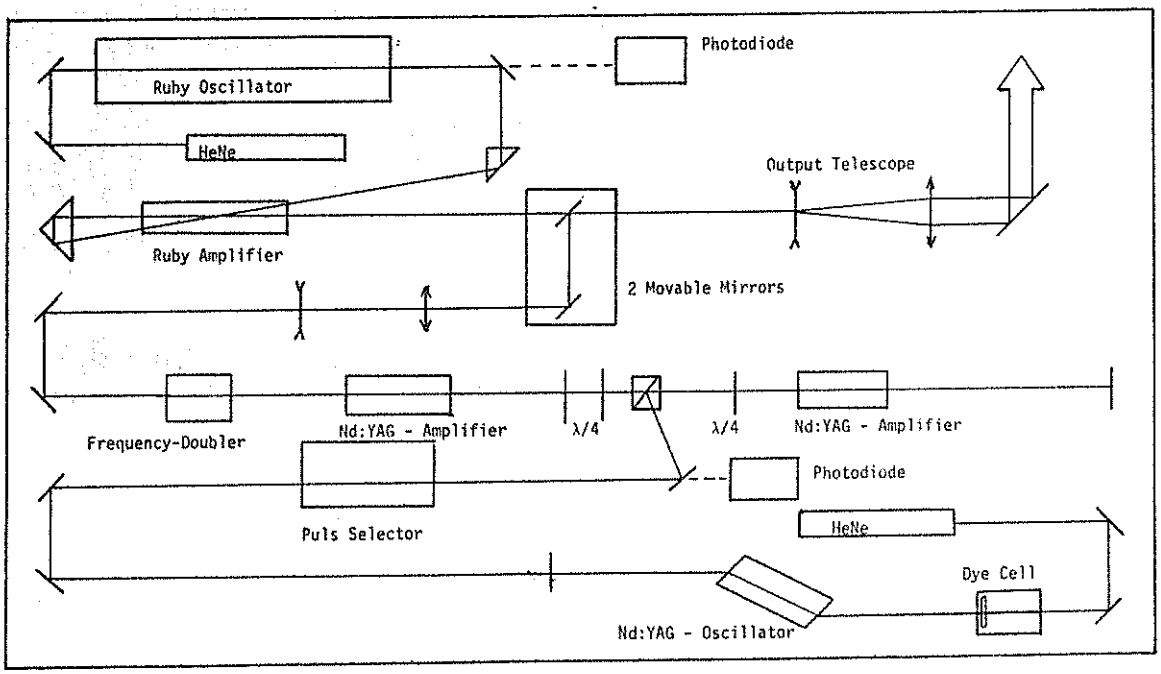

Figure 1: Block Diagram Of The Optical Lay - Out Of The QUANTEL Nd:YAG / Ruby - Lasersystem

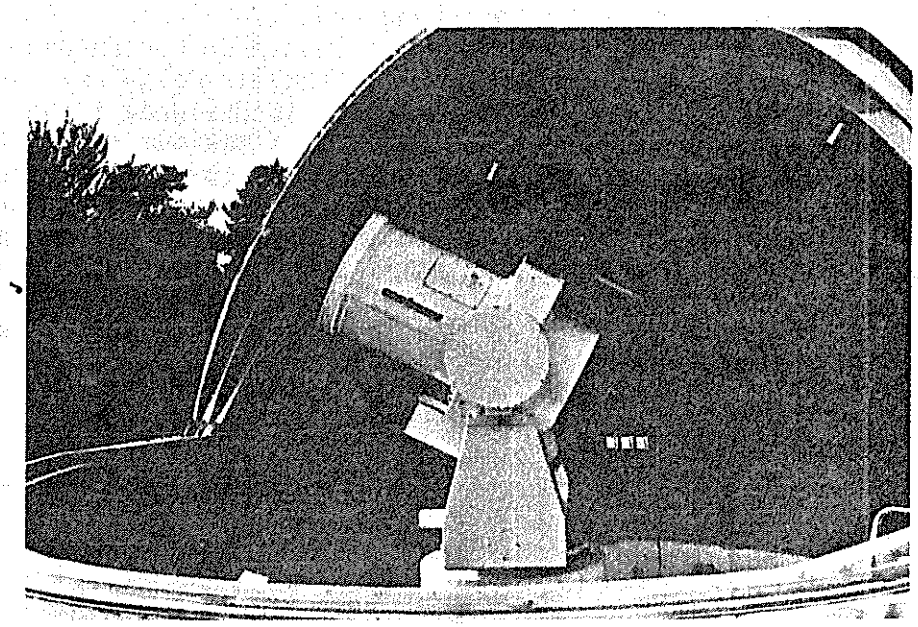

Figure 2: Mount And Telescope System

THE GERMAN/DUTCH MOBILE LASER RANGING SYSTEMS

PETER WILSON

INSTITUT FÜR ANGEWANDTE GEODÄSIE, FRANKFURT/MAIN
SONDERFORSCHUNGSBEREICH 78 (SATELLITENGEODÄSIE) DER TU MÜNCHEN

1. Introduction

In December 1980 the Institut für Angewandte Geodäsie, acting on behalf of the Sonderforschungsbereich 78 (Satellitengeodäsie) der TU München , entered into a contract with a Dutch group - Technisch Physikalische Dienst, TNO-TH, Delft - for the construction of a mobile laser ranging system. Financing for the contract was provided by the Bundesministerium für Forschung und Technologie (BMFT) through the Bereich Projektträgerschaften der Deutschen Forschungs- und Versuchsanstalt für Luft- und Raumfahrt (DFVLR) in Köln-Porz. With delivery to follow in early 1983 the system is designed to be capable of observing at the 1-2 cm noise level to a maximum range of approximately 12 000 km. As the result of efforts to co-ordinate the design, a second, identical system was ordered for the Satellite Observatory at Kootwijk in the Netherlands, with delivery to follow the first system by approximately 6 months. It is anticipated that the use of the two systems will also be co-ordinated in projects of common interest, particularly in the field of Crustal Dynamics and Earthquake Research such as that inaugurated by the NASA.

2. System configuration

The overall concept of the observing system is outlined in fig. 1, which illustrates the connecting links between major components. As can be seen from this block diagram, the system breaks down into

- the optical transmitter including telescope and laser;

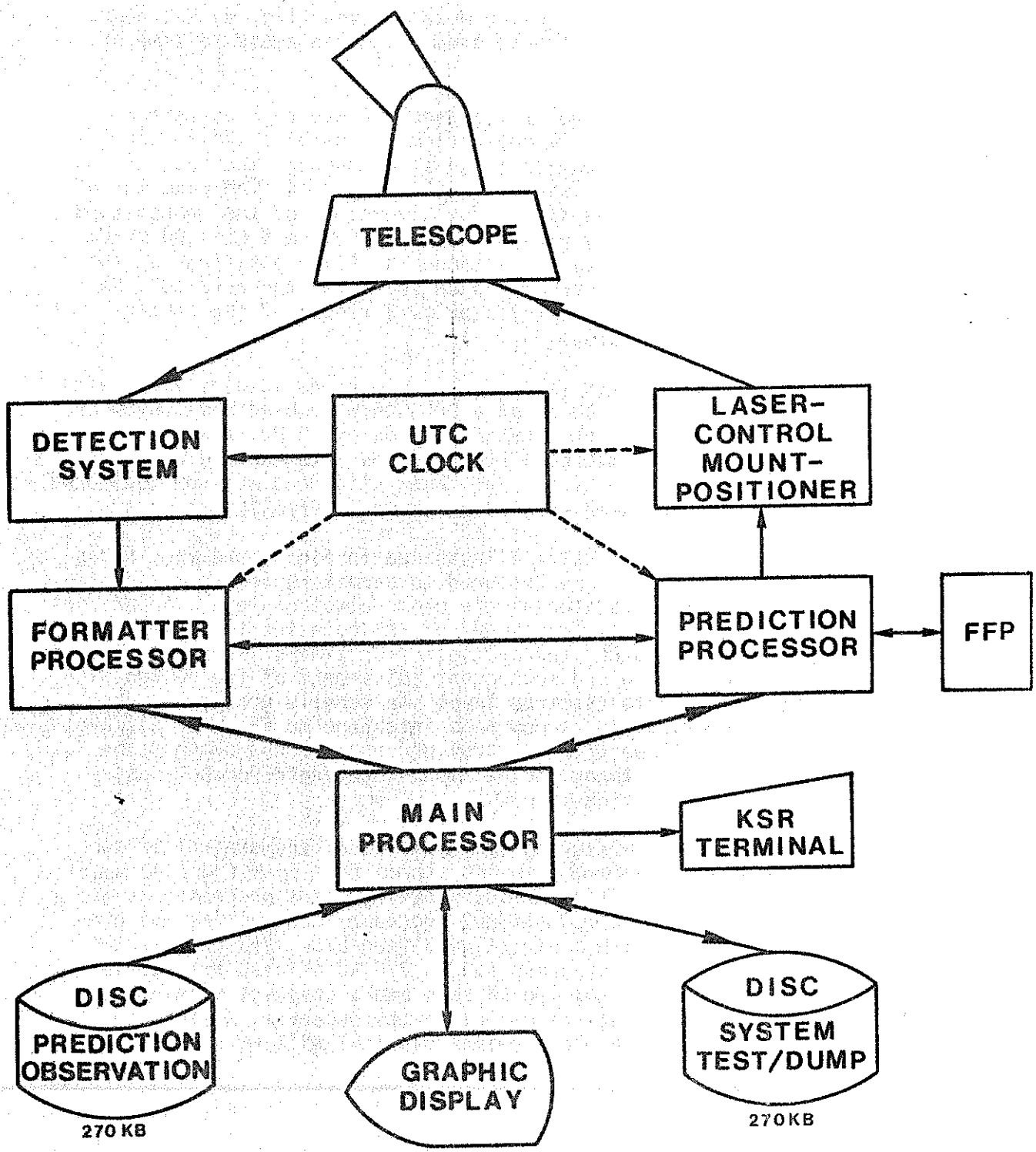

Fig. 1: The overall system concept

- the mount positioner and laser control unit;
- the detector package including UTC clock;
- the processors and their peripherals.

Although a discussion of the Coudé mount design (fig. 2) has been given in [1] it is useful here to draw attention again to some of the main features.

A single telescope is designed for use both as optical transmitter and receiver, the separation of outgoing and return pulses occurring at the beam splitter situated near the base of the mount, shortly before the laser and detector units. The diameter of the telescope objective is 40 cm. The divergence of the transmitted laser beam is continuously variable over the range 0,05-1,00 mrad. Laser and detector packages are attached in fixed positions at the base of the mount and are readily accessible for the operator. No loss of energy occurs at transmission as a result of the central obscuration of the telescope.

The Nd:YAP laser (fig. 3) [2] comprises an oscillator with one amplifier, producing 10 mJ at a frequency doubled wavelength of 539 nm (green) with a pulse repetition rate of 10 Hz. Alignment of the overall optical system will be performed with the aid of an externally mounted CW laser (fig. 2); laser alignment will be monitored via a separate He-Ne laser mounted as shown in fig. 3.

The detection system illustrated in fig. 4 and fig. 5 has been described in [3]. It is designed to permit rapid signal identification for observing at the single photo-electron level. A quadrant detector serves to enable adjustment of the pointing to maximise signal return at the main PMT and multiple-stop timing is used to facilitate signal recognition and subsequent adjustment of the return signal to the single photo-electron level. An echelle grating is used in place of the customary narrow band interference filter. This avoids the necessity for temperature control and permits use of the same optical configuration tuned to the laser wavelength for both day- and night-time observations.

The overall measuring system is under the control of two 8-bit Motorola 6809 micro-processors slaved to a 16-bit HP1000 model 5 micro-computer (fig. 1) [4]. A fast floating point processor is included to speed up the computational procedure controlling the prediction and pointing with a direct data feed-back link between the formater and prediction processors. 2 x 270 KB of disc storage is available to supplement the 128 KB core and a graphics terminal is included to provide visual feed-back to the observer. A TI-Silent 765 KSR (keyboard - send and receive) terminal will be used as an

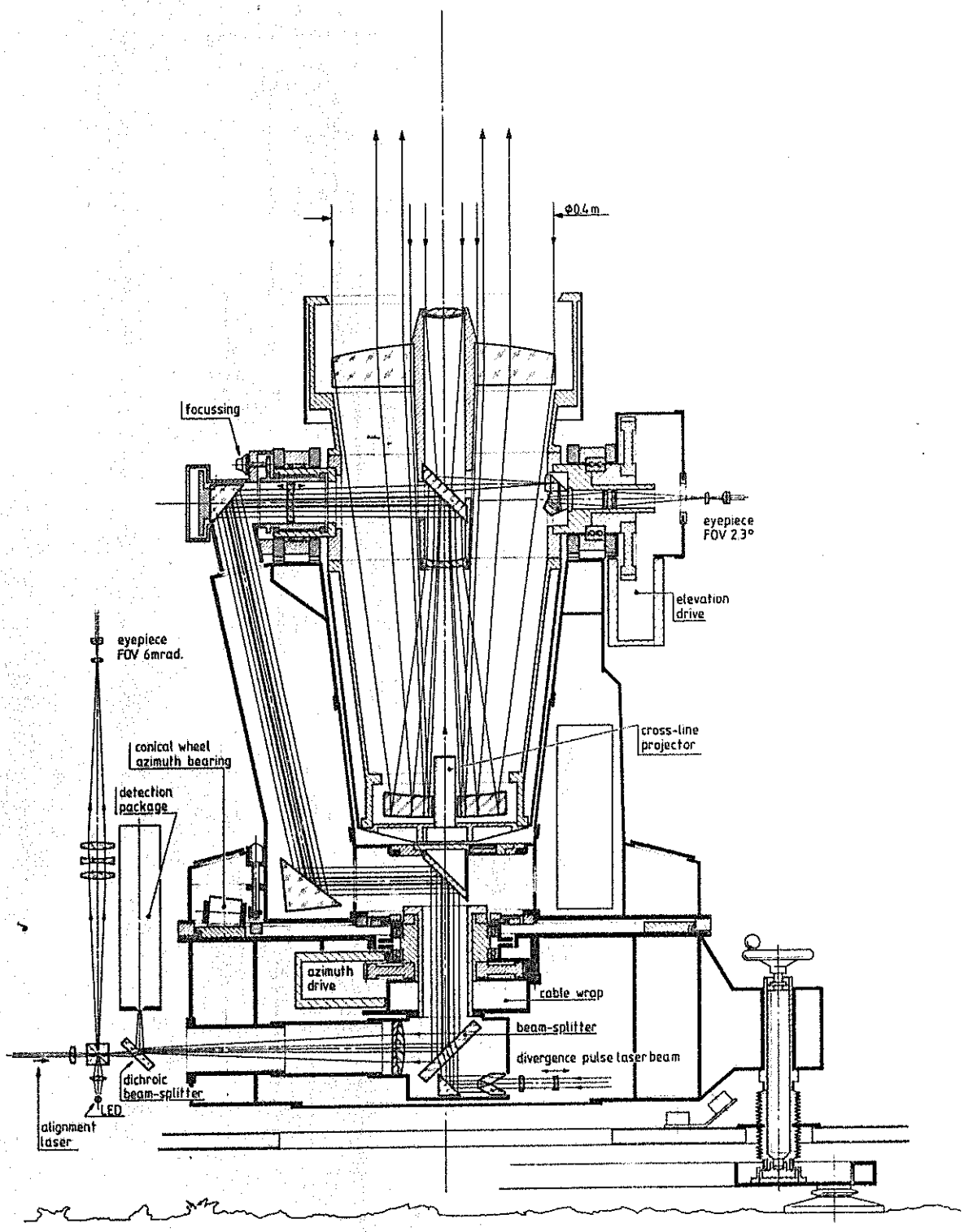

Fig. 2: Schematic of the mount and telescope

KLB - Nd:YAP-Lasersystem YL 143 S

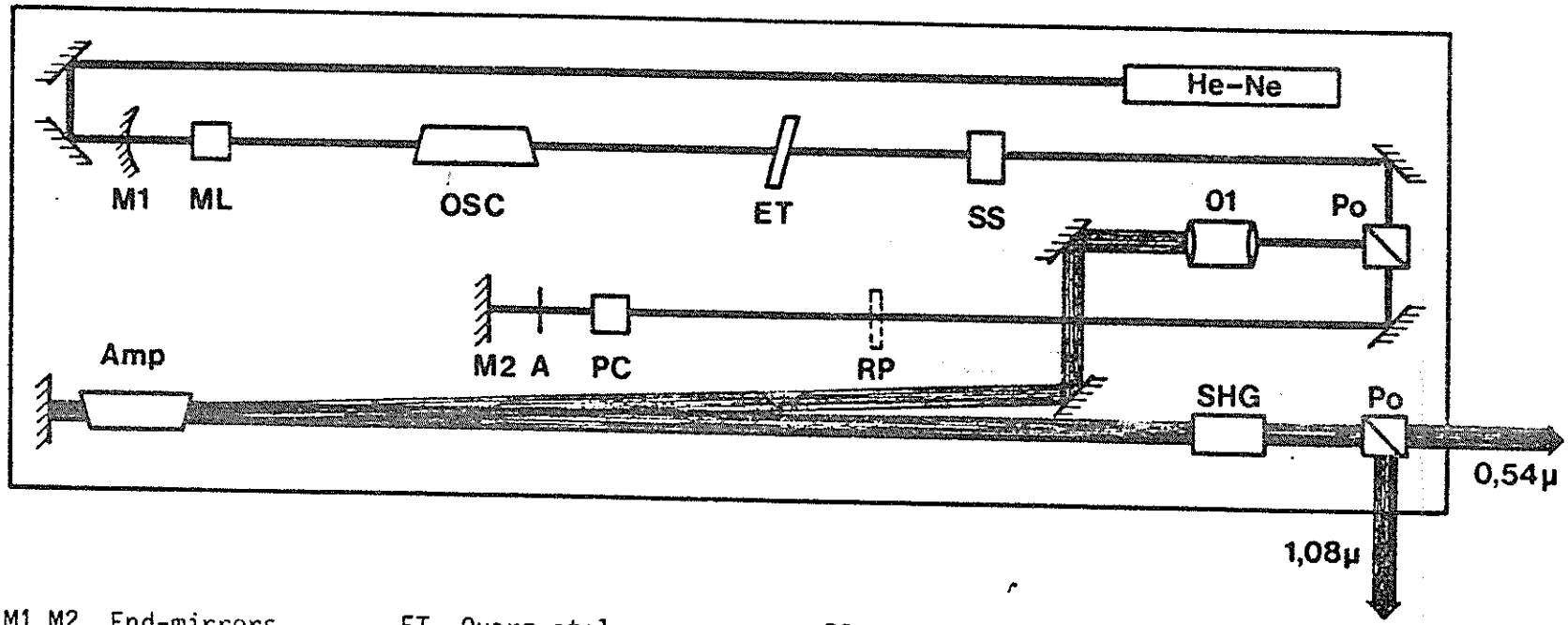

M1,M2	End-mirrors	ET	Quarz etalon	PC	Pockels cell
ML	KD*P mode-locker	SS	Safety shutter	A	Aperture
Po	Polarizer	01	Beam expander	Amp	Amplifier head
OSC	Oscillator head	RP	λ/2 Retardation plate	SHG	KD*P Frequency doubler

Fig. 3: Lay-out of the laser

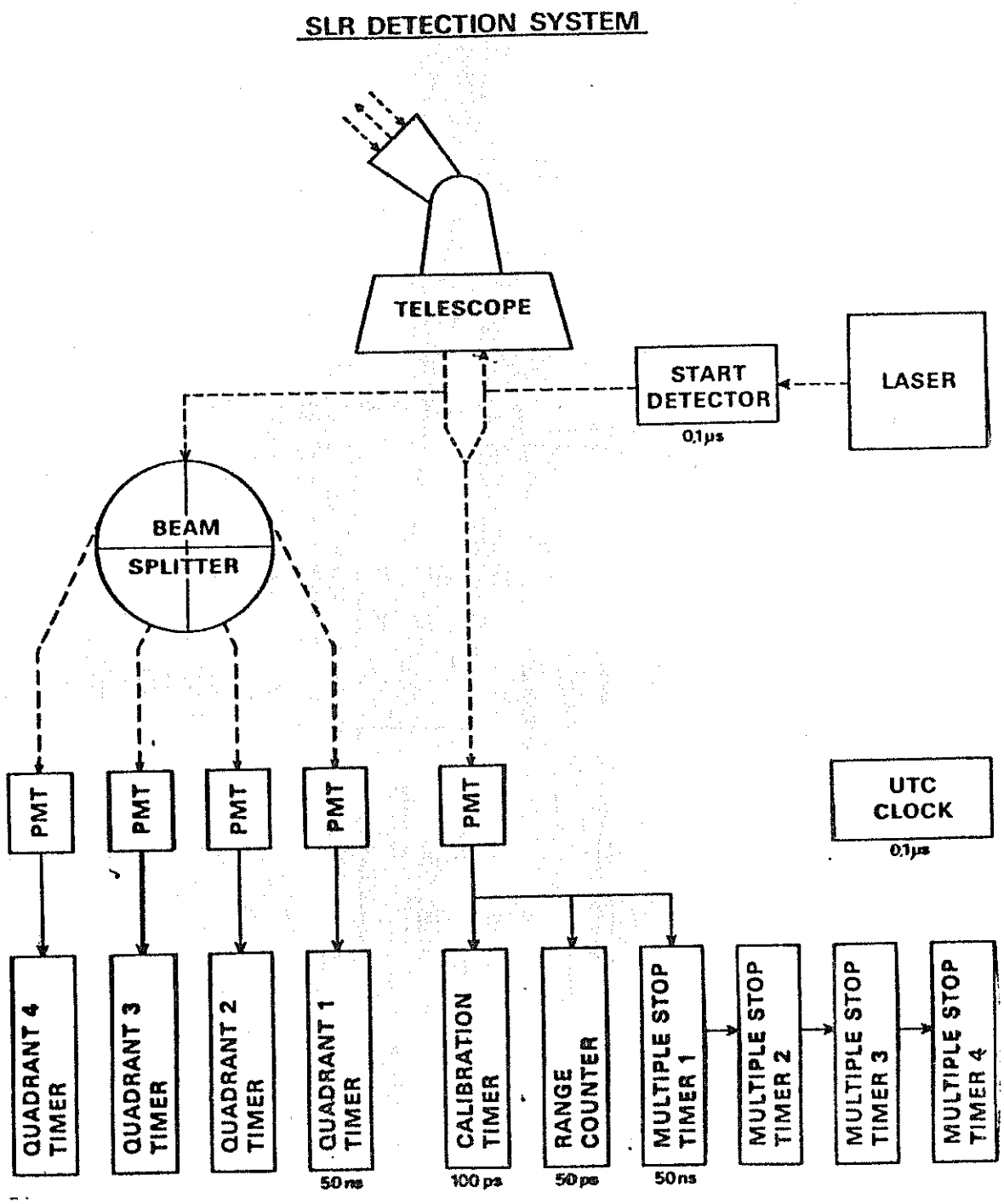

Fig. 4: Block diagram showing the detector concept

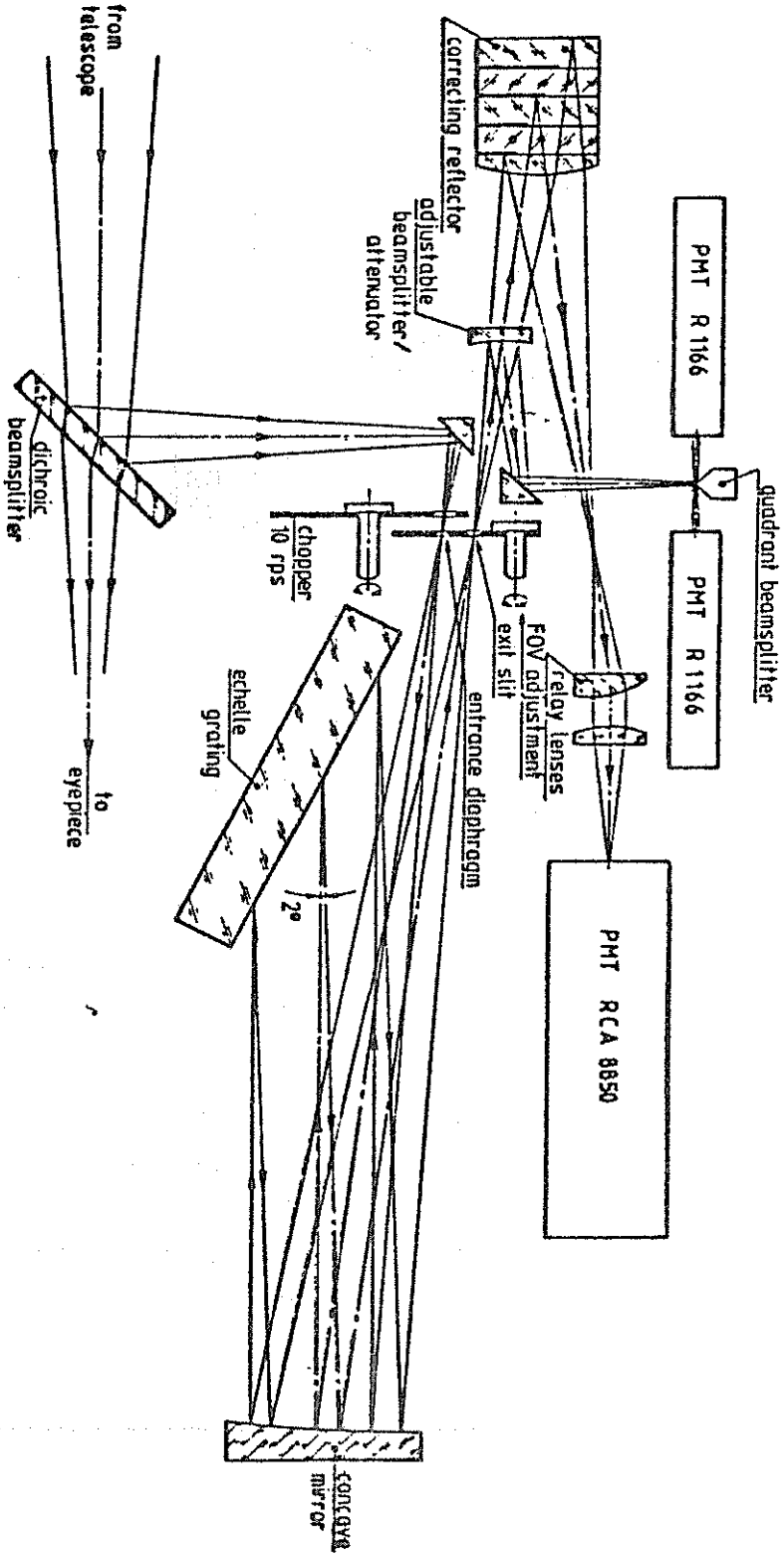

Fig. 5: Optical configuration of the detector package

input - output channel for communicating orbital updates and quick-look results between the system and the outside world.

The telescope, mount, laser (including power supply and cooling) and detector are configured together on a separate cart (fig. 6), which will be loaded into the vehicle for road transportation (fig. 7) and run out to a position adjacent to the ground marker for ranging operations (fig. 8). The system will be operated from its own independent power supply (fig. 7). In an air-freight configuration the total measuring system will fit onto a single standard freight pallet (fig. 9). Conversion from the air- to the road-transport or from road-transport to operational configuration will be possible within 24 hours, given suitable amenities and acceptable weather conditions.

3. The operational routine

The overall operational sequence is explained in fig. 10, whereby the most usual routine will be restricted to road travel, with only occasional air transfers necessary.

3.1 Setting up the system for observation

After arrival at the new site the system will first undergo routine checking and maintenance, during which time the time scale will be checked or reinstalled. The station position will usually be taken from a previously determined marker using a supplementary positioning device (fig. 11 and fig. 12). However, software is available which will enable the operators to determine station positions astronomically if required at the same time as the system orientation is made.

With the derived station position and the initiating vector provided via a data link such as GE-Mark III, telephone or telex, ephemerides will be calculated using an on-site prediction routine [5].

3.2 Range calibration

Much attention has been given to the design for range calibration. As it will be possible to range to terrestrial targets at arbitrary distances, the commonly practised technique of ranging to an external target board can also be used here. However, with the objective of eliminating any systematics identifiable at the 1 cm level, it is immediately apparent that

- an internally defined range undisturbed by atmospheric variations along the path,

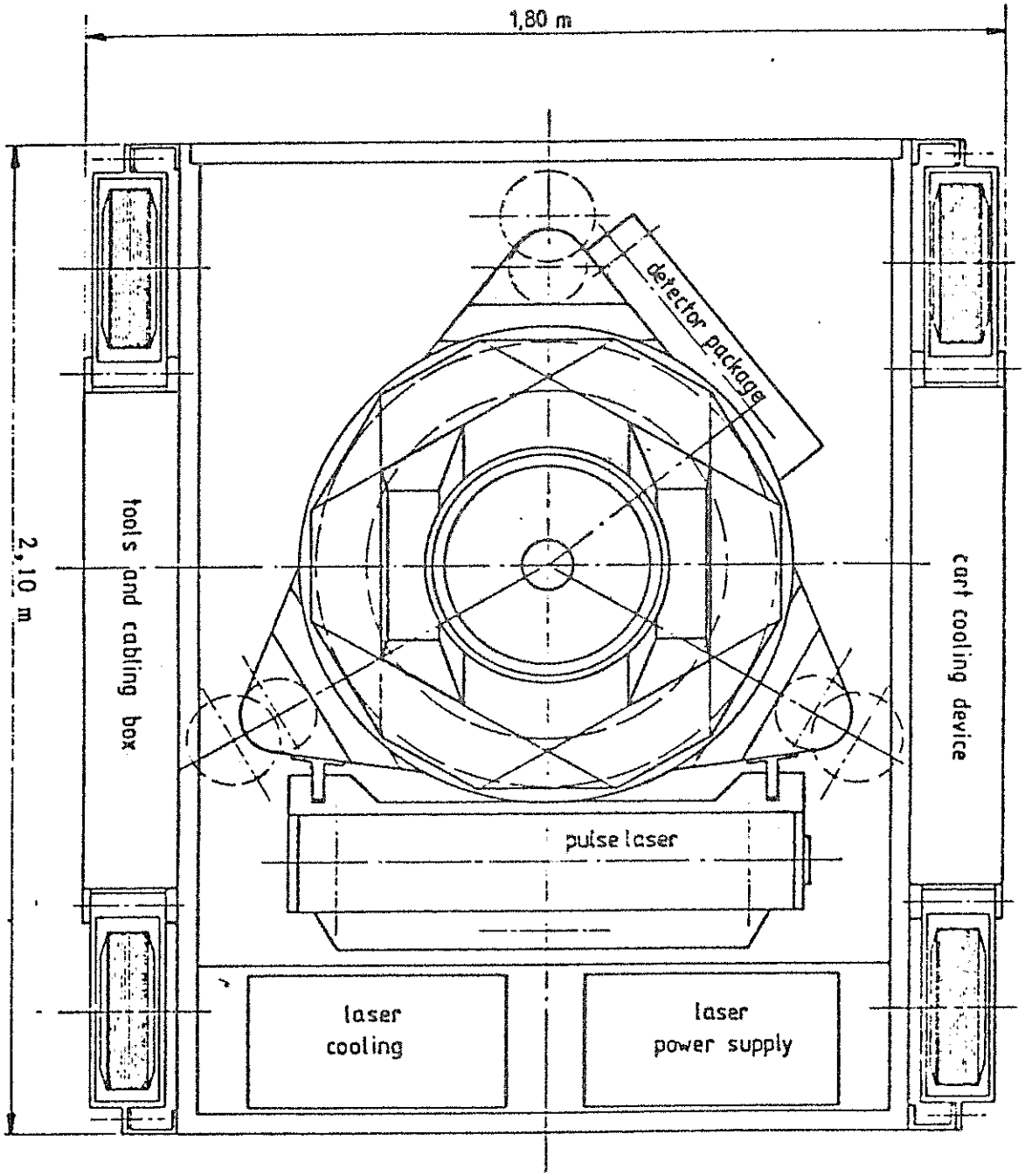

Fig. 6: Plan view of the observing cart

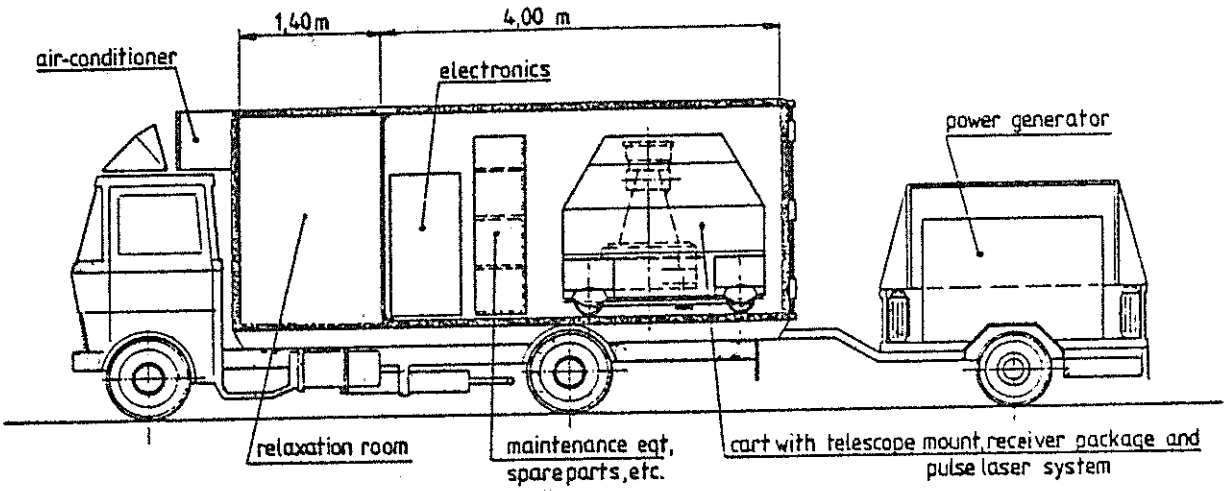

Fig. 7: The system assembled for road transportation

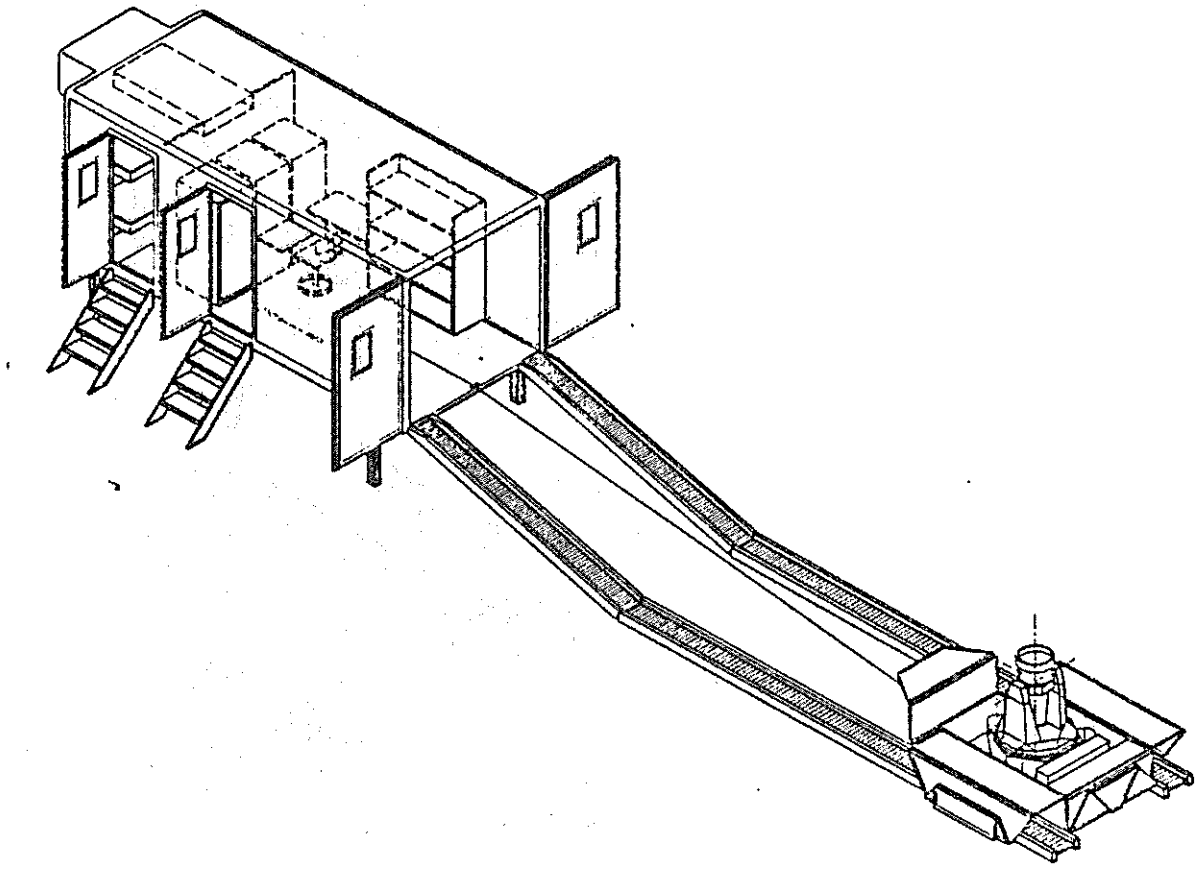

Fig. 8: The observing configuration

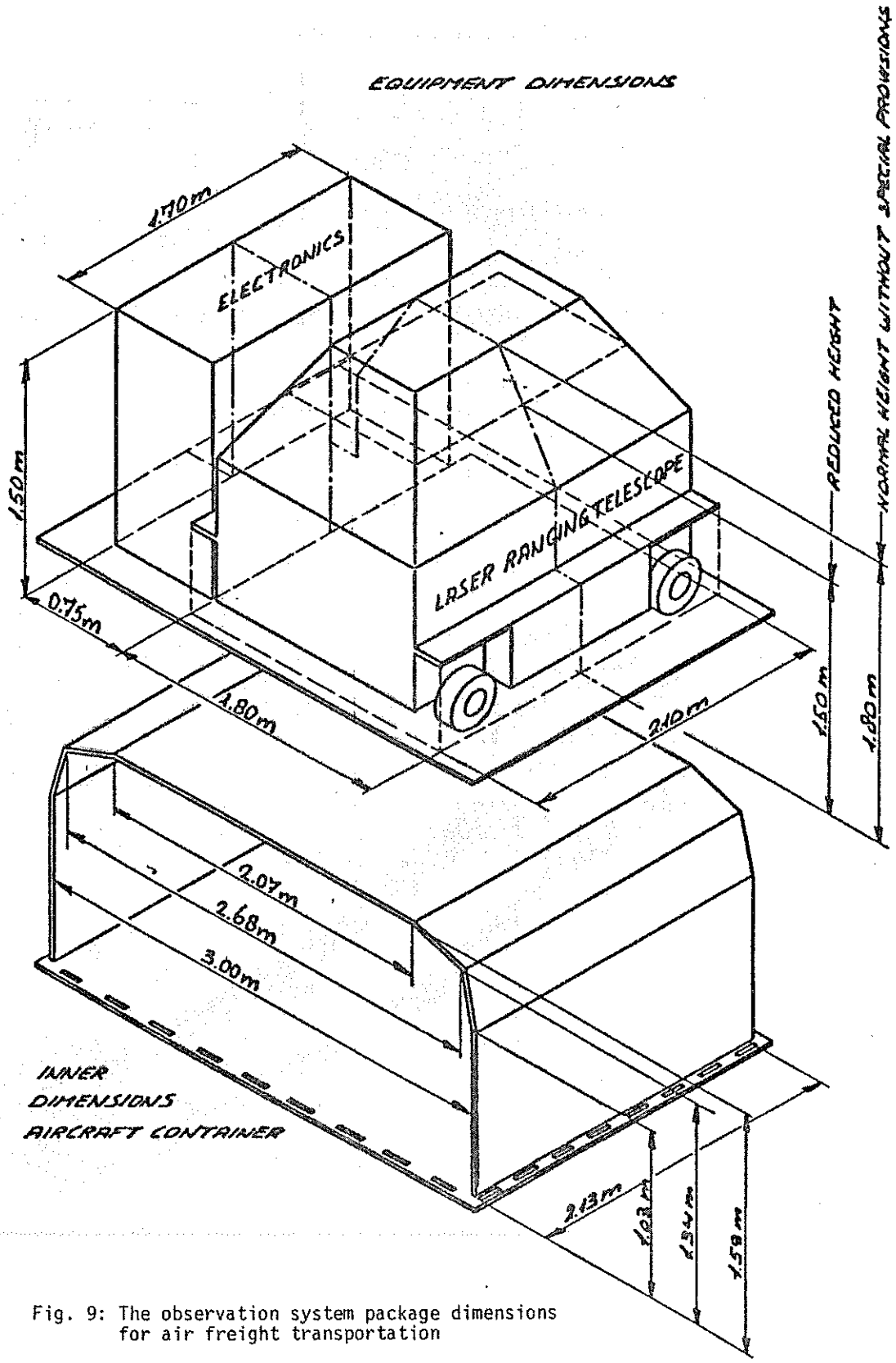

Fig. 9: The observation system package dimensions for air freight transportation

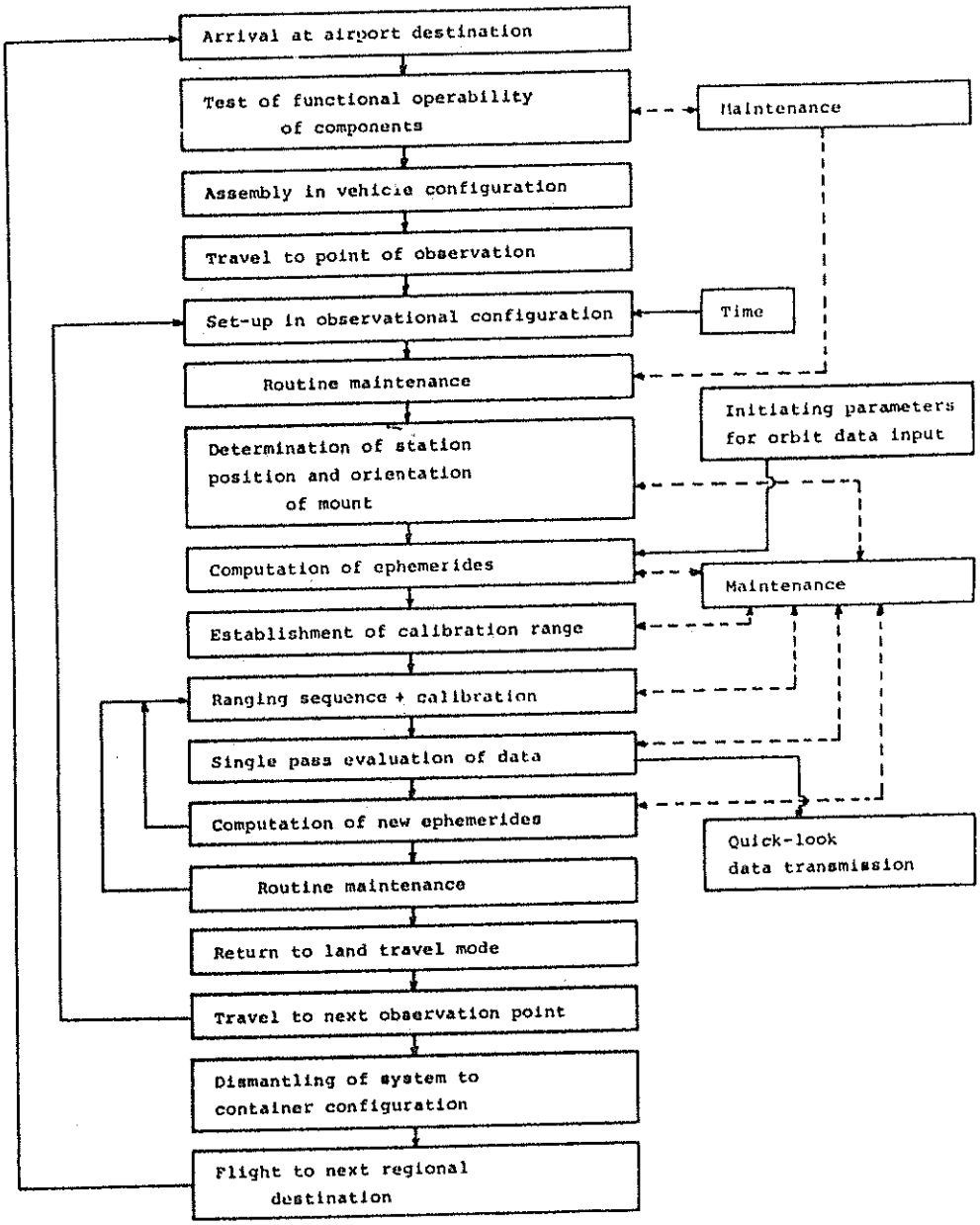

Fig. 10: The operational routine

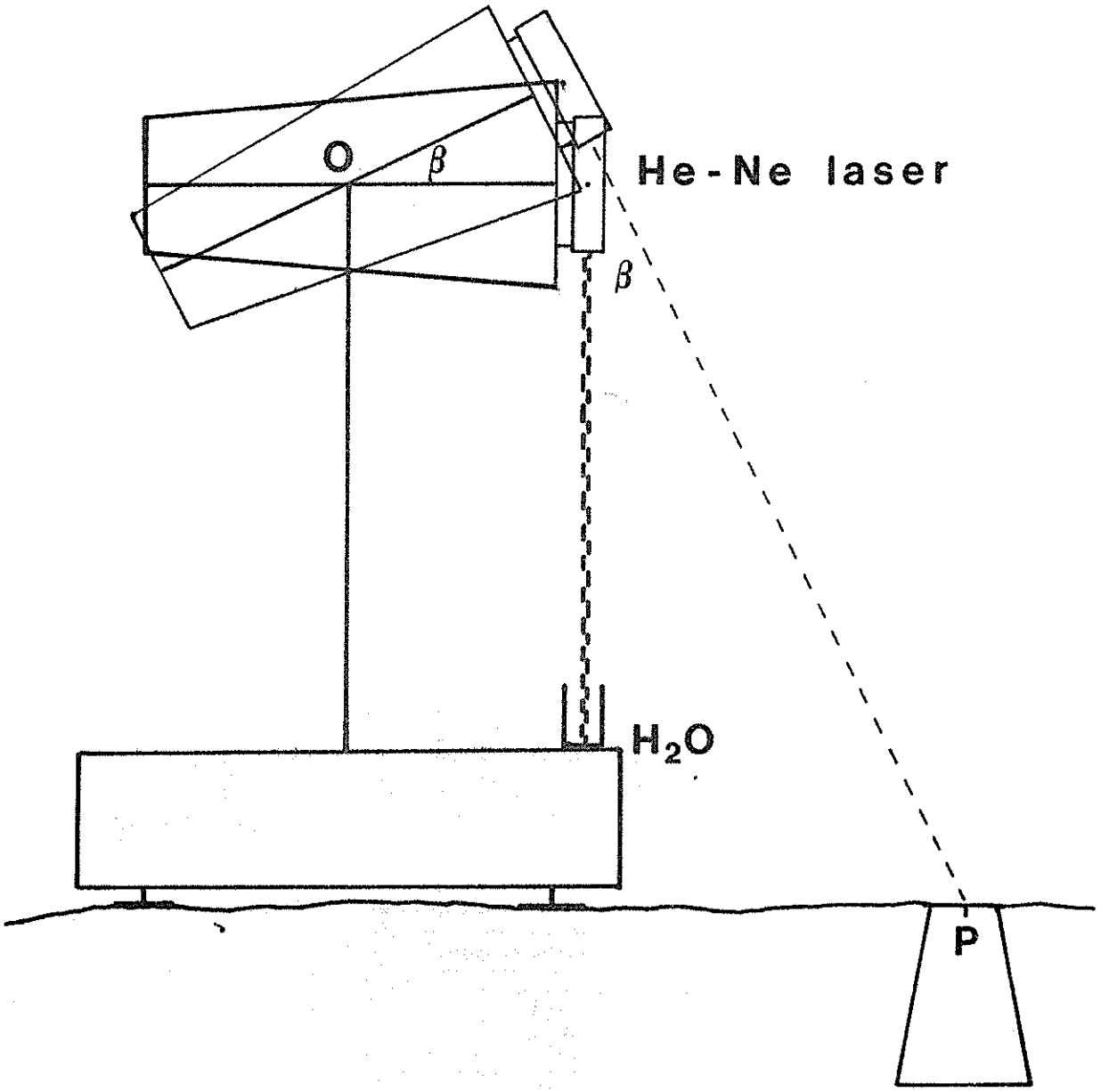

Fig. 11: Principle of transferring ground co-ordinates to the intersection of the axes of the mount

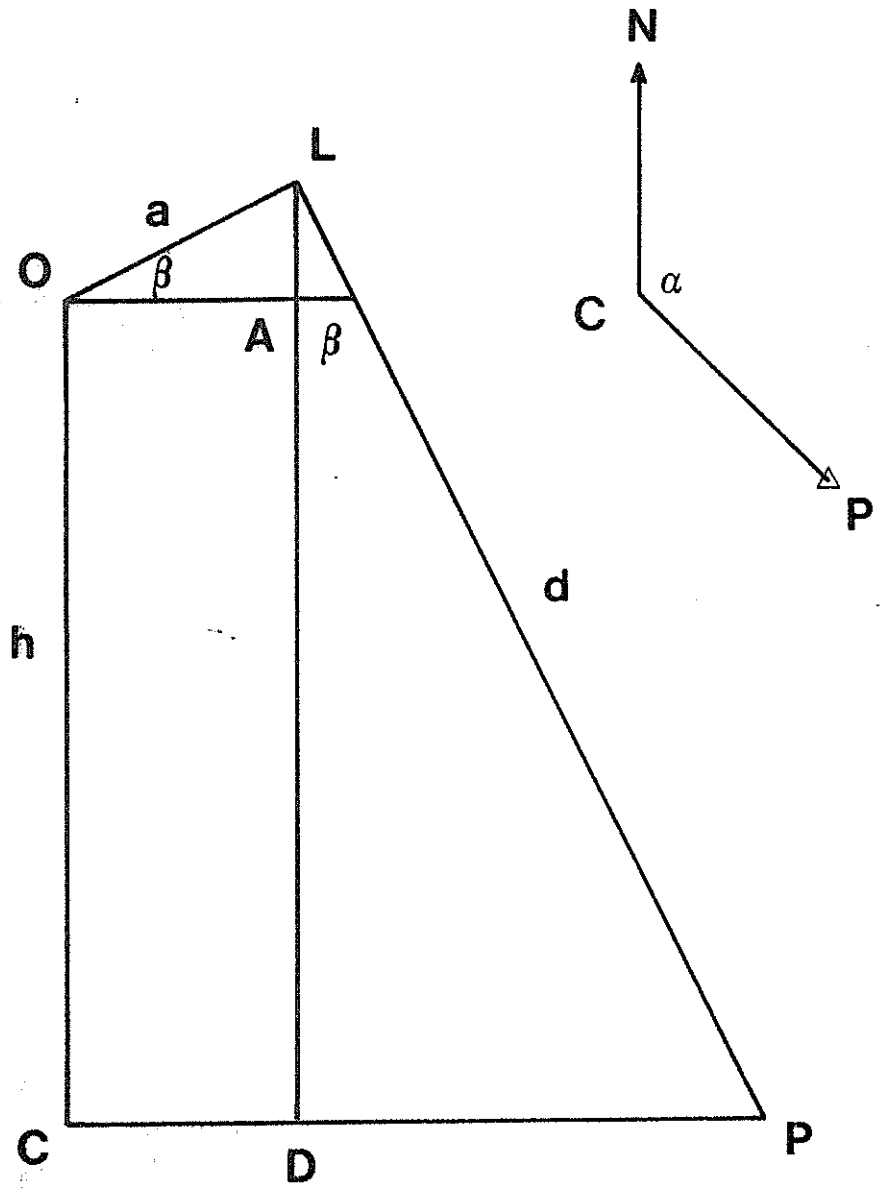

CP is the ex-centric distance, CO the ex-centric height. α is the azimuth of P from C.

$$CP = CD + DP = d \cdot \sin\beta + a \cdot \cos\beta$$

$$CO = DL - AL = d \cdot \cos\beta - a \cdot \sin\beta$$

Fig. 12: To transfer ground co-ordinates to O only d and ß must be measured. a is an instrumental constant

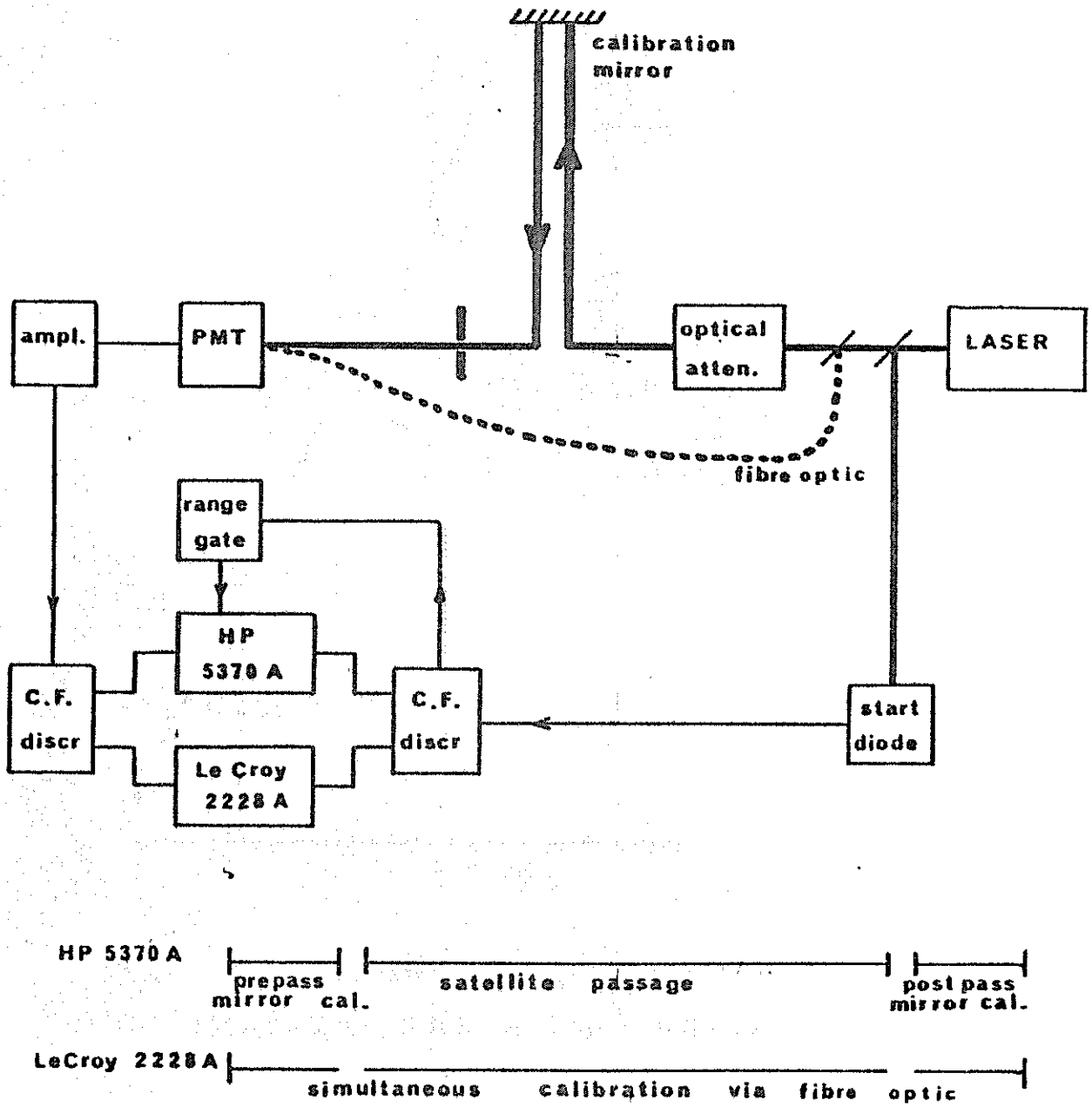

Fig. 13: The range calibration procedures

- and a pulse-by-pulse control of the ranged distance

are both desirable.

To achieve the first of these, pre- and post-pass calibrations are visualised using the defined range to a calibration mirror attached at the front of the telescope (fig. 13). For this, ranging is performed with the same HP 5370 A computing counter as that used to range to the satellite. At the same time, and throughout the satellite pass, parallel ranging will be performed over a second fixed range defined by a fibre-optic fed to the PMT (see also fig. 13). Constant fraction discriminators are used to furnish the start and stop signals to both the HP 5370 A and to a Le Croy 2228 A counter, whose task it will be to monitor the consistency of the fibre-optic calibration range throughout the pass.

4. Concluding comments

The systems described here have been designed with the objective of achieving high quality results with a mobile system, characterised by minimal systematic and a high level of alignment stability and operational reliability. To this end there has been some compromise of the requirement for diminishing volume and weight in the interest of accessibility and flexibility. The resulting systems will provide interesting alternatives in the growing family of relatively highly mobile laser ranging instrumentation.

5. Bibliography

[1] H. Visser and F.W. Zeeman - Mount and telescope for the German/Dutch mobile system - Fourth International Workshop on Laser Ranging Instrumentation, Austin, Texas, 1981.

[2] H. Puell - Subnanosecond laser systems for satellite ranging - Fourth International Workshop on Laser Ranging Instrumentation, Austin, Texas, 1981.

[3] H. Visser and F.W. Zeeman - Detection package for the German/Dutch mobile system - Fourth International Workshop on Laser Ranging Instrumentation, Austin, Texas, 1981.

[4] K.H. Otten - Software design for a multi-processor based mobile ranging system - Fourth International Workshop on Laser Ranging Instrumentation, Austin, Texas, 1981.

[5] E. Vermaat - Practical aspects of on-site prediction - Fourth International Workshop on Laser Ranging Instrumentation, Austin, Texas, 1981.

FIRST SATELLITE RANGING RESULTS USING A DUAL-PULSE RUBY LASER

L. Grunwaldt, R. Neubert, H. Fischer, R. Stecher

Central Earth Physics Institute of the Academy of Sciences of the GDR

DDR-1500 Potsdam, Telegrafenberg A17

1. Introduction

It has been demonstrated, that the simple passive Q-switched ruby laser may produce pulses of a few nanoseconds width [1],[2]. The new laser constructed for the Potsdam station transmits a diffraction limited TEMoo beam, but usually operates at two adjacent longitudinal modes. As a special feature, it may be adjusted so, that the modes oscillate at different times separated by 0 to 100 ns [3].

In this paper we report on first experiments directed to the use of both the pulses at low signal levels.

2. Hardware Description

The Potsdam laser radar system is based on a 4-axes camera mount modified for automatic tracking using an on-line computer. The main specifications are given in the station report contained in the proceedings.

The new ruby laser is a compact oscillator/preamplifier design with two rubies in the same pumping cavity (Fig.1).

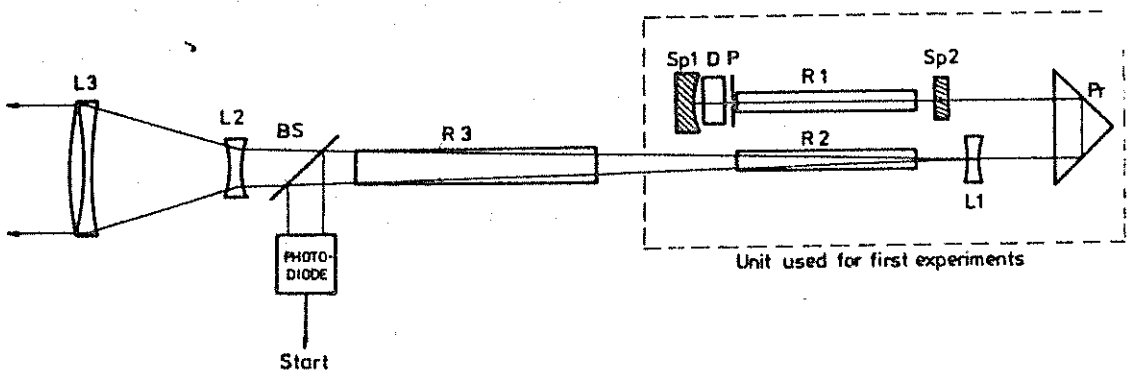

Fig.1 Optical Scheme of the Laser

For the experiments described here only the 1st laser head producing double pulses of 5ns width, 40 to 80 ns separation, and 20 to 30 mJ energy has been used. The

main specifications of the laser without the second amplifier stage are collected in Table 1. Using a beam expander of 5cm aperture only, a divergency of less than 30 arcsec is easily obtained.

To use both pulses it has been found necessary to measure their time separation for each shot, because the second pulse delay is fluctuating about 10%. For this purpose a pulse stretcher/ counter assembly has been designed giving a resolution of 0.1 ns. The real accuracy has been 1ns as yet. This pulse delay measurement system is the main modification of the electronics. Single stop time of flight method is used as before, the first laser pulse starts the counter in any case.

To minimize the noise of the time of flight measurements, both the start and stop trigger have been matched to 5ns pulses. The time walk effect of the stop trigger is now within 1ns for the full dynamical range from 1 to 10000 photoelectrons.

Table 1: Laser Parameters (Oscill.+Preamp.)

Ruby size	(6x120)mm, Czochralski
Resonator length	205mm (physical)
Q-switch	DDI* in methanol (45% SST)
Mirrors	100% dielectric, 51m curvature
	15% single glass etalon, flat
Pinhole	0.8mm diam.
Pulsewidth	5ns (2 pulses)
Output energy	20-30 mJ
Repetition rate	10/min

3. Experimental Results

3.1 Calibration Target Ranging

For the single stop system the second laser pulse is occuring in the range data for very low signal levels near to 1 photoelectron only. On the other hand this is the most interesting case, because for strong signals we have a sufficient amount of data even if the first pulse is used only.

Fig.2 is a histogram of calibration target results at single photoelectron level. The attenuation was chosen so, that the return rate was about 50%. For an amplitude ratio of the 1st to 2nd pulse of 3:1, we obtained about 20% second pulse returns. Note that in Fig.2 the second peak is plotted with 5 times enhanced amplitude. In Fig.2a (uncorrected data), the second peak has significantly greater spread in time than the first because of pulse delay fluctuations. In Fig.2b corrections are applied using the pulse separation data.

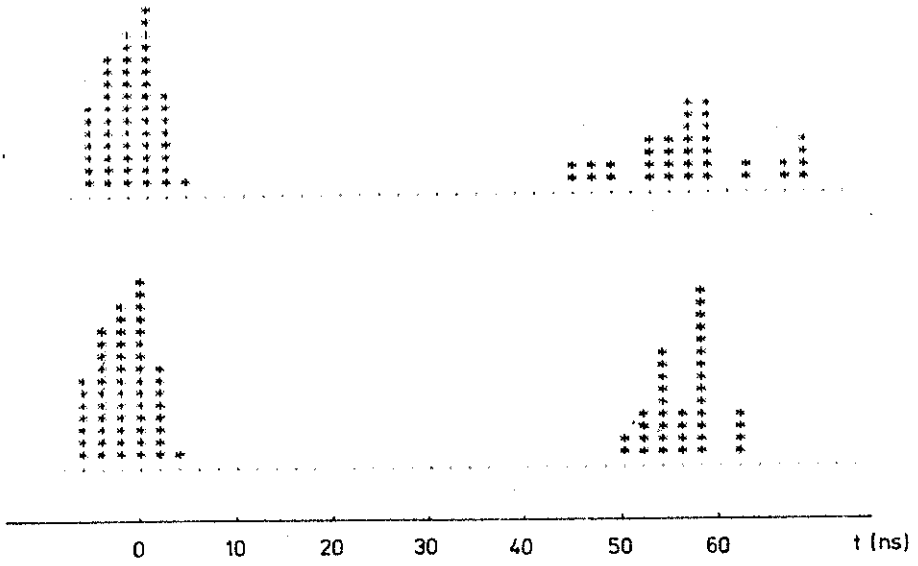

Fig.2 Histogram of Calibration Target Results

As a result both peaks have the same rms width of about 3ns.

For signal levels of about 100 photoelectrons the first pulse returns are dominating strongly. The rms noise of individual measurements is about 0.5 ns in this case.

3.2 Satellite Ranging

During August 1981 successful satellite ranging of all interesting satellites has been obtained using a 50 to 70 arcsec laser beam. Unfortunately, difficulties with the pulse delay measurement system have prevented the use of the second pulse returns as yet. Therefore the satellite ranging has been focused on satellites giving strong signals to test the ultimate precision. LAGEOS ranging will be continued as soon as the pulse separation can be measured reliably.
Table 2 is a summary of satellite ranging results. In the 4th column of this table the numbers of unambiguously identified returns from the second laser pulse are given. Their percentage is relatively low because of the strong signals.

To determine the rms noise of the individual measurements, each pass has been treated separately. After subtracting predicted ranges the remaining differences have been fitted by a low degree polynomial. The maximum and minimum range noise, determined in this way, are given in the table. The last column contains

the averages over all passes, weighted by the number of points of individual passes.

Table 2: Ranging Accuracy Summary

satellite	passes	returns 1st pulse	returns 2nd pulse	range noise/cm max	min	av.
7603901	2	15	2			<50
7502701	17	434	9	42	11	20
7501001	7	172	3	21	12	18
8107501	6	99	2	44	21	30

References

[1] M.Vrbova:
Damage limited pulsewidth of a passive Q-switched ruby oscillator
IEEE J.Quant.El. QE-14 (1978),No.8,pp.596-600

[2] J.Gaignebet:
New developments on laser transmitters for the GRGS/CERGA satellite and lunar ranging systems
Paper presented at the 3rd Workshop on Laser Tracking Instrumentation, Lagonissi, 1978

[3] L.Grunwaldt, R.Neubert, K.Hamal, H.Jelinkova
Generation of reproducible double pulses using a passive Q-switched two-mode ruby laser
Paper submitted to the 4th Internat. Conference on Lasers and their Appl., Leipzig, Oct. 1981

[4] R.Neubert:
On the use of pulse trains from a mode locking laser for satellite ranging
Paper submitted to the 3rd Workshop on Laser Tracking Instr., Lagonissi, 1978

[5] E.C.Silverberg:
The development of a highly transportable LAGEOS station: Status report
Paper presented at the 3rd Workshop on Laser Tracking Instr., Lagonissi , 1978
(see also these proceedings)

Mitteilung des Zentralinst. f. Phys. d. Erde Nr.1078

A Laser LockOut System Using X-Band Radar

D.R. Hall
Department of Applied Physics
University of Hull
Hull

C. Amess, N. Parker
Royal Greenwich Observatory
Herstmonceaux Castle,
Sussex

INTRODUCTION

A laser system designed to make high resolution ($\lesssim$ 5 cm) range measurements to satellites (Lageos, Geos and Starlette) in earth orbit will be installed at the Royal Greenwich Observatory during 1982. The laser to be used in this system will allow 30 mJ 150 psec pulses to be transmitted via the 10 cm aperture telescope at up to 10 hz in the green part of the spectrum at 532 nm. This corresponds to peak powers of 200 megawatts with average powers of 300 milliwatts.

One cause for concern is the possibility of aircraft flying through the laser beam during ranging operations. Under certain circumstances the optical energy density in the beam where it is intersected by the aircraft could exceed the Maximum Permissable Exposure. In this context it should be noted that the Gatwick International Airport is about 46 km from the Royal Greenwich Observatory. To prevent the occurrence of such an event it is proposed to design, install and operate a laser lock-out system. This will consist of an aircraft detection sensor, whose output is coupled directly to a control element in the laser. The objective here is to cause the laser to be effectively switched off in the event that an aircraft is detected, before the aircraft path intersects the laser beam pattern and puts the eyes of its passengers and crew at risk. This can be achieved by using an active microwave radar system to

detect aircraft, and by designing the radar antenna beam pattern to have a significantly larger spread in solid angle than the laser beam. In addition, the radar dish should be positioned close to the optical telescope, through which the laser beam is transmitted, and aligned such that the laser beam pattern passes up the centre of the radar beam pattern. Then, if the radar dish is slaved to track with the optical telescope, it is possible to detect an aircraft in the field of view of the radar dish before it is illuminated by the laser. This is illustrated in Figure 1(a). The radar receiver will be linked to a status monitor, and in parallel to an electro-mechanical shutter which, when activated will terminate laser oscillation (in about 10 milliseconds) by closing off the optical path within the laser resonator. A schematic of the proposed system is shown in Figure 1(b).

Minimum Eye Safe Range

In this context 'eye-safe range' is defined as the range at which the laser energy density drops to the level of maximum permissable exposure (MPE) defined by British Standard BS4803 (1). According to this standard, the range eye safe R_s from a laser emitting E joules per pulse at a repetition rate of p pulses per second at 532 nm, with a pulse duration τ ($< 10^{-9}$ sec) via a telescope of diameter D, producing a divergence θ is given by,

$$\frac{E}{\frac{\pi}{4}(R_s\theta+D)^2} < \frac{5 \times 10^6}{p} . \tau \qquad (1)$$

For our case E = 30 mJ, τ = 150 psec, p = 10 Hz D = 0.1 m, so we have

$$R_s\theta < 12.5 \qquad (2)$$

with R_s in metres and θ in radians. Evaluation of equation (2) for a 'worst case' value of $\theta = 10^{-4}$ radians yields the eye safe range R_s = 125 km.

Although it is clear that this in no way represents a range at which actual eye damage will occur since the MPE is considerably below the damage threshold, nevertheless it does indicate that to comply with BS4803, some technique for the detection of aircraft at all reasonable altitudes is required.

X-Band Radar Detection System

The geometry of the laser lock-out system is illustrated in Figure 2, which shows a laser beam of angular divergence ω tracking co-axially with the X band antenna, whose main lobe has an angular spread of Ω. We consider an aircraft flying horizontally at an altitude of h and at velocity V into the beams patterns. The maximum time T_{LO} available to shut down the laser assuming a successful radar detection is given by

$$T_{LO} = (h/2v \sin \theta) \ (\Omega - \omega) - \tau$$

where τ is the time taken to activate the electro mechanical shutter. T_{LO} is plotted against aircraft altitude for a range of speeds and elevation angles in Figure 3. The plots show that there is adequate time to achieve lockout for all likely combinations of aircraft altitude and speed, given that $\tau < 50$ m sec.

System Hardware

The lockout system to be installed at RGO will employ a 150 cm diameter X-band antenna dish mounted on an alt-az mount, slaved to the optical tracker telescope. The X-band transceiver is a commercial Marine Radar Unit manufactured by Racal-Decca. It produces 25 kw pulses at 9400 MHz, a pulse duration of 1 μsec and a repetition rate of 865 Hz. The receiver is fitted with a low noise (< 4db noise figure) front end and has a 5 MHz IF bandwidth.

Radar range equation calculations yield a received signal to noise ratio (single pulse case) dependence on range and radar cross section as indicated in Figure 4. However, because the time available for detection increases with range, one can use a cumulative probability of detection based on multiple pulses and a sliding window type integrator to improve the probability of detection, with a threshold level which will yidle an acceptably low false alarm rate and a high probability of detection at relevant ranges.

It is planned to complete installation of the lock-out system during 1981 and to carry out task and calibration procedures during early 1982.

Reference

(1) Radiation Safety of Laser Products and Equipment, Manufacturing Requirements, Ureis finde and Classification, British Standard, BS4803.

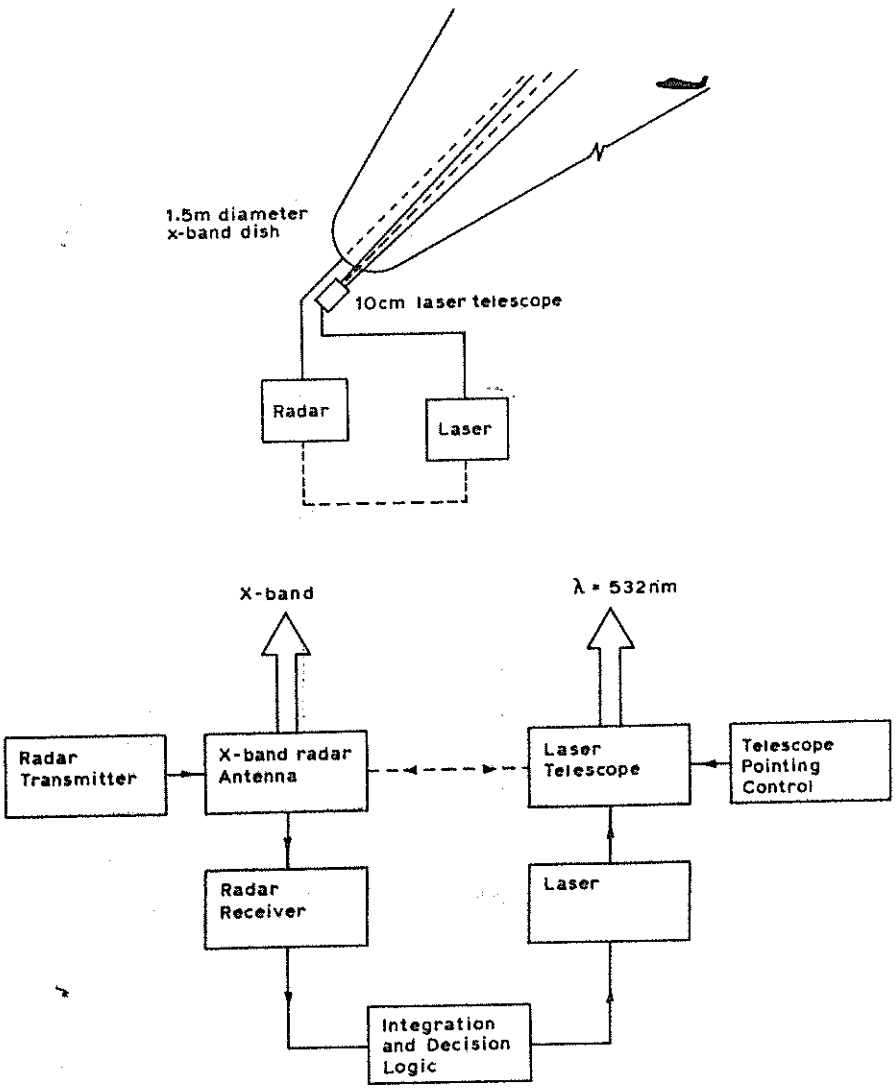

Fig. 1 Schematic of X-band Radar System for Aircraft Detection and Laser Lockout.

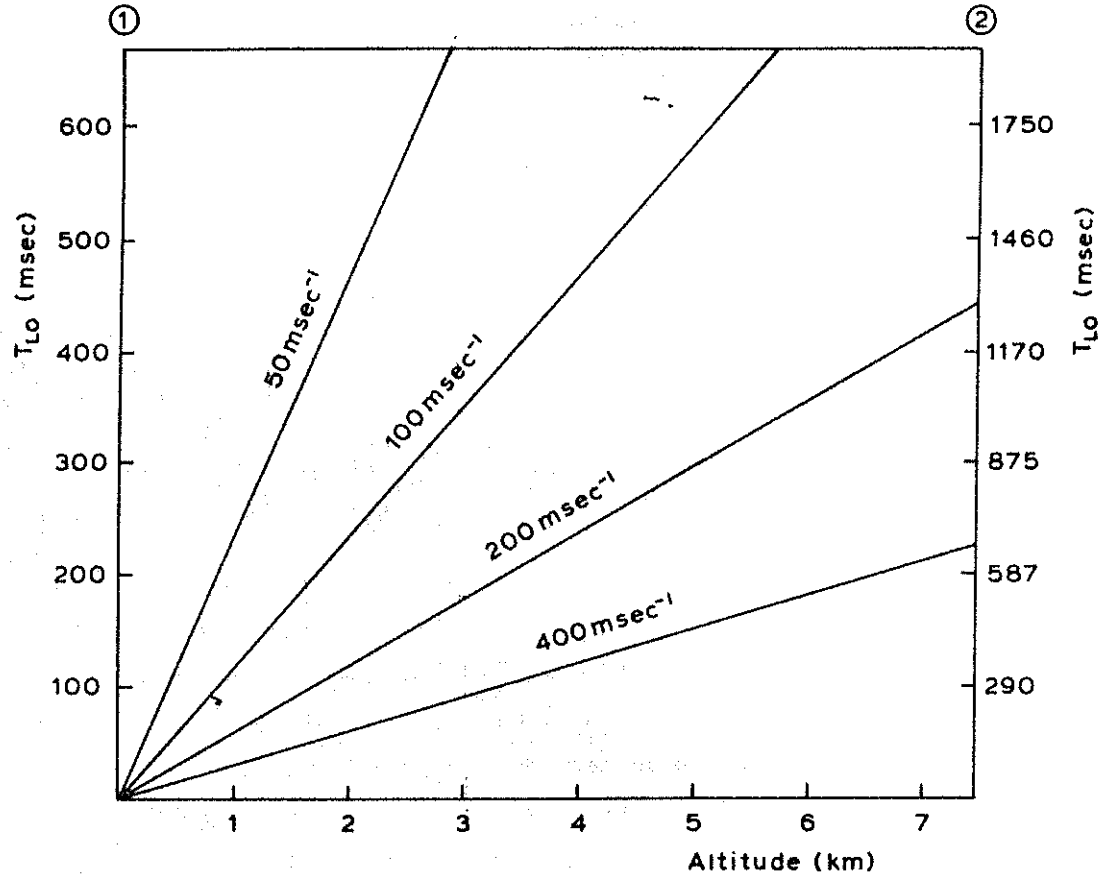

Fig. 3 Time Available for Aircraft Detection and Laser Lockout

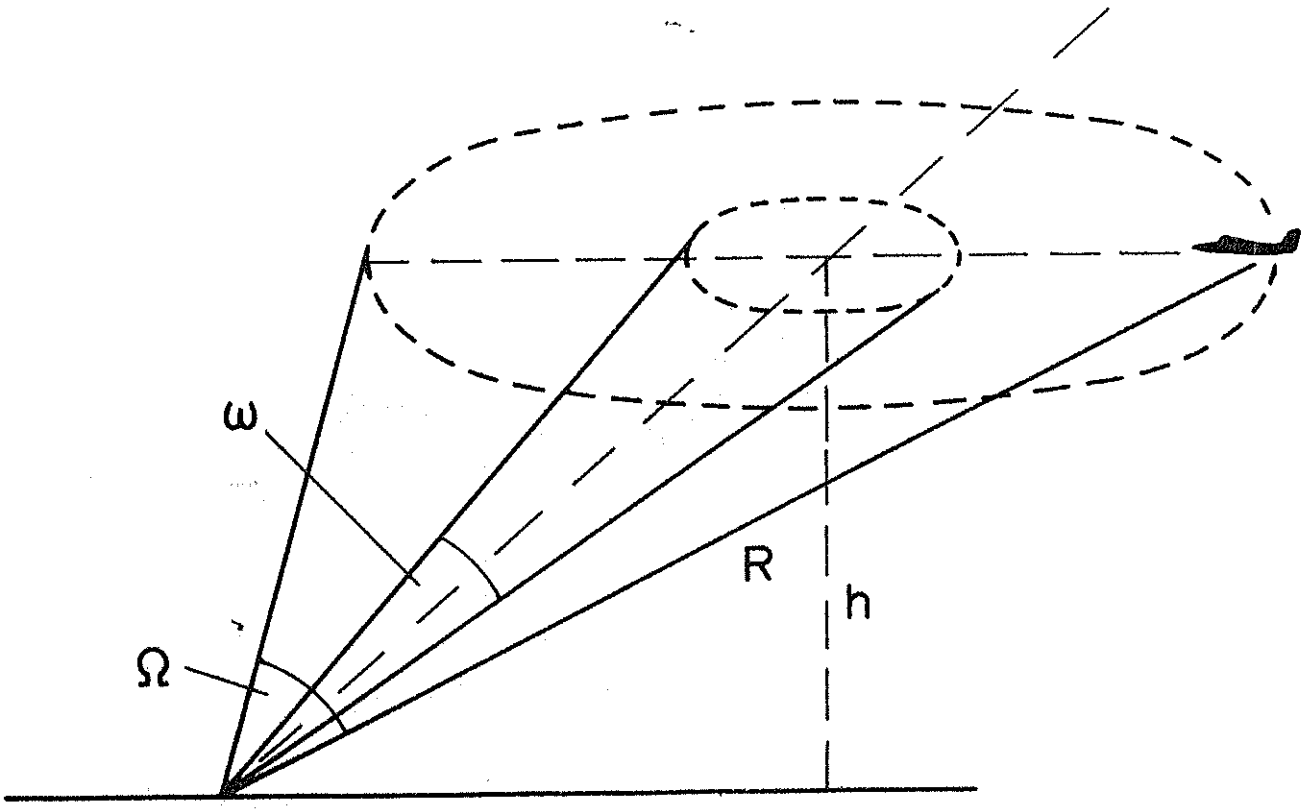

Fig. 2 Aircraft Detection Geometry

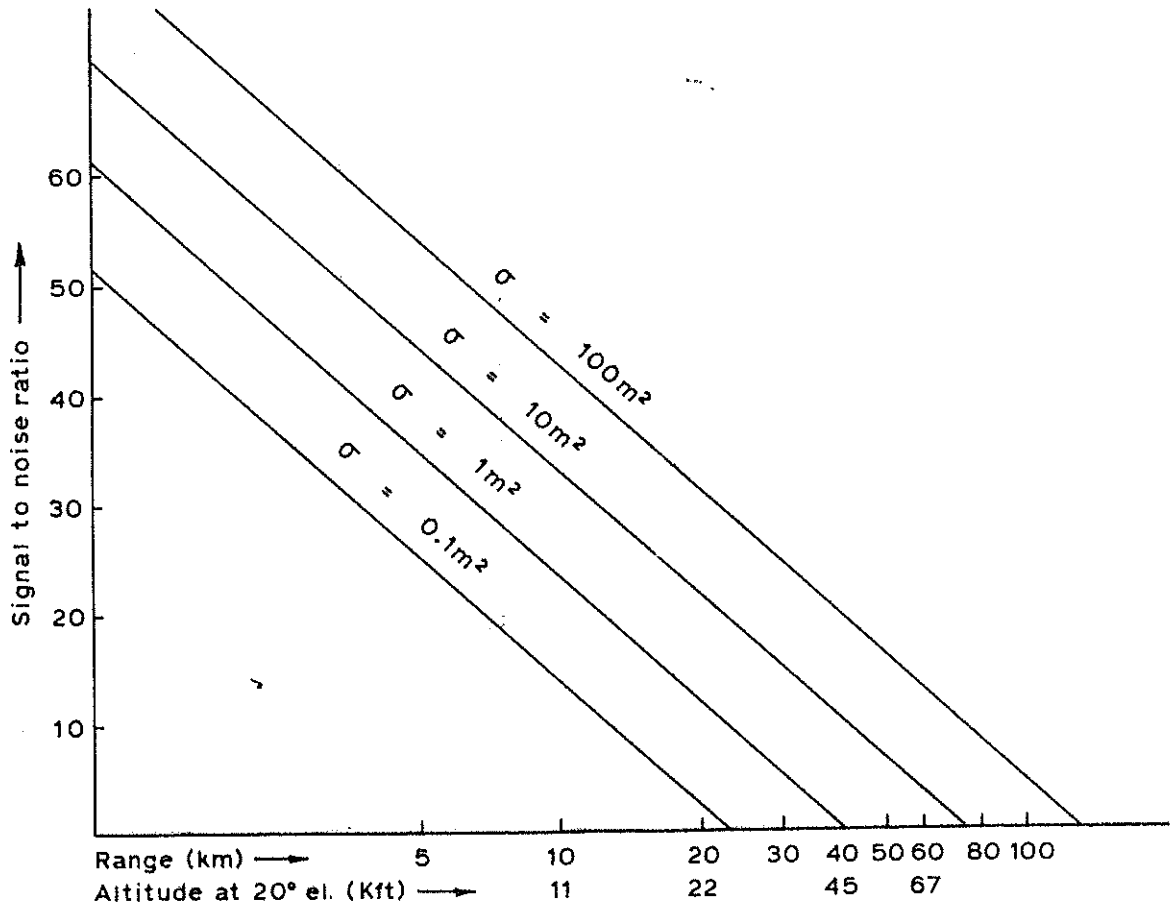

Fig. 4 Dependence of Received Signal-to-noise ratio on Target Cross-section and Range.

A FILTER FOR LAGEOS LASER RANGE DATA

E.G. Masters, B. Hirsch, and A. Stolz

Department of Geodesy
School of Surveying
University of New South Wales
Kensington, Australia

ABSTRACT

A simple filter for the Lageos range data is described. The basis of the technique is that the second time derivative of range should be constant over short time intervals. The method is well suited for use at observatory sites and as a means of cleaning the data prior to compressing it into normal points.

INTRODUCTION

We aim to use the high-accuracy laser range measurements to the Lageos satellite, obtained at existing fixed tracking stations in the Australasian region and possibly by one or more transportable units deployed at critically selected sites to measure baselines in order to determine the relative motion between the stations (Stolz, 1981). One problem that immediately arises is that the data contain a significant proportion of outliers. These outliers are commonly removed after comparing each observation with a modelled counterpart obtained from, amongst other things, an orbit computed using all the data (Dunn, 1981). Such a scheme is inefficient and in most cases unnecessary.

We have devised a much simpler method of detecting outliers in the Lageos range data which employs the fact that, over short intervals of time, the variation of the range measurement very nearly approximates to a degree two curve. We give only an outline of the technique and two examples of its application here. For details, we refer the reader to Masters et al. (1981).

METHOD

For orbital arcs which do not exceed 30 seconds in length, we find that the Lageos range measurements vary with time according to a degree two curve. In Fig. 1 we plot the root mean square difference between range data and the corresponding range as modelled by a second degree curve. The data span to which the curve is fitted has been varied from 0 to 300 seconds. The truncation error exceeds the 10 cm level around the 30 second mark. This implies that, for time intervals smaller than 30 seconds, the second time derivative of range can be considered to be constant. Moreover, the difference between consecutive second time derivatives should be small and essentially proportional to the data quality. An upper bound for the departure from this condition may be obtained by applying the law of propagation of variances to the second derivative calculations. Using this technique, we are able to trace an anomolous difference of the second time derivative to two satellite range values. The outlier is then determined by means of an iterative scheme.

RESULTS

In order to demonstrate the effectiveness of the filter, we have selected two Lageos passes each containing a number of outliers. In Figs. 2a and

3a we have plotted the residuals of the raw data with respect to an orbit computed from the good data. For convenience, residuals exceeding 5 m have been assigned a value of 5 m. The same passes, after applying the filter, are shown in Figs. 2b and 3b. For this study the rejection level for the range measurements was set at 2.5 m.

Stricter conditions can of course be imposed and the level of rejection can be tightened.

CONCLUSIONS

We have developed the filter for cleaning the data prior to compressing it into normal points. The method is a simple one and could therefore be adapted for use at observatory sites. Subsequent savings of computer time are substantial. The method is better suited for use with data gathered at the Moblas sites and by TLRS-type instruments than with SAO station data. This is because with the former the acquisition rate is higher and one is therefore less likely to encounter gaps in the data bigger than 30 seconds. The filter does not remove biases and long-period signals.

ACKNOWLEDGEMENTS

E.G. Masters is supported by a grant from the Australian Research Grants Committee. B. Hirsch is supported in part from the same grant as well as from funds provided by the School of Surveying.

REFERENCES

Dunn, P.J., 1981, personal communication.

Masters, E.G., Stolz, A. and Hirsch, B., 1981, A Method of Filtering and Compressing Lageos Range Data, in preparation.

Stolz, A., 1981, Determination of the Large-Scale Crustal Motion of Australasia by Satellite Laser Ranging, Proposal to NASA in response to Announcement of Opportunity AO No. OSTA 80-2.

FIGURE CAPTIONS

Fig. 1

Differences (r.m.s.) between Lageos range data and the corresponding range as modelled by a degree two curve for various time spans.

Fig. 2

(a) Residuals of raw Lageos range data with respect to an orbit computed from good data. Residuals exceeding 5 m have been assigned a value of 5 m.

(b) Same, except that the data are filtered. The rejection-level in this example is set at 2.5 m.

Fig. 3.

Same as Fig. 2, except for a different site and time.

FIGURE 1

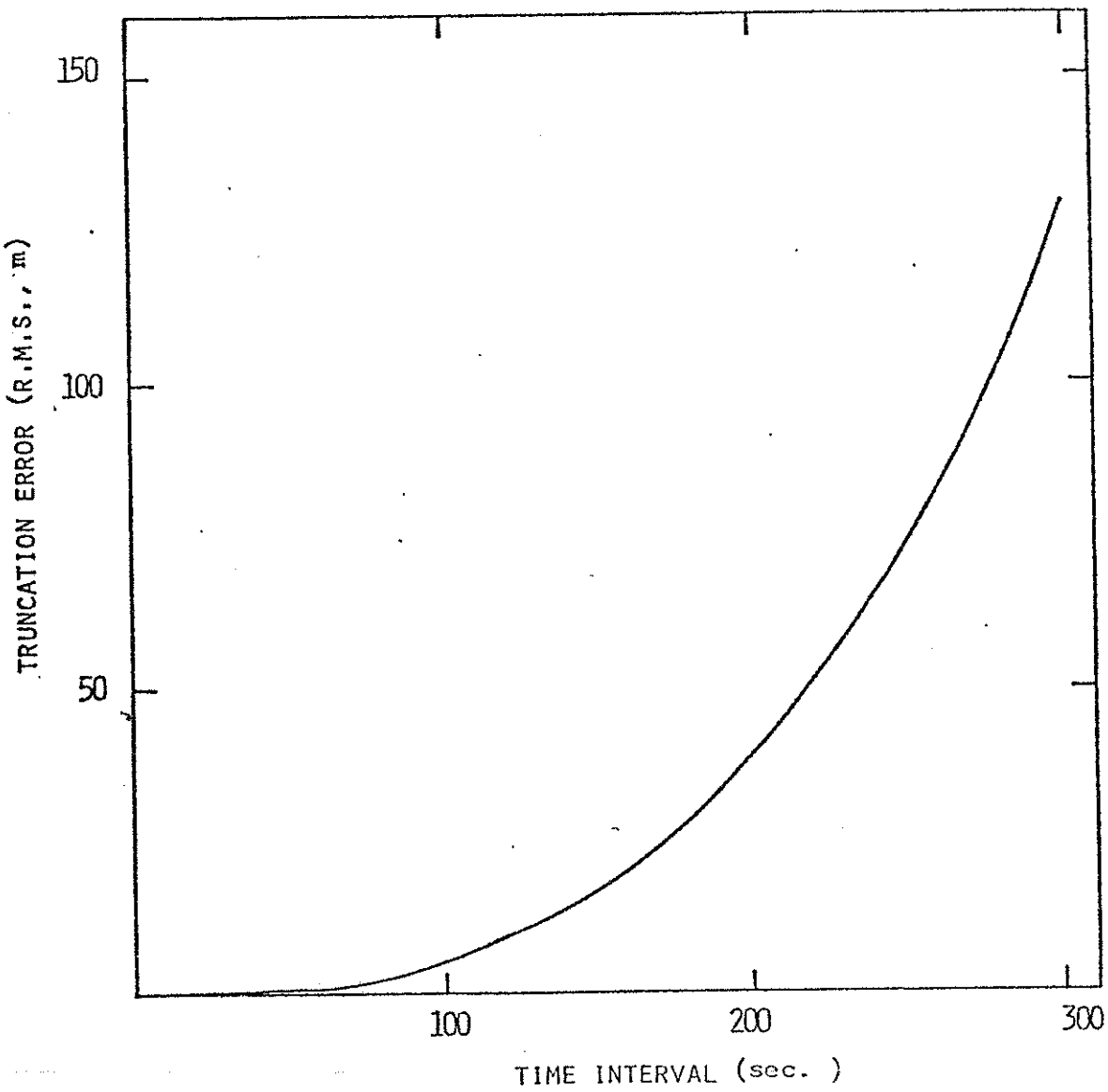
150
100
50
TRUNCATION ERROR (R.M.S., m)
100
200
300
TIME INTERVAL (sec.)

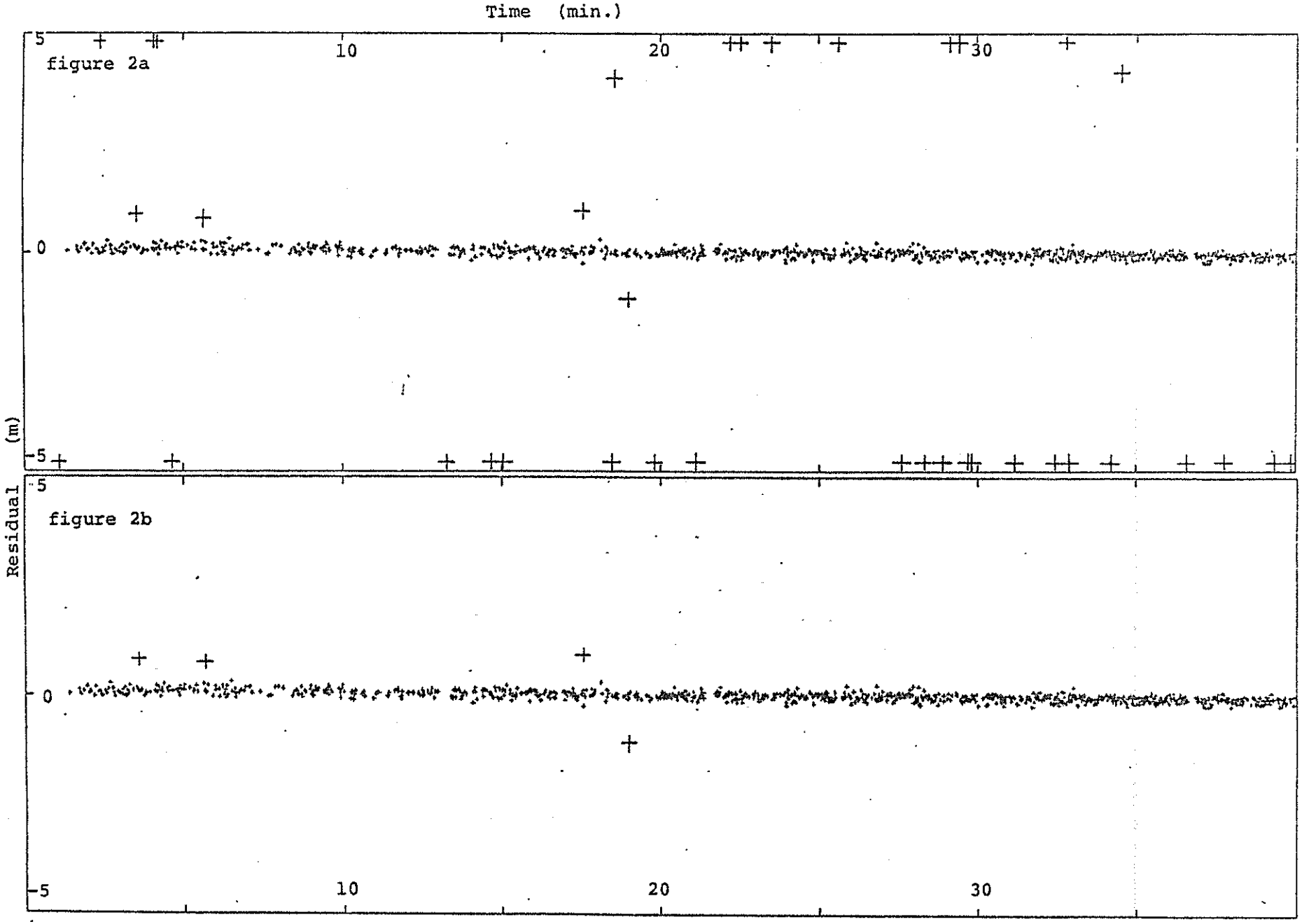
Time (min.)
5
10
20
30
figure 2a
0
-5
(m)
Residual
5
figure 2b
0
-5
10
20
30

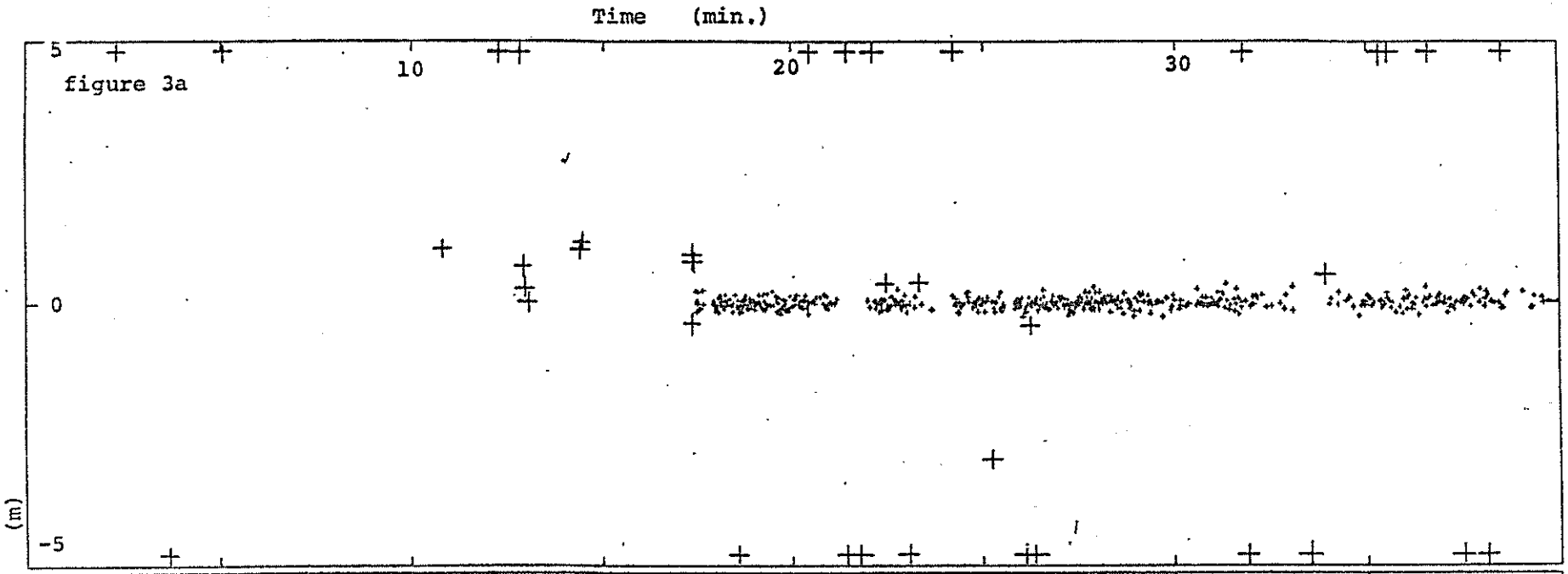
Time (min.)
5
10
20
30
figure 3a
0
-5
(m)

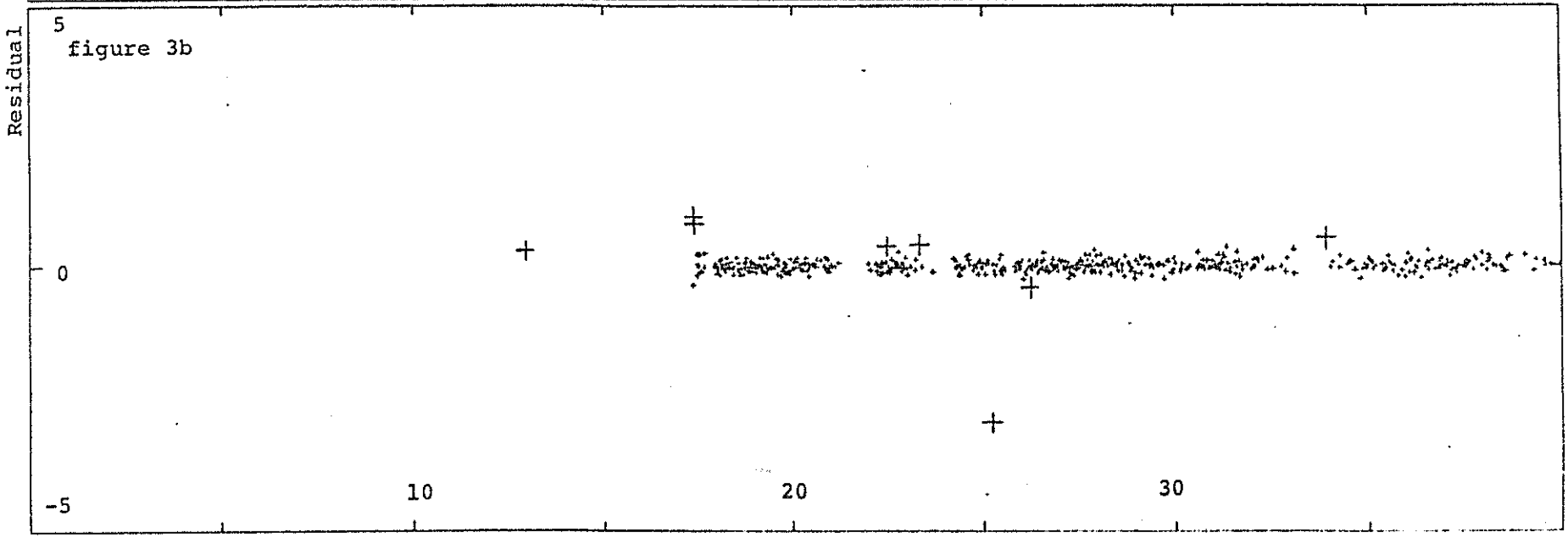
Residual
5
figure 3b
0
-5
10
20
30

SCIENTIFIC GOALS OF LASER RANGE MEASUREMENTS

Peter L. Bender

Joint Institute for Laboratory Astrophysics
National Bureau of Standards and University of Colorado
Boulder, Colorado 80309 U.S.A.

ABSTRACT

Two of the most important areas of geodynamics to which laser ranging appears capable of making fundamental contributions are discussed. These are worldwide plate tectonic motion measurements and the monitoring of the longer wavelength crustal movements in seismic zones. In both areas, the accuracy and reliability of the results are of great importance, since a factor 2 improvement in accuracy can reduce the time necessary for detecting anomalous motions by the same factor. The capabilities of other techniques are discussed briefly, and it is argued that laser ranging to satellites is likely to make major and unique contributions to geodynamics if it succeeds in demonstrating higher measurement accuracy than radio techniques. A strong emphasis on improving the measurement accuracy thus appears to be needed during the next two years.

INTRODUCTION

Accurate laser range measurements to satellites like LAGEOS can provide valuable and exciting new scientific information in geodynamics, as well as important information in several other fields. Rather than trying to cover most possible applications of laser ranging results, the next section will concentrate on discussing what I believe are the two most important scientific problems where laser ranging to satellites is likely to have a major impact in the 1980's. These are the measurement of present worldwide plate tectonic motion rates and the monitoring of the longer wavelength features of strain accumulation patterns in seismic zones.

An additional reason for focusing attention on these two topics, besides their intrinsic scientific importance, is that laser ranging may have a unique advantage in these cases. Other techniques are being developed which can address the same scientific problems, including particularly very long baseline radio interferometry (VLBI) for worldwide measurements and the use signals from the Global Positioning System (GPS) satellites for geodetic measurements in seismic zones. However, for both worldwide plate motions measurements and determining the longer wavelength strain changes in seismic zones, obtaining the highest possible accuracy is of great importance. The potential unique advantage of laser ranging is that its sensitivity to the water vapor content of the atmosphere is lower than for radio techniques. Thus, there appears to be very strong reason for the continued vigorous development of laser ranging, provided that the systematic measurement errors can be reduced to or below the level of uncertainties due to the dry part of the atmosphere.

In view of the importance of achieving high accuracy in laser ranging, some additional discussion of this topic will be given in the third section. Some of the capabilities of the radio techniques will then be reviewed in the fourth section, in order to encourage further discussion of the kinds of scientific problems for which laser ranging is most suitable.

The scientific returns expected from laser ranging and the other techniques include new information on the earth's rotation and polar motion. However, I won't say much about these topics because the network of stations needed for determining crustal movements is likely to produce very good results for earth rotation and polar motion also. Lunar ranging won't be discussed either, although it is likely to make important contributions both to determining the earth's rotation and nutation and to other important scientific questions such as the secular deceleration of the moon, lunar structure, and the validity of present gravitational theories.

SCIENTIFIC GOALS IN CRUSTAL DYNAMICS

One of the most important questions which laser ranging is likely to play a major role in answering is whether the rates of motion of the larger tectonic plates are within roughly 1 cm/yr of the presently estimated rates. Agreement with the estimates is likely if recent studies of the average motion rates over roughly the last 3 million years are correct and if variability over shorter times can be neglected. However, short-term variability appears to be a plausible possibility.

Over periods of up to roughly a thousand years it is possible to think of models where the back part of a plate moves quite uniformly away from a spreading center, but the front or sides of the plate move considerably less because of the lack of large earthquakes at the boundaries. Buildup of stress within the plates over such a period

would not necessarily be sufficient to trigger large earthquakes, and substantial distortion within the plate could occur. In looking for such internal distortions, one prime candidate is the Pacific plate, which is very large and also quite rapidly moving. Another candidate is the Australian plate, which might show distortion between India and Australia because of the episodic nature of crustal movement along the boundary between the Indian subcontinent and the Eurasian plate.

On the other hand, the present ideas of most geophysicists about the viscosity and thickness of the asthenosphere, which underlies the plates, would not permit such distortion away from the boundaries of even large and rapidly-moving plates. The reason is that the calculated time constant for the effect of a major earthquake at the boundary to propagate out into the plate is quite long. For this reason, the effects of changes in the boundary conditions for the plate motion would not have much effect beyond perhaps 300 kilometers from the boundary over periods characteristic of the recurrence times for large earthquakes, such as perhaps 100 or 200 years. Thus, according to this picture, the main part of the plate would continue to move quite uniformly, with earthquakes around the boundary causing episodic strain changes only near the edge. However, we should keep in mind that quite a bit of our present information on the viscosity of the asthenosphere comes from post-glacial rebound studies in Canada and Fennoscandia, which are continental areas. Thus our information concerning the asthenosphere under oceanic plates may be less reliable.

For periods of time longer than roughly 1,000 years, the main question is whether the forces driving plate tectonic motions are likely to be fairly constant. At present, the three types of forces which generally are believed to be the largest ones for a plate such as the Pacific plate are: the gravitational force associated with sliding of the back of the plate off the East Pacific rise; the negative buoyancy force on the down-going slab at the front of the plate because of its higher density; and the resistance of the mantle to the downward motion of the front of the plate. The last two forces may roughly cancel each other for a given rate of motion, with the gravitational sliding pushing on the main part of the plate to keep it pressing against the back of the down-going slab. If these forces really are the dominant ones, it seems unlikely that they would change dramatically over periods of less than perhaps a million years. However, measurements which give direct information on these questions would certainly be valuable. If the present motions of the major plates are not within roughly a centimeter per year of the presently estimated rates, this would require a substantial change in our picture of how the plate motions occur.

Direct measurements of present plate motion rates also will be important for other reasons. For some minor plates, there is not enough information available to determine the long-term average rates. Also, in order to interpret measurements of the apparent motion of a plate, it is necessary to check on the basic stability of a major part of

the plate interior. Otherwise, internal distortions within the plate could lead to errors in the deduced plate motion rate. The measurements of crustal movements in plate interiors will be important also for determining how tectonic forces modify the plates. However, the rates of distortion expected are generally very small, and accuracies of 2 or 3 mm/yr are needed for studying most questions of interest.

A second major question concerns the nature of the larger wavelength crustal movements in and near seismic zones. In this case, there are strong differences of opinion about what measurement accuracy is needed. A substantial number of scientists believe that large displacements occur fairly frequently in some major seismic zones, such as the uplifts characteristic of the reported Palmdale bulge and the horizontal displacements given by the initial interpretation of earlier VLBI mobile station data. On the other hand, it has been suggested that atmospheric refraction or other effects had an important influence on the leveling data used to deduce the existence of the Palmdale bulge, and it seems possible that the reported motion of roughly 20 centimeters for JPL with respect to Owens Valley was due to a combination of ionospheric, tropospheric, and instrumental systematic errors. Thus other scientists would say that the probability of learning about strain accumulation in seismic zones isn't increased much by making measurements more frequently than a characteristic time T, which depends on the accuracy of the measurements and the baselines of interest. T would be roughly the time required at the average strain accumulation rate for the area to accumulate displacements equal to the accuracy for measuring displacements. For the San Andreas fault system, the average rate is typically about 2 parts in 10^7 per year.

It seems to me that the strategy for measuring crustal movements by space techniques needs to be "robust" in the statistical sense. Namely, the strategy should be designed so that it is likely to lead to useful results, whichever of the two opinions about the nature of the motion we are looking for turns out to be correct. Thus, a major part of the effort should be devoted to making the measurements as accurately as possible. But there also is a need for making other measurements rapidly, even if the accuracy is somewhat lower, in case large motions actually are occurring or might occur a short time before a large earthquake.

Laser range measurements seem likely to contribute mainly through the monitoring of a moderate number of sites with as high accuracy as possible. In California, for example, the accurate monitoring of 15 to 20 sites once per year can provide valuable new information on strain accumulation out to large distances from the main fault system. These sites will be coordinated with the accurate trilateration networks of the U.S. Geological Survey so that they provide both ties between the networks and intercomparison lines across the networks.

For measurements in major seismic zones in other countries, the ways in which laser ranging can contribute the most will vary. In

Japan, where excellent ground measurement networks already exist and frequent measurements are made in special study zones, the role of laser ranging may be similar to that expected in California. In areas such as western South America, sites monitored by laser ranging are more likely to serve as reference points for measurements made using other types of instruments, such as GPS geodetic receivers. Such combined networks could provide quite high accuracy, at relatively low cost, for monitoring long-term strain accumulation patterns in areas where extensive ground measurement networks do not exist at present. They also would give valuable initial epoch measurements at an early date, so that coseismic and postseismic displacements after a large earthquake could be determined effectively.

A third type of seismic zone investigation is represented by proposed measurements in the Hellenic Arc, where substantial chances of a major earthquake in this century appear to exist, and other tectonically active areas of southern Europe and the Near East. Another application in the future might be to determine where the relative motion between the Indian subcontinent and central Asia is being accommodated. Ground measurements in the USSR have indicated relative motions of about 2 cm/yr between two mountain ranges in the region near Garm, but it is not known where the rest of the expected motion is occurring. Other important applications may be in New Zealand, where a major strike slip fault system can be studied relatively easily, and in the major seismic zones in China, India, Pakistan, and the USSR.

RELATED QUESTIONS CONCERNING MEASUREMENT ACCURACY

In view of the necessity of achieving high measurement accuracy and reliability for the scientific problems considered above, some additional discussion of accuracy seems desirable. Some useful methods for evaluating accuracy are as follows: (a) construction of systematic error budgets, (b) investigation of the stability and reasonableness of results, (c) comparisons with other laser ranging systems over short baselines, and (d) consistency of global solutions. While all of these methods have some advantages, none of them is sufficient by itself. For example, important effects can be left out of systematic error budgets, and the stability and reasonableness of experimental results over some period of time would not show up errors which correlate strongly with the azimuth or elevation angle of the observations, since they would produce consistent effects in the apparent station position. Also, consistency of global solutions cannot be established until after systems with high accuracy have collected data for a substantial period, such as a year or so. It thus seems necessary to proceed using all four of these approaches.

The confidence level for measuring crustal movements has to be high if the results are to influence geophysicists. Some prior information exists on long-term plate motions plus reasonable theoretical reasons for suspecting constancy of motion over long times, as

discussed earlier. Thus, geophysicists aren't likely to change their ideas based on discrepancies which have only 70% confidence limits, which really constitute "just another opinion." Testing hypotheses at the 95% confidence level is widely accepted in biology, medicine and other areas of science. It seems essential to reach the same level of confidence in deciding whether anomalous motions have been detected. This is particularly true for conclusions about whether the present rates of plate motion disagree with the long-term average rates.

It should be emphasized that dealing with 95% confidence intervals is substantially different than taking 70% confidence intervals and then roughly doubling them. That procedure would work for Gaussian error distributions or any other error distributions for which the tails cut off rapidly. But with some systematic error sources, the error level for 95% confidence may be 4 or 5 times larger than for 70% confidence. For example, wavefront corregation errors may average out fairly well at the 70% confidence interval because of changes in the pointing error during the course of a run or over a couple of days. However, at the 95% confidence level it is much harder to be sure that correlated effects aren't present, such as the pointing being considerably better later in the run than early in the run, coupled with smaller wavefront corregation errors in the center of the beam. This could give an apparent offset in the station position. It seems necessary to make up separate systematic error budgets at the 95% confidence level, rather than assuming that the ratio of 95% and 70% confidence estimates for different error sources is the same.

One particularly disturbing thing about systematic errors is associated with the fact that they can vary systematically with time during a pass so that they cause an error in the station position. The magnitude of the station error can then drift roughly linearly over long periods of time because of gradual changes in the instrumental errors. Thus, one could remeasure a baseline many times over a period of 2 or 3 years and see a roughly linear change in length. However, the confidence level for being able to say that a real change in length occurred may be little better than if most of the intermediate measurements hadn't been done. This is because, at the 95% confidence level, the magnitude of the systematic errors could indeed have changed roughly linearly 5% of the time. Additional intermediate measurements still are valuable, of course, in giving consistency checks.

The approach of constructing careful error budgets and publishing a discussion of how the individual error magnitudes were estimated has been used very widely in connection with measurement of the fundamental constants in physics. Realistic error estimates are needed so that the results of experiments measuring different combinations of the fundamental constant can be combined. While the degree of over-determination in the available experiments is not very high, it is sufficient to show how consistent the results are. Discrepancies certainly occur, but historically the number of experiments which have turned out to be in error by considerably more than the quoted uncertainties has been fairly small.

As an example of the extent of accuracy improvement which is needed, the error budgets for the NASA stations given in the Laser Ranging System Development Plan (NASA, 1980) are shown in Table 1. The error contribution due to the dry part of the atmosphere has been reduced to 0.7 cm to correspond to the results obtained by Gardner (1976) at 20° elevation from radiosonde data without any correction for horizontal gradients in the atmospheric density. Fortunately, at least one of the MOBLAS stations currently is being substantially upgraded in accuracy, as discussed in another paper, and it is planned to upgrade three of these stations to 1 to 2 cm accuracy at the 70% confidence level by 1983. However, further accuracy improvements certainly are needed in the next 2 years.

Table 1

Current Error Budgets* for the GSFC Satellite Laser Ranging Systems

Error Source	STALAS	MOBLAS 1-3	MOBLAS 4-8
Transmitter	0.5 cm	2.5 cm	6.0 cm
Atmosphere	0.7	0.7	0.7
Satellite (LAGEOS)	0.2	0.2	0.2
Receiver	1.5	4.0	8.0
Timing	0.7	0.7	0.7
Calibration	1.0	1.0	1.0
Total (RSS)	2.1 cm	4.9 cm	10.1 cm

*Normal point accuracy, 100-point average.

CAPABILITIES OF OTHER TECHNIQUES

In discussing the scientific contributions which laser ranging is likely to make, it is important not to underestimate the capabilities of other methods. Some of the capabilities demonstrated by VLBI measurements for determining baselines are listed in Table 2. The subcentimeter demonstrated accuracy and repeatability over a 1.24 kilometer baseline and the 3 centimeter repeatability over 4 years for a 3,929 kilometer baseline are accomplishments which laser ranging has not yet equaled. Also, actual measurement times as short as 1 day at a site have been demonstrated by the mobile 4 m ARIES VLBI station.

For measurements with either VLBI or GPS signals, the uncertainty in the tropospheric correction due to water vapor seems likely to be the most serious limitation. Even with water vapor radiometers in operation at each site, the uncertainty in the water vapor correction is likely to be about a centimeter, as discussed elsewhere (see e.g. Resch, 1980; Guiraud et al., 1979; and other references given in Bender, 1980). However, the situation is really too complicated to

Table 2

VLBI Baseline Measurements

Length (km)	Precision, Repeatability, or Accuracy (cm)	
1.24	0.3, 0.5, 0.7 (three components)	Repeatability (15 mo)
	≤0.6	Accuracy
42*	10	Accuracy
3929	3	Repeatability (4 yrs)
5600 to 7914†	6 to 8	Precision

*Difference of 353 and 387 km baselines measured by mobile station.

†U.S. to Sweden baselines; precision estimated from effects of different assumptions in analysis.

be described by a single number. In addition to the calibration errors of the water vapor radiometers, the effects of uncertainties in the effective emission temperature of the atmosphere and in the distribution of droplet sizes in clouds also have to be considered. Radiometer calibration errors are not likely to introduce azimuth-dependent measurement errors, so horizontal coordinates may be affected relatively little by this source of error. On the other hand, the one centimeter water vapor correction error estimate mentioned above has not yet been demonstrated experimentally, and the effect of such an error on the vertical coordinate of a station may be larger by as much as a factor 2.

The level of uncertainty in the range due to horizontal gradients in the dry part of the atmosphere also is uncertain. Since such uncertainties affect laser ranging as well as radio methods, the potential accuracy advantage of laser ranging would be small if the dry part of the atmosphere should turn out to introduce as much uncertainty as the water vapor does. Hopefully some reduction in the horizontal gradient error below the 0.7 cm value at 20° elevation angle found by Gardner (1976) can be achieved by using airport radiosonde data or other meteorological information, since much of the effect comes from gradients at the higher elevations. Such gradients may exist over fairly large areas and be stable over periods of a number of hours, except near frontal systems. However, Pearce et al. (1981) have raised the question of whether gradients with shorter wavelengths than those studied by Gardner may give larger uncertainties for an observation campaign of limited duration. Such questions certainly need to be resolved.

While the size of the effects discussed above is considerably more uncertain than we would like, it still seems fairly likely to me that the errors for laser ranging will be a factor 2 smaller than those for radio techniques. Thus, if we can make the other sources of systematic error for laser ranging small enough, I believe that the overall accuracy may be better than for any other technique.

The crustal dynamic problems for which an accuracy advantage would be particularly important are those discussed in Section 2; i.e. measurements of plate tectonic motions and of the longer wavelength distortions in seismic zones. For plate tectonic motions, in particular, the total number of measurements needed per year is limited, so the overall cost hopefully can be kept at a reasonable level. A factor 2 difference in accuracy will have a major impact scientifically, as mentioned earlier, because it reduces the time necessary to compare present motions with the expected rates by about the same factor. If this means obtaining new scientific information in 5 years which otherwise would have taken 10 years of measurements, then the probability of affecting the work done in a considerable area of geodynamics over a substantial period of time is considerably enhanced. For determining where large-scale distortion is taking place in plate interiors, the advantage of improved accuracy is equally strong.

There are important types of problems, however, for which laser ranging from mobile ground stations does not seem likely to be the most efficient approach. This includes, particularly, cases where large numbers of measurements need to be made per year, either with moderate times between measurements at a high density of points in seismic zones, or at very short repetition times for a lower density of points. In cases of this kind the cost per measurement is a very important factor, as well as the accuracy. It now appears likely that measurements using GPS receivers can be made with 1 or 2 centimeter accuracy in times as short as half an hour or less if the Global Positioning System is completed as planned. If not, VLBI measurements with highly mobile stations will still be quite competitive because of the considerable cloud cover problems for laser ranging, and the fact that one doesn't have to wait for a LAGEOS pass to make observations. While the cost of high mobility laser ranging stations is likely to be less than that for their VLBI counterparts, the operating budgets probably will be the most important factor over long times. However, if new information on the relative accuracies achievable by optical and radio methods favors laser ranging, the use of a larger number of high density satellites in lower orbits needs to be considered (Wilson et al., 1978). The launch of a second LAGEOS satellite also might be desirable in that case.

In addition to the measurements discussed above, a few words should be said about the possible future capabilities of airborne laser range measurements. NASA has been involved in investigating the accuracy achievable by pulsed laser range measurements from aircraft to ground reflectors. This approach might well be competitive for

frequent repeat measurements in seismic zones with the use of high mobility VLBI stations and possibly also with GPS receivers if higher accuracy can be achieved. In addition there is a possibility that airborne measurements using a line crossing method with microwave modulated cw lasers would be desirable in the future. The potential advantage would be high measurement accuracy, with the two-wavelength approach used to correct for atmospheric refraction. However, the vertical coordinate would not be determined well with this approach.

REFERENCES

Bender, P. L., Improved methods for measuring present crustal movements, Dynamics of Plate Interiors, Geodynamics Series, Vol. I, A. W. Bally, P. L. Bender, T. R. McGetchin and R. I. Walcott, eds., Am. Geophys. Union, Washington, D.C., and Geol. Soc. Am., Boulder, Colorado, pp. 155-162 (1980).

Gardner, C. S., Effects of horizontal refractivity gradients on the accuracy of laser ranging to satellites, Radio Science 11, 1037-1044 (1976).

Guiraud, F. O., J. Howard, and D. C. Hogg, A dual-channel microwave radiometer for measurement of precipitable water vapor and liquid, IEEE Trans. Geosci. Elec. GE-17, 129-136 (1979).

NASA, Laser ranging system development for crustal dynamics applications, Geodynamics Branch, NASA Headquarters, Washington, D.C. (1980).

Pearce, W., P. Dunn, and K. Borman, The effect of horizontal gradients in the dry atmosphere on geodetic observations, Trans. Amer. Geophys. Union 62, 261 (1981).

Resch, G. M., Water vapor — The wet blanket of microwave interferometry, Atmospheric Water Vapor, A. Deepak, T. D. Wilkerson and L. H. Ruhnke, eds., Academic Press, New York, pp. 265-282 (1980).

Wilson, P., E. Silverberg, R. Schutz, I. Malevich, and S. Ramsden, A proposal for the design and application of a high-mobility, low-cost satellite laser ranging system, Proceedings of the European Workshop on Space Oceanography, Navigation and Geodynamics, S. Hieber and T. D. Guyenne, eds., European Space Agency, SP-137, pp. 111-117 (1978).

Status of the networks for global and regional laser ranging

Peter Wilson

Institut für Angewandte Geodäsie, Richard-Strauss-Allee 11,
D-6000 Frankfurt/Main and
Sonderforschungsbereich 78 (Satellitengeodäsie) der TU München

1. Introduction - System review

A telescope count of all laser ranging equipment known to exist or to be under construction at this time (and to be fully operational by 1984) gives approximately 50 units. These systems differ widely in their capabilities and operate in the framework of one or more of the international networks.

Only four of the systems have been designed for relatively high mobility and of these only one, TLRS I, is currently in the field; a second, TLRS II, will follow shortly. The remaining two systems, a German and a Dutch, are undergoing construction and will be identical. Both systems will be handed over for field testing in 1983 and will go into full operation in 1984. All four systems will produce data of similar quality, characterised here by 1-3 cm normal points.
Details of all of these will be discussed in succeeding presentations.

There is some prospect that TLRS III and TLRS IV will be procured in the time-frame 1984-85, but this will depend upon a number of factors which are currently not predictable.

It is anticipated that there will be 4 further MOBLAS type stations plus some 8 permanent stations world-wide of the same ultimate quality in operation by 1984. Of these the stations at Herstmonceux (UK), Lustbühel (Austria), Mc Donald Observatory - MLRS - (U.S.A) and

Orroral - NATMAP - (Australia) are under construction and Simosato (Japan) is just about to be installed. Haleakala, MOBLAS 4,5,6,8 and Wettzell have been in operation with more or less success for some time. MOBLAS 7 has recently replaced STALAS as the Goddard reference, STALAS having been de-commissioned.

At a somewhat lower level of accuracy (2-5 cm normal points) there will then be 8 further systems available, of which the deployment of the SAO systems from Mt. Hopkins (U.S.A.), Natal (Brazil), and Orroral (Australia) is as yet uncertain. The remaining 5 are the systems at Arequipa (Peru), Kootwijk (Netherlands) and MOBLAS 1,2,3.

The system at Dionysos (Greece) is being upgraded with a Nd:YAG short-pulse laser, but the definitive plans and the time-table for completion of the work is not yet known. However it can be presumed that it will ultimately fit into one of the preceding categories and may reach 1-3 cm accuracy by 1983-84. Similarly, the accuracy for the systems at the Plateau de Calerne (France) and Dodaira (Japan) until the end of this period and for the recently upgraded system at San Fernando (Spain) are not known, but again there is some hope that there too, results will be sufficient to give at least the equivalent of 4-8 cm normal points if not better.

No attempt has been made to assess the remaining systems, but the majority will be inadequate for making significant contributions to satisfy current requirements, unless they undergo major upgrading in order to give Lageos ranging capabilities to one of the preceding levels.

The preceding discussion leads to the conclusion that only about 50 % of the systems in operation by 1984 will have the capacity to deliver data of adequate quality for use in MERIT and the ongoing Crustal Dynamics and Earthquake Research Program.

2. The Networks

Historically four networks of laser ranging instrumentation and a few individual systems have been operating. The networks were:

- the NASA network,
- the SAO network,
- the EROS network,
- the Interkosmos network.

In recent years, as the result of a number of influences, the co-operation between the networks has been improved to the point where nowadays there are essentially only two major network operations, each of which is addressing a multitude of tasks such as earth rotation, gravity field improvement and crustal dynamics. The NASA and SAO groups have continued to bear the brunt of the observational task during the years since the last Workshop, but with the anticipation of a closer international co-operation, the European (EROS) network for example is under pressure to make a more effective contribution to ongoin programs. This leads inevitably towards the integration of the first three of the aforementioned into one consolidated network.

Despite an apparent dependence on the SAO satellite ephemerides which are supplied to the centres in Prague and Moscow every week by telex via CNES in Toulouse, the Interkosmos network operates autonomously. Little is known of the real priorities set by this group in the way of scientific objectives, but from the literature it would appear that perhaps polar motion and the improvement of the gravity field model take pride of place. In any case it would be worthwhile to obtain more information on this topic in the course of the meeting.

3. Network response to project activities

Since the last workshop in 1978 three projects of world-wide interest have been addressed:

- SEASAT,
- Lageos,
- MERIT (preliminary campaign).

The
and a program for
- MERIT (long campaign)
- Crustal Dynamics and Earthquake Research

are in the course of preparation. The Lageos Project and the Crustal Dynamics Project were each conceived as long-term, on-going activities (the two will run jointly until expiration of the Lageos Project at the end of 1982) and MERIT as a co-ordinated, interdisciplinary effort of 3 + 12 + ... months observation in 1980, 1983-84 and ....

The network response to each of the projects addressed to date has served to show up the individual and collective weaknesses to which international co-operative efforts of this magnitude are susceptible. Problems of weather, maintenance, system-deployment, communication, standardisation of procedures, formatting, calibration and global coverage are just the first that come to mind from the catalogue of headaches that surfaced during the last three years.

Whereas the overall laser-ranging contribution to the success of the short-lived SEASAT project can only be described as disappointing - weather, system deployment, to some extent ephemerides and the sudden power failure onboard the satellite brought things to a halt before the observational campaign had fully atuned to the project in hand - the succeeding efforts for Lageos and MERIT have shown a vast improvement, both in the quality and quantity of data. Some problems still remain. After years of campaign oriented operations for which a few months of concentrated observation could be followed by a prolonged period of spasmodic activity interspersed between the times devoted to system improvement, the Lageos activities were the first for which the systems were to be put to a prolonged period of observation. Only SAO could respond immediately to this challenge, this having long been the cornerstone of their operational policy. NASA followed on, but the remaining portions of the network have been slow to respond. Perhaps a reason for this lies in the fact

that too little emphasis has been placed on the on-going characteristic of the Lageos Project and on the need for continuity in observations, two items which should receive more emphasis in encouraging contributions to the forthcoming Crustal Dynamics programme.

With a similar limitation,the preliminary MERIT campaign proved to be an outstanding success - both for the observers and the analysts. Again the observational contribution from European stations was disappointing, but the overall campaign opened up new and until then untried, possibilities for exploiting the quick-look data normally supplied to maintain the satellite ephemerides.

Generally, it can be said that 1979 proved to be the year in which a significant improvement in the data being submitted - quality and to some extent also quantity - became apparent. As a result:

- the quality of both the Lageos and Starlette orbits has improved considerably;
- the gravity model has been refined, both by the addition of altimeter data and the improved tracking;
- tuned gravity models are now available for both Lageos and Starlette;
- improved earth rotation parameters and earth and ocean tidal models are available for the analysts.

Still, more care is needed in the recording of reliable meteorological data - systematic ranging errors of up to 5 cm have been reported as a result of faulty data - and reliable calibration at the 2 cm level is evidently creating more problems than had been anticipated. Furthermore, despite the use of sophisticated measuring techniques, such as that shown previously for TLRS, the old problem of recording unambigvous measurements to a reference ground marker (for which more redundancy is required in the observations) has appeared for both SLR and VLBI stations. Each of these problems should be addressed in ensueing discussions.

4. Data exchange

Since 1978 there has been a great improvement in the readiness to exchange data between participating agencies and the analysts.

Quick-look data is made available to those requesting it (e.g. SAO and the University of Texas) immediately "after the event". The turn-around for pre-processed data during SEASAT and MERIT was of the order of 90 days, with some data being dispatched to the data centre within 28 days of its taking.

Whereas this schedule caused some difficulties during the SEASAT campaign, the data submissions for MERIT were prompt and effective. Increasing attention is being paid to the use of GE-Mk. III for transferring pre-processed information between data banks and some stations are also arranging to be connected to the system.

No information is available on data exchange within the Interkosmos community. Some Interkosmos stations expressed interest in participating in MERIT and e.g. a request to the IfAG for MERIT data was answered promptly and positively in accordance with the agreements reached for the project. Again, it would be helpful to have some comment on this from the Interkosmos participants.

5. Outlook

As we approach MERIT and enter the Crustal Dynamics programme the outlook is reasonably good. Whereas about 50 % of the existing systems will be in a position to deliver valuable, high quality data for the project by 1984, it must be anticipated that the knowledge of the Lageos orbit will be sufficient to justify a considerable cut-back in the global support network used to maintain it and a shift in emphasis towards a stronger support for regional investigations can be predicted, mainly resulting in an increased observational load for the highly mobile systems. At that time it can be anticipated that it may be unnecessary to occupy a station/site for longer than one week, if weather conditions are favourable.

Significant improvement in relative accuracy may also result from a more effective and concentrated use of mobile equipment in regional investigations. This is particularly important in the light of the time span over which we are forced to make our projections for Crustal Dynamics. New reduction techniques are currently being investigated for these problems.

A practical problem of some concern is to develop data compaction procedures applicable to all requirements. Proliferation of a number of differing techniques for this would put an unnecessary burden of work on stations reporting data. We already have too many formats for data exchange and there is no need to generate the same problem for reporting normal points.
Finally it is suggested that laser ranging suffers from a lack of standardisation of equipment and procedures. As the transition from the experimental to the operational era is made more effort is needed to ensure that the cm the analyst and the geophysicist is wanting to sec results from something external to the measuring system and not a systematic resulting from it. If this cannot be guaranteed the laser ranging community will lose its support in favour of other contenders. In a few words - we need results - we need high quality results - but we need guaranteed results. This workshop can contribute to attaining them.

Country	Station	Latitude (LSC 80.11)	Longitude	Height	Normal point accuracy 1981	1982	1983	1984	Remarks
Australia	Natmap	35 38S	148 57E					1-3	Lunar/Lageos
	Orroral-SAO IV	35 37S	148 57E	949	8-12	2-5	2-5		SAO
	Yarragadee	29 03S	115 21E	245	4-8	4-8	2-5		NASA (MOBLAS 5)
Austria	Lustbühel	47 04N	15 28E			1-3	1-3	1-3	EROS
Bolivia	Patacamaya	17 15S	292 06E		100				Interkosmos
Brazil	Natal-SAO I	5 56S	324 50E	39	8-12				SAO
Bulgaria	Plana				100				Interkosmos
China	Shanghai	31 12N	121 12E		60	60	8-12	8-12	
	Yunnan	25 01N	102 47E		100	100	100	100	
Cuba	Santiago de C.	20 01N	282 14E		100				Interkosmos
Czechoslo-	Hradec Kralowe	50 13N	15 50E		100				Interkosmos
vakia	Ondrejov	49 55N	14 47E		100				Interkosmos
Ecuador	Quito	0 12S	281 31E		100				Interkosmos
Egypt	Helwan I	29 52N	31 21E		100				Interkosmos/SAO
	Helwan II	29 52N	31 21E		8-12				Interkosmos/SAO

Country	Station	Latitude (LSC 80.11)	Longitude (LSC 80.11)	Height	Normal point accuracy 1981	1982	1983	1984	Remarks
F.R. Germany	Wettzell	49 09N	12 53E	661	1-3	1-3	1-3	1-3	EROS
	MSLRS						1-3	1-3	EROS
Finland	Metsähovi	60 13N	24 24E	78	50				EROS
France	Calerne LLRS	43 45N	6 56E	1306		8-12			Lunar/Lageos/ Starlette
	Calerne SLRS	43 45N	6 56E	1306	30				EROS
German D.R.	Potsdam	52 23N	13 04E		100				Interkosmos
Greece	Dionysos	38 05N	23 56E		100				EROS
Hungary	Penc	47 47N	19 17E		100				Interkosmos
India	Kavalur	12 54N	78 49E		100				Interkosmos
Italy	Cagliari	39 13N	9 07E						EROS
Japan	Dodaira LLRS	36 00N	139 12E						Lunar
	Dodaira SLRS	36 00N	139 12E		50				
	Simosato	34 07N	135 10E			1-3	1-3	1-3	
Netherlands	Kootwijk	52 11N	5 49E	93	8-12	8-12	2-5	2-5	EROS
	MSLRS						1-3	1-3	EROS

Country	Station	Latitude (LSC 80.11)	Longitude	Height	Normal point accuracy 1981	1982	1983	1984	Remarks
Peru	Arequipa-SAO II	16 28S	288 30E	2492	8-12	2-5	2-5	2-5	SAO
Poland	Borowiec	52 17N	17 04E		100				Interkosmos
Switzerland	Zimmerwald	46 53N	7 28E		100				EROS
Spain	San Fernando	36 28N	353 48E						EROS
United Kingdom	Herstmonceux	50 52N	0 20E			1-3	1-3	1-3	EROS
U.S.A.	Mc Donald	30 40N	255 59E		2-5				UT/NASA
	MLRS	30 40N	255 59E	1965		1-3	1-3	1-3	UT/NASA
	TLRS I				1-3	1-3	1-3	1-3	UT/NASA
	TLRS II					1-3	1-3	1-3	NASA
	Haleakala	20 43N	203 44E		2-5	1-3	1-3	1-3	UH/NASA
	MOBLAS 1 Mavi	20 42N	203 45E	3071	2-5	final plans uncer-tain			NASA
	MOBLAS 2 Boulder				2-5	2-5	2-5	2-5	NASA
	MOBLAS 3 Monument Peak				2-5	2-5	2-5	2-5	NASA
	MOBLAS 4 GSFC	39 01N	283 10E	21	4-8	4-8	2-5	1-3	NASA
	MOBLAS 6 GSFC	39 01N	283 10E	21	4-8	4-8	2-5	1-3	NASA
	MOBLAS 7 GSFC	39 01N	283 10E	21	1-3	1-3	1-3	1-3	NASA
	MOBLAS 8 Quincy	39 58N	239 04E	1064	4-8	4-8	2-5	1-3	NASA
	SAO 3					2-5	2-5	2-5	SAO

Country	Station	Latitude (LSC 80.11)	Longitude (LSC 80.11)	Height	Normal point accuracy 1981	1982	1983	1984	Remarks
U.S.S.R.	Riga	56 57N	24 04E		100				Interkosmos
	Simeis	44 24N	34 00E		100				Interkosmos
	Zvenigorod	55 42N	36 47E		100				Interkosmos

A CRITICAL ANALYSIS OF SATELLITE LASER RANGING DATA

B. D. Tapley, B. E. Schutz and R. J. Eanes

Department of Aerospace Engineering and Engineering Mechanics
The University of Texas at Austin
Austin, Texas 78712
512/471-1356

Abstract

The goals for satellite laser ranging, set forth in several international geodynamics programs establish challenging requirements on the observation accuracy, continuity in the observation program and geographical distribution of the laser tracking stations. The NASA Crustal Dynamics Project and the IAU/IUGG Program to Monitor Earth Rotation and Intercompare Techniques (MERIT) are two current programs which impose the most demanding requirements. In this discussion, the characteristics of the Lageos laser ranging data collected since its launch in May 1976 are reviewed. In particular, the quality of the data obtained during the last two years is contrasted with the pre-1980 data. A comparison of the precision of both the quick-look and full-rate data is presented. Finally, current limitations of the data base from the analyst point of view are noted.

Introduction

In recent years, laser ranging to near-earth satellites has been used for the determination of precise satellite orbits, the earth's gravity field, the earth's polar motion and rate of rotation, solid earth and ocean tide parameters, tectonic plate motion and crustal deformation [NRC Committee on Geodesy, 1978]. Further enhancement of results achieved in these applications will require a concentrated effort to ensure that the data set collected has adequate geographic and temporal distribution and small random and systematic errors. In particular, the goals set forth in several current international global earth dynamics programs, including the NASA Crustal Dynamics Project [NASA Office of Space and Terrestrial Applications, 1979], the San Andreas Fault Experiment [Smith, et al., 1976] and the IAU/IUGG MERIT Campaign [Wilkins, 1980], impose requirements on the observation program which are at the limit of the laser network observation efficiency and accuracy. Table 1 summarizes the geophysical measurement accuracy required for the Crustal Dynamics Project [NASA, 1979]. These requirements present a significant challenge to the laser ranging community. A dedicated effort in both the data analysis and the observation program will be required to achieve satisfactory results.

The following discussion reviews both the quick-look and full-rate Lageos laser ranging data and notes both the improvement in data quality and some of the current limitations on the data use for geophysical applications. In addition, the relative precision and productivity of the various systems which constitute the global laser tracking network are considered.

The Laser Range Measurement

Figure 1 illustrates the various elements in the laser range measurement. The primary measurement is the flight-time, Δt, between the laser pulse transmission and the return of the satellite reflected energy to the optical receiver at the tracking station. With appropriate corrections for atmospheric refraction and instrument delays, the measured time of flight can be used to give (with sufficient accuracy for this discussion) the range from the first non-moving point in the optical path of the laser (the reference point) to the average satellite corner-cube position at the time the pulse is reflected at the satellite. That is,

$$\rho = \frac{1}{2} c\Delta t - \eta_r - \eta_e - b + \varepsilon \qquad (1)$$

where

ρ is the range from the laser reference point to the average corner-cube reflector position,

Δt is the round-trip flight time,

c is the speed of light in a vacuum,

η_r is the atmospheric refraction correction,

η_e is the effect of systematic and random measurement errors,

b is the system delay as determined by calibration measurements, and

ε is the unmodeled observation error.

Eq. (1) suggests that the errors which corrupt the measurement of the round-trip time of flight can be separated into instrument or measurement errors and errors in the models used to correct the time of flight for atmospheric refraction and other effects [Plotkin, et al., 1973]. Corrections for these effects requires that other ancillary data, such as atmospheric pressure, temperature and reltive humidity be obtained [Marini and Murray; 1973; Rinner, 1974].

The equations of motion predict the position of the satellite's center of mass; hence, the location of the effective optical center, d_s, (Fig. 1) of the laser corner-cube array with respect to the spacecraft's mass center must be known precisely [Fitzmaurice, et al., 1977]. Since the laser reference point, O, will vary as different instruments occupy a given site, the surveyed distance, $\bar{r}$, between the laser reference point and the laser site benchmark must be precisely determined for each new site occupancy. Finally, since some applications will require intercomparison of positions and baselines determined by various techniques, the location of the laser station benchmark with respect to a specified survey mark ($\bar{s}$) must be precisely determined.

The instrument errors, η_e, include errors in the time standard, which can be separated into clock bias (relative to UTC), drift and discontinuous or anomalous time standard behavior. It is generally assumed that the transmitted pulse is symmetrical in shape. A non-gaussian pulse can lead to erroneous interpretation of time of flight for the returned signal unless corrections for this effect are included in the data pre-processing. The TLRS-1 which is based on a single-photon detection system uses a cross-correlation technique to correct for pulse distortion effects. For the systems which record the full wave-form, the two primary means of locating the returned pulse are leading edge discrimination and centroid location [Lehr, et al., 1975]. The centroid location requires integration of the total returned signal and, provided that sufficient attention is given to the process, can be made to yield a more accurate determination of the time of flight measurement. The effect of such pulse-dependent errors vary with both the laser and the detection system. For example, for

MOBLAS and SAO lasers, the far field diffraction patterns of the laser can cause systematic errors which vary with the position of the satellite in the laser beam [Fitzmaurice, et al., 1977]. However, single-photon systems like the one used for TLRS [Silverberg, et al., 1980] avoid this error source.

Another common error source occurs in the determination of the system delays from pre- and post-observation calibration measurements. Factors which influence the overall accuracy of the bias measurement are uncertainties in the measurement of the calibration target distance, d_c, background interference in ranging to the target, atmospheric instability in the calibration medium and differences in the signal strength of calibration versus satellite returns.

In most applications, the data analyst tacitly assumes that the instrument corrections have been properly modeled and that the bias and noise for the data lie within the specified accuracy bounds. If uncorrected errors remain in the data, the analysis results will be corrupted, and progress toward improving the requisite models will be slowed. Since systematic observation errors may be accommodated into adjusted parameters, such as orbit elements, gravity field coefficients and station positions, they are difficult for the analyst to confidently isolate. Consequently, the reduction of systematic errors in the observations is an essential requirement for achieving the scientific objectives of the international laser ranging programs.

The Lageos Data Set

The two fundamental requirements which the satellite laser ranging systems must satisfy to achieve the objectives of the current geodynamic programs are measurement accuracy and continuity of operation. A laser site which operates with high precision but operates over sparse time intervals will have little impact in the solution of most global geodynamic problems. At the present time, polar motion and earth rotation solutions require continuity in tracking by each station to ensure adequate temporal and spatial distribution of the data. Furthermore, the best determination of relative distance between tracking stations, which is an inherent element in regional and intercontinental baseline solutions, is obtained when the sites observe the satellite during the same time period. Because of the inability of most laser sites to track Lageos during the daylight hours, there will be extended periods during which only one or two passes per day will be observable from some sites, and weather conditions will reduce further the passes actually acquired. Consequently, to determine accurate global baselines, data must be gathered over a sufficiently long period to allow averaging of the effects of dynamical model error.

The tracking stations which have ranged to the Lageos satellite are shown in Figure 2. The laser ranging data set for the Lageos satellite for the period May 1976 to November 1981 is summarized in Table 2. The set of stations which have contributed to this data base, along with the number of observations from each station (based on samples at one-minute intervals) are tabulated. The question of the relative accuracy of the data from the various sites will be considered in the subsequent discussion. Figure 3 shows the temporal distribution of the passes for this data set, as summarized in the number of passes per five-day interval for the period up to December 1981. There are obvious time periods when substantially more data is collected than at other periods, and some stations have contributed a much larger number of observations than other stations. The five-day interval is used for the current University of Texas polar motion and earth rotation solutions [Schutz, et al., 1981] and, when the number of passes during the five-day period approaches ten or less, the accuracy of the solution is questionable. As is evident from Table 2, the contribution from the various stations is not uniform.

A number of factors influence the variation in the quantity of data collected at any given station. As an example, Figure 4 shows the number of passes contributed in each five-day interval by the Orroral tracking site. The station was not operating during the first 100 days of the Lageos mission which began in May 1976 (MJD = 42905). Note that there is an apparent periodic character to the number of passes in each five-day interval. The dominant variation is at a period of 560 days and is associated with the motion of the Lageos node relative to the sun. This effect is a function of the ratio of daytime passes to nighttime passes at each tracking site and is introduced by the limited ability of most tracking stations to range to Lageos during the daylight hours. Additional variations with an annual period may also be present due to seasonal meteorological variations and changes in the number of hours of daylight.

There are also shorter period variations in the amount of data gathered introduced by the tracking schedule adopted for the laser operation. This effect can be evaluated by considering the data set collected during the Preliminary MERIT Campaign. This data set, collected during a period of 92 days, represents the best satellite laser ranging data available with regard to quantity and global data distribution. The daily amount of tracking varies from 40 to approximately 320 minutes. The mean is 107 minutes, and the RMS about the mean is 74 minutes. Figure 5 shows the results obtained by analyzing the histogram of the data collected each day using a maximum entropy spectral analysis. Presumably the peaks at 7.0 and 3.5 days occur because the five-day work week is uniformly scheduled at most sites on Monday through Friday, leading to limited data being collected on Saturday and Sunday. Figure 6 shows the actual data collected in minutes per day for the Preliminary MERIT Campaign. Superimposed on this figure is a best fit trigonometric function containing terms with

7-day and 3.5-day periods. Note that the phase determined by the data is such that each Saturday (shown by the solid circle) is at a minimum of the data. A rotated schedule to ensure tracking by an adequate number of stations during the weekend could eliminate this schedule-induced void in the tracking data.

Figure 7 shows the number of passes obtained by the stationary laser (Stalas) operated at the Goddard Space Flight Center. While the measurements from this instrument are some of the most precise of any consistently operating laser system, the number of passes contributed is substantially fewer than those provided by the SAO sites. Because of the limited data distribution, the impact of the Stalas-gathered data on the global station coordinate solutions, orbit accuracy results and polar motion solutions is far less than the Stalas system precision would promise. Problems with weather, instrument malfunctions and the use of the system for development work are cited as the primary reasons for the sparse data collected by Stalas. The weather factor can be modulated by site location; however, the design inherent in achieving the high-accuracy range measurements must be such that reliable system operation can be achieved as well.

Accuracy Assessment for Laser Range Data

To obtain an overall assessment of the performance of the laser network, several factors should be considered. In addition to the amount of data contributed by the respective laser systems, the number of observations edited, the noise level and systematic error signals in the data are other factors which must be considered. In order to obtain relative comparisons of these quantities, the capability for computing an orbit which yields an accurate fit to the data is necessary.

In the approach presented in the subsequent discussion, a single long-arc solution for the orbit of the Lageos satellite was computed using the UTOPIA orbit computation system at the University of Texas [Schutz and Tapley, 1980]. There will be residual error in the orbit due to unmodeled orbit effects. The effects of the long-period orbit error were removed by using a smoothed solution through a set of short-arc orbit element adjustments. In this approach, the residuals from the long-arc solution were separated into five-day batches, and average orbit element corrections were determined for each of these five-day batches. The orbit element corrections were smoothed using a method proposed by Vondrak [1977], and corrections to the long-arc solution were obtained using the smoothed orbit element corrections. This corrected solution removes essentially all of the long-period orbit error. However, the residuals computed from the corrected orbit will contain measurement errors and short-period orbit error.

If the corrected long-arc orbit solution is used to obtain a computed value of the range, ρ^*_i, then the raw range residual, $\delta\rho_i$, is defined as follows:

$$\delta\rho_i = \rho_i - \rho^*_i \tag{2}$$

where ρ_i is the observed value of the range.

The raw range residual RMS for the entire set of data is given then as follows:

$$\sigma_\varepsilon = \left[\frac{1}{m} \sum_{i=1}^{m} (\delta\rho_i)^2 \right]^{1/2} \tag{3}$$

The value of σ_ε is nominally on the order of 40 cm for the 100-day fit interval used in the subsequent discussions. The raw range residuals, $\delta\rho_i$, still contain the effect of orbit error with shorter periods than those included in the orbit element smoothing, as well as the effects of inaccuracies in the station location, inaccuracies in the atmospheric refraction corrections and other measurement model errors. The systematic trend in a single pass of residuals can be mostly removed with a two parameter least squares adjustment of an apparent range bias and time bias. To achieve this effect, the following equation is used:

$$\delta\rho_i = b + \dot{\rho}_i \tau + \tilde{\varepsilon}_i \tag{4}$$

where b is the apparent range bias, τ is the time bias, $\dot{\rho}_i$ is the range rate, and $\tilde{\varepsilon}_i$ is the remaining error. The residuals, ε_i, will consist of random measurement noise, as well as trends not accommodated by the time bias adjustment. The RMS of the $\tilde{\varepsilon}_i$ is referred to as the range bias-time bias (RB-TB) RMS. Next, a kth-order polynomial, usually selected as a quadratic, is fit to the residuals in each pass using the following model

$$\tilde{\varepsilon}_i = \sum_{j=0}^{k} c_j t^j + \varepsilon_i \tag{5}$$

where c_j, $j=0,\ldots,k$ are constant coefficients whose values are to be estimated from the residuals $\tilde{\varepsilon}_i$ for any given pass and where ε_i is the remaining residual. The RMS of the ε_i is referred to as the polynomial (POLY) RMS.

The polynomial RMS is predominantly due to high frequency and random observation error and can be used as a good measure of the single-pass internal precision of the laser tracking systems. The estimates for the range bias b and time bias τ, as well as their uncertainties, can be used as a measure of the systematic errors which still remain. These errors occur due to inaccurate solutions for the orbit, the tracking station coordinates, polar motion, the various

models for correcting the laser range measurements, as well as systematic measurement error with periods comparable to the duration of a pass or longer.

Comparison of the Quick-Look and Full-Rate Data

The laser range data is transmitted to the NASA Goddard Space Flight Center in two modes.

1. The quick-look data, sampled at approximately 50 points per pass, is used primarily for orbit maintenance and overall data quality checks. These data are transmitted to the Goddard Space Flight Center over the NASA Communications (NASCOM) Network from the individual Goddard laser tracking sites and from the Smithsonian Astrophysical Observatory for data collected by Telex from the SAO and participating foreign laser sites. In either case, data can be made available with delays as short as a few hours.

2. The full-rate data is the complete data set collected by the tracking sites and corrected for all known errors and stored in the National Space Science Data Center at the NASA Goddard Space Flight Center as an archival data record. This data set is used for precise orbit computation and for geodynamic parameter determinations. The full-rate data set requires substantially more computational effort and, as a consequence, is not available for a period of approximately 90 days after the data are collected at the tracking site.

Although the primary use for the quick-look data is in the preliminary orbit determination application to support tracking station acquisition predictions, there are a number of other applications which require data availability within a few days of its collection. These include the determination of rapid service polar motion and earth rotation values and preliminary accuracy assessment of TLRS site solutions. In addition, the quick-look data can be used to detect data abnormalities, such as timing anomalies, systematic bias or increased noise levels in the data from the various stations.

Since the quick-look data is the only source for satisfying these rapid response requirements, a comparison of the the quick-look and the full-rate data is of interest. Figures 8 through 11 summarize a comparison of the quick-look data gathered by the SAO Orroral laser system and the NASA Stalas system operated at the Goddard Space Flight Center during the MERIT Short Campaign from August 1, 1980, through October 31, 1980.

The complete pass statistics during this 92-day time interval are summarized into two parameters, the mean range difference and

the mean time difference. These statistics are formed by identifying the measurements in the full-rate data which correspond to each quick-look observation. The differences in the associated range measurements, y_i , and the differences in the time tags, t_i , are formed for each individual quick-look measurement. That is,

$$y_i = \rho_i - \rho^*_i \quad , \qquad t_i = T_i - T^*_i \tag{6}$$

where ρ_i is the full-rate range at the time, T_i , and ρ^*_i is the quick-look range at the indicated quick-look time, T^*_i . Then, for each pass, the mean and standard deviation is computed for both the range differences and the time differences as follows:

$$\bar{y} = \frac{1}{m} \sum_{i=1}^{m} y_i \quad , \qquad \sigma_y^2 = \frac{1}{m} \sum_{i=1}^{m} (y_i - \bar{y})^2 \tag{7}$$

$$\bar{t} = \frac{1}{m} \sum_{i=1}^{m} t_i \quad , \qquad \sigma_t^2 = \frac{1}{m} \sum_{i=1}^{m} (t_i - \bar{t})^2 \tag{8}$$

where m is the number of quick-look measurements in the pass.

Figures 8 and 9 show the mean range and time differences for each pass of Stalas laser data collected during the MERIT Campaign, while Figures 10 and 11 show similar results for Orroral. The error bars indicate the pass standard deviation. From Figures 8 and 10, it can be seen that there are significant differences in the character of the mean range difference for the Goddard stations as compared with the SAO stations. The data for the Orroral station in Figure 10 have an overall mean of -0.6 cm with an RMS about the mean of 3 cm. The overall mean for the Stalas data is 3.2 cm with an RMS of 5.4 cm. The range difference between the quick-look and full-rate Stalas data is relatively constant from pass to pass, but the RMS for each individual pass is about 5 cm. On the other hand, the mean of the range difference for the Orroral data may vary from pass to pass by as much as $\pm$ 10 cm, while the scatter within a pass is less than 1 cm.

Figures 9 and 11 show that the time difference for the Stalas data is on the order of 0.8 μs and is uniform throughout the entire MERIT Campaign. For the Orroral data, the time difference varies from -3 μs at the beginning of the MERIT Campaign to about 9 μsec at the end of the MERIT Campaign. This growth in the time difference is due to a drift in the station clock which is corrected in the final processing. While a time tag difference of 9 μsec would lead to apparent range differences of only 3 cm, if this error growth continues uncorrected it could lead to non-negligible degradation in the quality of the quick-look data as compared to the full-rate data. In order to avoid this, efforts should be made to recalibrate the SAO station clocks often enough to ensure that polar motion solutions obtained using the quick-look data are not degraded.

As pointed out previously, the data obtained in the MERIT Short-Campaign is the most complete set of laser ranging data collected to date. Consequently, these data form an excellent set for evaluating the overall quality of the quick-look data. Table 3 shows the mean range and time differences for several of the stations which tracked throughout the MERIT Campaign. Note that the characteristics of the differences identified in considering Figures 8 through 11 are present in this table. That is, the mean time differences between the quick-look and full-rate data for the Goddard stations is negligibly small. On the other hand, the mean time differences for the SAO stations are larger, varying from a -0.93 μsec to 4.8 μsec with the RMS about the mean varying from 3 to 5 μsec. The range difference for the SAO stations is on the order of 0.5 cm with an RMS of the order of 3 cm. The range difference for the NASA MOBLAS stations, on the other hand, varies from station to station with a maximum mean difference of 8 cm for the Yarragadee site with RMS values which range from 3 cm to 6 cm.

From the previous comparison, it can be concluded that the precision of the quick-look data is comparable to that of the full rate data and is thus quite valuable for rapid determinations of polar motion and other geophysical phenomena. After further examination of the differences, changes might be made to improve the precision of the quick-look data.

Improvements in the Laser Range Accuracy

In addition to the need for tracking continuity and global coverage, the accuracy of geophysical parameter determinations is dependent on the accuracy with which the laser range measurements are made. Since launch of the Lageos satellite in May 1976, there have been significant improvements in the accuracy of the laser measurements. The increased accuracy has resulted from improvements in the hardware used to make the measurements and in the understanding of the error sources which influence it.

For the purposes of this discussion, errors in the range are considered to be composed of a random part which is uncorrelated from pulse to pulse and a systematic part that could vary on several time scales. There could be a bias that is constant over several passes, biases that vary from pass to pass and errors that change during the course of a pass both continuously and discontinuously. The spectrum of range errors for periods of less than about 10 minutes (about 1/4 of a Lageos pass) can be separated confidently from the geophysically interesting signal. Also, the existence of dual populations from a double laser pulse or of discontinuous range error is easily detectable when the size of the error is large compared to the internal precision of the data. Consequently, the internal precision of the range measurements in a single pass can be estimated from appropriately

filtered residuals.

On the other hand, the error spectrum for periods comparable to the duration of a pass and longer is difficult to separate from signal due to gravity, station coordinate and earth rotation errors. As a result, the size of these range errors must be estimated indirectly from analysis of the deviaton of polar motion or orbit element solutions from suitably smoothed curves. Any systematic range error that can lead to errors in the polar motion and orbit elements that is correlated over more than about 40 days will be impossible to detect.

At Lageos launch, the precision of the laser systems in the SAO network was on the order of 1 m. Figure 12 shows estimates of the range precision for each pass of Lageos data collected by the SAO system at Arequipa, Peru. Note that the single-pass noise is estimated to be on the order of 1 m with occasional excursions as high as 1.4 m during the first part of the Lageos mission. In late 1978 and early 1979, the SAO laser systems were modified to include a pulse chopper which reduced the 25 nsec pulse to a width of 6 nsec. The effect of this modification is readily evident in Figure 12, where around day 900 in the Lageos mission, one can see a significant reduction in the noise level for the Arequipa laser. The noise level for the SAO systems following the pulse chopper modification is on the order of 40 cm. With the SAO pulse-repetition rate of 8 pulses per minute, the 40 cm data collected for the continuing period since November 1978 have played a significant role in the quality of the polar motion and tracking station coordinate solutions determined with the Lageos data.

The NASA Mobile Laser Ranging Systems (MOBLAS) have operated with precisions which vary from 9 cm to 30 cm during the time period since Lageos launch. One problem with a number of the MOBLAS sites is the lack of continuity in the tracking operations. Figure 13 shows the range precision estimates for the Stalas tracking station. Note that since the beginning of 1978, the noise level has been systematically below the 10 cm level.

Figures 14 through 16 show a sample of the quick-look data from a 40-minute Lageos pass taken by MOBLAS-7 at the Goddard Space Flight Center following a recent modification in which a Sylvania laser replaced the original Q-switched system. Figure 14 shows the corrected long-arc residuals with the RB-TB fit obtained using Eq. (4). The residuals from the solid curve in Figure 14 are shown in Figure 15. The solid line in Figure 15 is the quadratic polynomial fit described by Eq. (5). The polynomial residuals, which are obtained when the polynomial is subtracted from the results in Figure 15, are shown in Figure 16. The polynomial RMS, which is used to approximate the measurement noise RMS, is 3.3 cm for this 40-minute pass. Similar data collected over a 100-day interval had a measurement noise RMS of 4.8 cm, indicating that the new laser will yield

routine Lageos laser ranging at the sub-5 cm level. Normal points created from the raw range measurements at the rate of one per second should approach a sub-centimeter noise level for one-minute normal points.

In an alternate development, the University of Texas McDonald Observatory has developed for NASA a Transportable Laser Ranging System, referred to as the TLRS-1, based on a single photoelectron detection design. The key design goals for this system are [Silverberg, et al., 1980]:

- air-transportable without disassembly,
- eye safe (i.e., no safety radar required),
- a 2 cm Lageos normal point precision for 3-minute averages.

Figure 17 shows the internal precision of the TLRS as a function of the number of single-shot returns in the normal points formed for three separate passes in November and December, 1980. Note that for normal points based on twenty or more returns, the precision is below 2.0 cm.

From the previous discussion, it is apparent that the precision of the laser tracking data has improved significantly since the Lageos satellite was launched. However, as pointed out in the previous discussion, continuity in tracking from the sites in the network and the geographical distribution of the stations are additional factors which influence the accuracy of geophysical parameter estimates. In addition to the improvements in the tracking precision, continuity in operation and the distribution of the tracking network have both improved significantly during the five-year lifetime of the Lageos mission. The effect of these improvements are manifested in improved geodynamic parameter recovery.

As an example, Figures 18 and 19 show the improvement in the x-component of the polar motion determined with the Lageos range observations collected during this time period. Figure 18 shows the difference between the estimate of the x-component of the polar motion using five-day values [Schutz, et al., 1981] from a smoothed curve [Vondrak, 1977] through the individual values. The RMS of the fit during the period from satellite launch through 1979 was 16 mas. Following the introduction of the pulse chopper in the SAO networks in November 1978 and early 1979 and the global deployment of the MOBLAS network in October 1979, the RMS value for the x-component of polar motion was reduced to about 6 mas.

When the 5-day arc residuals are combined into 100-day averages, the evolution of the improvement is shown in an even more dramatic fashion. Figure 19 shows the standard error of the mean x_p

residual for 100-day averages. In each point, 20 five-day arc solutions are combined into a single point. Note that the standard error for the 100-day averages at the beginning of the Lageos mission were on the order of 4 mas. The standard error was reduced to the order of 1.5 mas during the MERIT Campaign which occurred around 1600 days after satellite launch. Figure 17 also shows the degradation in the accuracy at the beginning of 1981 when a number of the NASA sites were taken out of operation for a network move. By late 1981, the lasers were re-deployed and operating, and the standard error was reduced again to the order of 1.5 mas. Note that the 1.5 mas standard error corresponds to roughly 6 mas in RMS value. It is also significant to note the reduction in the standard error which occurred around the beginning of 1979 as the SAO sites were modified to include the pulse chopper.

An important additional problem is the determination of baseline and station coordinate heights. A major factor in this determination will be the accuracy with which the Lageos satellite orbit can be determined. Figure 20 shows the improvement in the orbit inclination precision during this time period. The figure plots the difference between raw and smoothed values for independent 10-day arc determinations of the inclination. Note that the scatter about the smoothed curve is as large as .014 arcsec during the early part of the mission, while during 1980, the value is below .005 arcsec. A linear improvement with time is shown in Figure 20. The results obtained during 1980 demonstrate the potential of the laser data for geophysical parameter determinations, and if a global laser network can be operated with reasonable continuity and with the measurement precision at a level consistent with current capability, the geophysical objectives called for in the Crustal Dynamics Project can be achieved within the next half-decade.

However, at the present time, the reliability of the laser network is not uniform, the geographic coverage is not global, and there is some disparity in the accuracy with which the various systems are tracking. The following section discusses the overall quality of the data obtained from the global network.

An Assessment of Current Laser Range Accuracy

As a means of assessing the accuracy of the current laser tracking network, two sets of global laser range data were selected for detailed analysis. In the first of these, a 100-day interval spanning the period from September 23, 1980, through December 31, 1980, was analyzed using the full-rate laser range data archived in the National Space Science Data Center. In a second set, a 100-day interval of laser quick-look data spanning the period from July 17, 1981, through October 9, 1981, was analyzed.

Table 4 gives a list of the laser stations along with the station identification number for the lasers which contributed data to the full-rate and quick-look solutions. Table 5 summarizes the results obtained from the 100-day analysis of the full-rate data. Table 6 shows similar results for the analysis of the quick-look data. In addition to the data contributed by each station, these tables give the raw RMS, RB-TB RMS and POLY RMS statistics described previously. Estimates of the range bias and time bias for each station are also given.

For the full-rate data given in Table 5, the noise levels for the three SAO stations, Station No. 9907 (Arequipa), 9929 (Natal) and 9943 (Orroral), have internal precisions which vary between 33 and 36 cm. These numbers are consistent with the expected accuracy of the SAO systems following the addition of the pulse chopper. The Goddard systems, on the other hand, have noise levels in the range of 10 to 15 cm. The noise level for the TLRS-1 (7896) system was approximately 9 cm during this time period. It should be noted that the European stations, Kootwijk, Metsahovi, Grasse and Potsdam, have noise levels which vary from 23 cm to 62 cm. The Kootwijk (7833) and Grasse (7835) sites appear to be particularly important in terms of their performance levels. The range bias and time bias solutions contain both the average effects of orbit errors, polar motion errors and tracking station location errors. Since the station coordinates used for the solution are currently expected to be accurate to about 30 cm RMS, a significant portion of the range bias-time bias values can be attributed to station location error. Time bias values in excess of 100 ms are of concern, and further analysis of the data must be performed to understand the nature of these values.

In Table 6 similar results are presented for the quick-look data. In contrast to Table 5, where there were no edited observations since a previously edited data set was processed, Table 6 shows the amount of data edited for each of the stations. Note that the percent of data edited varies from approximately 2% to as high as 85%. The most significant of these statistics is the fact that, out of the 84 passes collected by Haleakala (7210), essentially 80% of the data were edited. Note that the quick-look data contains data from Wettzell (7834) and from Helwan (7831). The Helwan data have an internal precision of 70 cm, while Wettzell is operating at 20 cm. A current problem exists in interpreting the quick-look data messages from Metsahovi (7805) and from Grasse (7835). A 4 m bias was removed from the Metsahovi data, and a 13 m bias was removed from the Grasse data. Analysis of the Grasse data suggests that a 13 m preprocessing error was made in preparing the quick-look data from this site. It should be further noted that the stations consisting of Kootwijk, Grasse, Wettzell, Metsahovi and Helwan could be significant contributors to the strength of the global tracking solutions if these stations operate on a regular basis.

Note that the quick-look polynomial RMS for MOBLAS-4 (7102) is 3.2 cm. This can be contrasted with the 16.9 cm RMS for station 7102 during the 100-day full-rate data solution. The difference between these two data sources is due to substantial system improvements including a new Quantel laser and represents the level at which the improved NASA systems should be operating in the future. This performance level was achieved also for MOBLAS-7 which produced 47 passes with a polynomial RMS of 4.8 cm. Analysis of the range biases indicates that, with the exception of three sites, the range biases are all on the order of 10 cm or less.

In examining the data shown in Tables 5 and 6, it is apparent that the quality of the global laser data has improved substantially since the Lageos launch. However, it is also apparent that to achieve the goals of the Crustal Dynamics Project, further reduction in the systematic error components and some improvement in the measurement precision will be required. In this regard, the instances of anomalous performance of individual tracking stations is still present.

As an example, Figure 21 shows a history of the time bias determinations obtained using the quick-look data from the Platteville tracking station during the month of August 1981. Note that during the first portion of the month the time bias determinations are below .4 ms. However, on August 13, the time bias jumped to the order of 5 ms. After this time bias value was confirmed through several successive days of data, the anomaly was brought to the attention of the appropriate personnel at the NASA Goddard Space Flight Center. In early September, a portable atomic clock was taken to the Platteville site for checking the time bias, and a 4.79 ms jump in the station's cesium clock was confirmed. Note that the actual value of the discontinuity suggested by the results shown in Figure 21 is 4.98 - .24 = 4.74 ms.

The results shown in this figure illustrate another valuable use for the quick-look data, i.e., monitoring the performance of the global laser network. Such quality checks are valuable to assure the quality of the real-time polar motion products and to allow preliminary quality checks on TLRS site determinations and baselines.

Conclusions

Based on the results presented in the previous sections, it can be concluded that the laser tracking network has undergone dramatic improvement during the lifetime of the Lageos mission. There is, however, a very strong need for continuous tracking by a subset of stations satisfying the global distribution conditions. In this regard, it is extremely important that the stations on the European continent track continuously to provide strength to the polar motion

solutions and to allow complete geographic and temporal monitoring of the satellite orbit for the purpose of dynamic model development. The global distribution of tracking data for continuous periods of time will also be important in obtaining the requisite accuracies for the baseline and tracking station coordinates needed for the measurement of crustal motion. To achieve the extremely ambitious goals of the Crustal Dynamics Project, further refinements in the accuracy with which the laser measurements can be made will be required. Finally, in addition to the improvements in instrument accuracy, a careful effort should be made to obtain precise surveys of the distance to the target boards and/or the development of techniques for performing internal calibrations to reduce the uncertainties in the pre- and post-calibration measurements.

Acknowledgements

This research was supported by NASA under Contract No. NAS5-25991.

REFERENCES

Fitzmaurice, M. W., P. O. Minott, J. B. Abshire and H. E. Rowe, "Pre-launch Testing of the Laser Geodynamic Satellite," NASA TP-1062, October 1977.

Lehr, C. G., C. R. H. Tsiang, G. M. Mendes and R. J. Eldred, "Laser Pulse Analysis," The Use of Artificial Satellites for Geodesy and Geodynamics, Ed. by G. Veis, National Technical Univ. of Athens, 1973.

Marini, J. W. and C. W. Murray, "Correction of Laser Range Tracking Data for Atmospheric Refraction at Elevations Above 10 Degrees," NASA TM X-70555, 1973.

NASA Office of Space and Terrestrial Applications, "Application of Space Technology to Crustal Dynamics and Earthquake Research," National Aeronautics and Space Administration, NASA Technical Paper 1464, August, 1979.

NRC Committee on Geodesy, "Geodesy: Trends and Prospects," Assembly of Mathematical and Physical Sciences, National Research Council, 1978.

Plotkin, H. H., T. S. Johnson and P. O. Minott, "Progress in Laser Ranging to Satellites: Achievements and Plans," The Use of Artificial Satellites for Geodesy and Geodynamics, Ed. by G. Veis, National Technical Univ. of Athens, 1973.

Rinner, K., "Distance Measurement with the Aid of Electromagnetic Waves," Geophysical Surveys I, pp. 459-479, D. Reidel Publ. Co., Dordrecht, 1974.

Schutz, B. E. and B. D. Tapley, "UTOPIA: University of Texas Orbit Processor," Inst. for Advanced Study in Orbital Mechanics, University of Texas at Austin, IASOM TR 80-1, 1980.

Schutz, B. E., B. D. Tapley and R. J. Eanes, "Earth Rotation from Lageos Laser Ranging," Annual Report for 1980, Bureau International de l'Heure, pp. D27-D29, Paris, 1981.

Silverberg, E. C., "The TLRS and the Change in Mobile Station Design Since 1978," Proc. Laser Ranging Workshop, Austin, Texas, 1981.

Smith, D. E., F. J. Lerch, J. G. Marsh, C. A. Wagner, R. Kolenkiewicz and W. D. Kahn, "Contributions to the National Geodetic Satellite Program by Goddard Space Flight Center," J. Geophys. Res. 81 (5), pp. 1006-1026, February 1976.

Vondrak, J., "Problem of Smoothing Observational Data II," Bull. Astron. Inst. of Czech., 28, 84-89, 1977.

Wilkins, G. A., Ed., "Project MERIT," Report from the IAU/IUGG Joint Working Group, Royal Greenwich Observatory, 1980.

TABLE 1

GEOPHYSICAL MEASUREMENT ACCURACY FOR THE CRUSTAL DYNAMICS PROJECT

	σ_v, cm/yr	ΔT, yr	σ_d, cm	σ_n, cm
Current	2	5	11	8
Near future	1	5	6	4
Goal	.4, .7	5, 3	2	1

σ_v, velocity (baseline change) determination accuracy

ΔT, measurement span.

σ_d, precision determination accuracy

σ_n, laser range normal point accuracy

TABLE 2

SUMMARY OF LAGEOS LASER DATA CATALOG
UNIVERSITY OF TEXAS LAGEOS LONG ARC 8112.2
DATA SAMPLED TO 1 MINUTE SPACING, 7 MAY 76 - 14 NOV 81

STA ID	NO. OF PASSES	GOOD OBS	LASER SYSTEM; LOCATION
9921	675	16168	SAO 4 ; MT. HOPKINS, AZ.
9907	1566	35298	SAO 2 ; AREQUIPA, PERU
7063	429	9964	STALAS ; GREENBELT, MD.
9929	363	5485	SAO 1 ; NATAL, BRAZIL
7065	4	50	MOBLAS 3 ; GREENBELT, MD
7067	28	341	MOBLAS 1 ; BERMUDA ISLAND
7051A	26	333	MOBLAS 2 ; QUINCY, CA.
7062A	209	3903	MOBLAS 3 ; OTAY MT., CA.
7833	215	3245	KOOTWIJK, NETHERLANDS
9943	1341	35755	SAO 3 ; ORRORAL, AUSTRALIA
7082A	77	1389	MOBLAS 1; BEAR LAKE, UT.
7100	5	82	MOBLAS 3 AND 4 ; GREENBELT, MD.
7084	21	331	MOBLAS 2; OWENS VALLEY, CA.
7091A	32	395	MOBLAS 3; HAYSTACK, MA.
7085	20	318	MOBLAS 1 ; GOLDSTONE, CA. (DSS-14)
7834	118	1419	WETTZELL, GERMANY
7068	4	34	MOBLAS 2 ; GRAND TURK ISLAND
7101	8	131	MOBLAS 6 ; GREENBELT, MD.
7104	13	281	MOBLAS 7 ; GREENBELT, MD.
7103	18	348	MOBLAS 6 ; GREENBELT, MD.
7102	128	2654	MOBLAS 5 AND 4 ; GREENBELT, MD.
7069	17	141	RAMLAS ; PATRICK AFB, FL.
7210	68	1250	HOLLAS ; MT. HALEAKALA, MAUI, HI.
7091B	285	6841	MOBLAS 7 ; HAYSTACK, MA.
7096	124	2211	MOBLAS 6 ; AMERICAN SAMOA
7114A	288	6816	MOBLAS 2 ; OWENS VALLEY, CA.
7115	377	8333	MOBLAS 3 ; GOLDSTONE, CA. (DSS-13)
7086A	169	3828	MOBLAS 1 ; MCDONALD OBS., TX.
7090	1008	25292	MOBLAS 5 ; YARAGADEE, AUSTRALIA
7092	57	1121	MOBLAS 8 ; KWAJALEIN ATOLL
7120	353	7372	MOBLAS 1 ; MT. HALEAKALA, MAUI, HI.
7899	47	582	TLRS 1 ; GREENBELT, MD.
7805	24	386	METSAHOVI, FINLAND
7835	31	685	GRASSE, FRANCE
7896	66	1214	TLRS 1 ; PASADENA, CA.
7105	86	1893	MOBLAS 7 ; GREENBELT MD.
7086B	17	225	TLRS 1 ; MCDONALD OBS., TX.
7892	36	761	TLRS 1 ; VERNAL, UT.
7891	38	700	TLRS 1 ; FLAGSTAFF, AZ.
7831	22	253	HELWAN, EGYPT
7112	136	2360	MOBLAS 2 ; PLATTEVILLE, CO.
7110	85	1309	MOBLAS 3 ; MONUMENT PEAK, CA.
7051B	103	2895	MOBLAS 8 ; QUINCY, CA.
7082B	29	621	TLRS 1 ; BEAR LAKE, UT.
7114B	29	436	TLRS 1 ; OWENS VALLEY, CA.
7109	15	314	MOBLAS 8 ; QUINCY, CA.
7062B	31	363	TLRS 1 ; OTAY MT., CA.
TOTALS	8841	196126	

TABLE 3

QUICK-LOOK MINUS FULL-RATE DATA FOR
THE MERIT SHORT CAMPAIGN

	Time Tag (μsec)	Range (cm)
Owens Valley (MOBLAS 2)	0.82 ± 0.44	2.4 ± 6.2
Goldstone (MOBLAS 3)	0.87 ± 0.39	-4.9 ± 5.2
Yarragadee (MOBLAS 5)	0.54 ± 0.21	8.2 ± 2.7
Stalas	0.78 ± 0.43	3.2 ± 5.4
Orroral	-0.93 ± 2.99	-0.6 ± 2.9
Arequipa	1.30 ± 3.41	-0.6 ± 3.2
Natal	4.80 ± 5.23	-0.7 ± 3.1

TABLE 4

LASER STATION IDENTIFICATION

Station Name	Station No.	System No.
Arequipa, Peru	9907	SAO-3
Natal, Brazil	9929	SAO-2
Orroral, Australia	9943	
GORF, GSFC	7063	STALAS
Maui, Hawaii	7120	MOBLAS-1
Owens Valley, CA	7114	MOBLAS-2
Goldstone, CA	7115	MOBLAS-3
GORF, GSFC	7102	MOBLAS-4
Yarragadee, Aus.	7090	MOBLAS-5
American Samoa	7096	MOBLAS-6
Haystack, MA	7091	MOBLAS-7
Kwajelein Atoll	7092	MOBLAS-8
GORF, GSFC	7899	TLRS-1
Pasadena, CA	7896	TLRS-1
Kootwijk, Netherlands	7833	
Grasse, France	7835	
Metsahovi, Finland	7805	
Haleakala, Hawaii	7210	HOLLAS
Wettzell, Germany	7834	
Platteville, CO	7112	MOBLAS-2
Monument Peak, CA	7110	MOBLAS-3
Helwan, Eqypt	7831	
GORF, GSFC	7105	MOBLAS-7
Quincy, CA	7109	MOBLAS-8

TABLE 5

SUMMARY OF RESIDUAL ANALYSIS FOR 100 DAY INTERVAL FROM
80 SEP 23 - 80 DEC 31 FROM LAGEOS LONG ARC 8109.3

STA ID	NO. OF PASSES	TOTAL OBS	EDITED OBS	PCT EDITED	GOOD OBS	RAW RMS	RB TB RMS	POLY RMS
9907	68	1130	0	0.0	1128	48.2	36.4	34.3
7063	23	414	0	0.0	414	32.1	11.4	10.1
9929	24	214	0	0.0	214	76.8	37.1	33.4
7833	5	115	0	0.0	115	58.4	46.5	42.6
9943	94	2227	0	0.0	2227	44.5	38.2	36.7
7102	23	355	0	0.0	355	37.7	18.7	16 9
7091	59	1534	0	0.0	1533	37.3	19.2	17.6
7096	22	376	0	0.0	376	25.4	12.2	11.5
7114	68	1421	0	0.0	1421	34.2	15.4	13.3
7115	72	1329	0	0.0	1329	28.7	11.3	9.4
7090	144	3965	0	0.0	3964	34.8	14.7	14.0
7092	13	292	0	0.0	292	45.7	23.5	22.0
7120	69	1362	0	0.0	1359	34.3	12.5	11 4
7899	10	125	0	0.0	125	31.9	15.1	12.4
7805	18	275	0	0.0	275	102.6	68.4	57.3
7835	24	569	0	0.0	569	48.3	24.2	23.0
7896	66	1219	0	0.0	1219	33.7	11.0	8.8
TOTALS	802	16922	0	0.0	16915	40.3	23.8	22.1

MULTIPLE PASS RANGE BIAS AND TIMING BIAS SOLUTIONS

STATION	PASSES	RBIAS	STD ERR	SIGMA	TBIAS	STD ERR	SIGMA
9907	66	-9.5	2.7	3.0	81.3	17.2	19.4
7063	23	3.2	5.7	4.9	35.7	18.9	31.8
9929	24	-49.5	5.7	10.0	47.6	52.0	64.1
7833	5	10.2	10.8	9.4	-134.8	65.8	57.0
9943	94	-6.1	1.5	2.2	-34.8	10.9	13 3
7102	23	9.4	6.7	5.6	-57.0	17.2	35.7
7091	58	18.0	2.2	2.6	-31.7	17.4	16 5
7096	22	-4.8	4.2	5.2	29.4	17.5	32 7
7114	68	15.5	1.6	2.7	-102.5	11 4	16.9
7115	72	6.4	1.8	2.7	-19.1	16.1	19.7
7090	143	21.1	1.2	1.6	33.1	9.0	9.8
7092	13	-10.0	9.6	5.9	76.1	19.7	35.9
7120	67	5.5	3.0	2.8	57.4	11.0	17.2
7899	10	13.5	4.4	9.0	-46.8	34.8	54.2
7805	18	-30.1	9.2	6.0	53.3	108.6	41.9
7835	24	7.8	5.7	4.5	-147.7	31.8	28.7
7896	66	-.2	1.9	2.9	-94.3	17.4	18.0

TABLE 6

SUMMARY OF RESIDUAL ANALYSIS FOR 85 DAY FIT TO QUICKLOOK DATA
81 JUL 17.5 - 81 OCT 9.5

STA ID	NO. OF PASSES	TOTAL OBS	EDITED OBS	PCT EDITED	GOOD OBS	RAW RMS	RB TB RMS	POLY RMS
7063	21	956	103	10.8	853	30.0	16.0	12.6
7102	7	348	298	85.6	50	23.6	10.2	3.2
7090	118	5397	163	3.0	5234	26.3	13.3	12.7
7210	84	3658	2934	80.2	724	39.2	22.0	19.7
9907	115	6101	1016	16.7	5085	43.0	37.9	37.3
9943	54	2310	442	19.1	1868	56.1	51.3	50.3
9929	42	2067	806	39.0	1261	46.8	43.9	42.9
7805	8	197	140	71.1	57	100.1	83.7	73.7
7833	7	104	17	16.3	87	42.6	34.7	32.3
7120	78	3752	233	6.2	3519	27.1	10.9	9.9
7835	7	183	115	62.8	68	22.2	18.9	18.7
7834	16	507	334	65.9	173	37.2	23.7	23.6
7105	47	2134	105	4.9	2029	18.8	6.8	4.8
7112	77	2750	963	35.0	1787	26.9	16.8	15.8
7110	50	2025	398	19.7	1627	28.1	21.1	19.4
7831	32	1930	983	50.9	947	88.2	72.8	69.6
7109	4	196	3	1.5	193	26.0	19.2	16.9
TOTALS	767	34615	9053	26.2	25562	38.5	30.4	29.3

MULTIPLE PASS RANGE BIAS AND TIMING BIAS SOLUTIONS

STATION	PASSES	RBIAS	STD ERR	SIGMA	TBIAS	STD ERR	SIGMA
7063	21	21.4	2.4	3.5	15.7	10.1	26.2
7102	7	15.6	2.9	14.3	-41.1	36.5	107.1
7090	116	3.2	1.9	1.4	2.6	7.0	9.5
7210	17	-2.2	6.3	3.7	40.4	40.4	28.7
9907	111	1.6	1.3	1.6	-80.9	8.3	10.3
9943	45	-7.7	2.4	2.4	61.0	15.9	17.2
9929	40	-3.0	2.1	2.8	3.7	14.9	23.5
7805	4	-37.3	13.6	13.3	69.3	144.0	90.7
7833	5	-2.5	9.7	11.5	81.9	39.5	85.5
7120	73	-8.4	1.2	1.7	82.7	12.8	11.5
7835	2	2.0	13.6	13.3	-22.8	83.3	88.4
7834	5	.2	14.0	19.8	13.9	157.3	141.7
7105	45	5.2	2.1	2.2	12.0	10.0	17.2
7112	52	-1.1	2.6	2.4	41.6	12.3	15.7
7110	41	-5.2	2.1	2.5	13.8	14.7	17.4
7831	22	-2.1	10.0	3.3	22.7	41.7	29.1
7109	4	-6.7	5.9	7.2	64.1	63.9	55.4

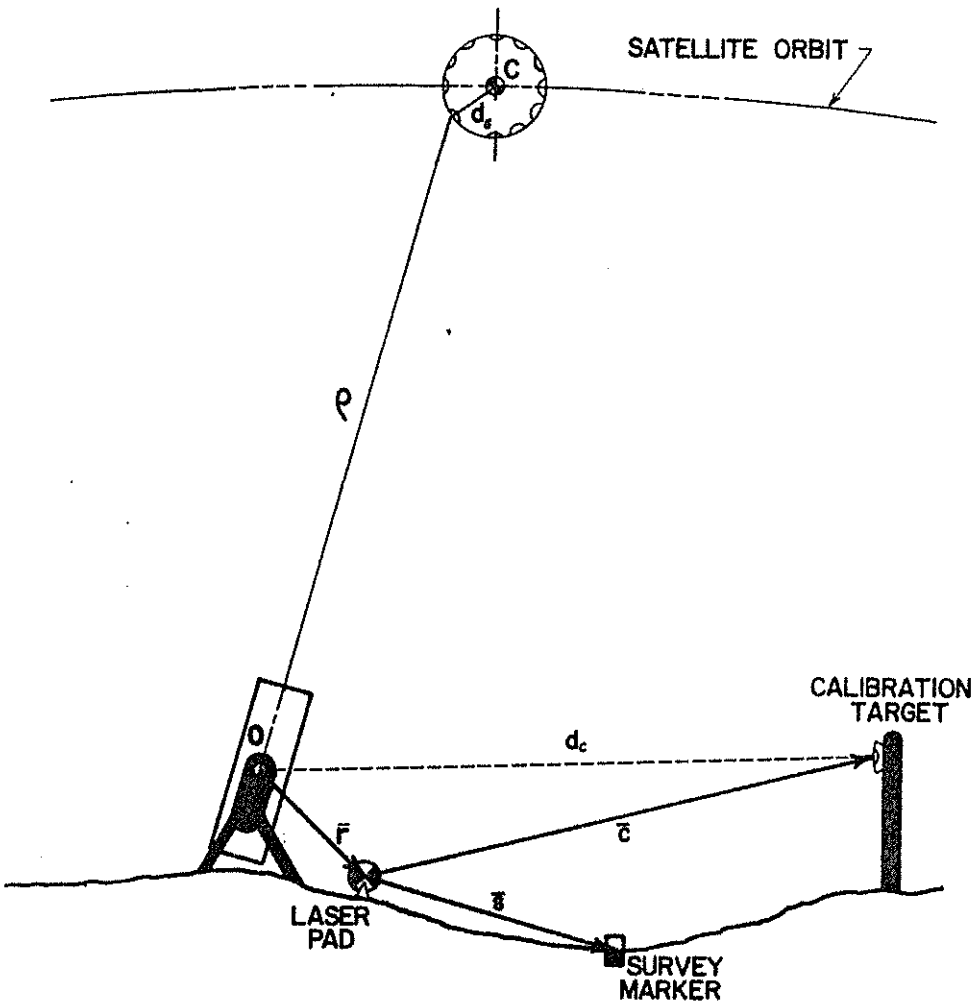

Figure I. Satellite Laser Range Measurement

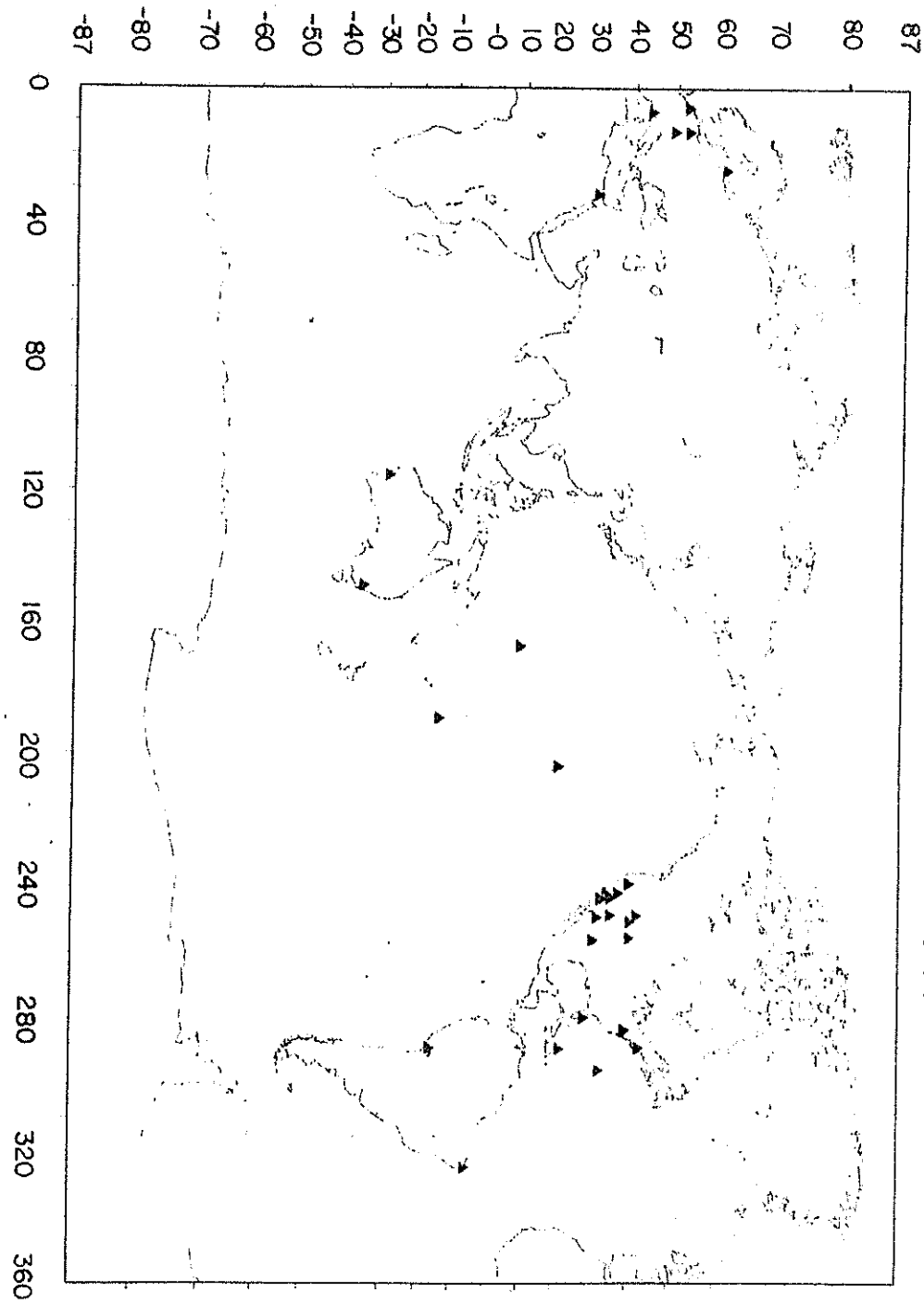

FIGURE 2
LAGEOS TRACKING STATION NETWORK

FIGURE 3

NUMBER OF LAGEOS PASSES OBSERVED IN EACH 5-DAY POLAR MOTION ARC
FROM 42909 (11 MAY 76) TO 44944 (06 DEC 81)

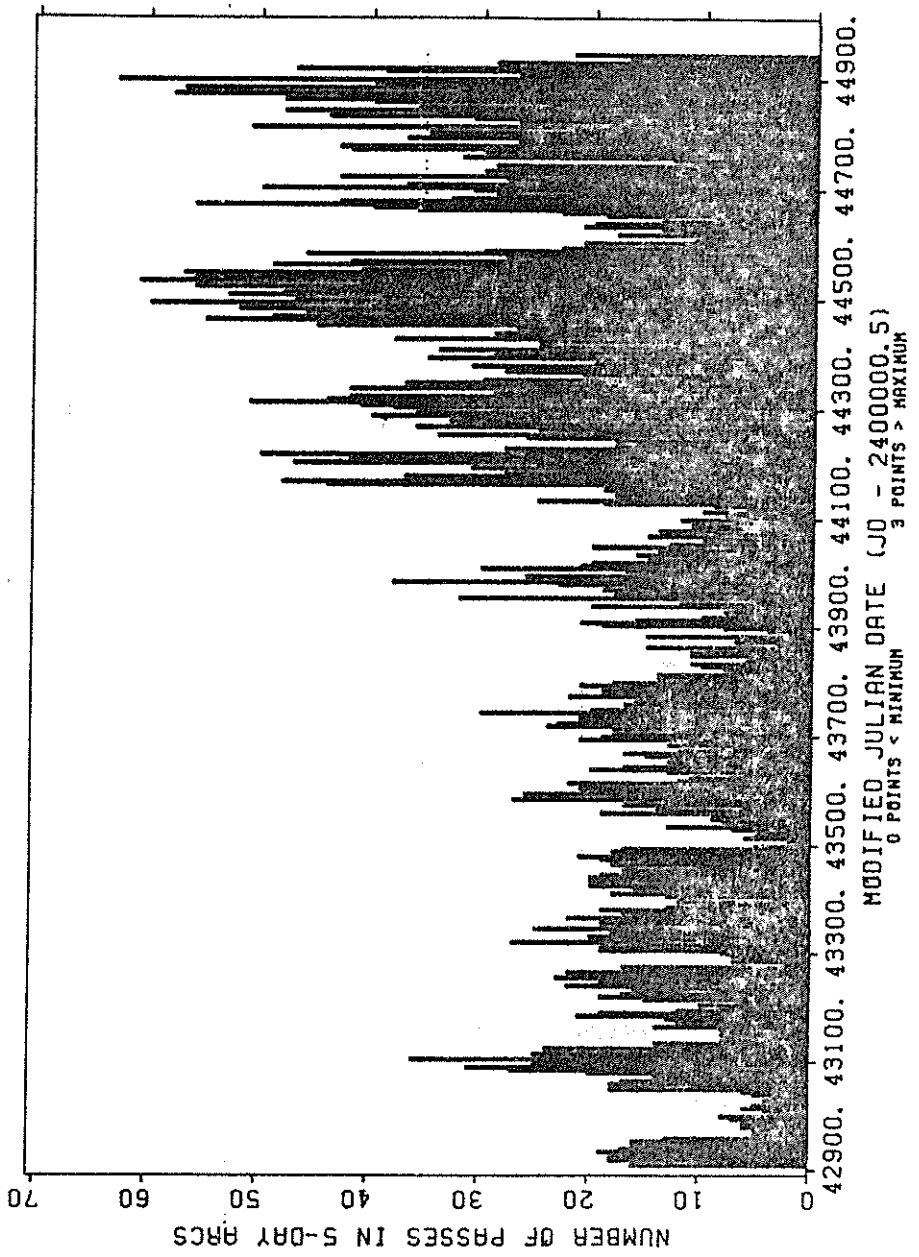

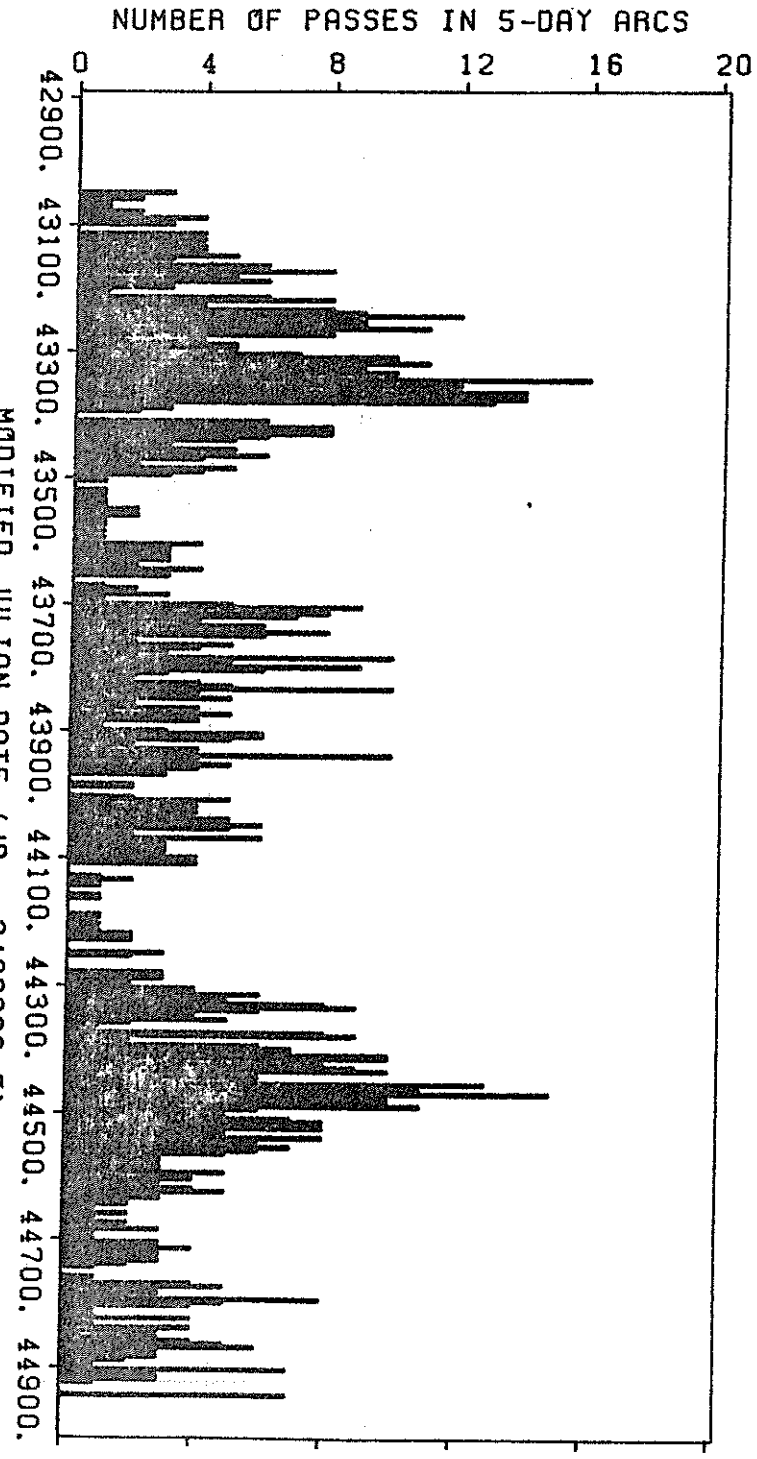

FIGURE 4

NUMBER OF LAGEOS PASSES OBSERVED BY ORORAL IN EACH 5-DAY POLAR MOTION ARC FROM 42909 (11 MAY 76) TO 44944 (06 DEC 81)

FIGURE 5

MAXIMUM ENTROPY SPECTRAL ANALYSIS OF
LAGEOS OBSERVATION DISTRIBUTION

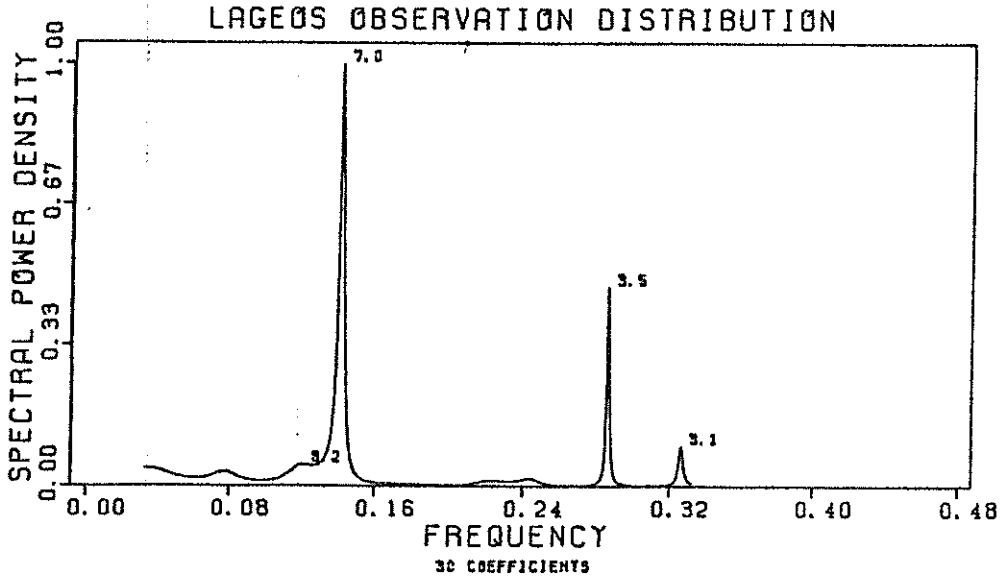

FIGURE 6

VARIATION OF THE QUANTITY OF LAGEOS DATA OBTAINED DURING THE MERIT SHORT CAMPAIGN. FIT WITH 7 AND 3.5 DAY PERIODS

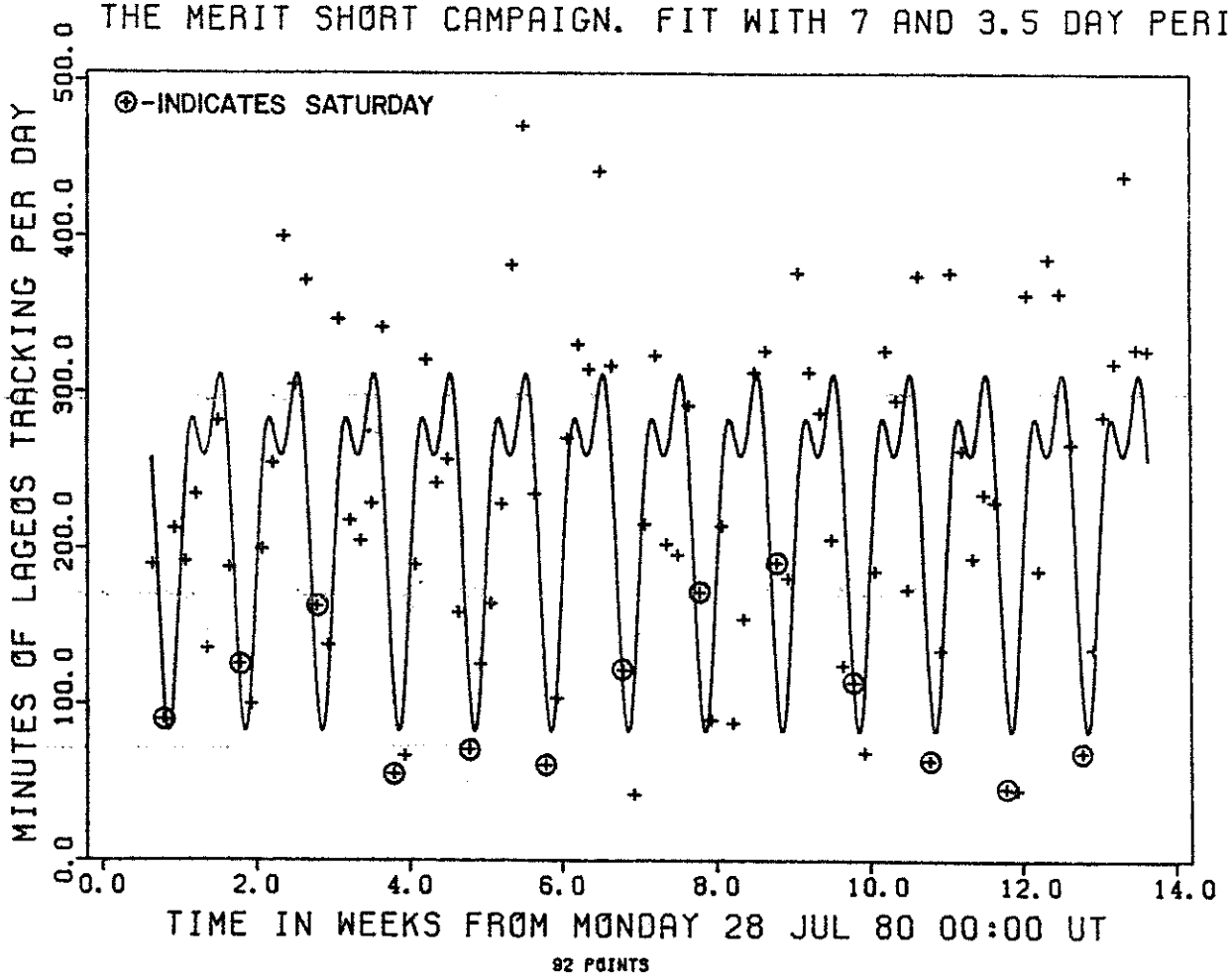

FIGURE 7

NUMBER OF LAGEOS PASSES OBSERVED BY STALAS IN EACH 5-DAY
POLAR MOTION ARC FROM 42909 (11 MAY 76) TO 44944 (06 DEC 81)

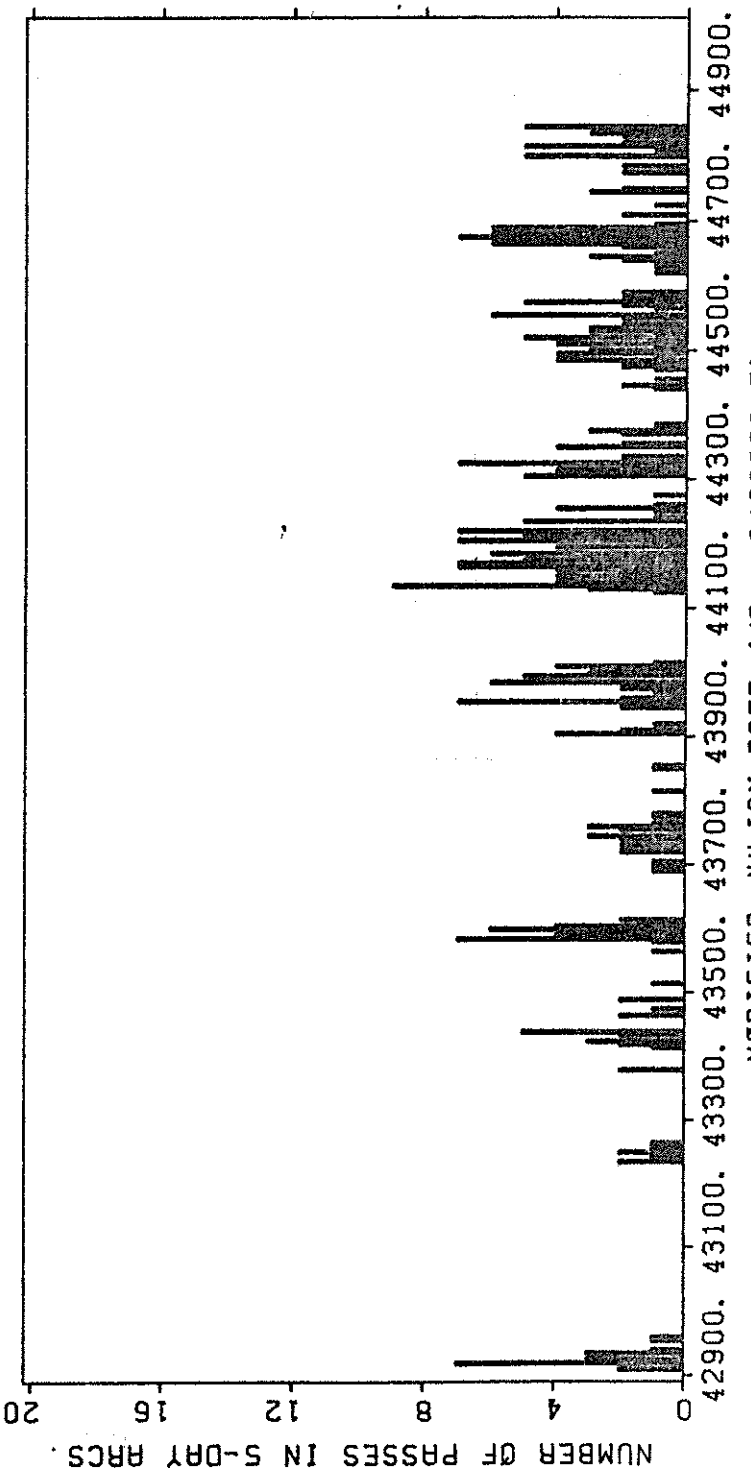

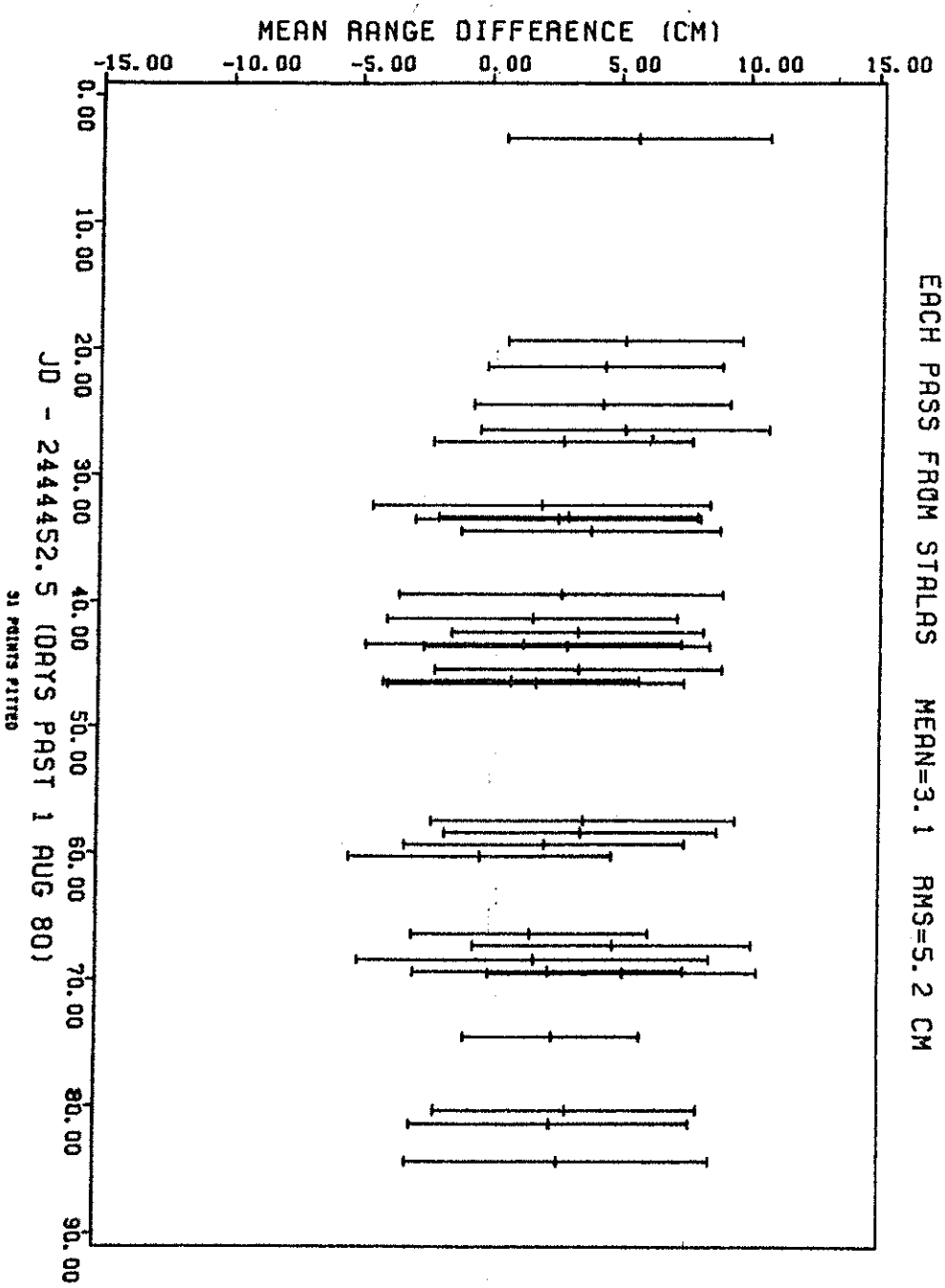

FIGURE 8

FINAL - QUICKLOOK DATA MEAN RANGE DIFFERENCE FOR EACH PASS FROM STALAS MEAN=3.1 RMS=5.2 CM

FIGURE 9

FINAL - QUICKLOOK DATA MEAN TIME DIFFERENCE FOR EACH PASS FROM STALAS MEAN=0.8 RMS=0.4 MICROSEC

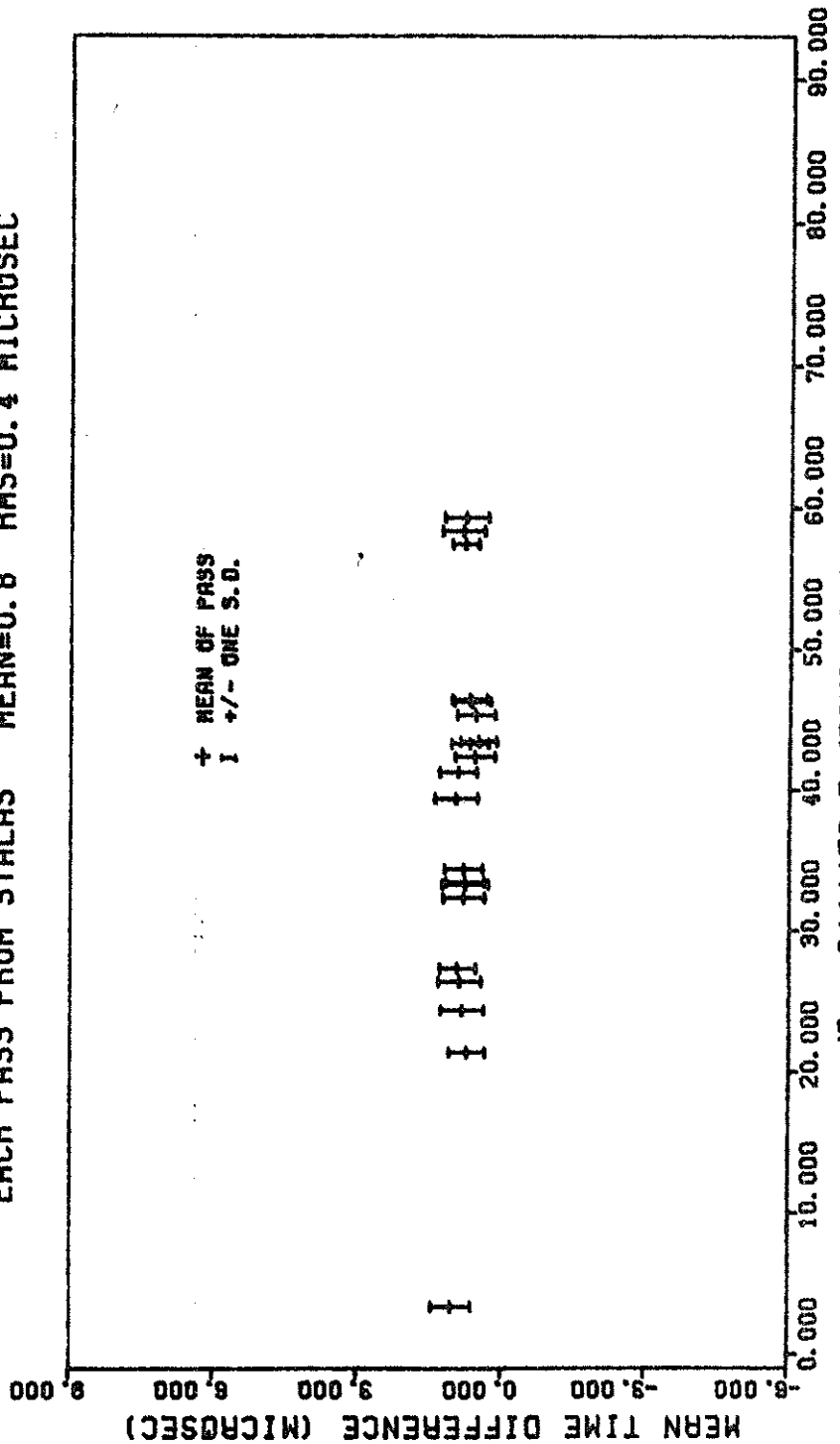

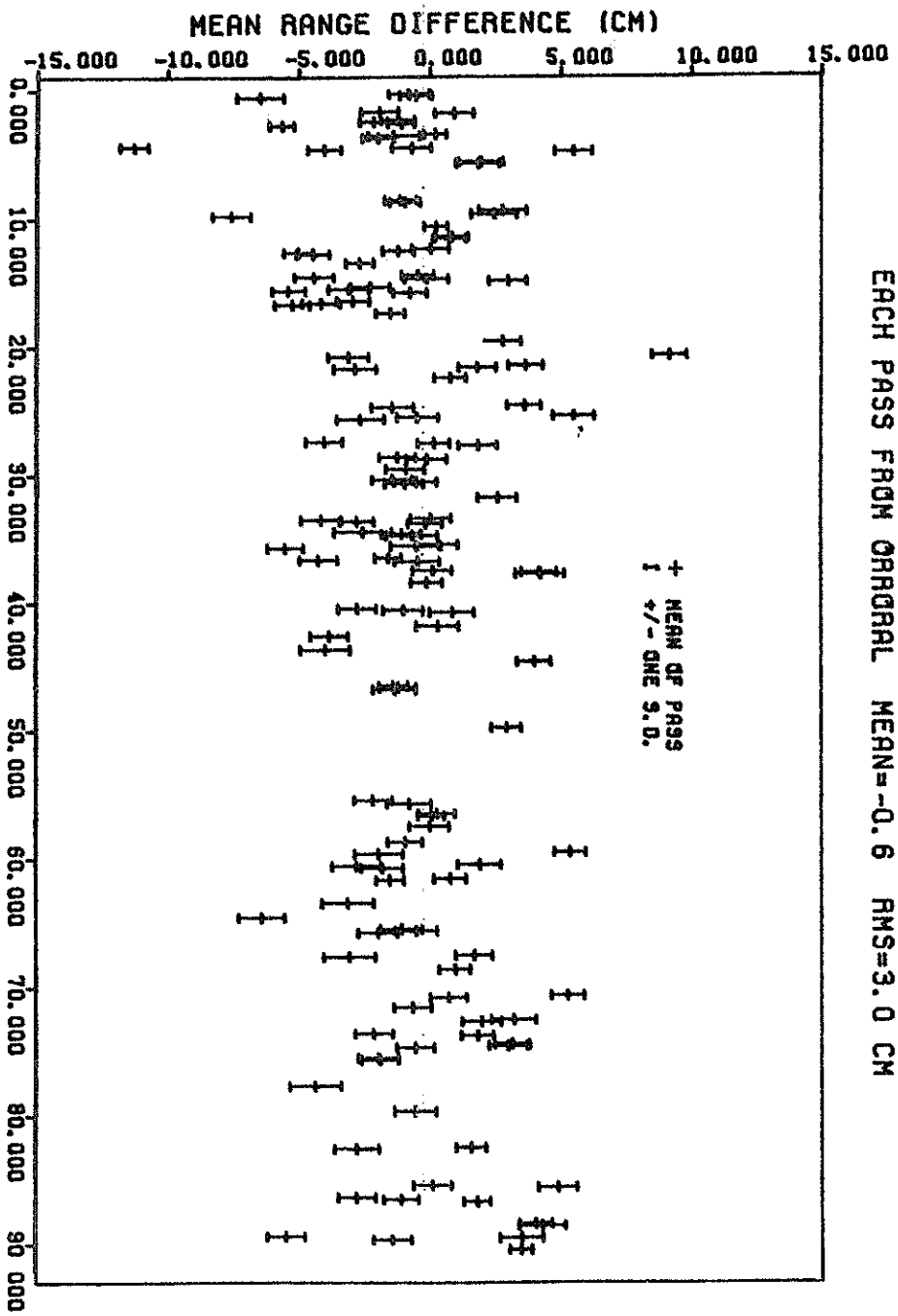

FIGURE 10
FINAL - QUICKLOOK DATA MEAN RANGE DIFFERENCE FOR EACH PASS FROM ORORAL MEAN=-0.6 RMS=3.0 CM

FIGURE 11
FINAL - QUICKLOOK DATA MEAN TIME DIFFERENCE FOR
EACH PASS FROM ORORAL MEAN=-0.9 RMS=3.0 MICROSEC

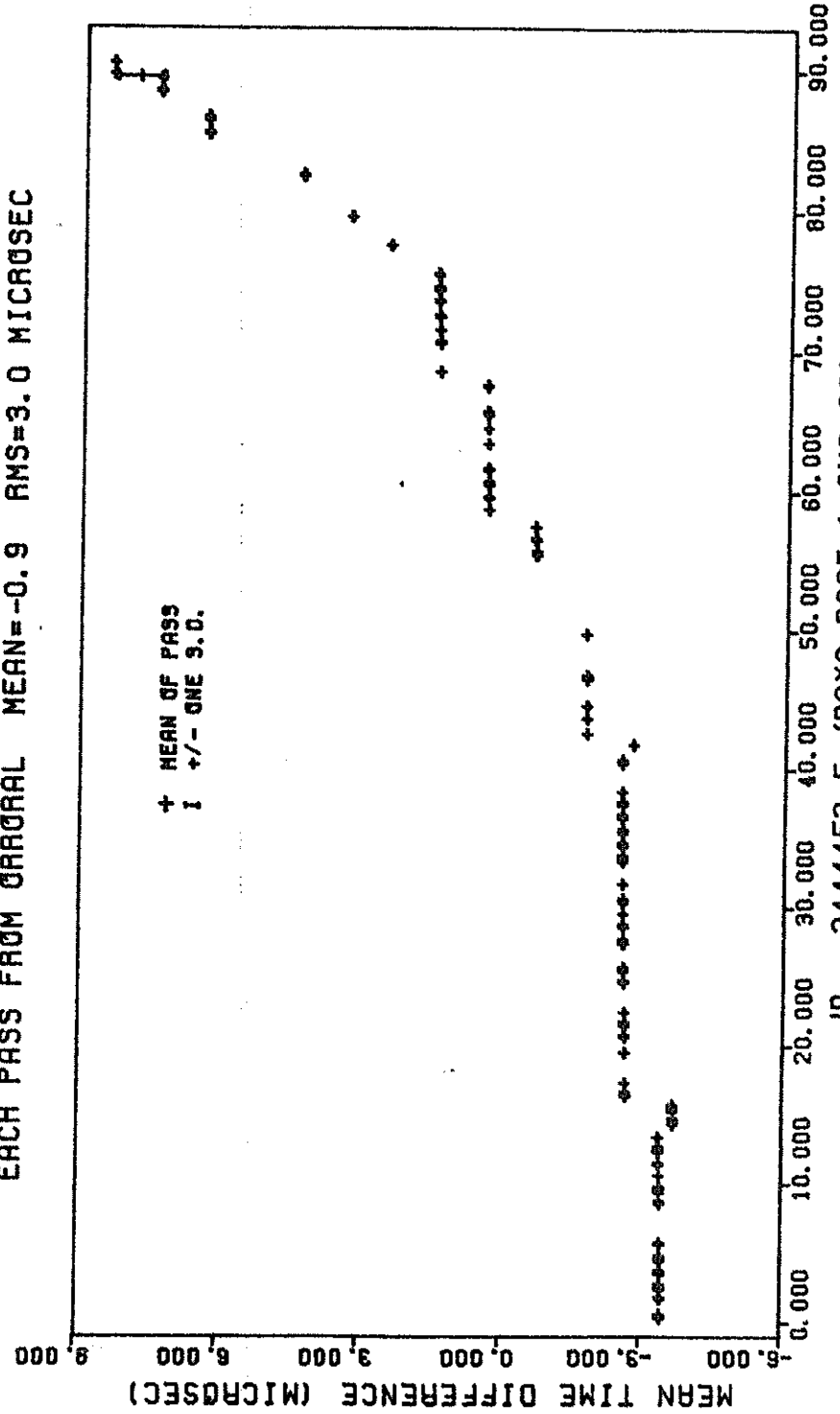

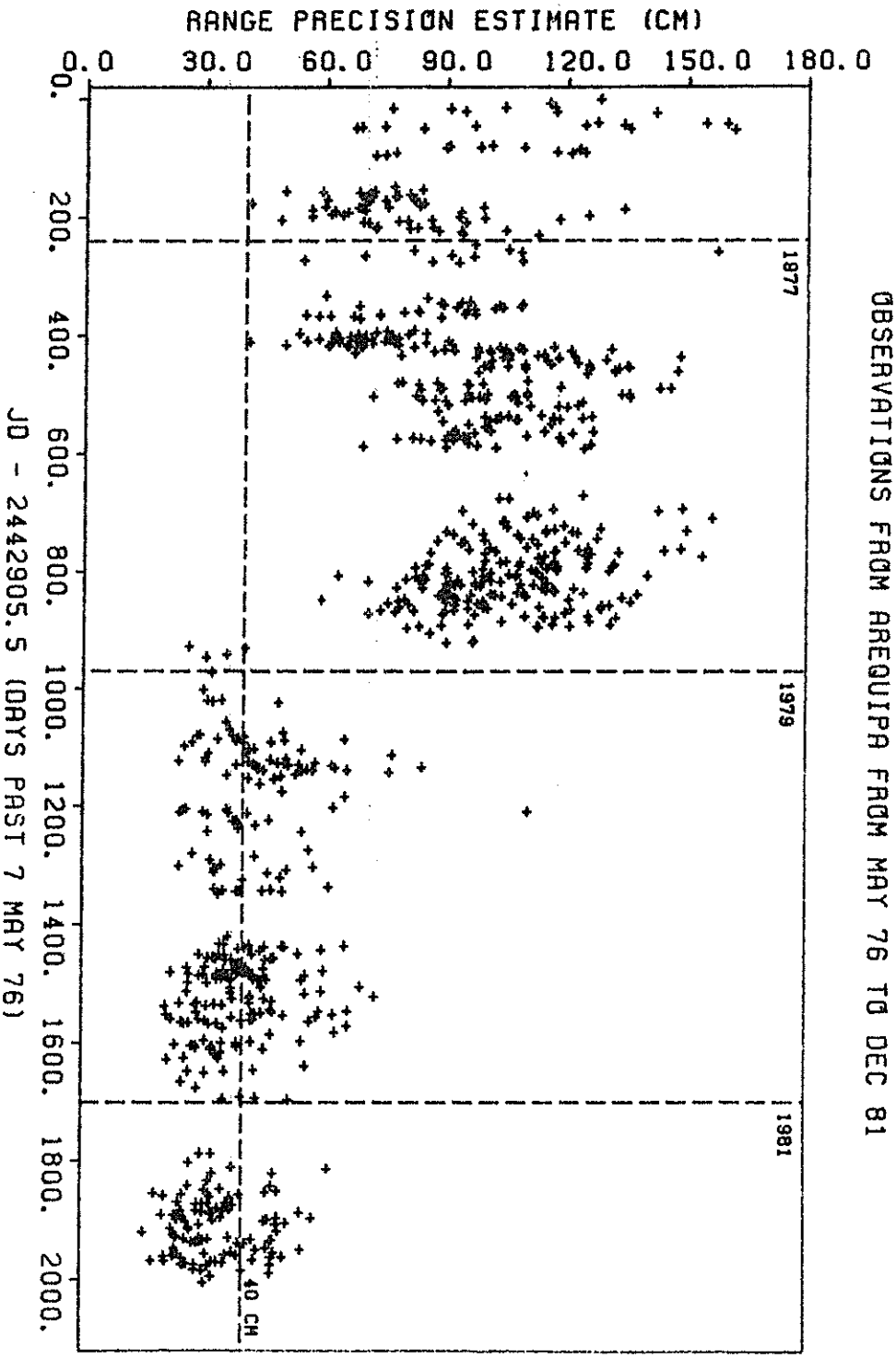

FIGURE 12

PASS BY PASS ESTIMATES OF THE INTERNAL PRECISION OF LAGEOS OBSERVATIONS FROM AREQUIPA FROM MAY 76 TO DEC 81

FIGURE 13

PASS BY PASS ESTIMATES OF THE INTERNAL PRECISION OF LAGEOS OBSERVATIONS FROM STALAS FROM MAY 76 TO DEACTIVATION IN OCT 81

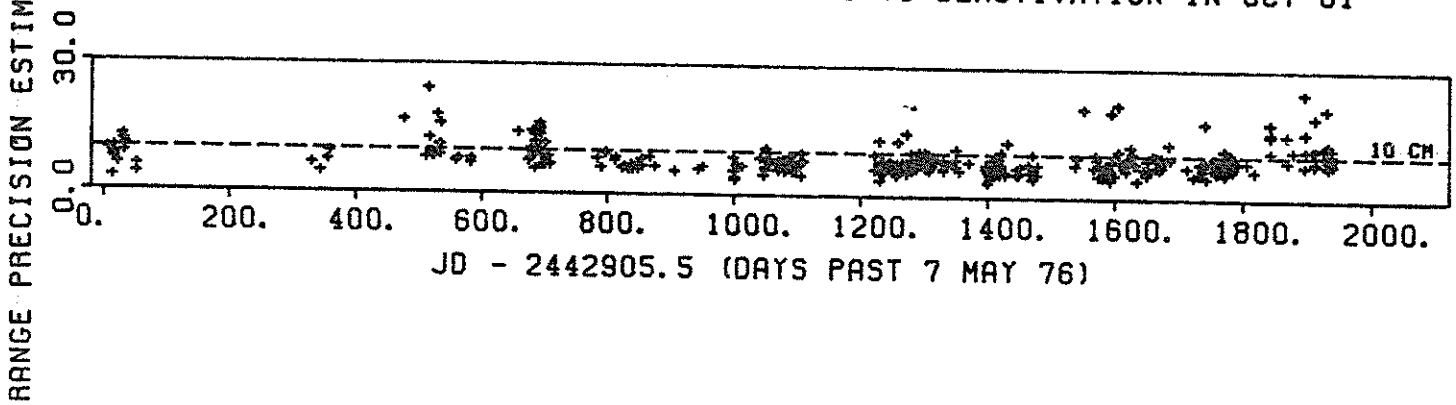

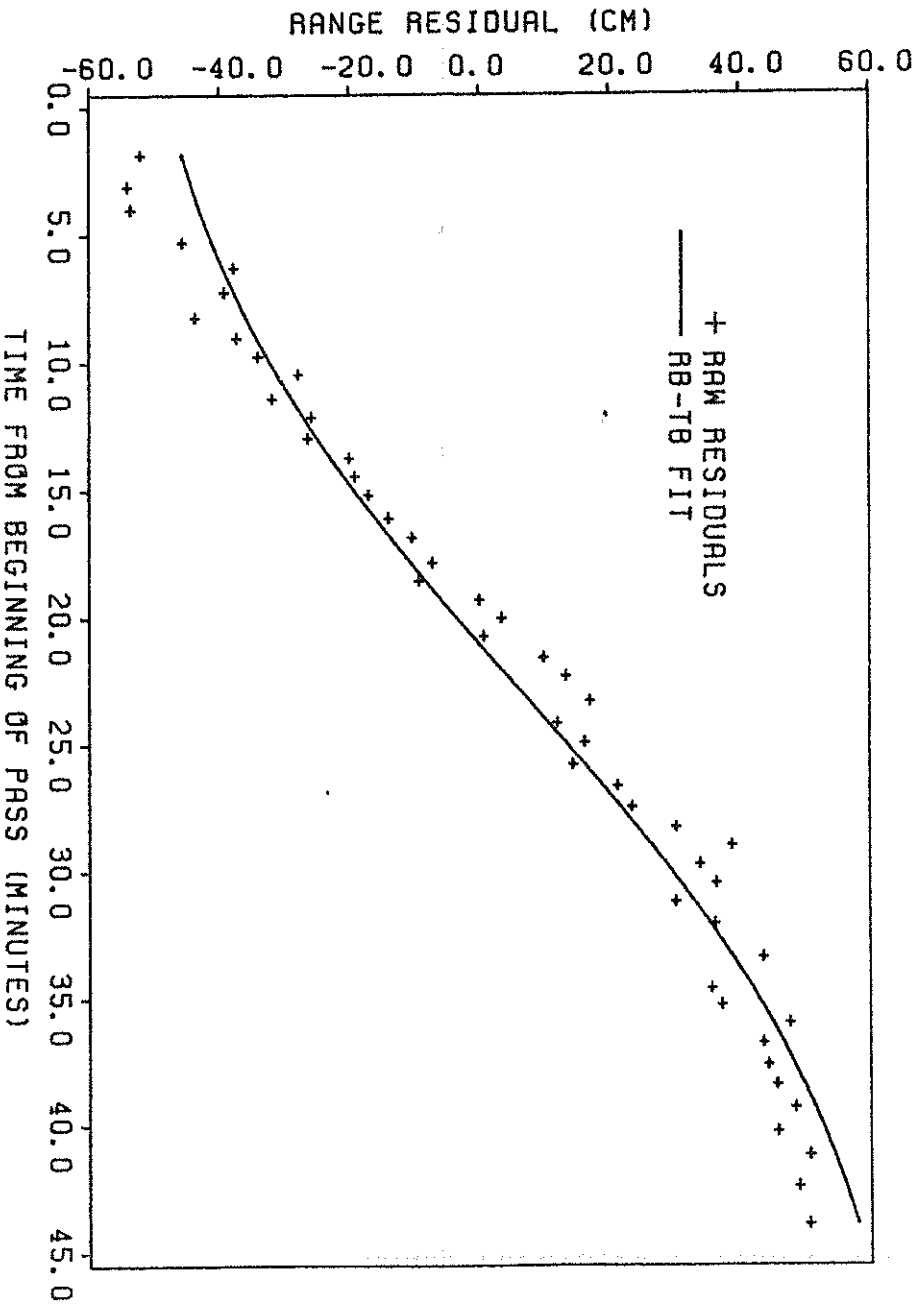

FIGURE 14

RANGE RESIDUALS FROM MOBLAS 7 PASS OF 8 JAN 82, 10 HRS UT
THE RAW RESIDUALS ARE SHOWN WITH THE RANGE BIAS-TIME BIAS FIT

FIGURE 15
RANGE RESIDUALS FROM MOBLAS 7 PASS OF 8 JAN 82, 10 HRS UT
THE RB-TB RESIDS ARE SHOWN WITH THE POLYNOMIAL FIT

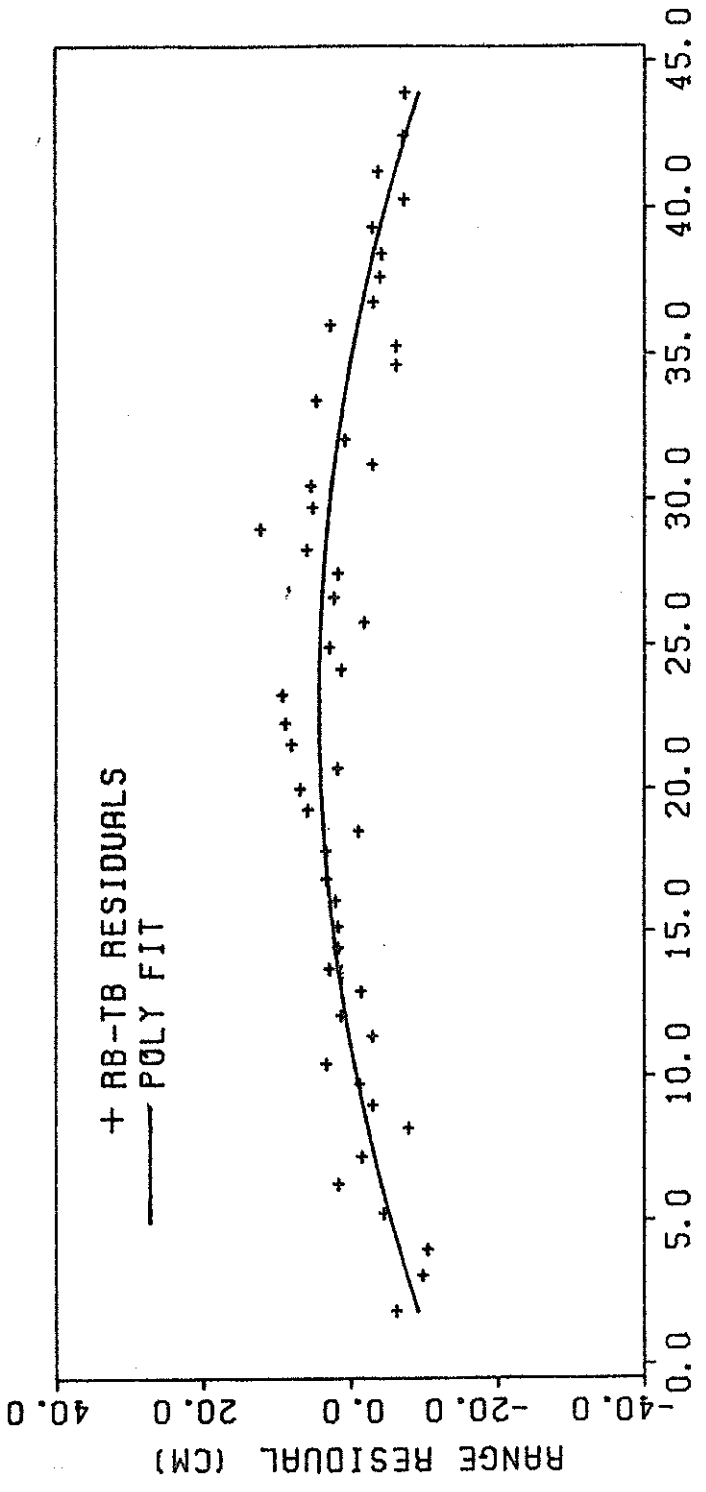

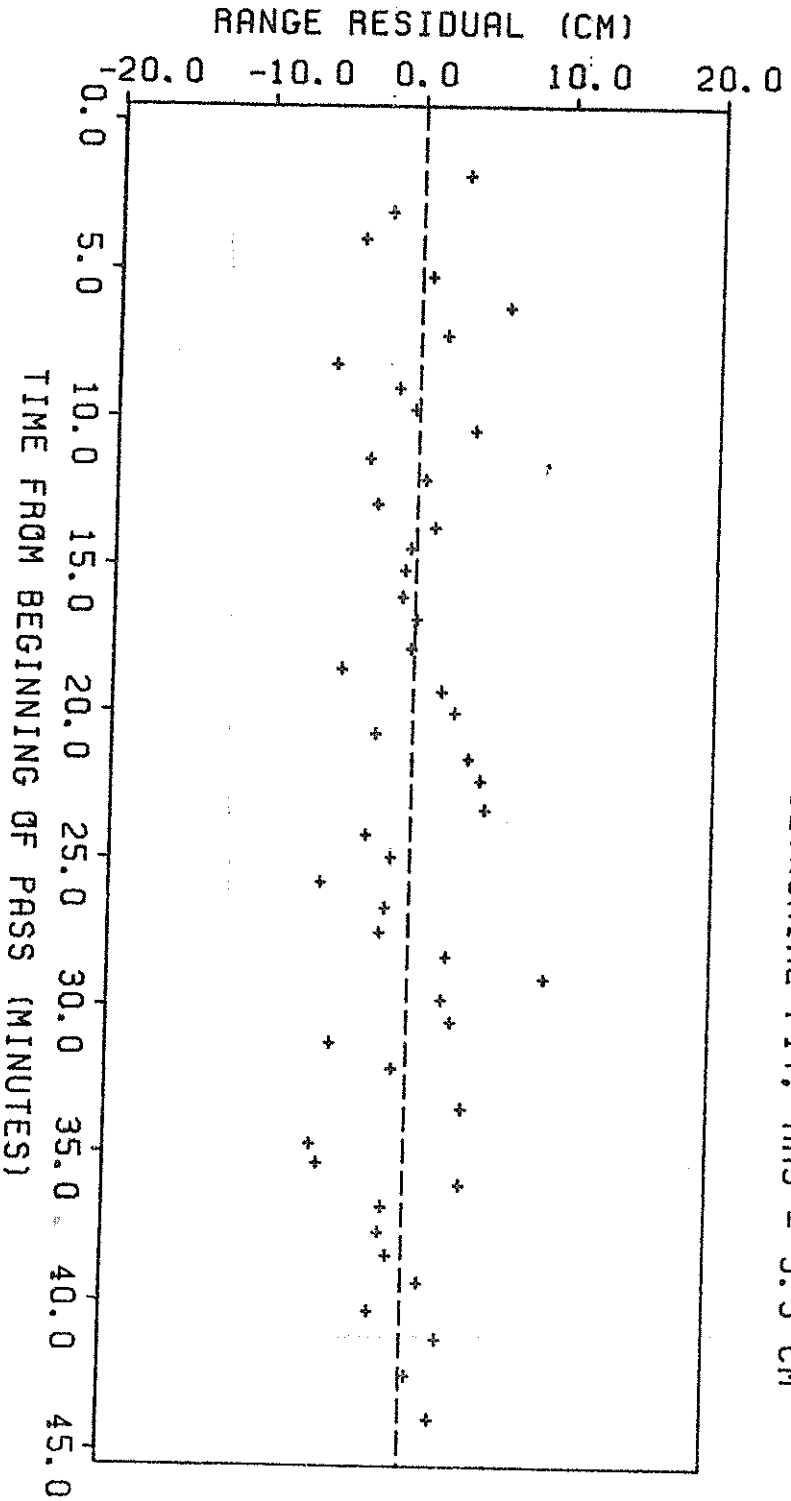

FIGURE 16

RANGE RESIDUALS FROM MOBLAS 7 PASS OF 8 JAN 82, 10 HRS UT
QUICKLOOK RESIDUALS AFTER POLYNOMIAL FIT, RMS = 3.3 CM

FIGURE 17
INTERNAL PRECISION OF TLRS NORMAL POINTS
DATA FROM SITE 8, PASADENA, CA.

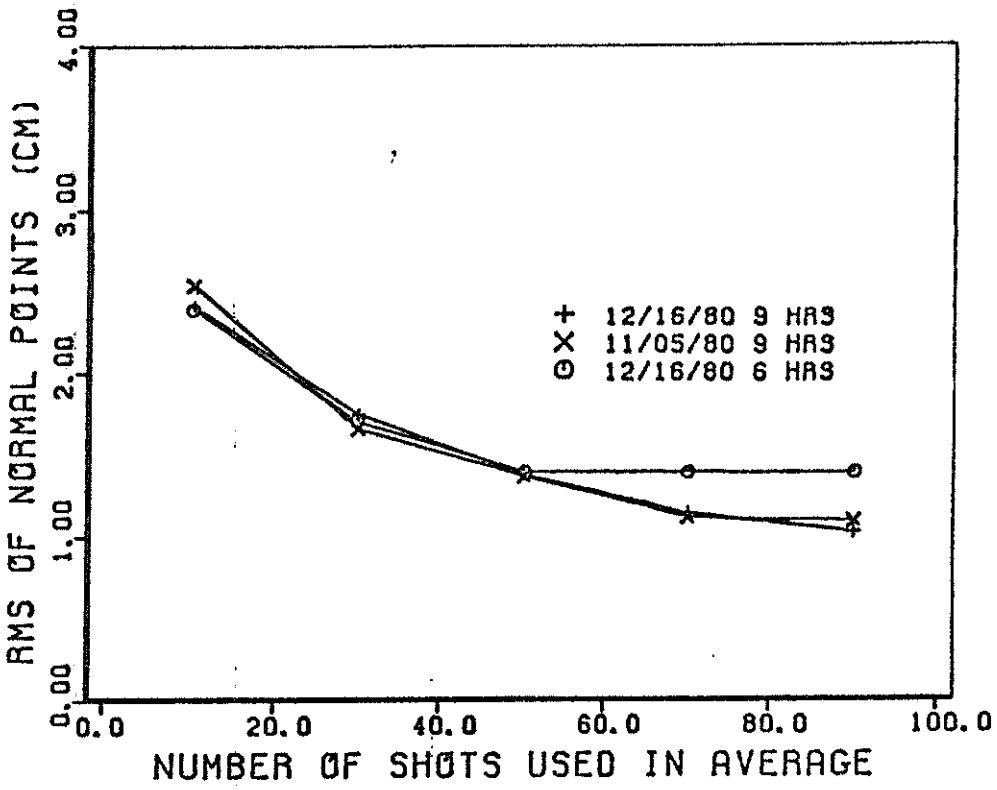

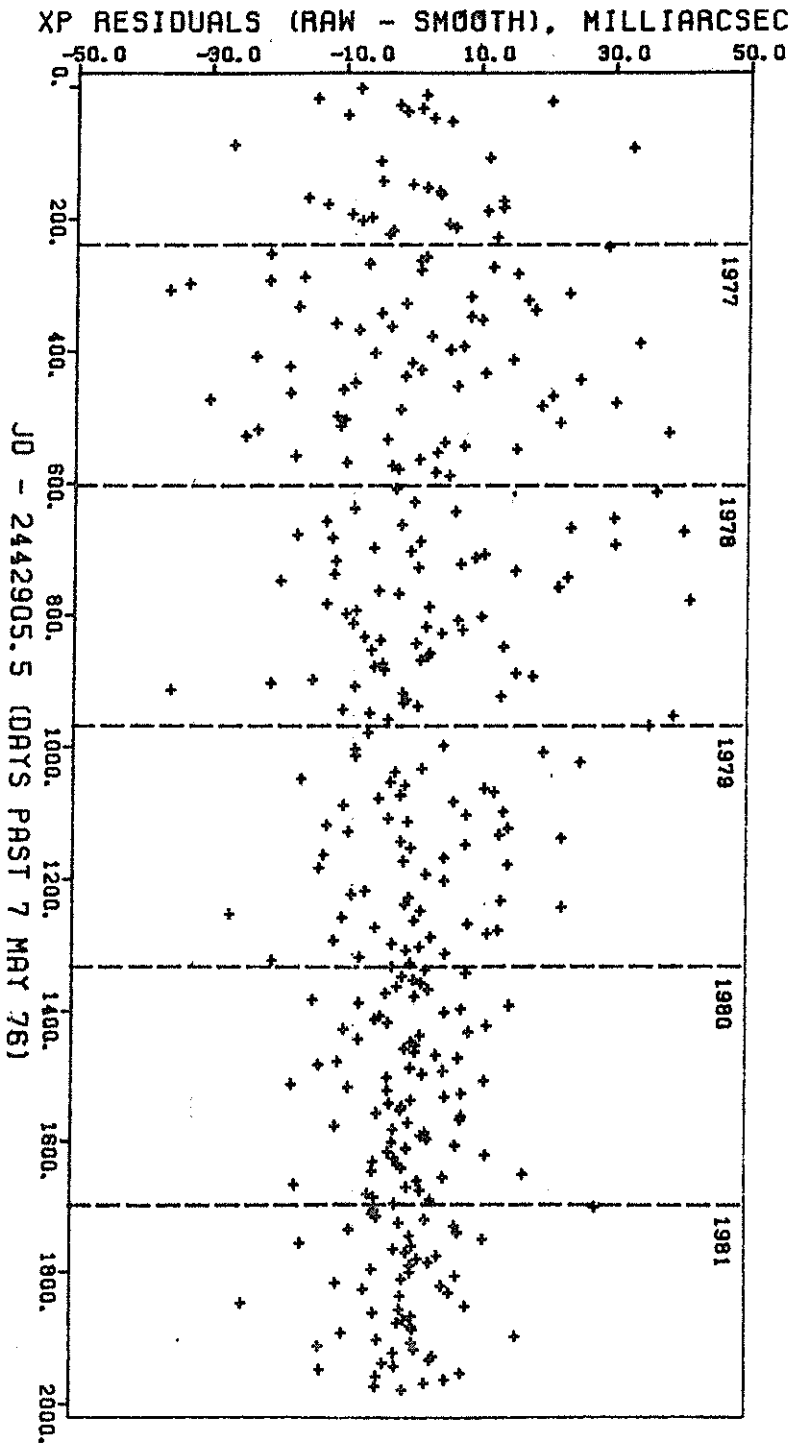

FIGURE 18

LAGEOS POLAR MOTION SOLUTION RESIDUALS FROM SMOOTHING
SHOWING IMPROVEMENT IN INTERNAL CONSISTENCY

FIGURE 19

STANDARD ERROR OF THE MEAN XP SMOOTHING RESIDUAL FOR
100 DAY AVERAGES (20 FIVE-DAY ARC SOLUTIONS)

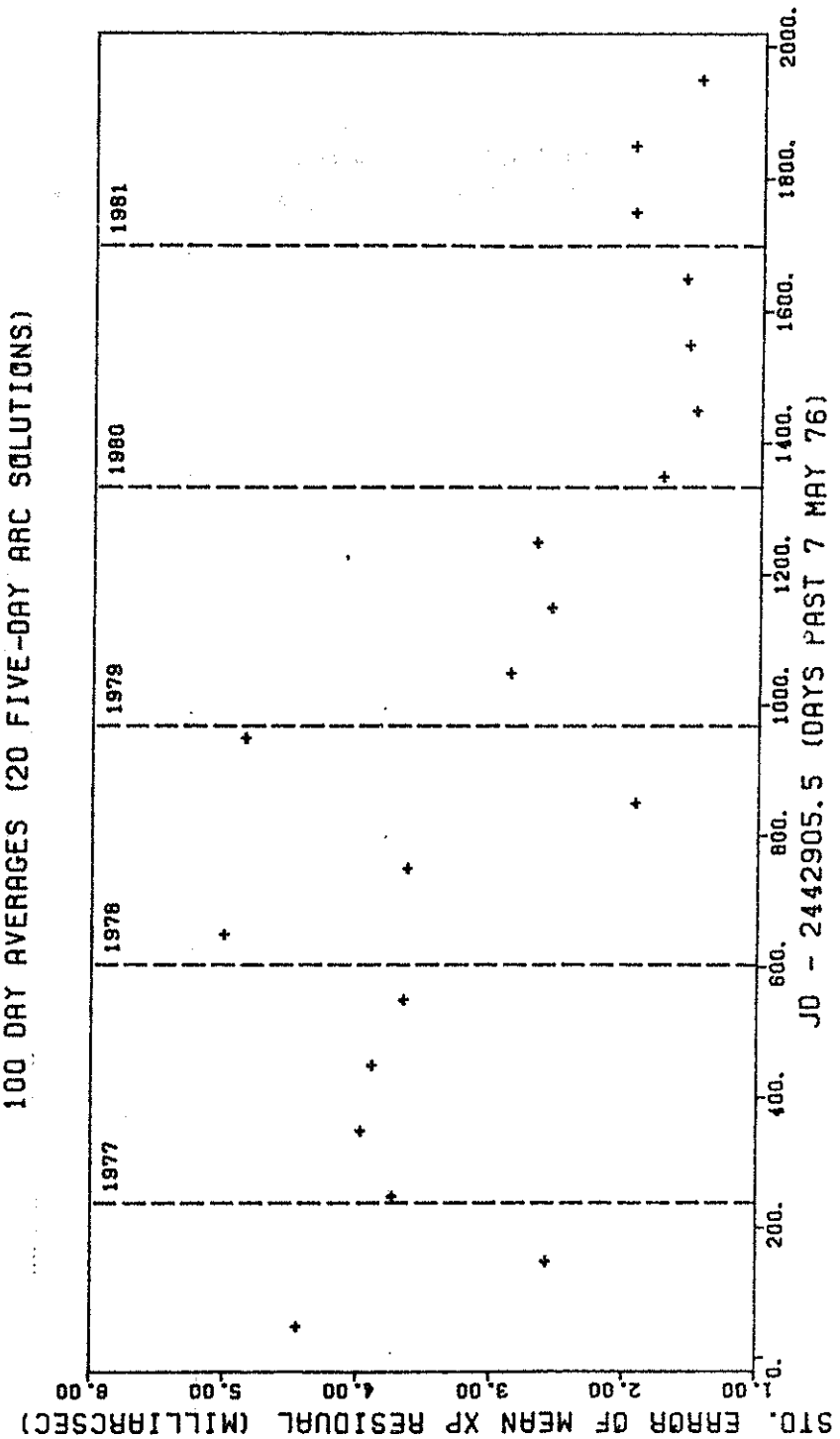

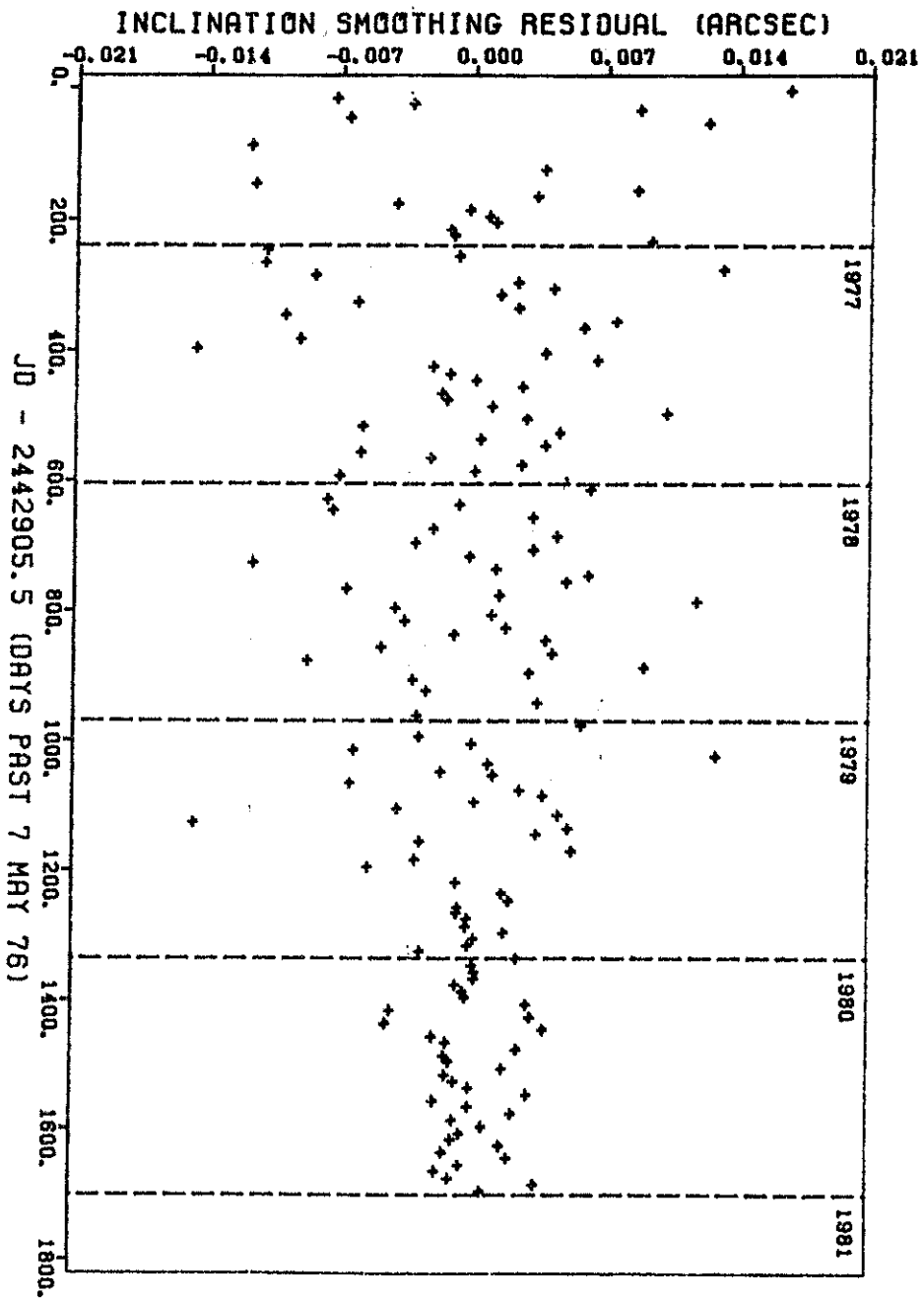

FIGURE 20

LAGEOS 10 DAY ARC INCLINATION RESIDUALS (RAW - SMOOTHED)
SHOWING IMPROVEMENT IN INTERNAL CONSISTENCY

FIGURE 21

APPARENT TIME BIAS FOR EVERY PLATTEVILLE (MOBLAS 2) PASS FROM 16 JULY 81

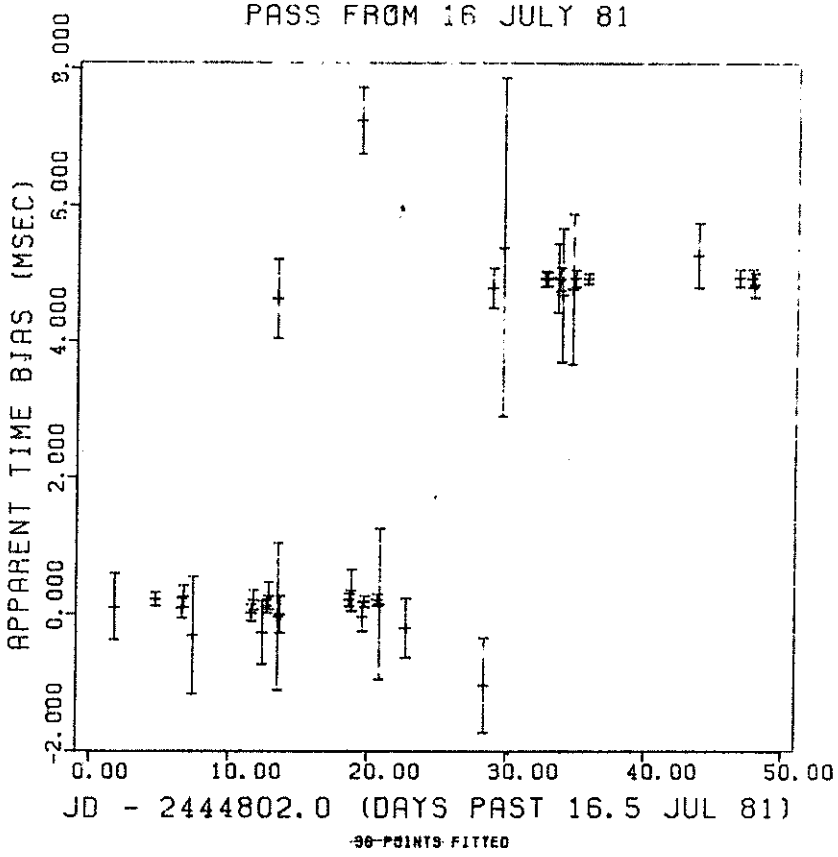

SOME CURRENT ISSUES IN SATELLITE LASER RANGING

M. R. Pearlman

SMITHSONIAN ASTROPHYSICAL OBSERVATORY
60 Garden Street
Cambridge, Massachusetts 02138

The Laser Workshops have provided an important forum for us to discuss hardware and now software status and development. We have also had the opportunity to hear an elaboration of requirements and an assessment of present data quality.

In this paper we will address several very critical issues that have not been given sufficient attention to date. These include: (1) current trends in data capability, (2) accuracy, and (3) data aggregation. Recommendations are provided as a means to stimulate discussion and hopefully some organized action.

1.0 Applications and Current Trends

At the last Laser Workshop at Lagonnissi, Dr. E. M. Gaposchkin (1978) gave an overview of the applications that could be addressed in geophysics at different levels of ranging accuracy. A summary of this, with some more recent input from the NASA Crustal Dynamics Program appears in figure 1.

At the 10 cm/year level of accuracy, which is probably satisfied by many systems in the field, we should be able to make reasonable contributions to the studies of tides and polar motion. These studies are in fact underway with very promising results. Measurements accuracies of about 3 cm/year will be required to study plate tectonics and regional fault motion. Some operational lasers may be

performing at this level or are on the verge of doing so. The most stringent requirement is for the measurement of intra-plate deformation that will require accuracies of 1 cm/year.

The message that was evident from the NASA Crustal Dynamics Meeting at GSFC in early September was that some investigators want ultimate measurement accuracies of 1 cm/year with at least 3 sigma assurance.

If we examine the history of ranging accuracy of operational systems from 1965 to date (see figure 2) it appears that we are improving accuracy by a factor of three every five years. Projecting forward at this rate it will be at least 1990 before we can fully satisfy the needs of the scientific community.

The technology is now available to reach the required 1 cm accuracy. It is now probably a matter of experience to refine the techniques and put them into widespread operation. Basically the current trend is toward:

1. Subnanosecond pulse width lasers for higher accuracy and lower noise
2. High repetition-low output power for reliability and eye safety
3. Single photoelectron detection to take maximum advantage of the quantum statistical properties
4. Small optics for mobility
5. High resolution timing for higher accuracy
6. Software intensive systems for lower costs and greater flexibility

It is essential that we exploit and impliment these new techniques as rapidly as possible to accelerate the evaluation in satellite laser ranging field capability. We have developed a user community, but its interest and support will wane if we are not responsive to its needs.

2.0 UNIFORM STANDARD OF RANGING ACCURACY

2.1 Requirement

As workers in the field of satellite laser ranging (SLR), we have long avoided the issue of a uniform standard (definition) of accuracy. This is in part due to the complicated nature of the error sources and the variety of system configurations that now exist. At the moment, we have the whole spectrum of concern about accuracy: Some groups have taken their whole system apart piece-by-piece to examine the characteristics of each component; at the other extreme, some groups really do nothing.

We are now at the stage where laser data is being examined for decimeter and even centimeter effects. However, current modeling capability does not permit the analyst to detect and diagnose errors at this level. In fact, historically, evolving laser data quality has always been a primary driver for model development. As a result, the analyst must rely on us, the experts in the systems, to specify data quality and error model.

In addition to our responsibility to the analysts, we ourselves suffer from a lack of uniform means of comparing one system with another and even comparing different stages of development in an individual systems.

In view of our current reticence over the definition and measurement of accuracy, and the ambitious programs that lay ahead of us, it is essential that we adopt a uniform error model to characterize our laser systems.

This standard error model should:

1. Represent a "good" estimate of the known error sources
2. Specify relevant time period or periods
3. Define a means of measuring and specifying each error component
4. Specify a means of aggregating the error components
5. Be practicable

2.2 Suggested Model

Recognizing the diversity in the nature of the error sources and the range of applications in which the data will be used, we recommend a standard error model that:

1. Is restricted to the ranging machine only, leaving the atmospheric corrections and the satellite center-of-mass for separate consideration
2. Includes two estimates of error: epoch bias and range bias
3. Uses one sigma estimates of error components
4. Characterizes system performance over a period of a satellite pass (30-45 minutes)

Epoch bias is the uncertainity in our correction of station time to a uniform standard (USNO). This is determined through the quality of: portable clock checks, frequency and epoch broadcast readings, and the timing data analysis.

Range bias estimates should consist of several components including:

1. Wavefront distortion
2. Uncorrected system drift
3. Error in target distance survey including atmospheric effects
4. Uncorrected variation in system delay with signal strength
5. Uncorrected variation in system delay with P.M.T. saturation level.

2.3 Measurements

The wavefront distortion should be measured by mapping the laser beam in the far field with a retroreflector.

System drift should be quantified by aggregating experience of pre-pass calibration minus post-pass calibration differences or through some other form of direct measurement if appropriate.

The error in target distance is the estimated accuracy of the target survey.

The uncorreced variation in system delay with signal strength should be determined from extended target calibrations over the full dynamic operating range of the system.

The uncorrected variation in system delay with PMT saturation should be estimated from extended target calibration under anticipated extreme conditions.

2.4 Aggregation of Range Bias Components

For simplicity we have suggested that the range bias error sources be assumed independent and that an rss of the 1 sigma contributions be formed to provide a single range bias characterization parameter.

2.5 Special Cases

Some of the range bias error components will not be pertinent to particular ranging systems currently in operation or under development. Those groups operating systems at the single photoelectron level will probably not be concerned with issues of dynamic range; those that have internal pulse-by-pulse calibration may compensate completely for system drift. Systems that operate only at night may not present problems with PMT saturation.

2.6 Comments from the Workshop Participants

The need for a uniform standard of Ranging Accuracy was well recognized by the membership. Comments included:

1. Estimates of bias over longer periods of time such as a month and a year should also be included.

2. The rss is not the proper way to aggregate the error component as it tends to give biased results; a more rigourous formula should be used.

A committee was formed under the leadership of Dr. Peter Wilson to formulate a recommended error model for review of the membership and the scientific community.

3.0 Uniform Method of Data Aggregation

3.1 Requirement

The current trend in satellite laser ranging is toward higher pulse repetition rates and lower return energy. Systems with repetition rates of 5-10 pulses per second are now being implemented by some groups, and many are now using or planning to use single photoelectron detection in their ranging operation.

As a result of this trend, we are already faced with occasional passes containing as many as 2000-3000 data points, and we expect this to become far more common as time goes on. This data volume is far more than the data analysts would ordinarily choose to use. However, he would very much like the averaging potential that such a data yield could provide.

Several groups already are aggregating data in a normal point formulation or are planning to do so. Unfortunately to date there is no agreed standard for data aggregation. In order to avoid the proliferation of different techniques, the satellite laser ranging community including both data acquisition and analysis people should adopt a standard method for data aggregation.

As a minimum, the model must preserve the accuracy of the full data set, including all short period orbital effects. It must also be reasonably easy to impliment which means it can not rely on long arc orbital analysis techniques which some groups may not have available.

3.2 Standard Models

In an operational sense, data aggregation is intimately coupled with data screening. We eliminate bad data through some type of fitting process, perform an aggregation on the residuals, and then construct normal points.

Although there are many different techniques for screening data, most consist of the same basic processing steps in slightly different arrangements. The largest difference is in the initial step: Some groups use a long arc orbital fit to obtain "first" residuals that are then subjected to bias and/or polynominal fits. Others avoid the long arc fit by starting with the observed minus predicted residuals and then use gross-screening measures, bias fits, and local and/or single orbit polynomial fits. At a first glance, it appears that both techniques give similar results.

We recommend that the community adopt a Standard Data Aggregation Method that:

1. Relies on current data screening techniques currently available at each group to separate data from noise.

2. Aggregates data into time periods of fixed duration: one minute for Lageos and 0.5 minutes for lower orbiting satellites.

3. Determines normal points by:

   a. Aggregating residuals to the screening process into the appropriate time bias

   b. Calculating a normal point residual at a data point epoch closest to the center of the bin using a straight line fit to the data in the bin

   c. Reconstructing the normal point range value

4. Requires that the following data be furnished:

   a. Normal points

   b. Number of points in each bin

   c. RMS of each bin

   d. RMS of the pass (full rate)

Naturally, the full data set should be made available for verification of the technique and to those who require it for specialized analysis.

3.2 Comments from the Workshop Participants

The need for a uniform standard for Data Aggregation was recognized by the participants. Comments included:

1. The full data set should still be submitted to the Data Centers

2. It would be most advantageous if normal points could be made available through the Quick-Look process

3. We must be careful that the screening processes used do not inadvertantly alias the data toward a particular result

A committee was formed under the leadership of Dr. Michael R. Pearlman to formulate a recommended Method of Data Aggregation for the membership and the scientific community.

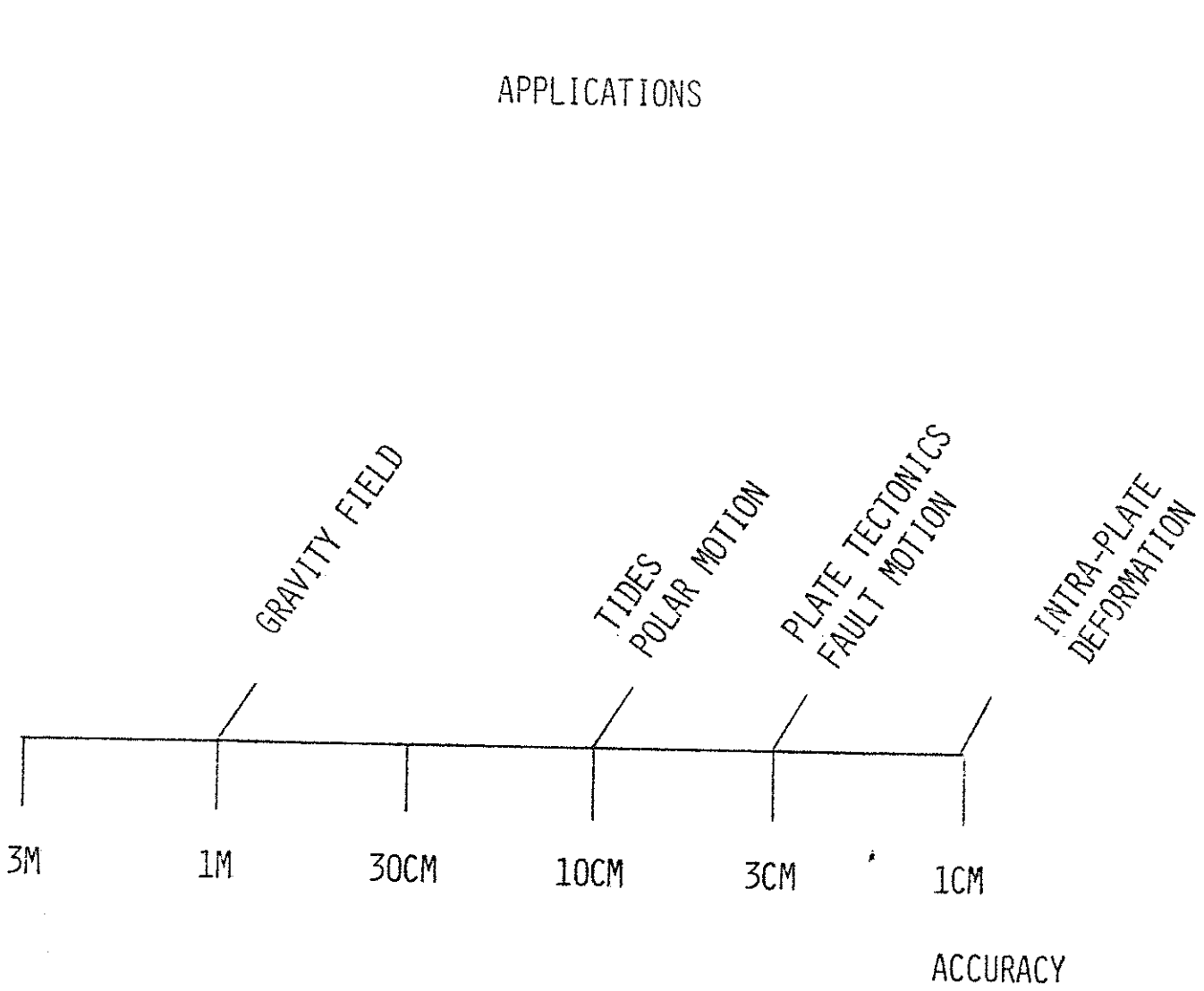
APPLICATIONS
GRAVITY FIELD
TIDES
POLAR MOTION
PLATE TECTONICS
FAULT MOTION
INTRA-PLATE
DEFORMATION
3M
1M
30CM
10CM
3CM
1CM
ACCURACY

Figure 1.

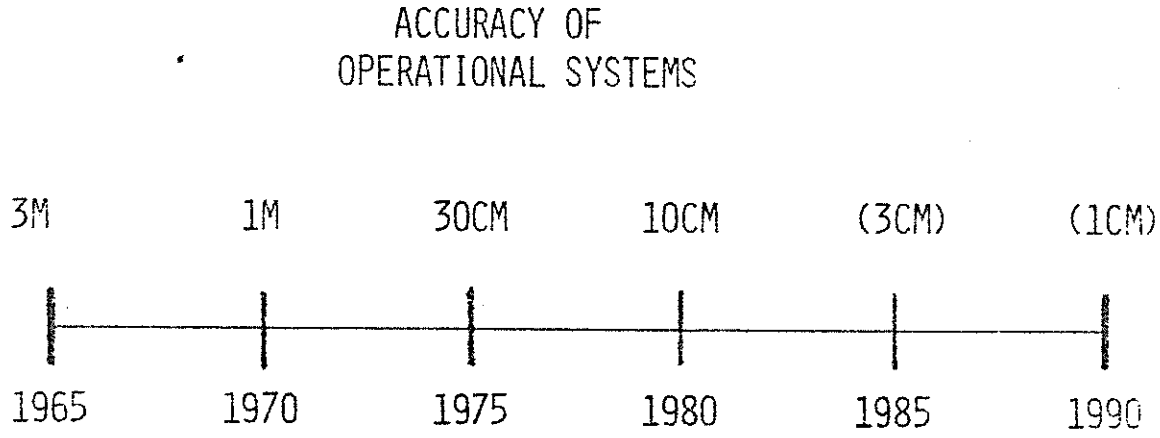
ACCURACY OF
OPERATIONAL SYSTEMS
3M
1M
30CM
10CM
(3CM)
(1CM)
1965
1970
1975
1980
1985
1990

Figure 2.

References

1978 Gaposchkin, E. M., Geophysical Uses of Laser Range Data and Related Questions. Presented at the Third International Workshop on Laser Ranging Instrumentation, Lagonissi, Greece, May.

Recommendation No. 1

Recognising: The importance of high quality laser range observations over the full 14 month period of the MERIT campaign to determine:

1. The potential contribution that satellite laser ranging may be able to make a future earth rotation service;
2. possible shorter period periodic variations in the earth rotation vector;
3. the possible existence or systematic differences between conventional inertial systems.

This workshop Recommends that operation of satellite laser rangers be configured from the present until the commencement of MERIT to ensure that systems are in the best state of readiness to commence the MERIT campaign and with the best capability to perform over the MERIT campaign with the highest possible accuracy.

Recommendation No. 2

The 4th International Workshop on Laser Ranging Instrumentation,

Considering the importance of an objective estimate of the accuracy of laser ranging instruments,

Realising that for a full and proper utilisation of ranging data such information is valuable

and Noting that commonly acceptable procedures and standards do not exist for the estimation of instrumental accuracy,

Requests the chairman of W.G. 2,33 to set up a small group of experts to prepare such procedures and standards.

Recommendation No. 3

The 4th International Workshop on Laser Ranging Instrumentation,

Considering that for several applications of satellite laser ranging there are advantages to aggregating data in the form of "normal" points and Emphasing that the original data should be preserved,

Requests the chairman of S.S.G. 2,33 to set up a group of experts to recommend standard procedures for the calculation of "normal" points which will preserve the information contained in the original data.

At the close of the meeting unanimous approval was given to the following resolution:

This Workshop, accustomed to the very high standards of performance of University of Texas personnel, acknowledges the excellent organization and running of the Workshop on our behalf. The opportunity to meet with our colleagues in congenial surroundings, in formal sessions and in formal social gatherings has enhanced the prospects of being in the desired state of readiness for the Crustal Dynamics Project and Project MERIT.

Our thanks are extended to the University of Texas at Austin, and the Director of the Mc Donald Observatory - Dr. Smith, for their support of the organizers - Drs. Eric Silverberg and Peter Shelus who we congratulate on maintaining the highest standards of excellence. Finally we extend our warmest thanks and appreciation to the Workshop organizer's staff. - Cynthia Straub and Pam Johnson, without whose hard work and dedication this workshop would have failed.

STATION REPORTS

STATION REPORT

STATION NAME:	Moblas 5
LOCATION:	Yarragadee, Western Australia
MAILING ADDRESS:	NASA Tracking Station P. O. Box 137 Dongara, 6525 Western Australia
TELEPHONE NO:	GSFC SCAMA TWX NO. GXEE
PERIOD OF OPERATION:	October, 1979 to present
DATA REPORTED TO:	GSFC

APERTURE:	30 inch	MOUNT TYPE:	AZ-EL
TRANSMITTED POWER:	250 MJ	REP. RATE:	1PPS
WAVELENGTH:	532 NM	PULSE WIDTH:	5 - 7 nsec

DETECTOR TYPE:	2233 Amperex
PRIMARY TIME STANDARD:	Caesium
TIME OF FLIGHT EQUIPMENT:	HP 5360
COMPUTER TYPE & CAPACITY:	Modular Computer II - 64K

MAJOR SUBSYSTEMS UNDER COMPUTER CONTROL:	Peripherals, Mount Servo Control Console, Data Measuring System		
CALIBRATION METHOD:	Pre-post ranging of fixed calibration target		
PRINCIPLE TARGETS:	Lageos	Starlette	BE-3
TRACKS IN 1980:	524	108	0
PRECISION ON TARGET:	15 cm	10	
ENVIRONMENTAL MONITORING:	Temperature, Air Pressure, Humidity		
GEODETIC MONITORING:			
READINESS TO TRACK IN '82:			
READINESS TO TRACK IN MERIT '83-'84:			
COMMENTS:			

STATION REPORT

STATION NAME:	7943 - SAO
LOCATION:	Orroral Valley, Australia
MAILING ADDRESS:	Station Director, NASA/STDN Orroral Valley Tracking Station P. O. Box 40, Kingston ACT 2604 Australia
TELEPHONE NO:	TWX No. via NASCOM
PERIOD OF OPERATION:	full time, 2 shifts
DATA REPORTED TO:	SAO

APERTURE:	20"cassegrain	MOUNT TYPE:	Alt/Azi, Stepping
TRANSMITTED POWER:	350 MW	REP. RATE:	8ppm
WAVELENGTH:	694.3 nm	PULSE WIDTH:	6 nsec

DETECTOR TYPE:	RCA 7265
PRIMARY TIME STANDARD:	Caesium UTC (USNO)
TIME OF FLIGHT EQUIPMENT:	0.1 nsec counter, 20 channel digitizer, A/D converters
COMPUTER TYPE & CAPACITY:	D.G. Nova 1200, 32K

MAJOR SUBSYSTEMS UNDER COMPUTER CONTROL:	Mount, data system, paper tape reader and punch, linc tape			
CALIBRATION METHOD:	pre/post pass calibration, weekly start electronics, monthly system calibration			
PRINCIPLE TARGETS:	Lageos	Starlette	Geos 3	Geos 1
TRACKS IN 1980:	378	316	233	254
PRECISION ON TARGET:	10cm	10cm	10cm	10cm
ENVIRONMENTAL MONITORING:	Temperature, Humidity, Pressure			
GEODETIC MONITORING:	Periodic slant			
READINESS TO TRACK IN '82:	201 nights/ 266 days			
READINESS TO TRACK IN MERIT '83-'84:	201 nights/ 201 days			

COMMENTS:

STATION REPORT

STATION NAME:		National Mapping LLR, Orroral Valley	
LOCATION:		Orroral Valley, ACT, Australia	
MAILING ADDRESS:		Division of National Mapping P. O. Box 31 Belconnen, ACT, Australia	
TELEPHONE NO:		062-357215	TWX No. AA 62230
PERIOD OF OPERATION:		continuous	
DATA REPORTED TO:		University of Texas	
APERTURE:	1.5 M	MOUNT TYPE:	Equatorial
TRANSMITTED POWER:	1 J.	REP. RATE:	12 ppm
WAVELENGTH:	694.3 nm	PULSE WIDTH:	6 nsec
DETECTOR TYPE:		RCA 31034	
PRIMARY TIME STANDARD:		Caesium	
TIME OF FLIGHT EQUIPMENT:		HP5370A	
COMPUTER TYPE & CAPACITY:		HP 21MX, 176K	

MAJOR SUBSYSTEMS UNDER COMPUTER CONTROL:	Mount, Timing System, Data Storage
CALIBRATION METHOD:	pre/post pass calibration
PRINCIPLE TARGETS:	Apollo 15
TRACKS IN 1980:	approx. 100
PRECISION ON TARGET:	30 cm
ENVIRONMENTAL MONITORING:	temperature, air pressure, humidity
GEODETIC MONITORING:	1st order horizontal and vertical control net to AGD and AHD respectively
READINESS TO TRACK IN '82:	refurbishment phase
READINESS TO TRACK IN MERIT '83-'84:	300 days, 300 nights

COMMENTS: _____

STATION REPORT

STATION NAME:	Observatory Lustbuhel
LOCATION:	Graz - Austria
MAILING ADDRESS:	Observatory Lustbuhel Lustbuhelstrasse 46 A - 8042 GRAZ AUSTRIA
TELEPHONE NO:	(0)316/41332/21 TWX No. 31078 obslgz a
PERIOD OF OPERATION:	
DATA REPORTED TO:	

APERTURE:	50 cm	MOUNT TYPE:	Azimuth/Elevation
TRANSMITTED POWER:	100 mJ (a) 2.5 J, 4 J (b)	REP. RATE:	up to 10 Hz (a) up to 0.25 Hz (b)
WAVELENGTH:	530 nm (a) 694.3 nm (b)	PULSE WIDTH:	100 pps (a) 3 ns, 6 ns (b)

DETECTOR TYPE:

PRIMARY TIME STANDARD:	B.I.H. Laboratory TUG (Graz), with: 2 Caesium Beam Frequency Standards 4 LORAN - C Receivers; 3 VLF - Receivers
TIME OF FLIGHT EQUIPMENT:	HP 5370A Time Interval Counter
COMPUTER TYPE & CAPACITY:	HP 1000, Model 40, 128kByte

MAJOR SUBSYSTEMS UNDER
COMPUTER CONTROL:

CALIBRATION METHOD:

PRINCIPLE TARGETS:

TRACKS IN 1980:

PRECISION ON TARGET:

ENVIRONMENTAL MONITORING:

GEODETIC MONITORING:

READINESS TO TRACK IN '82:

READINESS TO TRACK IN
MERIT '83-'84:

COMMENTS:

Hardware integration and software development are going on during 1981, test phase is expected to start beginning of 1982.

STATION REPORT

STATION NAME:	7929 - SAO		
LOCATION:	Natal, Brazil		
MAILING ADDRESS:	Smithsonian Astrophysical Observatory US Consulate Recife APO Miami, FL 34030		
TELEPHONE NO:	TWX No. RTTY - via SAO		
PERIOD OF OPERATION:	full time, 3 shifts		
DATA REPORTED TO:	SAO		
APERTURE:	20"cassegrain	MOUNT TYPE:	Alt/Azi, stepping
TRANSMITTED POWER:	350 MW	REP. RATE:	8ppm
WAVELENGTH:	694.3 nm	PULSE WIDTH:	6 nsec
DETECTOR TYPE:	RCA 7265		
PRIMARY TIME STANDARD:	Caesium UTC (USNO)		
TIME OF FLIGHT EQUIPMENT:	0.1 nsec counter, 20 channel digitizer, A/D converters		
COMPUTER TYPE & CAPACITY:	Nova 1200, 32K		

MAJOR SUBSYSTEMS UNDER COMPUTER CONTROL:	mount, data system, paper tape reader and punch Linc tape				
CALIBRATION METHOD:	pre/post pass calibration, daily counter				
PRINCIPLE TARGETS:	Lageos	Starlette	Geos 3	Geos 1	BEC
TRACKS IN 1980:	65	167	262	241	113
PRECISION ON TARGET:	10cm	10cm	10cm	10cm	10cm
ENVIRONMENTAL MONITORING:	temperature, humidity, air pressure				
GEODETIC MONITORING:	periodic slant range				
READINESS TO TRACK IN '82:	0				
READINESS TO TRACK IN MERIT '83-'84:	0				

COMMENTS:

STATION REPORT

STATION NAME:	Shanghai Observatory
LOCATION:	Shanghai, China
MAILING ADDRESS:	Shanghai Observatory Shanghai, China
TELEPHONE NO:	
PERIOD OF OPERATION:	Sept., 1980 to January, 1981
DATA REPORTED TO:	SAO, USA

APERTURE:	300 mm	MOUNT TYPE:	A--h
TRANSMITTED POWER:	20 MW	REP. RATE:	1 Hz
WAVELENGTH:	532 nm	PULSE WIDTH:	5nsec

DETECTOR TYPE:	PMT GDB 49
PRIMARY TIME STANDARD:	Rubidium
TIME OF FLIGHT EQUIPMENT:	Computing Counter with 0.1 ns resolution
COMPUTER TYPE & CAPACITY:	none

MAJOR SUBSYSTEMS UNDER COMPUTER CONTROL:	n/a	
CALIBRATION METHOD:	range to the fixed target on ground	
PRINCIPLE TARGETS:	Geos - 3	Geos - 1
TRACKS IN 1980:	60	30
PRECISION ON TARGET:	60cm	30cm
ENVIRONMENTAL MONITORING:	Air pressure, temperature	
GEODETIC MONITORING:		
READINESS TO TRACK IN '82:	300 nights	
READINESS TO TRACK IN MERIT '83-'84:	300 nights/300 days	

COMMENTS:

A new laser system made in China will be installed at the Shanghai Observatory by the Fall of 1982. The main parameters are:

Telescope: 600mm aperture with Coude optics,

Nd: YAG Laser, 0.25 joules, 5ns, 1Hz

Controlled by a microprocessor (Z--80)

Can track Lageos, maybe by daylight

STATION REPORT

STATION NAME:	Yunnan Observatory, Academia Sinica
LOCATION:	$\lambda = 102^{\circ}47'$ $\phi = 25^{\circ}01'$
MAILING ADDRESS:	Yunnan Observatory P. O. Box 110 Kunming, Yunnan Province China
TELEPHONE NO:	Kunming 2034-75
PERIOD OF OPERATION:	1979 to present
DATA REPORTED TO:	Shanghai Observatory

APERTURE:	430 mm	MOUNT TYPE:	4th axis
TRANSMITTED POWER:	80 MW	REP. RATE:	30/min.
WAVELENGTH:	694.3 nm	PULSE WIDTH:	20 nsec

DETECTOR TYPE:

PRIMARY TIME STANDARD:

TIME OF FLIGHT EQUIPMENT:

COMPUTER TYPE & CAPACITY:

MAJOR SUBSYSTEMS UNDER COMPUTER CONTROL:			
CALIBRATION METHOD:			
PRINCIPLE TARGETS:	65321	65891	75271
TRACKS IN 1980:			
PRECISION ON TARGET:	100 cm	100 cm	100 cm
ENVIRONMENTAL MONITORING:			
GEODETIC MONITORING:			
READINESS TO TRACK IN '82:	200 nights (not including weather)		
READINESS TO TRACK IN MERIT '83-'84:			
COMMENTS:			

STATION REPORT

STATION NAME:	Santiago de Cuba
LOCATION:	Santiago de Cuba
MAILING ADDRESS:	Institute of Geophysics and Astronomy ACC.212 ST. 2906 Havana, Cuba
TELEPHONE NO:	TWX No. 511240 geoastro cu
PERIOD OF OPERATION:	1979
DATA REPORTED TO:	Interkosmos

APERTURE:	32 cm	MOUNT TYPE:	4 axes
TRANSMITTED POWER:	50 MW	REP. RATE:	15 ppm
WAVELENGTH:	694 nm	PULSE WIDTH:	30 ns

DETECTOR TYPE:	RCA 8852
PRIMARY TIME STANDARD:	VLF
TIME OF FLIGHT EQUIPMENT:	
COMPUTER TYPE & CAPACITY:	

MAJOR SUBSYSTEMS UNDER COMPUTER CONTROL:			
CALIBRATION METHOD:	Fixed target		
PRINCIPLE TARGETS:	GEA	GEC	BEC
TRACKS IN 1980:			
PRECISION ON TARGET:	100cm	100cm	100cm
ENVIRONMENTAL MONITORING:			
GEODETIC MONITORING:			
READINESS TO TRACK IN '82:	150 nights		
READINESS TO TRACK IN MERIT '83-'84:	300 nights		

COMMENTS:

STATION REPORT

STATION NAME:	Intercosmos - 1867, Quito		
LOCATION:	ℓ = 0°12'25.5" λ = 281°31'47" h = 2860 m		
MAILING ADDRESS:	Ecuador, R. Oreliana Escuela Politecnica Nacional Apartado 2759 Quito		
TELEPHONE NO:			
PERIOD OF OPERATION:	day time		
DATA REPORTED TO:	Data Center of the A. S.		
APERTURE:	340 mm	MOUNT TYPE:	4-axis
TRANSMITTED POWER:	1 J.	REP. RATE:	0.25 per sec.
WAVELENGTH:	694.3 nm	PULSE WIDTH:	35 nsec
DETECTOR TYPE:	FEU-84		
PRIMARY TIME STANDARD:	Cuarz System AFU-75		
TIME OF FLIGHT EQUIPMENT:	CV-receiver		
COMPUTER TYPE & CAPACITY:			

MAJOR SUBSYSTEMS UNDER COMPUTER CONTROL:	printing device MT-1016	
CALIBRATION METHOD:	stand.target at dist. of 2181.34 m	
PRINCIPLE TARGETS:	Geos A	Geos C
TRACKS IN 1980:	2	9
PRECISION ON TARGET:	135 cm	170 cm
ENVIRONMENTAL MONITORING:	visual control	
GEODETIC MONITORING:		
READINESS TO TRACK IN '82:		
READINESS TO TRACK IN MERIT '83-'84:		

COMMENTS:

STATION REPORT

STATION NAME:	Helwan I		
LOCATION:	Helwan, Egypt		
MAILING ADDRESS:	Helwan Institute of Astronomy and Geophysics Helwan, Egypt		
TELEPHONE NO:	TWX No. 93 070		
PERIOD OF OPERATION:	1974 to present		
DATA REPORTED TO:	Interkosmos, SAO		
APERTURE:	32 cm	MOUNT TYPE:	4 axis
TRANSMITTED POWER:	50 MW	REP. RATE:	15 ppm
WAVELENGTH:	694 nm	PULSE WIDTH:	30 nsec
DETECTOR TYPE:	RCA 8852		
PRIMARY TIME STANDARD:	Loran C, HP Cs clock		
TIME OF FLIGHT EQUIPMENT:			
COMPUTER TYPE & CAPACITY:	HP 9830, 16k		

MAJOR SUBSYSTEMS UNDER COMPUTER CONTROL:	time gate, range counter, epoch counter		
CALIBRATION METHOD:	fixed target		
PRINCIPLE TARGETS:	GEA	GEC	BEC
TRACKS IN 1980:			
PRECISION ON TARGET:	100cm	100cm	100cm
ENVIRONMENTAL MONITORING:			
GEODETIC MONITORING:			
READINESS TO TRACK IN '82:	100 nights		
READINESS TO TRACK IN MERIT '83-'84:	100 nights		

COMMENTS:

STATION REPORT

STATION NAME:	Helwan II
LOCATION:	Helwan, Egypt
MAILING ADDRESS:	Helwan Institute of Astronomy and Geophysics Helwan, Egypt
TELEPHONE NO:	TWX No. 93-070
PERIOD OF OPERATION:	1981 to Present
DATA REPORTED TO:	Interkosmos, SAO

APERTURE:	40 cm	MOUNT TYPE:	AZ/ALT
TRANSMITTED POWER:	200 MW	REP. RATE:	15ppm
WAVELENGTH:	694 nm	PULSE WIDTH:	4 nsec

DETECTOR TYPE:	RCA 8852
PRIMARY TIME STANDARD:	Loran c, H-P Cs clock
TIME OF FLIGHT EQUIPMENT:	
COMPUTER TYPE & CAPACITY:	HP 2100S, 64 KByte

MAJOR SUBSYSTEMS UNDER COMPUTER CONTROL:	range counter, epoch counter, time gate, laser mount			
INPUT/OUTPUT FORMATS:	SAO coded			
CALIBRATION METHOD:	fixed target			
PRINCIPLE TARGETS:	gea	GEC	BEC	Starlette
TRACKS IN 1980:				
PRECISION ON TARGET:	20cm	20cm	20cm	20cm
ENVIRONMENTAL MONITORING:				
GEODETIC MONITORING:				
READINESS TO TRACK IN '82:	150 nights/50 days			
READINESS TO TRACK IN MERIT '83-'84:	200 nights/100 days			

COMMENTS:

STATION REPORT

STATION NAME:	Wettzell
LOCATION:	Germany (F.R)
MAILING ADDRESS:	Institut F. Angew. Geodaesie Sat. Beob. Station Wettzell D-8493 Koetzting Germany (F.R.)
TELEPHONE NO:	09941-8643 TWX No. 069937 WESAT-D
PERIOD OF OPERATION:	1972 to present (3 weeks per month)
DATA REPORTED TO:	SAO, CNES

APERTURE:	60 cm	MOUNT TYPE:	Alt/Azim.
TRANSMITTED POWER:	0.25 J	REP. RATE:	4 pps
WAVELENGTH:	532 nm	PULSE WIDTH:	0.2 nsec

DETECTOR TYPE:	Varian Static Crossed Field 154 (153)
PRIMARY TIME STANDARD:	3 Caesium clocks, sev. Rub.-Cls.
TIME OF FLIGHT EQUIPMENT:	Hewlitt-Packard Computing Counter 5360A
COMPUTER TYPE & CAPACITY:	DEC 11/45, 82K

MAJOR SUBSYSTEMS UNDER COMPUTER CONTROL:	look.angles, mount-control, laser contr., detector, data handling		
CALIBRATION METHOD:	terrestrial target measurement		
PRINCIPLE TARGETS:	Lageos	Starlette	Geos 3
TRACKS IN 1980:	21	39	20
PRECISION ON TARGET:	4-50cm (depending on state of laser eqpt.)	4-50cm	4-50cm
ENVIRONMENTAL MONITORING:	temperature, pressure, humidity		
GEODETIC MONITORING:	geodetic control net (angle, distance, height, gravity) in preparation, earth tides (observations in preparation)		
READINESS TO TRACK IN '82:			
READINESS TO TRACK IN MERIT '83-'84:			
COMMENTS:			

STATION REPORT

STATION NAME:	Mobile Laser Ranging System
LOCATION:	under development
MAILING ADDRESS:	Institut für Angewandte Geodäsie Richard Strauss Allee 11 D-6000 Frankfurt 70
TELEPHONE NO:	0611-638091 Telex 04 13 592 ifag d
PERIOD OF OPERATION:	from mid-year 1983
DATA REPORTED TO:	

APERTURE:	40 cm	MOUNT TYPE:	Az-El, coude
TRANSMITTED POWER:	50 MW	REP. RATE:	10 Hz
WAVELENGTH:	539 nm	PULSE WIDTH:	0.2 nsec

DETECTOR TYPE:	RCA 8850 (preliminary)
PRIMARY TIME STANDARD:	to be decided
TIME OF FLIGHT EQUIPMENT:	HP 5370 A + constant fraction discriminators
COMPUTER TYPE & CAPACITY:	multi-microprocessor system

MAJOR SUBSYSTEMS UNDER COMPUTER CONTROL:	mount, detection system		
CALIBRATION METHOD:	pre/postcalibration + simultaneous internal calibration		
PRINCIPLE TARGETS:	Lageos	Starlette	Ground
TRACKS IN 1980:			
PRECISION ON TARGET:	2 cm	2 cm	1cm
ENVIRONMENTAL MONITORING:	pressure, temperature, relative humidity		
GEODETIC MONITORING:	geodetic locator		
READINESS TO TRACK IN '82:			
READINESS TO TRACK IN MERIT '83-'84:			

COMMENTS:

STATION REPORT

STATION NAME:	Metsahovi (7805)		
LOCATION:	Finland		
MAILING ADDRESS:	Finnish Geodetic Institute Ilmalankatu 1 A SF-00240 Helsinki 24, Finland		
TELEPHONE NO:	410433		
PERIOD OF OPERATION:	March to December		
DATA REPORTED TO:	SAO, University of Texas, NSSDC, CNES, IfAG, Kootwijk		
APERTURE:	630mm	MOUNT TYPE:	Equatorial
TRANSMITTED POWER:	50 MW	REP. RATE:	1/15 Hz
WAVELENGTH:	694.3 nm	PULSE WIDTH:	20 nsec
DETECTOR TYPE:	RCA C 31034, 8852		
PRIMARY TIME STANDARD:	Quartz, phase-locked to LORAN C		
TIME OF FLIGHT EQUIPMENT:	Nanofast 536 B counter+ M/2 half-max plug-in		
COMPUTER TYPE & CAPACITY:	32k Words		

MAJOR SUBSYSTEMS UNDER COMPUTER CONTROL:	tracking, data registration			
CALIBRATION METHOD:	flat target, 333 m distance			
PRINCIPLE TARGETS:	Lageos	Geos 1	Geos 3	Starlette
TRACKS IN 1980:	41	30	25	19
PRECISION ON TARGET:	100cm	50cm	50cm	50cm
ENVIRONMENTAL MONITORING:	air pressure, temperature, humidity			
GEODETIC MONITORING:				
READINESS TO TRACK IN '82:	240 nights			
READINESS TO TRACK IN MERIT '83-'84:	300 nights			

COMMENTS:

STATION REPORT

STATION NAME:	Laser-Lune, C.E.R.G.A.		
LOCATION:	Observatoire de Calern		
MAILING ADDRESS:	06460 St. Vallier de Thiey		
TELEPHONE NO:	42-62-70 (93)	TWX No.	461402
PERIOD OF OPERATION:	all year		
DATA REPORTED TO:	first experiment in June and July, 1981		
APERTURE:	1.5m	MOUNT TYPE:	Azimuthal
TRANSMITTED POWER:	1.5 J	REP. RATE:	6 S
WAVELENGTH:	694.3 nm	PULSE WIDTH:	3 nsec
DETECTOR TYPE:	RCA 31034 A		
PRIMARY TIME STANDARD:	Caesium		
TIME OF FLIGHT EQUIPMENT:			
COMPUTER TYPE & CAPACITY:	Eclipse - Data General		

MAJOR SUBSYSTEMS UNDER COMPUTER CONTROL:	32 K + Nova - Data General		
CALIBRATION METHOD:	internal + external targets at several kms		
PRINCIPLE TARGETS:	Starlette	Geos A	Geos C
TRACKS IN 1980:	2	1	1
PRECISION ON TARGET:	25 cm	25cm	25cm

ENVIRONMENTAL MONITORING:

GEODETIC MONITORING:

READINESS TO TRACK IN '82: 120 nights, 0 days

READINESS TO TRACK IN MERIT '83-'84: 120 nights

COMMENTS:

This station can track also Lageos and geostationary satellite; it will participate to LASSO experiment in 1982 (intercontinental synchronization at 1ns through a geostationary satellite).

STATION REPORT

STATION NAME:	Laser Satellite Grasse (7835)		
LOCATION:	GRASSE		
MAILING ADDRESS:	Station Laser Satellite Observatoire de Calern 06460 St. Vallier de Thiey		
TELEPHONE NO:	(93) 42-62-70 TWX No. 461402		
PERIOD OF OPERATION:			
DATA REPORTED TO:	CNES - Toulouse		
APERTURE:	1.00 m	MOUNT TYPE:	Azimuthal
TRANSMITTED POWER:	3 J.	REP. RATE:	5 S
WAVELENGTH:	694 nm	PULSE WIDTH:	3 nsec
DETECTOR TYPE:	Centroid detection		
PRIMARY TIME STANDARD:	Caesium		
TIME OF FLIGHT EQUIPMENT:			
COMPUTER TYPE & CAPACITY:	T/1600 Telemecanique 48K octets		

MAJOR SUBSYSTEMS UNDER COMPUTER CONTROL:			
INPUT/OUTPUT FORMATS:	SEASAT format		
CALIBRATION METHOD:	external targets at several kms. simple and return way		
PRINCIPLE TARGETS:	7501001	7502701	76303901
TRACKS IN 1980:	111	36	78
PRECISION ON TARGET:	20cm	50 cm	20cm
ENVIRONMENTAL MONITORING:			
GEODETIC MONITORING:			
READINESS TO TRACK IN '82:	100 nights/50 days		
READINESS TO TRACK IN MERIT '83-'84:	20 nights/100 days		

COMMENTS:

This station can be moved (but not very quickly); its accuracy will be improved in the next years at level of a few centimeters.

This station can track geostationary satellite and will participate in LASSO experiment in 1982 (intercontinental synchronization at 1ns through a geostationary satellite).

STATION REPORT

STATION NAME:	Potsdam, Helmertturm; No. 1181
LOCATION:	X=3800596 Y=881989 Z=5028865
MAILING ADDRESS:	Zentralinst.Physik d. Erde Telegrafenberg A 17 DDR-1500 Potsdam G.D.R.
TELEPHONE NO:	4551 TWX No. 15305
PERIOD OF OPERATION:	1974 to present
DATA REPORTED TO:	Astrosoviet, CNES

APERTURE:	40 cm	MOUNT TYPE:	4-ax., SBG
TRANSMITTED POWER:	0.5 to 1 J	REP. RATE:	10/min.
WAVELENGTH:	694.3 nm	PULSE WIDTH:	20 nsec

DETECTOR TYPE:	RCA C 34034A
PRIMARY TIME STANDARD:	Cs-Clock HP 5061 A
TIME OF FLIGHT EQUIPMENT:	HP 5370 A
COMPUTER TYPE & CAPACITY:	HP 9825S, 23 K Byte

MAJOR SUBSYSTEMS UNDER COMPUTER CONTROL:	Mount drive, laser, gate, counter			
CALIBRATION METHOD:	Terrestrial Targets 500 m and 2000 m distance			
PRINCIPLE TARGETS:	Geos A	Geos C	Starlette	Lageos
TRACKS IN 1980:	89	72	47	24
PRECISION ON TARGET:	80 cm	60 cm	60 cm	150 cm
ENVIRONMENTAL MONITORING:	pressure, temperature			
GEODETIC MONITORING:				
READINESS TO TRACK IN '82:	180 nights/180 days			
READINESS TO TRACK IN MERIT '83-'84:	200 nights/200 days			

COMMENTS:

Availability of long term classical astronomical, seismic and gravimetric data from the same observatory.

STATION REPORT

STATION NAME:	DIONYSOS
LOCATION:	Athens, Greece
MAILING ADDRESS:	9 K Zografou Athens 624 GREECE
TELEPHONE NO:	(01) 8131961 TELEX: 215032
PERIOD OF OPERATION:	1969 to Present
DATA REPORTED TO:	EROS and SAO

APERTURE:	40 CM	MOUNT TYPE:	Coude
TRANSMITTED POWER:	4.5 Joule	REP. RATE:	8 PPM
WAVELENGTH:	694.3 NM	PULSE WIDTH:	25 nsec

DETECTOR TYPE:	PMT RCA 7265
PRIMARY TIME STANDARD:	HP Cesium Standard 5061 A
TIME OF FLIGHT EQUIPMENT:	HP Counter 5360 A
COMPUTER TYPE & CAPACITY:	CDC Cyber 171

MAJOR SUBSYSTEMS UNDER COMPUTER CONTROL:	Local Terminal			
CALIBRATION METHOD:	Paper Tape and/or Cassette			
PRINCIPLE TARGETS:	GEOS 1	GEOS 3	LAGEOS	STARLETTE
TRACKS IN 1980:	30	23	22	50
PRECISION ON TARGET:	60 CM	60 CM	60 CM	60 CM
ENVIRONMENTAL MONITORING:	Temperature (±0.1C), Pressure (±1 MBAR), Humidity (5%)			
GEODETIC MONITORING:	Earth Tides and Local Deformations			
READINESS TO TRACK IN '82:	Refurbishment Phase			
READINESS TO TRACK IN MERIT '83-'84:	300 days, 300 nights			

COMMENTS:

A new green laser of 100 mJ, 200 psec at 10 Hz is expected to be delivered in March and go into operation in June.

STATION REPORT

STATION NAME:	Satellite Geodetic Obs.
LOCATION:	Penc, Hungary
MAILING ADDRESS:	H-1373 Budapest, Pf.546 Hungary
TELEPHONE NO:	27-10980 TWX No. 282241
PERIOD OF OPERATION:	10-04-80 to 20-10-80
DATA REPORTED TO:	

APERTURE:	43 cm	MOUNT TYPE:	4 axes
TRANSMITTED POWER:	0.5J	REP. RATE:	0.5 Hz
WAVELENGTH:	694 nm	PULSE WIDTH:	20 nsec

DETECTOR TYPE:	PMT, FEU-84
PRIMARY TIME STANDARD:	Rubidium Atomic
TIME OF FLIGHT EQUIPMENT:	Modified EMG 1646 , 100MHz counter
COMPUTER TYPE & CAPACITY:	HP 9830

MAJOR SUBSYSTEMS UNDER COMPUTER CONTROL:		
CALIBRATION METHOD:	pre/post target measurements	
PRINCIPLE TARGETS:	Geos 3	Geos 1
TRACKS IN 1980:	33	18
PRECISION ON TARGET:	100cm	100cm
ENVIRONMENTAL MONITORING:		
GEODETIC MONITORING:		
READINESS TO TRACK IN '82:	100 nights	
READINESS TO TRACK IN MERIT '83-'84:	150 nights	

COMMENTS:

Photographic and laser measurements are possible from the same SBG telescope mount.

STATION REPORT

STATION NAME:		Kavalur	
LOCATION:		India	
MAILING ADDRESS:		STARS Project 6th Floor, Shastri Bhavan, Haddows Road, Madras 600 006 INDIA	
TELEPHONE NO:		811046	Telex No. 041-394 & 7353
PERIOD OF OPERATION:		January through May; September through October and the month of December	
DATA REPORTED TO:		AS-USSR (Moscow) Co-ordinator, Interkosmos Laser Radar working group (Prague) and ISRO	
APERTURE:	32 cm	MOUNT TYPE:	4 axis
TRANSMITTED POWER:	1 J.	REP. RATE:	1 pps
WAVELENGTH:	694.3 nm	PULSE WIDTH:	20 nsec
DETECTOR TYPE:		RCA 8852 and USSR equivalent (RCA C31034A)	
PRIMARY TIME STANDARD:		Caesium Beam Frequency Standard HP 5061A (with option 004)	
TIME OF FLIGHT EQUIPMENT:		Polish FL 103B + BT2 and Hewlett Packard 5335A with options 010 and 030	
COMPUTER TYPE & CAPACITY:		IBM 370/155	

MAJOR SUBSYSTEMS UNDER COMPUTER CONTROL:	None	
CALIBRATION METHOD:	Fixed target board method	
PRINCIPLE TARGETS:	(1)	(2)
TRACKS IN 1980:	1500	1500
	at the rate of 10 shots per calibration	
PRECISION ON TARGET:	15 cm	15 cm
ENVIRONMENTAL MONITORING:	p mm Hg	T°per C H%
GEODETIC MONITORING:	yes	
READINESS TO TRACK IN '82:	150 nights	
READINESS TO TRACK IN MERIT '83-'84:	150 nights	

COMMENTS:

The station is established in the campus of Indian Institute of Astrophysics, Kavalur (12°34'N, 78°51'E, 800m MSL) as a scientific collaboration between Indian Space Research Organization (ISRO) and the Astronomical Council of the USSR (AC-AS USSR). The station is equipped with A F U-75 tracking camera, laser radar and precise timing equipment.

Highly accurate time service exist at the station. The current epoch accuracy is 10 μ seconds (UTC) with respect to BIH (Paris).

STATION REPORT

STATION NAME:	Dodaira Station
LOCATION:	Long. 139°11' 43".159E Lat. 36°00' 08".606N H. 855.89 m
MAILING ADDRESS:	Dodaira Station, Tokyo Astronomical Observatory Ohno, Tokigawa-Mura, Hiki-Gun, Saitama-Ken 355-05 JAPAN
Main office:	Univ.of Tokyo, Mitaka, Tokyo 181, JAPAN
TELEPHONE NO:	Dodaira (0) 493-67-0224 TWX 02933106 Mitaka (0) 422-32-5111 TWX 02822307 (0) is necessary only in Japan
PERIOD OF OPERATION:	All Year
DATA REPORTED TO:	Smithsonian Astrophysical Observatory

APERTURE:	RX=50cm TX=10cm	MOUNT TYPE:	XY mount
TRANSMITTED POWER:	0.3J	REP. RATE:	0.1 ppm
WAVELENGTH:	694.3 nm	PULSE WIDTH:	15 ns (without slicer) 4 ns (with slicer)

DETECTOR TYPE:	RCA 7265(will be replaced soon by HTV R-1333, similar to RCA-8852)
PRIMARY TIME STANDARD:	Rubidium Frequency Standard which is linked to caesium frequency standards at Mitaka through VHF radio
TIME OF FLIGHT EQUIPMENT:	
COMPUTER TYPE & CAPACITY:	HP-2100 with 64 K

MAJOR SUBSYSTEMS UNDER COMPUTER CONTROL:	telescope driving, ranging system control and data acquisition, disc drive (5MByte) CRT terminal, line printer, TEX tape reader
CALIBRATION METHOD:	Electrical: HP1900 series pulse generator Optical: ground based standard target
PRINCIPLE TARGETS:	GEOS A GEOS C BEACON C STARLETTE
TRACKS IN 1980:	approx. 40 successful passes for above four satellites
PRECISION ON TARGET:	approx. 50 cm for above four targets
ENVIRONMENTAL MONITORING:	temperature, humidity, atmospheric pressure, wind, etc.
GEODETIC MONITORING:	one of the 1st order triangulation points at Mt. Dodaira
READINESS TO TRACK IN '82:	100 nights/20 days (including weather
READINESS TO TRACK IN MERIT '83-'84:	120 nights/50 days (including weather)

COMMENTS:

Our 50 cm receiving telescope was modified to a standard Cassgrain type from off-axis Herschel type in 1979. The telescope is to be used for lunar laser transmitting. The lunar laser receiving is done by a 3.8 meters' metallic reflector on an elevation-azimuth mount. The lunar system is now under adjustments.

STATION REPORT

STATION NAME:	Simosato Hydrographic Observatory
LOCATION:	Simosato, Wakayama Pref.
MAILING ADDRESS:	Simosato, Nachi-Katsu-ura-cho Higasi-Muro-gun, Wakayama 649-51 JAPAN
TELEPHONE NO:	07355-8-0084 TWX No. to be installed
PERIOD OF OPERATION:	December, 1981
DATA REPORTED TO:	

APERTURE:	60 cm	MOUNT TYPE:	Alt-Az
TRANSMITTED POWER:	250 mJ	REP. RATE:	4 pps
WAVELENGTH:	532 nm	PULSE WIDTH:	0.2, 0.4 nsec

DETECTOR TYPE:	Photo-multiplier tube, leading-edge detection
PRIMARY TIME STANDARD:	Rubidium frequency standard
TIME OF FLIGHT EQUIPMENT:	high resolution electronic counter with 20 ps resolution
COMPUTER TYPE & CAPACITY:	PDP 11/60 with 64 kw memory

MAJOR SUBSYSTEMS UNDER COMPUTER CONTROL:	entire system under computer control		
CALIBRATION METHOD:	one ground target for ranging and three ground targets for levelling calibrations		
PRINCIPLE TARGETS:	Lageos	Geos	Starlette
TRACKS IN 1980:			
PRECISION ON TARGET:	10cm	20cm	10cm
ENVIRONMENTAL MONITORING:	temperature, humidity, air pressure		
GEODETIC MONITORING:			
READINESS TO TRACK IN '82:	300 nights		
READINESS TO TRACK IN MERIT '83-'84:	300 nights		

COMMENTS:

This station is scheduled to be in operation on December 1, 1981.
The laser ranging system is almost the same as the Wettzel's.

STATION REPORT

STATION NAME:	Kootwijk Observatory
LOCATION:	Kootwijk (The Netherlands)
MAILING ADDRESS:	P. O. Box 581 7300 AN Apeldoorn The Netherlands
TELEPHONE NO:	5769-341 TWX No. 36442
PERIOD OF OPERATION:	1/9/76 to Present
DATA REPORTED TO:	NSSDC up to 31/ 12- 1980

APERTURE:	50cm	MOUNT TYPE:	Az-El, coude
TRANSMITTED POWER:	700 MW	REP. RATE:	15 ppm
WAVELENGTH:	694.3 nm	PULSE WIDTH:	1.8 nsec

DETECTOR TYPE:	RCA 8852
PRIMARY TIME STANDARD:	Rb standard HP 5065 A
TIME OF FLIGHT EQUIPMENT:	HP 5360 A + constant fraction discriminators
COMPUTER TYPE & CAPACITY:	HP 21 MX-E, 128k

MAJOR SUBSYSTEMS UNDER COMPUTER CONTROL:	none, predictions only		
CALIBRATION METHOD:	pre/postcalibration using internal light path		
PRINCIPLE TARGETS:	Lageos	Starlette	Geos 3
TRACKS IN 1980:	53	157	160
PRECISION ON TARGET:	15 cm	10cm	15cm
ENVIRONMENTAL MONITORING:	pressure, temperature, relative humidity		
GEODETIC MONITORING:			
READINESS TO TRACK IN '82:	240 nights/240 days		
READINESS TO TRACK IN MERIT '83-'84:	300 nights/300 days		

COMMENTS:

STATION REPORT

STATION NAME:	Mobile Laser Ranging System
LOCATION:	under development
MAILING ADDRESS:	Delft University of Technology Kootwijk Observatory P. O. Box 581, 7300 AN Apeldoorn, The Netherlands
TELEPHONE NO:	5769-341 TWX No. 36442
PERIOD OF OPERATION:	September, 1983
DATA REPORTED TO:	

APERTURE:	40 cm	MOUNT TYPE:	Az-El, coude
TRANSMITTED POWER:	50 MW	REP. RATE:	10 Hz
WAVELENGTH:	539 nm	PULSE WIDTH:	0.2 nsec

DETECTOR TYPE:	RCA 8850 (preliminary)
PRIMARY TIME STANDARD:	to be decided
TIME OF FLIGHT EQUIPMENT:	HP 5370 A + constant fraction discriminators
COMPUTER TYPE & CAPACITY:	multi-microprocessor system

MAJOR SUBSYSTEMS UNDER COMPUTER CONTROL:	mount, detection system		
CALIBRATION METHOD:	pre/postcalibration + simultaneous internal calibration		
PRINCIPLE TARGETS:	Lageos	Starlette	Ground
TRACKS IN 1980:			
PRECISION ON TARGET:	2 cm	2 cm	1cm
ENVIRONMENTAL MONITORING:	pressure, temperature, relative humidity		
GEODETIC MONITORING:	geodetic locator		
READINESS TO TRACK IN '82:			
READINESS TO TRACK IN MERIT '83-'84:			

COMMENTS:

STATION REPORT

STATION NAME:	7907 - SAO		
LOCATION:	Arequipa, Peru		
MAILING ADDRESS:	Smithsonian Astrophysical Observatory Casilla 751 Arequipa, Peru 224038		
TELEPHONE NO:	Arequipa 215959	TWX No.	RTTY-via SAO
PERIOD OF OPERATION:	full time, 3 shifts		
DATA REPORTED TO:	SAO		
APERTURE:	20"cassegrain	MOUNT TYPE:	Alt/Azi, Stepping
TRANSMITTED POWER:	350 MW	REP. RATE:	8ppm
WAVELENGTH:	694.3 nm	PULSE WIDTH:	6 nsec
DETECTOR TYPE:	RCA 7265		
PRIMARY TIME STANDARD:	Caesium UTC (USNO)		
TIME OF FLIGHT EQUIPMENT:	0.1 nsec counter, 20 channel digitizer, A/D converters		
COMPUTER TYPE & CAPACITY:	Nova 1200, 32K		

MAJOR SUBSYSTEMS UNDER COMPUTER CONTROL:	Mount, data system, paper tape reader, and punch, Linc tape				
CALIBRATION METHOD:	pre/post pass calibration, weekly start electronics, monthly system calibration, daily counter calibration				
PRINCIPLE TARGETS:	Lageos	Starlette	Geos 3	Geos 1	BEC
TRACKS IN 1980:	340	536	685	590	494
PRECISION ON TARGET:	10cm	10cm	10cm	10cm	10cm
ENVIRONMENTAL MONITORING:	temperature, humidity, pressure				
GEODETIC MONITORING:	periodic slant range				
READINESS TO TRACK IN '82:	261 nights/261 days				
READINESS TO TRACK IN MERIT '83-'84:	261 nights/261 days				

COMMENTS:

STATION REPORT

STATION NAME:	Borowiec		
LOCATION:	lat=52°16'38", long=$1^h08^m18^s$, 80m over sea level		
MAILING ADDRESS:	Astronomical Latitude Observatory Borowiec 62-035 Kornik POLAND		
TELEPHONE NO:	Kornik 188	TWX NO.	0412623
PERIOD OF OPERATION:	1.IV to 31.X		
DATA REPORTED TO:	Interkosmos		
APERTURE:	32 cm	MOUNT TYPE:	4-axis, manual, Interkosmos
TRANSMITTED POWER:	1.5 J	REP. RATE:	7/min
WAVELENGTH:	694 nm	PULSE WIDTH:	25 nsec
DETECTOR TYPE:	RCA 8852 followed by constant fraction discriminator		
PRIMARY TIME STANDARD:	Atom Clock - Rhode and Schwarz/Ces.		
TIME OF FLIGHT EQUIPMENT:	Fl 102, 5 ns resolution		
COMPUTER TYPE & CAPACITY:	not used		

MAJOR SUBSYSTEMS UNDER COMPUTER CONTROL:	n/a
CALIBRATION METHOD:	pre-post ground target calibration 1478.907 m
PRINCIPLE TARGETS:	Geos C Geos A
TRACKS IN 1980:	no observations - damage to the laser
PRECISION ON TARGET:	46 23 (1979)
ENVIRONMENTAL MONITORING:	Temperature, air pressure, humidity
GEODETIC MONITORING:	
READINESS TO TRACK IN '82:	100 nights
READINESS TO TRACK IN MERIT '83-'84:	expecting new laser system

COMMENTS:

STATION REPORT

STATION NAME:	Laser Satellite San-Fernando (7824)
LOCATION:	San-Fernando, Spain
MAILING ADDRESS:	Estacion Laser Observatorio de Marina San-Fernando (Cadiz) ESPANA
TELEPHONE NO:	(56) 883548 Telex: 76108 IOM E
PERIOD OF OPERATION:	1975 to present
DATA REPORTED TO:	CNES - TOULOUSE

APERTURE:	60 cms	MOUNT TYPE:	AZ-EL
TRANSMITTED POWER:	0,7 J	REP. RATE:	6 s
WAVELENGTH:	694 nm	PULSE WIDTH:	27 ns

DETECTOR TYPE:	RCA 31034 A
PRIMARY TIME STANDARD:	Caesium
TIME OF FLIGHT EQUIPMENT:	1 ns counter CGE design
COMPUTER TYPE & CAPACITY:	WANT 2200 - 16 K

MAJOR SUBSYSTEMS UNDER COMPUTER CONTROL:	Peripherals, Mount Servo Control, Data Measuring System
CALIBRATION METHOD:	Pre-Post ranging on fixed calibration target
PRINCIPLE TARGETS:	
TRACKS IN 1980:	No operation from April to December
PRECISION ON TARGET:	100 cms
ENVIRONMENTAL MONITORING:	Temperature, pressure
GEODETIC MONITORING:	
READINESS TO TRACK IN '82:	200 nights
READINESS TO TRACK IN MERIT '83-'84:	200 nights

COMMENTS:

The observations were discontinued on the 10th of April 1980 in order to move the GRGS mobile station to its new location in the observatory's main building.

Following the difficulties experienced with the dome opening, the laser station is now operating. (From December of 1980).

Presently, we are fitting up a new laser which characteristics are: 2-3 J, 6-10 ns.

The ranging accuracy will be 50 cms and the system will be able to get regular ranging on Lageos.

The Event-Timer required for the LASSO experiment is expected soon. The model selected by the Naval Observatory is: Thomson TSN 634 H.

STATION REPORT

STATION NAME:	Zimmerwald Laser Ranging Station
LOCATION:	Zimmerwald near Bern
MAILING ADDRESS:	Astronomisches Institut Universitat Bern Sidlerstrasse 5 3012 Bern, SWITZERLAND
TELEPHONE NO:	+41 31658591 TWX No. 32 320
PERIOD OF OPERATION:	August 1, 1980 to September 30, 1980
DATA REPORTED TO:	C.N.E.S.

APERTURE:	525 mm	MOUNT TYPE:	Alt/AZ
TRANSMITTED POWER:	1.5 J	REP. RATE:	.25 Hz
WAVELENGTH:	694 nm	PULSE WIDTH:	17 nsec

DETECTOR TYPE:	RCA 7265
PRIMARY TIME STANDARD:	Loran-C
TIME OF FLIGHT EQUIPMENT:	Eldorado + Octal TDC's
COMPUTER TYPE & CAPACITY:	PDP-11/40 64 kb

MAJOR SUBSYSTEMS UNDER COMPUTER CONTROL:	Mount and Laser Radar - CAMAC			
CALIBRATION METHOD:	Internal, pre and post track			
PRINCIPLE TARGETS:	Geos 1	Geos 3	Starlette	BE-C
TRACKS IN 1980:	5	2	5	2
PRECISION ON TARGET:	60cm	80cm	80cm	60cm
ENVIRONMENTAL MONITORING:	pressure, temperature, humidity			
GEODETIC MONITORING:	Doppler (visiting)			
READINESS TO TRACK IN '82:	40 nights			
READINESS TO TRACK IN MERIT '83-'84:	60 nights			

COMMENTS:

Video recording and processing for direction measurement

STATION REPORT

STATION NAME:	RGO Herstmonceux		
LOCATION:	Herstmonceux, East Sussex England 50°52'N, 0°20'E		
MAILING ADDRESS:	Royal Greenwich Observatory Hailsham, East Sussex, BN27 1RP United Kingdom		
TELEPHONE NO:	(UK) 032-181-3171 Telex (UK) 87451 RGOBSY G from 1982 032-383-3171		
PERIOD OF OPERATION:	from early 1982		
DATA REPORTED TO:			
APERTURE:	T 100mm/ R 508mm	MOUNT TYPE:	Alt-az
TRANSMITTED POWER:	30 mJ pulse	REP. RATE:	10Hz
WAVELENGTH:	532 nm	PULSE WIDTH:	0.15 ns
DETECTOR TYPE:	Varian VPM 152S, RCA 8850 available		
PRIMARY TIME STANDARD:	Cs ensemble on site, Loran C links		
TIME OF FLIGHT EQUIPMENT:	University of Maryland 4-stop		
COMPUTER TYPE & CAPACITY:	PDP 11/34a, 128K x 16 bit, RSX 11M V3.2; LSI 11/2		

MAJOR SUBSYSTEMS UNDER COMPUTER CONTROL:	Telescope, laser, receiver, timer, data storage
CALIBRATION METHOD:	under consideration
INPUT/OUTPUT FORMATS:	9-track magnetic tape, 1600 bpi phase encoded
PRINCIPLE TARGETS:	Lageos Starlette
TRACKS IN 1980:	none
PRECISION ON TARGET:	better than 100 mm expected
ENVIRONMENTAL MONITORING:	under consideration
GEODETIC MONITORING:	linked to UK geodetic net, 4 Doppler campaigns on site since mid-1979
READINESS TO TRACK IN '82:	100 days or nights
READINESS TO TRACK IN MERIT '83-'84:	200 days or nights

COMMENTS:

The RGO Herstmonceux station will use a short-pulse laser of relatively low power, a telescope steered with unusual accuracy under computer control, single-photon detection and a multi-stop timing system. The option of working in pulse-comb mode will be investigated. The system is expected to be capable of tracking Lageos with sub-decimeter range uncertainty in daylight, but the small divergence of the emitted beam needed to reach the more distant targets may make acquisition difficult unless more accurate predictions can be obtained. The receiver and timing electronics will be controlled by a microcomputer slaved to the main computer, partly to reduce the load on the main computer and partly to simplify development of the system at two centres (RGO and the University of Hull).

The site is close to one of the holding patterns of London-Gatwick airport, and the station will include a radar system, slaved to the telescope drive, which will automatically shut off the laser whenever an aircraft approaches the laser beam.

STATION REPORT

STATION NAME:	McDonald Lunar Ranging
LOCATION:	Fort Davis, Texas USA
MAILING ADDRESS:	McDonald Observatory University of Texas Austin, Texas 78712 USA
TELEPHONE NO:	(512) 471-4471 TWX No. 910 8741351
PERIOD OF OPERATION:	August, 1969 to January, 1982
DATA REPORTED TO:	Goddard Space Flight Center

APERTURE:	2.7M	MOUNT TYPE:	Equatorial
TRANSMITTED POWER:	0.4W	REP. RATE:	20ppm
WAVELENGTH:	694.3 nm	PULSE WIDTH:	3 nsec

DETECTOR TYPE:	RCA 31034A
PRIMARY TIME STANDARD:	X-tal with Loran C
TIME OF FLIGHT EQUIPMENT:	TDC 100 in epoch recording mode
COMPUTER TYPE & CAPACITY:	Varian 620L 12K

MAJOR SUBSYSTEMS UNDER COMPUTER CONTROL:	timing, timekeeping, lunar pointing
CALIBRATION METHOD:	internal target
PRINCIPLE TARGETS:	Moon
TRACKS IN 1980:	
PRECISION ON TARGET:	10cm
ENVIRONMENTAL MONITORING:	pressure, temperature, humidity
GEODETIC MONITORING:	seismometer, accurate local survey
READINESS TO TRACK IN '82:	30 nights/30 days
READINESS TO TRACK IN MERIT '83-'84:	0

COMMENTS:

Station to be discontinued in early 1982, in favor of dual purpose installation at same location

STATION REPORT

STATION NAME:	MLRS
LOCATION:	Fort Davis, Texas, USA
MAILING ADDRESS:	McDonald Observatory University of Texas Austin, Texas 78712 USA
TELEPHONE NO:	(512)471-4471 TWX No. 910-874-1351
PERIOD OF OPERATION:	Nov., 1981 to
DATA REPORTED TO:	Goddard Space Flight Center

APERTURE:	0.76 M	MOUNT TYPE:	X-Y
TRANSMITTED POWER:	~4 W	REP. RATE:	10 Hz
WAVELENGTH:	532 nm	PULSE WIDTH:	0.1 nsec

DETECTOR TYPE:	RCA 8852
PRIMARY TIME STANDARD:	Rubidium + Loran C
TIME OF FLIGHT EQUIPMENT:	EG & G TD811 units in an epoch measuring mode
COMPUTER TYPE & CAPACITY:	Nova IV, 128K

MAJOR SUBSYSTEMS UNDER COMPUTER CONTROL:	timing, pointing, weather, clocks
CALIBRATION METHOD:	internal target returns cross correlated with satellite
PRINCIPLE TARGETS:	Lageos Moon Starlette
TRACKS IN 1980:	
PRECISION ON TARGET:	2cm 5cm 2cm normal point
ENVIRONMENTAL MONITORING:	pressure, temperature, humidity
GEODETIC MONITORING:	accurate local survey, seismometer
READINESS TO TRACK IN '82:	300 nights/300 days
READINESS TO TRACK IN MERIT '83-'84:	350 nights/350 days

COMMENTS:

System uses two lasers, a 3-5 W, 3 nsec unit for lunar work and a 20 mw, 011 nsec mode locked unit for satellites.

Telescope is a yoke mounted X-Y configuration with both cass. and coude focus position. System uses a roller drive with both high accuracy incremental as well as 18 bit absolute encoders.

System is in a transportable carrier about 16 x 3M is size.

STATION REPORT

STATION NAME:	TLRS
LOCATION:	variable
MAILING ADDRESS:	McDonald Observatory University of Texas Austin, Texas 78712 USA
TELEPHONE NO:	(512) 471-4471 TWX No. 910 874 1351
PERIOD OF OPERATION:	August, 1980 to Present
DATA REPORTED TO:	Goddard Space Flight Center

APERTURE:	0.3M	MOUNT TYPE:	Alt-Az
TRANSMITTED POWER:	35 MW	REP. RATE:	10Hz
WAVELENGTH:	532.nm	PULSE WIDTH:	0.1nsec

DETECTOR TYPE:	Varian 152 S
PRIMARY TIME STANDARD:	Caesium + Rubidium
TIME OF FLIGHT EQUIPMENT:	TD811 in epoch recording mode
COMPUTER TYPE & CAPACITY:	Nova III 32K

MAJOR SUBSYSTEMS UNDER COMPUTER CONTROL:	all
CALIBRATION METHOD:	internal target
PRINCIPLE TARGETS:	Lageos
TRACKS IN 1980:	50
PRECISION ON TARGET:	2 cm normal point
ENVIRONMENTAL MONITORING:	pressure, temperature, humidity
GEODETIC MONITORING:	variable
READINESS TO TRACK IN '82:	300 nights/300days
READINESS TO TRACK IN MERIT '83-'84:	300 nights/300days

COMMENTS:

Station is highly mobile and built in a single chassis vehicle.

The system uses a mode-locked laser with no pulse selection, identifying the pulses by cross correlating the single photon returns with the data from an internal target.

Computer intensive system which can perform a mount model prior to every pass if necessary at an unprepared site.

STATION REPORT

STATION NAME:	Moblas 1
LOCATION:	Mt. Haleakala, Hawaii
MAILING ADDRESS:	NASA Tracking Station P. O. Box 521 Puunene, Maui, Hawaii 96784 USA
TELEPHONE NO:	(808) 242-5563 TWX No. GXAA
PERIOD OF OPERATION:	July, 1980 to Present
DATA REPORTED TO:	GSFC

APERTURE:	16 inch	MOUNT TYPE:	AZ-EL
TRANSMITTED POWER:	750 MJ	REP. RATE:	1PPS
WAVELENGTH:	694 NM	PULSE WIDTH:	5 nsec

DETECTOR TYPE:	56 TVP
PRIMARY TIME STANDARD:	Caesium
TIME OF FLIGHT EQUIPMENT:	HP5360
COMPUTER TYPE & CAPACITY:	Honeywell DDP516, 16K

MAJOR SUBSYSTEMS UNDER COMPUTER CONTROL:	Peripherals, Mount Servo Control Console, Data Measuring System		
CALIBRATION METHOD:	Pre-post ranging of fixed calibration target		
PRINCIPLE TARGETS:	Lageos	Starlette	BE-3
TRACKS IN 1980:	216	141	229
PRECISION ON TARGET:	10cm	10cm	10cm
ENVIRONMENTAL MONITORING:	Temperature, Air Pressure, Humidity		
GEODETIC MONITORING:			
READINESS TO TRACK IN '82:			
READINESS TO TRACK IN MERIT '83-'84:			

COMMENTS:

Moblas 1 was operational at Ft. Davis, Texas prior to May, 1980. 1980 data figures include passes obtained at that location.

STATION REPORT

STATION NAME:	Moblas 2
LOCATION:	Platteville, Colorado
MAILING ADDRESS:	NASA Tracking Station P. O. Box 749 Platteville, Co. 80651 USA
TELEPHONE NO:	(303) 785-6366 TWX. No. GXBB
PERIOD OF OPERATION:	February, 1981 to Present
DATA REPORTED TO:	GSFC

APERTURE:	20 inch	MOUNT TYPE:	AZ-EL
TRANSMITTED POWER:	750 MJ	REP. RATE:	1PPS
WAVELENGTH:	694 NM	PULSE WIDTH:	5 nsec

DETECTOR TYPE:	56 TVP
PRIMARY TIME STANDARD:	Caesium
TIME OF FLIGHT EQUIPMENT:	HP 5360
COMPUTER TYPE & CAPACITY:	Honeywell DDP516, 16K

MAJOR SUBSYSTEMS UNDER COMPUTER CONTROL:	Peripherals, Mount Servo Control Console, Data Measuring System		
CALIBRATION METHOD:	Pre-post ranging of fixed calibration target		
PRINCIPLE TARGETS:	Lageos	Starlette	BE-3
TRACKS IN 1980:	184	135	225
PRECISION ON TARGET:	10cm	10cm	10cm
ENVIRONMENTAL MONITORING:	Temperature, Air Pressure, Humidity		
GEODETIC MONITORING:			
READINESS TO TRACK IN '82:			
READINESS TO TRACK IN MERIT '83-'84:			

COMMENTS:

Moblas 2 was operational at Owens Valley, CA. prior to January, 1981. Data figures include passes obtained at that location.

STATION REPORT

STATION NAME:	Moblas 3
LOCATION:	Monument Peak, CA
MAILING ADDRESS:	NASA Tracking Station P. O. Box 130 Mt. Laguna, CA 92048 USA
TELEPHONE NO:	(714) 473-9754 TWX NO. GXCC
PERIOD OF OPERATION:	July, 1981 to Present
DATA REPORTED TO:	GSFC

APERTURE:	20 inch	MOUNT TYPE:	AZ-EL
TRANSMITTED POWER:	750MJ	REP. RATE:	1PPS
WAVELENGTH:	694NM	PULSE WIDTH:	5 nsec

DETECTOR TYPE:	56TVP
PRIMARY TIME STANDARD:	Caesium
TIME OF FLIGHT EQUIPMENT:	HP5360
COMPUTER TYPE & CAPACITY:	Honeywell DDP516, 16K

MAJOR SUBSYSTEMS UNDER COMPUTER CONTROL: Peripherals, Mount Servo Control Console, Data Measuring System

CALIBRATION METHOD: Pre-post ranging of fixed calibration target

PRINCIPLE TARGETS:	Lageos	Starlette	BE-3
TRACKS IN 1980:	213	71	161
PRECISION ON TARGET:	10cm	10cm	10cm

ENVIRONMENTAL MONITORING: Temperature, Air Pressure, Humidity

GEODETIC MONITORING:

READINESS TO TRACK IN '82:

READINESS TO TRACK IN MERIT '83-'84:

COMMENTS:

Moblas 3 was operational at Goldstone, CA during 1980. Data figures reflect passes obtained at that location.

STATION REPORT

STATION NAME:	Moblas 4		
LOCATION:	GORF/GSFC		
MAILING ADDRESS:	Route 2, Box 274 Laurel, Md. 20708 USA		
TELEPHONE NO:	(301) 344-5800	TWX No. GXDD	
PERIOD OF OPERATION:	N/A		
DATA REPORTED TO:	GSFC		
APERTURE:	30 inch	MOUNT TYPE:	AZ-EL
TRANSMITTED POWER:	varied	REP. RATE:	1PPS
WAVELENGTH:	532 NM	PULSE WIDTH:	varied
DETECTOR TYPE:	56 TVP		
PRIMARY TIME STANDARD:	Caesium		
TIME OF FLIGHT EQUIPMENT:	HP 5360		
COMPUTER TYPE & CAPACITY:	Modular Computer II		

MAJOR SUBSYSTEMS UNDER COMPUTER CONTROL:	Peripherals, Mount Servo Control Console, Data Measuring System		
CALIBRATION METHOD:	Pre-post ranging of fixed calibration target		
PRINCIPLE TARGETS:	Lageos	Starlette	BE-3
TRACKS IN 1980:	76	34	68
PRECISION ON TARGET:	test	test	test
ENVIRONMENTAL MONITORING:	Temperature, Air Pressure, Humidity		
GEODETIC MONITORING:			
READINESS TO TRACK IN '82:			
READINESS TO TRACK IN MERIT '83-'84:			

COMMENTS:

Moblas 4 has been used as an engineering test bed. Data from this station, therefore, is subject to change in quality depending upon system configuration.

STATION REPORT

STATION NAME:	Moblas 6		
LOCATION:	GSFC		
MAILING ADDRESS:	Route 2, Box 274 Laurel, MD 20708 USA		
TELEPHONE NO:	(301) 344-6573	TWX NO.	GLSM
PERIOD OF OPERATION:	N/A		
DATA REPORTED TO:	GSFC		
APERTURE:	30 inch	MOUNT TYPE:	AZ-EL
TRANSMITTED POWER:	250 MJ	REP. RATE:	1 PPS
WAVELENGTH:	532 NM	PULSE WIDTH:	5-7 nsec
DETECTOR TYPE:	56TVP Amperex		
PRIMARY TIME STANDARD:	Caesium		
TIME OF FLIGHT EQUIPMENT:	HP 5360		
COMPUTER TYPE & CAPACITY:	Modular Computer II - 64K		

MAJOR SUBSYSTEMS UNDER COMPUTER CONTROL:	Peripherals, Mount Servo Control Console, Data Measuring System		
CALIBRATION METHOD:	Pre-post ranging of fixed calibration target		
PRINCIPLE TARGETS:	Lageos	Starlette	BE-3
TRACKS IN 1980:	103	30	24
PRECISION ON TARGET:	15cm	10cm	10cm
ENVIRONMENTAL MONITORING:	Temperature, air pressure, humidity		
GEODETIC MONITORING:			
READINESS TO TRACK IN '82:			
READINESS TO TRACK IN MERIT '83-'84:			

COMMENTS:

Moblas 6 was operational during 1980 in American Samoa. Presently this system is being held in caretaker status at GSFC.

STATION REPORT

STATION NAME:	Moblas 7		
LOCATION:	GORF/GSFC		
MAILING ADDRESS:	Route 2, Box 274 Laurel, MD 20708 USA		
TELEPHONE NO:	(301)344-5800	TWX NO.	GXGG
PERIOD OF OPERATION:	January, 1981 to Present		
DATA REPORTED TO:	GSFC		
APERTURE:	30 inch	MOUNT TYPE:	AZ-EL
TRANSMITTED POWER:	250 MJ	REP. RATE:	1PPS
WAVELENGTH:	532 NM	PULSE WIDTH:	.2-.4 nsec
DETECTOR TYPE:	56 TVP Amperex		
PRIMARY TIME STANDARD:	Caesium		
TIME OF FLIGHT EQUIPMENT:	HP 5360 Computing Counter		
COMPUTER TYPE & CAPACITY:	Modular Computer II - 64K		

MAJOR SUBSYSTEMS UNDER COMPUTER CONTROL:	Peripherals, Mount Servo Control Console, Data Measuring System		
CALIBRATION METHOD:	Pre-post ranging of fixed calibration target		
PRINCIPLE TARGETS:	Lageos	Starlette	BE-3
TRACKS IN 1980:	198	129	99
PRECISION ON TARGET:	15cm	10cm	10cm
ENVIRONMENTAL MONITORING:	Temperature, Air Pressure, Humidity		
GEODETIC MONITORING:			
READINESS TO TRACK IN '82:			
READINESS TO TRACK IN MERIT '83-'84:			

COMMENTS:

Moblas 7 was operational during 1980 at Haystack, Mass. The data reported was obtained in that location using a 5-7 nsec laser.

STATION REPORT

STATION NAME:	Moblas 8		
LOCATION:	Quincy, CA		
MAILING ADDRESS:	NASA Tracking Station P. O. Box BB Quincy, CA 95971 USA		
TELEPHONE NO:	(916) 283-1396 (temp) TWX NO. GXGG		
PERIOD OF OPERATION:	February, 1981 to Present		
DATA REPORTED TO:	GSFC		
APERTURE:	30 inch	MOUNT TYPE:	AZ-EL
TRANSMITTED POWER:	250 MJ	REP. RATE:	1PPS
WAVELENGTH:	532 NM	PULSE WIDTH:	5-7 nsec
DETECTOR TYPE:	56TVP Amperex		
PRIMARY TIME STANDARD:	Caesium		
TIME OF FLIGHT EQUIPMENT:	HP 5360 Computing Counter		
COMPUTER TYPE & CAPACITY:	Modular Computer II - 64K		

MAJOR SUBSYSTEMS UNDER COMPUTER CONTROL:	Peripherals, Mount Servo Control Console, Data Measuring System		
CALIBRATION METHOD:	Pre-post ranging of fixed calibration target		
PRINCIPLE TARGETS:	Lageos	Starlette	BE-3
TRACKS IN 1980:	65	20	67
PRECISION ON TARGET:	15cm	10cm	10cm
ENVIRONMENTAL MONITORING:	Temperature, air pressure, humidity		
GEODETIC MONITORING:			
READINESS TO TRACK IN '82:			
READINESS TO TRACK IN MERIT '83-'84:			

COMMENTS:

Moblas 8 was operational during 1980 at Kwajelein, M.I. The data reported was obtained in that location.

STATION REPORT

STATION NAME:	Stalas
LOCATION:	GORF/GSFC
MAILING ADDRESS:	Route 2, Box 274 Laurel MD 20708 USA
TELEPHONE NO:	(301) 344-7874 TWX No. GLTF
PERIOD OF OPERATION:	May, 1975 to Sept. 1, 1981
DATA REPORTED TO:	GSFC

APERTURE:	24 inch	MOUNT TYPE:	X-Y
TRANSMITTED POWER:	250 MJ	REP. RATE:	1PPS
WAVELENGTH:	532 nm	PULSE WIDTH:	.2 - .4 nsec

DETECTOR TYPE:	56TVP
PRIMARY TIME STANDARD:	Caesium
TIME OF FLIGHT EQUIPMENT:	HP 5360
COMPUTER TYPE & CAPACITY:	Honeywell DDP516, 16K

MAJOR SUBSYSTEMS UNDER COMPUTER CONTROL:	Peripherals, Mount Servo Control Console, Data Measuring System		
CALIBRATION METHOD:	Pre-post ranging of fixed calibration target		
PRINCIPLE TARGETS:	Lageos	Starlette	BE-3
TRACKS IN 1980:	167	52	56
PRECISION ON TARGET:	10 cm	10cm	10cm
ENVIRONMENTAL MONITORING:	Temperature, Air pressure, Humidity		
GEODETIC MONITORING:			
READINESS TO TRACK IN '82:			
READINESS TO TRACK IN MERIT '83-'84:			

COMMENTS:

Stalas was operational prior to May, 1975, but not in the configuration specified.

STATION REPORT

STATION NAME:	Maui, Lure Observatory
LOCATION:	Haleakala, Maui, Hawaii, U.S.A.
MAILING ADDRESS:	Institute for Astronomy P. O. Box 209 Kula, Maui 96790
TELEPHONE NO:	(808) 244-9108 NASCOM
PERIOD OF OPERATION:	November 81 -
DATA REPORTED TO:	GSFC

APERTURE:	0.4M	MOUNT TYPE:	ACT-A2 Seliostat
TRANSMITTED POWER:	0.6W	REP. RATE:	3Hz
WAVELENGTH:	532 NM	PULSE WIDTH:	500 PS

DETECTOR TYPE:	AMPEREX XP2233
PRIMARY TIME STANDARD:	Caesium Clock
TIME OF FLIGHT EQUIPMENT:	Univ. of Maryland Multistop Timer
COMPUTER TYPE & CAPACITY:	LSI 11/23, 90K

MAJOR SUBSYSTEMS UNDER COMPUTER CONTROL:	Telescope, Timer, Dome		
CALIBRATION METHOD:	Target Board		
PRINCIPLE TARGETS:	LAGEOS	BEC	STARLETTE
TRACKS IN 1980:	-	-	-
PRECISION ON TARGET:	5 CM	5 CM	5 CM
ENVIRONMENTAL MONITORING:	Pressure, Temperature, Humidity, Wind		
GEODETIC MONITORING:	None		
READINESS TO TRACK IN '82:	16 hrs./day, 5 day/week		
READINESS TO TRACK IN MERIT '83-'84:	16 hrs./day, 5 day/week		

COMMENTS:

Expect relocation testing with Moblas 1 to begin 1 October '81 beginning to interface lurescope for lunar operations sometime in '82.

STATION REPORT

STATION NAME:	Intercosmos - 1873 Simeiz
LOCATION:	ℓ=44°24'11".6 λ=34°00'08" h= 346m
MAILING ADDRESS:	USSR, Crimea, Observatory, Simeiz
TELEPHONE NO:	77-13-70
PERIOD OF OPERATION:	
DATA REPORTED TO:	

APERTURE:	320 mm	MOUNT TYPE:	4th axis
TRANSMITTED POWER:	50 mgvt	REP. RATE:	0.7 htz
WAVELENGTH:	694.3 nm	PULSE WIDTH:	20 nsec

DETECTOR TYPE:	FEU-79
PRIMARY TIME STANDARD:	Hewlett Packard
TIME OF FLIGHT EQUIPMENT:	
COMPUTER TYPE & CAPACITY:	M-222

MAJOR SUBSYSTEMS UNDER COMPUTER CONTROL:

CALIBRATION METHOD: stand. target 800 m

PRINCIPLE TARGETS:	Geos A	Geos C	BEC	BEB
TRACKS IN 1980:	970	958	6	17

PRECISION ON TARGET: 100 cm

ENVIRONMENTAL MONITORING:

GEODETIC MONITORING:

READINESS TO TRACK IN '82: 60 nights

READINESS TO TRACK IN MERIT '83-'84: 120 nights

COMMENTS:

STATION REPORT

STATION NAME:	Intercosmos - 1072, Svenigozod
LOCATION:	ℓ= 55°41' 39.2" λ= 2h26m45.9s, h= 134m
MAILING ADDRESS:	109017 Moscow, Pyatnitskaya, 48, The Astronomical Council USSR
TELEPHONE NO:	231-54-61
PERIOD OF OPERATION:	day time
DATA REPORTED TO:	Data Center of the A. S.

APERTURE:	340 mm	MOUNT TYPE:	4th-axis, Crypton
TRANSMITTED POWER:	1 J.	REP. RATE:	0.33 per sec.
WAVELENGTH:	694.3 nm	PULSE WIDTH:	25 nsec

DETECTOR TYPE:	photomultiplier type FEU-84
PRIMARY TIME STANDARD:	Kvarz system
TIME OF FLIGHT EQUIPMENT:	LV-receiver and TV-reciever
COMPUTER TYPE & CAPACITY:	ES-1032, ES-9002.01

MAJOR SUBSYSTEMS UNDER COMPUTER CONTROL:	MT-1016, printing device	
CALIBRATION METHOD:	standard target at distance of 250.887m testing by series to 20 pulse	
PRINCIPLE TARGETS:	Geos A	Geos C
TRACKS IN 1980:	17	22
PRECISION ON TARGET:	100 cm	100 cm
ENVIRONMENTAL MONITORING:	VLS control	
GEODETIC MONITORING:		
READINESS TO TRACK IN '82:	50 nights	
READINESS TO TRACK IN MERIT '83-'84:	100 nights	

COMMENTS:

Automatic system for counter's gate operation

Analog system for receiving energy measurements

Sensitive counting system for calibration of the receiving system